27

ORNL
MASTER COPY

ORNL-2584
Chemistry-General

# CHEMISTRY DIVISION ANNUAL PROGRESS REPORT

## FOR PERIOD ENDING JUNE 20, 1958

**OAK RIDGE NATIONAL LABORATORY**
operated by
UNION CARBIDE CORPORATION
for the
U.S. ATOMIC ENERGY COMMISSION

Printed in USA. Price 2.75 cents. Available from the

Office of Technical Services
U. S. Department of Commerce
Washington 25, D. C.

LEGAL NOTICE

This report was prepared as an account of Government sponsored work. Neither the United States, nor the Commission, nor any person acting on behalf of the Commission:

A. Makes any warranty or representation, express or implied, with respect to the accuracy, completeness, or usefulness of the information contained in this report, or that the use of any information, apparatus, method, or process disclosed in this report may not intringe privately owned rights; or

B. Assumes any liabilities with respect to the use of, or for damages resulting from the use of any information, apparatus, method, or process disclosed in this report.

As used in the above, "person acting on behalf of the Commission" includes any employee or contractor of the Commission to the extent that such employee or contractor prepares, handles or distributes, or provides access to, any information pursuant to his employment or contract with the Commission.

ORNL-2584
Chemistry-General

Contract No. W-7405-eng-26

# CHEMISTRY DIVISION ANNUAL PROGRESS REPORT

## for Period Ending June 20, 1958

E. H. Taylor, Director
M. A. Bredig, Associate Director

DATE ISSUED

SEP 30 1958

OAK RIDGE NATIONAL LABORATORY
Oak Ridge, Tennessee
operated by
UNION CARBIDE CORPORATION
for the
U.S. ATOMIC ENERGY COMMISSION

# CHEMISTRY DIVISION ANNUAL PROGRESS REPORT FOR PERIOD ENDING JUNE 20, 1958

| Page | Column | Line | Errata |
|---|---|---|---|
| viii | 2 | 13 | *for* the evidence of a polymeric species of $UO_2F_2$ (trimer) was confirmed *read* the existence of a polymeric species of $UO_2F_2$ was confirmed |
| 4 | (see below for revised table) | | |
| 13 | Fig. 4 | | the experimental points correspond to $M$ = 1, 7, and 10 |
| 17 | Table 8 | | *for* 364 *read* 426; *for* 426 *read* 364 |
| 33 | 2 | 11 | *for* carbonyl *read* carboxyl |
| 60 | 1 | 25 | *for* Resin Phase *read* Resin Phase[51] |
| 60 | 2 | 12 | delete ref 51 |
| 60 | 2 | | *for* ref 52 *read* To be published in the proceedings of the symposium on "Structure of Electrolytes," held at the 1957 Spring Meeting of the Electrochemical Society, Washington, D.C. |
| 80 | Table 23 | | delete $\times 10^{-3}$ from last column |
| 82 | Fig. 41 | | *for* present caption *read* Heats and Entropies of Solution of HF in $NaF\text{-}ZrF_4$ Mixtures |
| 85 | 2 | 32 | *for* 20% *read* 5.0% |
| 88 | 1 | | *for* ref 18 *read* R. E. Thoma, H. Insley, B. S. Landau, H. A. Friedman, and W. R. Grimes, *J. Am. Ceram. Soc.* (in press) |
| 88 | 1 | | *for* ref 19 *read* C. J. Barton, W. R. Grimes, H. Insley, R. E. Moore, and R. E. Thoma, *J. Phys. Chem.* **62**, 665–76 (1958) |

**Table 1. Preferred Values of Heavy-Nuclide Cross Sections**

| Nuclide | Process[(a)] | $\sigma_0$ (barns) | $g\sigma_0$ (barns) | $I_0$ (barns) | $\sigma_{eff}$[(b)] (barns) |
|---|---|---|---|---|---|
| $Th^{233}$ | c | (1350 ± 150) | 1350 ± 150 | 450 ± 150 | 1400 ± 150 |
| $Pa^{233}$ | c | (70 ± 20 | 70 ± 20 | 1200 ± 300 | 170 ± 20 |
| $U^{233}$ | c | 52 ± 10 | 48 ± 10 | 150 ± 40 | 60 ± 15 |
| | abs | 580 ± 20 | 590 ± 30 | 1000 ± 200 | 670 ± 50 |
| $U^{234}$ | c | 95 ± 10 | 95 ± 10 | 700 ± 70 | 150 ± 15 |
| $U^{236}$ | c | 6 ± 2 | 6 ± 2 | 400 ± 50 | 38 ± 10 |
| $U^{238}$ | c | 2.75 ± 0.05 | 2.75 ± 0.05 | 280 ± 10 | 26 ± 3 |
| $Pu^{239}$ | c | 310 ± 20 | 350 ± 20 | 1500 ± 300[(c)] | 500 ± 80 |
| | abs | 1040 ± 30 | 1100 ± 30 | 3600 ± 1000[(c)] | 1400 ± 200 |
| $Pu^{240}$ | c | 280 ± 15 | 320 ± 20 | 9000 ± 1000 | 1100 ± 150 |

[(a)] c and abs represent capture and absorption, respectively.
[(b)] Values of $\sigma_{eff}$ are for $\phi_r/\phi_{th} = 1/12$.
[(c)] These values are for the resonance integral $I_0'$, with a lower limit of 0.15 ev.

## SUMMARY

### NUCLEAR CHEMISTRY

The gamma-ray spectrum of 16-sec $Tc^{100}$ was determined by scintillation spectrometry. It exhibits two strong lines at 0.542 and 0.600 Mev, and at least eight more lines of low intensity. The maximum energy of the beta ray to the ground state of $Ru^{100}$ is 3.38 ± 0.06 Mev.

Fast neutrons have been used to produce a (7.8 ± 0.2)-min activity by means of the reaction $Ge^{74}(n,p)Ga^{74}$. The assignment of this period to $Ga^{74}$ was established by chemical identification and by the correlation of the yield of the 7.8-min activity with the target isotope enrichment. Preliminary investigations of the decay scheme were made.

Both 86-sec $I^{136}$ and 2.9-min $Rb^{90}$ decay with emission of energetic beta and gamma radiations. Partial decay schemes were formulated.

A level scheme for $Zr^{90}$ was formulated by studies on the decay of 14.6-hr $Nb^{90}$. Excited states at 1.76 (0+), 2.19 (2+), 2.32 (5−), 3.08 (4+), 3.45 (6+), 3.59 (8+), 4.44, 5.05, and 5.45 Mev were established. The spins and parities of these levels may be understood qualitatively in terms of an independent-particle model.

The polarization of electrons emitted in the beta decay of $P^{32}$ is being measured in cooperation with members of the Physics Division to determine whether the degree of polarization is accurately equal to $-v/c$, as predicted by theory.

A "fast-slow" coincidence assembly was developed for the measurement of lifetimes of energy levels populated by electron capture decay or by gamma emission. This equipment was used to measure the lifetimes of levels in $Pm^{145}$ and $Nd^{145}$.

A critical review of neutron cross sections pertinent to thermal reactor operation includes the nuclides $Th^{233}$, $Pa^{233}$, $U^{233}$, $U^{234}$, $U^{236}$, $U^{238}$, $Pu^{239}$, and $Pu^{240}$.

### ISOLATION AND CHEMICAL PROPERTIES OF SYNTHETIC ELEMENTS

A spectrophotometric examination of several compounds or oxidation states of technetium and rhenium in solution was made. Compounds of technetium prepared and studied were $K_2TcCl_6$, $K_2TcBr_6$, $K_2TcI_6$, and $TcO_3Cl$. The corresponding rhenium compounds were prepared, and their spectra and stability in solution were compared with those of the technetium compounds. The existence of Re(VI) in 18 *M* $H_2SO_4$ was established. Neither the corresponding Tc(VI) nor Tc(V) appears to exist in this medium.

Comprehensive measurements of the solvent extraction of heptavalent technetium, present in aqueous solutions as pertechnetate ion, contributed to a better understanding of the factors operative in the extraction of the $MX_4^-$ type of metal complex ions. This extraction, which may be highly efficient, appears to be governed by an ion exchange mechanism requiring the presence or formation of an "onium" salt in the organic phase. The dependence of the extraction coefficient for Tc(VII) on acid type and concentration, salt type and concentration, pertechnetate ion concentration, and on the composition of the organic phase is consistent with the view that an anion exchange equilibrium with $TcO_4^-$ is operative. The ultraviolet absorption spectra observed with the equilibrium organic phases showed the same characteristic features of the pertechnetate ion observed in aqueous solutions, thereby lending support to the hypothesis that this simple ion only is involved.

Some details are given of the procedure used for the isolation of an additional amount, 115 g, of $Np^{237}$ from Gaseous Diffusion Plant fluorination residues of depleted $UO_3$. In order to increase the efficiency of the neptunium production, a thorium partitioning step was incorporated in the initial fluorination extraction process.

The collection, on a set of two filters, of particle-forming fission elements released from APPR fuel plates melted in air yielded practically exclusively cesium hydroxide.

### CHEMICAL SEPARATION OF ISOTOPES

Fractionation of lithium isotopes between aqueous lithium ions and lithium ions on various ion exchange resins was observed to vary as a function of resin type, resin cross-linkage, and the nature of the complexing agent in the aqueous phase.

Studies dealing with the chemical separation of boron isotopes were continued, with emphasis on systems involving thioether complexes of $BF_3$. The single-stage separation factors, vapor pressures, and heats of association for the system

gaseous $BF_3$ vs *n*-butyl sulfide–$BF_3$ complex were measured over a wide temperature range.

The separation factor in the Nitrox system was observed to vary in a predictable manner over the temperature range between 25 and 70°C.

Two chemical exchange reactions having attractive carbon isotope fractionation factors were found.

Separation factors for a number of systems involving the amine complex of $SO_2$ were measured.

Infrared spectra of isotopic species of $N_2O$, NOCl, and $BF_3$ were observed. The Raman spectra of several metal-ammonia complexes were studied.

## RADIATION CHEMISTRY

The yield of molecular hydrogen in the radiolysis of water was found to be independent of pH and added sodium sulfate. The yield is diminished by added sodium nitrate, the decrease being proportional to the cube root of the nitrate activity. The "molecular" peroxide yield is the same for both light and heavy water. The yield is diminished by the same amount in both solutions by added KBr. The decrease in yield is again proportional to the cube root of the activity of added solute. The results are consistent with the radical-diffusion model of Magee.

Radiation induces reaction between Fe(III) and Sn(II), and between Ce(VI) and As(III). Mechanisms consistent with the observed results and with known radical yields in radiolysis of water were derived. Relative rate constants for reactions with radicals were evaluated.

From studies of the kinetics of the radiation-induced reduction of Ce(IV) in solutions containing Ce(IV), Ce(III), $H_2$, and $H_2SO_4$, the reactivities of Ce(III), $H_2$, and $H_2SO_4$ with OH radical were found to be as 650:135:1.

Kinetics of formation and disappearance of nitrous oxide, nitrogen dioxide, nitrogen pentoxide, nitric acid, and ozone in the radiolysis of moist air were studied.

The alpha-particle radiolysis of CO produced $CO_2$ and solid products which are mainly $(C_3O_2)_x$ and C. The solid material, when degassed and irradiated, gave $CO_2$ and a new solid.

The radiolysis of biphenyl with radon alpha particles produced hydrogen, methane, and a polymer with yields (*G*) of 0.03, 0.003, and 0.5, respectively.

The effect of ionizing radiation upon heterogeneous catalysts was investigated. The study included the role played by high-temperature activation and by catalyst poisons, $H_2$, $H_2O$, or $C_2H_4$, in the catalysis of $H_2$-$D_2$ exchange by $\gamma$-$Al_2O_3$, and the decay rate of the radiation-induced catalytic acitivity. Electron trapping, for gamma irradiation, and atom displacement, for heavy particles, are suggested for explanation of the effects observed. Other catalysts investigated included ZnO, $ThO_2$, $TiO_2$, $SiO_2$, $V_2O_3$, and $SiO_2$-$Al_2O_3$; the enhancement factors ranged from 0.1 (retardation) to 50,000.

## ORGANIC CHEMISTRY

Further evidence was obtained for the mechanism of the rearrangement of phenyl-di-*p*-tolylacetaldehyde in the presence of cold concentrated sulfuric acid. The kinetics of the rearrangements of threo- and erythro-1,2-diphenyl-1-*o*-tolylethylene glycol were studied.

Kinetic rate data for the isotope position isomerization of variously labeled 1,2,2-triphenylethyl acetates and for the racemization of optically active 1,2,2-triphenylethyl acetate in the presence of *p*-toluenesulfonic acid were analyzed by means of the Oracle. It was shown that the ordinary least-squares treatment would lead, in the present instance, to erroneous conclusions.

The stereochemistry of the deamination of (+)-1,2,2-triphenylethyl-1-$C^{14}$-amine at 25°C was studied by a determination of the fractions of rearrangement of the $C^{14}$ labels in the enantiomeric products.

The optical configurations of (+)-1,2,2-triphenylethylamine and (+)-1,2,2-triphenylethanol have been related.

During the reduction of triphenylacetonitrile in the presence of benzylmagnesium chloride, the source of hydrogen was shown to be the $\alpha$-hydrogen of the benzyl group.

The reaction of cyanogen with various benzyl-type Grignard reagents was shown to proceed with ortho addition.

The carbon isotope effect in the pinacol-pinacolone rearrangement, previously reported elsewhere by other investigators to be astonishingly large, was reinvestigated and found to be in a normal range of 0 to 3% ($k^*/k = 0.97$ to 1.0).

From isotopic studies of the decarbonylation of carboxylic acids in concentrated sulfuric acid, it is inferred that the mechanism depends upon the substituent groups present in the acids studied.

It was demonstrated by $O^{18}$ tracer studies that the oxygen of carbon monoxide undergoes exchange with the oxygen of concentrated sulfuric acid.

Mass spectrometric studies of deuterium-labeled formic acids were carried out. From these studies, the mode of hydrogen loss upon electron impact was determined. When a homogeneous beam of $HCOO^-$ ions was passed through nitrogen gas, a negative ion was produced which is believed to be $CN^-$.

The dispersion of $ThO_2$ in nonpolar solvents was studied. Several additives were effective as dispersing agents.

Relatively inert esters of sulfur and phosphorus acids were converted to salts of compounds such as ethanolamine. These salts were decomposed with cation exchange resins, thus permitting equivalent weight determinations to be made by titration of the liberated acids with standard alkali.

The solubilities of tributyl phosphate in water solutions of several electrolytes were shown to be adequately represented by the Setchenow equation. The extraction of tributyl phosphate from nonpolar solvents was studied.

The distribution of univalent electrolytes between tributyl phosphate and aqueous phase was measured as a function of electrolyte type and concentration. Two mechanisms of extraction are apparent; water accompanies the electrolyte in one case but is rejected by the organic phase in the other.

## CHEMISTRY OF AQUEOUS SYSTEMS

The equilibrium and rate behavior of several new organic ion exchangers was examined. The properties of a new strong-base anion exchanger containing structurally bound tertiary sulfonium cationic groups were found to be similar to those of the quaternary ammonium types. This finding suggests that the unusually high selectivities sometimes shown for transition metal ions in concentrated aqueous chloride ion solutions by strong-base anion exchangers cannot be attributed to the nature of the ionogenic groups in these materials. Equilibrium ion exchange distributions measured with specially prepared variable capacity, monofunctional polystyrene sulfonic acid cation exchangers and quaternary-ammonium-type anion exchangers gave selectivity coefficients which decreased as the exchange capacity increased. This finding is the reverse of that predicted by polyelectrolyte theory and suggests that important contributions to the total free energy of ion exchangers may have been overlooked in the theory.

Survey investigations with four types of liquid ion exchangers were completed. Because of the rapidity with which exchange equilibrium can be established and because of the absence of complications in the exchanger phase, liquid ion exchangers promise to be of use in the elucidation of ion exchange mechanisms, particularly those involving concentrated aqueous electrolyte solutions.

Calorimetric measurements of the differential heats of ion exchange of $Na^+$ ion with $H^+$, $Li^+$, $K^+$, and $Cs^+$ ions in a series of six differently cross-linked polystyrene sulfonate-type cation exchangers, and of $Br^-$ ion with $F^-$, $Cl^-$, and $I^-$ ions in a series of five differently cross-linked polystyrene quaternary-ammonium-type anion exchangers were performed at 25°C as a function of the resin "loading." Previous equilibrium selectivity coefficient measurements on these systems permit the estimation of standard free energies, $\Delta F^0$, of the ion exchange, and these, together with $\Delta H^0$ values from the heat measurements, make possible the evaluation of the standard entropy, $\Delta S^0$, of exchange. The magnitudes of $\Delta H^0$ and $\Delta S^0$ found with the cation and anion exchangers, respectively, show that the standard free energy changes, and hence the ionic selectivities, for these two types are determined by quite different factors. With the cation exchanges studied, ion binding is relatively unimportant, and the heat and entropy changes appear to originate in strong ion-solvent interactions. In contrast, ion binding is a predominant effect with the anion exchanges examined, and polymer network entropies may be of some importance.

A rotor which allows simultaneous ultracentrifugation of five solutions was tested and found satisfactory. Light-scattering measurements on the two-component system, silicotungstic acid–water, confirmed that, contrary to statements in the literature, the molecular weight obtained by extrapolation of data for a polymeric electrolyte (in the absence of supporting electrolyte) to infinite dilution is a number average ionic weight. Ultracentrifugation of polymolybdate solutions confirmed, in general, the assumption of predominant species in the hexameric to octameric range for $HClO_4/Na_2MoO_4$ ratios of 1 to 1.5.

The performance and general reliability of the first high-temperature spectrophotometric cell are

described. Measurements made on a solution of $Np^{237}$ in the range from 4.5 to 252°C indicate that Np(VI) is quantitatively and irreversibly reduced to Np(V). The Np(V) was stable throughout the remainder of the heating and cooling cycle. Plans for the design of a more versatile cell assembly are mentioned.

It was noted that with a proper choice of parameters, experimental solubilities of salts in aqueous solution could be described by expressions of the Debye-Hückel type over wide ranges of temperature and concentration. This agreement between theory and experiment is demonstrated by extensive measurements of the solubility of $Ag_2SO_4$ in $KNO_3$, $K_2SO_4$, $H_2SO_4$, and $HNO_3$ solutions. A high-speed digital computer was used in making the calculations. The principal species in solution at all temperatures were found not to be drastically different from those assumed, although additional species might exist at low to moderate concentrations.

The pH values of $UO_2SO_4$ solutions were measured in the range 25 to 180°C with a high-temperature pH meter.

Temperatures for the transition from a homogeneous to a two-liquid system were determined for the system $UO_2SO_4$-$CuSO_4$-$H_2SO_4$-$H_2O$ at elevated temperature. These data indicate maximum temperature and composition limits within which particular homogeneous reactor fuels can be used in order to avoid the appearance of a solid or a second liquid phase.

Simplified calculations were carried out for the solubility of antlerite ($3CuO{\cdot}SO_3{\cdot}2H_2O$) in the four-component system $UO_3$-$CuO$-$SO_3$-$H_2O$ at 290°C utilizing only data for the independent three-component systems $UO_3$-$SO_3$-$H_2O$ and $CuO$-$SO_3$-$H_2O$. The calculated values are compared with experimental values in the four-component system and show some consistent agreement. The results of further solubility studies will be used in an attempt to develop a modified treatment for multicomponent systems.

Phase equilibrium data from the system $NiO$-$SO_3$-$H_2O$ were obtained from 150 to 300°C and from 1 to $10^{-4}$ $m$ $SO_3$. These data indicate $NiSO_4{\cdot}H_2O$ to be the stable solid phase at high concentration of $SO_3$ and at the higher temperatures, whereas several basic nickel sulfates appear to exist as stable species in lower concentration ranges. The completed phase equilibrium data are to be combined with data for other three-component systems such as $UO_3$-$SO_3$-$H_2O$ and $CuO$-$SO_3$-$H_2O$ in an attempt to correlate solubility interactions in reactor fuel solutions.

The measurement of vapor pressures of aqueous systems at elevated temperature was resumed. The current goal of this investigation is to attain a method for measuring absolute vapor pressures to a high degree of precision and accuracy to temperatures approaching the critical temperature of water. The use of a differential manometer for measurement at high temperature is actively being investigated.

An investigation is under way to measure the equilibrium compositions of the light and heavy liquid phases in the systems $UO_3$-$SO_3$-$H_2O$ and $UO_3$-$SO_3$-$D_2O$.

The homogeneous catalysis of the oxidation of dissolved hydrogen in aqueous solutions was studied in heavy-water solutions of approximately the composition of the fuel solution of the HRT. The substitution of dichromate for oxygen gas as the oxidizing agent in light-water solutions did not alter the observed rate of the reaction as measured by the rate of change of hydrogen partial pressure. Improvements in the experimental technique permitted simultaneous determination of reaction rates and hydrogen distribution coefficients with higher precision.

The decomposition of peroxide in uranyl sulfate solutions was found to proceed 13% faster in heavy-water solutions than in corresponding light-water solutions. This indicates that breaking of an O-H or O-D bond is not involved and suggests that acid catalysis may be operating. The addition of cupric copper to a uranyl sulfate solution containing low amounts of iron increased the rate of decomposition of peroxide over the temperature range 60 to 100°C but did not lower the activation energy for the reaction.

A method of measuring the pH of thoria slurries was developed which minimizes or eliminates errors normally resulting from contact of the slurry with the calomel electrode. This method was shown to give reproducible results when applied to several slurry samples containing varying amounts of nitric acid. This technique in combination with minimizing $CO_2$ contamination gave significantly different results from those by regular procedures.

In the study of dispersions of high-molecular-weight, hydrolytic Th(IV) polymer, the apparent

enthalpy change for HCl adsorption and the activity of HCl in a concentrated polymer dispersion were determined. Work on the adsorptive and ion exchange properties of inorganic materials was continued. A qualitative investigation was made of the adsorption of acidic gases such as $SO_2$ on hydrous oxides at high temperatures; oxides of Al(III) and Th(IV) showed the highest uptake.

In the program of investigating the properties of anion exchangers and the adsorptive behavior of elements in complexing media, adsorbability of rare-earth and other elements from HCl-HF and from acidified $LiNO_3$ or $NH_4NO_3$ media was studied. A systematic investigation was begun of the oxidation states of transuranic elements adsorbed on an anion exchange resin. Gaseous $SO_2$ was found to be adsorbable by organic anion exchangers. Activity coefficients of HCl in the resin, determined as a function of HCl activity and of cross-linking, could, with the use of Harned's rule, be correlated by a concentrated-electrolyte model of the exchanger.

The study of the temperature dependence of ion exchange equilibria in pressurized systems up to 200°C was continued. The apparent enthalpy change for the cation exchange equilibrium was found to increase with temperature. A greater tendency to anion complex formation at higher temperature is implied from the measurements with Zn(II) and Ga(III). A packed-column technique was used to measure the solubility of silver chloride in HCl solutions between 25 and 200°C.

## CHEMISTRY OF CORROSION

It was demonstrated that a deaerated pertechnetate solution does not convert ferrous ions to a precipitated oxide under conditions which permit inhibition of corrosion. It was also shown that reduction of pertechnetate ions occurs on active sites, rather than on the cathodic film of a heterogeneous iron or steel surface. The results indicate the inapplicability of the two main hypotheses of the action of $XO_4^{n-}$ inhibitors in vogue prior to the suggestion that an electrostatically induced space charge is involved.

With the use of the galvanostatic and potentiostatic procedures for which the theory was previously presented, the kinetics of the reduction of uranyl ions at a passive stainless steel electrode in sulfuric acid was investigated. A study of the theory of the potential-time relationship of polarized electrodes led to a useful technique for obtaining the differential capacity of an electrode-solution interphase, along with other kinetically significant quantities. Potentiostatic and galvanostatic measurements were made also on systems of crystal-bar zirconium in a variety of solutions and atmospheres for the determination of kinetic factors.

## NONAQUEOUS SYSTEMS AT HIGH TEMPERATURES

In the continued study of isotopic fluorine exchange between gaseous fluorocarbons and solid inorganic fluorides, the exchange between radioactive perfluoropropene and specially prepared alkali fluoride crystals was measured.

The self-diffusion coefficients of the ions in molten lithium and silver nitrates and their temperature dependence were determined by using radioactive $Ag^{110}$ and stable $Li^6$ and $N^{15}$.

The liquid-liquid phase equilibria of the systems Li-LiF and Rb-RbF were found to fit the series of the alkali metal–fluoride systems in the expected regular manner. The maximum degree of ideality among the chloride, bromide, and iodide systems of rubidium was again found in the bromide system, as had been the case with the corresponding sodium and potassium systems. An empirical relationship between the symmetry of the liquid-liquid coexistence areas and the sizes of the anion, cation, and metal atom was noted.

Measurements of the electrical conductivity of sodium and potassium metal solutions in their molten iodides confirmed the previously observed connection with the degree of ideality of the solution, or the degree of association of the metal, possibly to $Na_2$ and $K_2$ molecules.

Measurements in molten potassium nitrate of the activities of silver nitrate in the presence of chloride ions and of the solubility of silver chloride were successfully interpreted in terms of the preferential distribution of $Cl^-$ ions about the $Ag^+$ ions. The physical theory was proposed as an alternate to the vague concept of complex ions.

The solubility of noble gases in molten fluoride mixtures was found to increase with gas pressure, with temperature, and with decreasing atomic number of the noble gas. Enthalpy and entropy changes on dissolution were determined. By means of a theoretical model, it was possible (despite

probable oversimplification) to estimate inert gas solubility fairly well from the surface tension of the molten salts and the size of the gas molecules. The solubility of HF in molten $NaF-ZrF_4$ mixtures was found to vary directly with the HF pressure and to decrease with increasing temperature. The total pressure of all gaseous species resulting from vaporization of various molten fluorides was determined. A comparison with pressures measured in the literature by the transpiration method gave some indication of the degree of association in the vapor state.

The solubility of some fission product fluorides in molten fluoride mixtures was determined. It is suggested that removal of rare-earth elements from nuclear fuel melts might be achieved by solid-solution formation with solid $CeF_3$. The solubility of plutonium trifluoride in molten alkali fluoride–beryllium fluoride mixtures was found to increase with temperature. It appears to be of sufficient magnitude to allow operation of a plutonium burner fueled with plutonium solutions in molten $LiF-BeF_2$ or $NaF-BeF_2$ mixtures. Many new measurements and observations of phase behavior in fluoride systems potentially useful for various types of molten salt mixtures are summarized.

## CHEMICAL PHYSICS

Atomic hydrogen assays by the paramagnetic resonance method were made on frozen solutions of sulfuric, phosphoric, and perchloric acids at 77°K after irradiation with gamma rays from $Co^{60}$. There is a correlation between the molecular hydrogen yields, determined after melting, and the atomic hydrogen yields.

An apparatus for observing paramagnetic resonance spectra of free radicals formed in liquids during intense electron irradiation from a Van de Graaff generator is being constructed.

Paramagnetic resonance was studied in normal and deuterated ethanol and methanol irradiated at 77°K with $Co^{60}$ gamma rays.

A theoretical study of the satellite lines which arise from environmental nuclei and appear in electron spin resonance spectra was completed.

The results of the completed single-crystal neutron diffraction study of $H_2O_2$ are given in detail. An Oracle program for processing results of crystal structure refinements was prepared which takes the least-square parameters, the variance-covariance matrix, and the unit-cell dimensions with their standard errors and computes various functions of these parameters, together with their standard errors. Also, a method offering computational advantages in the determination of the principal axes of anisotropic temperature factors is described.

A refinement of the structure determination of acetylglycine by means of neutron diffraction resulted in considerably improved precision. Preliminary results of a structure determination of potassium hydrogen maleate are presented.

In x-ray diffraction studies of aqueous solutions, the evidence of a polymeric species of $UO_2F_2$ (trimer) was confirmed. Evidence was also obtained for the existence in an aqueous $BiOClO_4$ solution of a complex species, $Bi_6(OH)_{12}^{6+}$, having an octahedral arrangement of bismuth atoms and for the structure of the aqueous $SiW_{12}O_{40}^{4-}$ ion, which is similar to that of $PW_{12}O_{40}^{3-}$ in the crystal form.

A doubly bent and ground, point-focusing crystal monochromator for single-crystal x-ray diffraction studies was designed and built. A precision x-ray diffraction refinement of the unit-cell dimensions of dimethyl-γ-pyrone was obtained.

Continued experiments on the transformation of calcite into metastable aragonite by grinding are mentioned.

The construction of an apparatus for the measurement of high-temperature heat contents, utilizing a Bunsen ice calorimeter, and of a calorimeter for the measurement of specific heats between 10 to 310°K was completed.

The dissociation of $C_6H_5T$ into 31 singly charged fragments following beta decay was studied by means of a specially designed mass spectrometer and compared with the processes found in electron impact studies.

The development of the apparatus designed for the study of chemically interesting collisions between a beam of low-energy protons and a deuterium molecular beam was continued.

A study of the thermal emission of alkali positive ion pulses from clean and oxygenated tungsten was made. It is suggested that the method used may be applied as a general tool in investigations of high-temperature behavior, such as diffusion of impurities, crystallite reorientation, stability of oxide films, etc.

The degree of association in alkali-metal salt vapors is being determined by the most direct

and unambiguous technique: measurement of the vapor density. Preliminary results gave semi-quantitative agreement with recent literature data obtained by molecular beam velocity measurements.

A study of processes such as ion-molecule collisions, charge exchange, etc., with a multiple-stage mass spectrometer (at least two stages) was initiated. As a first step, a single-stage 6-in-radius instrument was improved. By use of isotopically labeled formic acid reactants, the cross sections for forming fragment ions and the origin of the fragments resulting from collisions of formic acid ions with $H_2$, $D_2$, He, $N_2$, A, and Kr molecules were determined. The differences in the effect of mass of the noble gas atoms with which $HCOOH^+$, $CO^+$, and $N_2^+$ were made to collide, with resulting dissociation, was found to be related to the dissociation energy of the ions. Also studied were bimolecular ion-molecule reactions of isotopically labeled aliphatic acids of the type $HCOOH^+ + HCOOH \rightarrow HCOOH{\cdot}H^+ + COOH$. Rupture of the C-H bond was found to be more frequent than that of the O-H bond. Charge permutation on collision of either negative or positive formic acid ions with inert gas molecules was also studied. Triatomic ions were (for the first time) observed experimentally in $Cl_2$ and $Br_2$ gases.

## CONTENTS


SUMMARY ..... iii

NUCLEAR CHEMISTRY ..... 1

- Polarization of $P^{32}$ Electrons ..... 1
- Lifetimes of Energy Levels Populated by Electron Capture ..... 1
- Characterization of Short-Lived Fission Products ..... 2
  - Nuclear Spectra of $Tc^{100}$ ..... 2
  - Production of $Ga^{74}$ ..... 2
  - Radiations from $I^{136}$ ..... 2
  - Nuclear Spectra of $Rb^{90}$ ..... 2
  - Nuclear Structure of $Zr^{90}$ ..... 3
- A Review of Some Neutron Absorption Cross Sections of Interest to Reactor Operation ..... 3
- Thermal-Neutron Absorption Cross Section of $Pu^{240}$ ..... 4
- Apparent "Solubility" of Fission Products in the Homogeneous Reactor ..... 4

ISOLATION AND CHEMICAL PROPERTIES OF SYNTHETIC ELEMENTS ..... 5

- Chemistry of Technetium ..... 5
  - Solvent Extraction of Technetium ..... 5
  - Spectrophotometric Examination of Certain Oxidation States of Technetium and Rhenium ..... 5
- Isolation of Neptunium. Extraction Studies and Flow Plans ..... 7
- Experiments on the Release of Fission Products from Molten Reactor Fuels ..... 8
  - Particle-Forming Fission Elements Released from APPR Fuel Plate Melted in Air ..... 8

CHEMICAL SEPARATION OF ISOTOPES ..... 10

- Lithium Isotope Separation by Ion Exchange Chromatography ..... 10
- Separation of Boron Isotopes ..... 10
- Oxygen Isotope Fractionation Studies ..... 12
- Separation of $N^{15}$ ..... 12
  - Separation Factor Measurements ..... 12
  - Production of $N^{15}$ ..... 13
- Enrichment of $C^{13}$ ..... 13
- Enrichment of Sulfur Isotopes ..... 13
- Infrared and Raman Spectra of Isotopic Molecules ..... 14
  - Infrared Spectra of the Isotopic Nitrous Oxides ..... 14
  - Infrared Studies of NOCl ..... 15
  - Raman Studies of Metal-Ammonia Complexes ..... 17
  - Infrared Spectrum of $BF_3$ ..... 17

RADIATION CHEMISTRY ..... 18

- Effect of Ionizing Radiation on Catalysts ..... 18
- Radiolysis of Carbon Monoxide by Alpha Particles ..... 18
- Radiolysis of Biphenyl by Alpha Particles from Radon ..... 20
- Effects of Solutes on the "Molecular" Yields ($H_2$ and $H_2O_2$) in the Decomposition of Water by Gamma Rays ..... 21
  - Effect of Sodium Nitrate Concentration on $H_2$ Yield ..... 21
  - The Activity Coefficient in Radiation Chemistry ..... 21
  - Effect of pH on "Molecular" Hydrogen Yield ..... 21
  - Effect of Sodium Sulfate Concentration on Hydrogen Yield ..... 22

Comparison of the Effect of KBr on the Molecular Peroxide Yield in Light and Heavy Water ..... 22
Radiation-Induced Reaction of Redox Couples ..... 22
Radiation-Induced Reaction of Fe(III) and Sn(II) ..... 22
Radiation-Induced Reaction of As(III) with Ce(IV) ..... 22
Kinetics of the Radiation-Induced Reduction of Ce(IV) in Solutions Containing Ce(IV), Ce(III), $H_2$, and $H_2SO_4$ ..... 23
Chemical Features of the Fixation of Nitrogen by Irradiation of Moist Air ..... 23

ORGANIC CHEMISTRY ..... 24

The Pinacol Rearrangement ..... 24
The Phenyl-di-*p*-tolyl System ..... 24
The 1,2-Diphenyl-1-*o*-tolyl System ..... 24
Analysis of Kinetic Rate Data by Means of the Oracle ..... 25
Stereochemistry of the Deamination of 1,2,2-Triphenylethylamine ..... 27
Optical Configuration of (+)-1,2,2-Triphenylethylamine and (+)-1,2,2-Triphenylethanol ..... 28
Chemical Methods ..... 28
Physical Methods ..... 28
Determination of Active Hydrogen by Means of Tritium Exchange ..... 29
Reduction of Triphenylacetonitrile by the $\alpha$-Hydrogen Atom of Benzylmagnesium Chloride ..... 29
Reaction of Cyanogen with Arylmethylmagnesium Halide ..... 30
The Carbon Isotope Effect in the Pinacol-Pinacolone Rearrangement: A Reinvestigation ..... 31
Isotopic Studies of the Decarbonylation of Carboxylic Acids in Concentrated Sulfuric Acid ..... 32
Exchange of Carbon Monoxide-$O^{18}$ with 96% Sulfuric Acid ..... 33
Mass Spectrometric Studies of Labeled Formic Acids ..... 34
Detection of Cyanide ($CN^-$) in a Mixture of Formic Acid and Nitrogen in a Research Mass Spectrometer ..... 34
Extraction of Tributyl Phosphate from Nonpolar Solvents ..... 35
Effects of Electrolytes and Temperature on the Solubility of Tributyl Phosphate in Water ..... 36
Distribution of Monovalent Electrolytes Between Water and Tributyl Phosphate ..... 36
Dispersion of Thorium Dioxide in Nonpolar Solvents ..... 36
Determination of Equivalent Weight and of Esters and Halides with Cation Exchange Resins ..... 37

CHEMISTRY OF AQUEOUS SYSTEMS ..... 38

Physical Chemistry of Ion Exchangers ..... 38
Properties of a New Strong-Base Anion Exchanger Containing Structurally Bound Tertiary Sulfonium Cations ..... 38
Equilibrium Measurements with Cation and Anion Exchangers of Variable Capacity ..... 38
Model Studies of Ion Exchange Mechanisms with Liquid Ion Exchangers ..... 38
Calorimetric Measurements of the Heats of Cation Exchange ..... 39
Calorimetric Measurements of the Heats of Anion Exchange ..... 39
Temperature Dependence of the Solubility of Silver Sulfate in Various Electrolyte Media ..... 40
Liquid-Phase Spectrophotometry at Elevated Temperatures and Pressures ..... 43
The pH of $UO_2SO_4$ Solutions as a Function of Temperature and Concentration ..... 45
Observations on the Phase Behavior of the System $UO_2SO_4$-$CuSO_4$-$H_2SO_4$-$H_2O$ at Elevated Temperatures ..... 46

Calculations of Solubility in Multicomponent Systems from Solubilities in Simpler Systems ..... 47
Solubility Equilibrium in the System $NiO-SO_3-H_2O$ at High Temperature ..... 49
Measurement of Aqueous Vapor Pressure at Elevated Temperature and Pressure ..... 51
Equilibrium Compositions of the Light and Heavy Liquid Phases in the System $UO_3-SO_3-H_2O$ ..... 52
Homogeneous Catalysis of the Oxidation of Dissolved Hydrogen ..... 52
Decomposition of Peroxide in Aqueous Solutions ..... 53
pH Measurements of $ThO_2$ Slurries ..... 54
Dispersions of Thorium Oxide ..... 56
Ultracentrifugation and Light-Scattering Studies of Inorganic Polymerization ..... 56
Adsorption on Inorganic Materials ..... 58
Adsorption of $SO_2$ by Hydrous Oxides ..... 58
Anion Exchange Studies ..... 58
Temperature Dependence of Ion Exchange Equilibra ..... 60
Solubility of Silver Chloride in the Temperature Range 25 to 200°C ..... 63

CHEMISTRY OF CORROSION ..... 64

Studies on Inhibition ..... 64
Kinetic Studies on Corrosion Systems ..... 65
Kinetics of the Reduction of Uranyl Ion ..... 65
Measurement of Differential Capacity ..... 67
Electrochemistry of Zirconium ..... 69

NONAQUEOUS SYSTEMS AT HIGH TEMPERATURES ..... 72

Heterogeneous Isotopic Exchange Reactions of Fluorine-Containing Compounds ..... 72
Self-Diffusion in Molten Salts ..... 72
Molten Salt–Metal Solutions ..... 73
Phase Equilibria ..... 73
Electrical Conductivity of Solutions of Sodium and Potassium Metals in Their Molten Iodides ..... 75
Thermodynamics of Dilute Solutions of $AgNO_3$ and KCl in Molten $KNO_3$ from EMF Measurements ..... 76
Solubilities of Noble Gases in Molten Fluoride Mixtures ..... 77
A Simple Method for the Estimation of Gas Solubilities ..... 79
Solubility of HF in Molten $NaF-ZrF_4$ Mixtures ..... 81
Solubility Relations Among Some Fission Product Fluorides in Molten Fluoride Mixtures ..... 82
Vapor Pressure Measurements on Molten Fluorides ..... 84
Solubility and Stability of $PuF_3$ in Molten Alkali Fluoride–Beryllium Fluoride Mixtures ..... 85
Phase Behavior in Fluoride Systems ..... 86

CHEMICAL PHYSICS ..... 89

Microwave and Radio-Frequency Spectroscopy ..... 89
Hydrogen Gas and Atomic Hydrogen Yields from Irradiated Acids ..... 89
Effect of Environmental Nuclei in Electron Spin Resonance Spectroscopy ..... 89
Paramagnetic Resonance Studies of Liquids During Intense Irradiation ..... 89
Paramagnetic Resonance Studies of Methanol and Ethanol Irradiated at 77°K ..... 90
Neutron and X-Ray Diffraction Studies ..... 90
Single-Crystal Neutron Diffraction Study of Hydrogen Peroxide ..... 90
Computer Program To Process the Results of Crystal Structure Refinements ..... 91

Determination of the Principal Axes of the Anisotropic Temperature Factor ..... 91
Structure of Acetylglycine ..... 92
Crystal Structure of Potassium Hydrogen Maleate ..... 92
Diffraction Studies of Liquids ..... 94
Crystal Phase Transformations by Mechanical Deformation (Grinding) ..... 95
Bent-Crystal Monochromator for Single-Crystal X-Ray Diffraction Studies ..... 95
Cell Size of Dimethyl-$\gamma$-Pyrone ..... 95
Calorimetry ..... 95
Low-Temperature Heat Capacity Calorimeter ..... 95
High-Temperature Heat Content Calorimeter ..... 96
Molecular and Ionic Beam Studies in Chemical Kinetics ..... 96
Thermal Emission of Alkali Positive Ion Pulses from Clean and Oxygenated Tungsten ..... 97
Determination of Vapor Densities of Alkali Halide Salts ..... 97
Dissociation of $C_6H_5T$ Following Beta Decay ..... 97
Mass Spectrometry and Related Techniques ..... 98
Research Mass Spectrometers ..... 98
Dissociation of Ions of Formic Acid and Deuteroformic Acids by Ion-Molecule Collision ..... 98
Bimolecular, Ion-Molecule Reactions of Aliphatic Acids and of Deuteroaliphatic Acids ..... 99
Charge Permutation of Ion-Molecule Collision ..... 100
Mass Spectrometric Observations of Triatomic Ions in Chlorine and Bromine Gases ..... 101

PUBLICATIONS ..... 103

PAPERS PRESENTED AT SCIENTIFIC AND TECHNICAL MEETINGS ..... 107

# NUCLEAR CHEMISTRY

## POLARIZATION OF $P^{32}$ ELECTRONS

B. H. Ketelle A. R. Brosi

As a consequence of the nonconservation of parity, it follows that beta decay electrons are polarized with respect to the direction in which they are emitted. The polarization of beta particles has been confirmed in several experiments, but none have shown whether the degree of polarization is accurately equal to $-v/c$, as predicted by theory, where $v$ is the electron velocity, and $c$ is the velocity of light.

In the present experiment the electrons from the beta decay of $P^{32}$ are bent through an angle of 136 deg, with the electric field in a 1-cm gap between two spherical aluminum plates which have a mean radius of 25 cm. This converts the longitudinal spin of the electrons into a transverse spin. The transverse polarization of the electron beam is then measured by observing the asymmetry in Mott scattering from a thin gold foil.

Because of the large losses in intensity in the electrostatic spectrometer and in the scattering process, it is necessary to work with sources containing hundreds of millicuries of $P^{32}$. For proper focusing of the beam the source must be small, and for prevention of scattering in the source the $P^{32}$ must have a very high specific activity.

Techniques have been developed for the preparation of high-specific-activity $P^{32}$ in cooperation with the Operations Division. Sources approximately 1 mm in diameter which contain about 0.5 curie of $P^{32}$ have been prepared. Because the $P^{32}$ sources have been slightly volatile it has been necessary to seal them from the rest of the spectrometer and let the electron beam pass through a thin plastic window.

Although a large asymmetry is observed in the Mott scattering, the polarization computed from the scattering data has never been as large as $-v/c$, the value predicted by theory. The deviations are much larger than the standard deviations of the measurements. At present several experimental factors which would tend to reduce the polarization are being studied.

This work is being done in cooperation with H. B. Willard and A. Galonsky of the Physics Division.

## LIFETIMES OF ENERGY LEVELS POPULATED BY ELECTRON CAPTURE

H. C. Thomas B. H. Ketelle
A. R. Brosi

A "fast-slow" coincidence assembly has been developed for the measurement of lifetimes of energy levels populated by electron-capture decay or by gamma-ray emission. Used in the assembly are thallium-activated NaI crystals mounted on 14-stage 6810A RCA photomultiplier tubes as radiation detectors. The photomultipliers are operated at a voltage high enough so that the coincidence circuit is triggered by the first electron from the photocathode. The coincidence resolving time depends on the average time of arrival of the first photoelectron, which to a first approximation is inversely proportional to the energy of the radiation and directly proportional to the lifetime of the scintillator light pulse. Because NaI scintillators have a much longer decay time than organic scintillators (250 vs about 10 m$\mu$sec), NaI detectors have not been used in fast-coincidence work even though they offer decided advantages from the standpoint of energy resolution.

In preliminary work the $1.5 \times 10^{-9}$-sec half life of the 166-kev level in $La^{139}$ formed by electron capture in $Ce^{139}$ was measured. The lifetime of this level when formed by beta decay of $Ba^{139}$ had been measured previously by other workers using organic scintillators. This work with $Ce^{139}$ showed that level half lives in the millimicrosecond region could be measured with NaI detectors when the formation of the level was announced by radiation as soft as the 33-kev lanthanum $K$ x ray.

The half life of the 61-kev level in $Pm^{145}$, which is populated by electron capture in $Sm^{145}$, was found to be $2.6 \times 10^{-9}$ sec. The 67-kev level in $Nd^{145}$ was found to have a half life of $3.3 \times 10^{-8}$ sec. The half life of the 72-kev level in $Nd^{145}$ and that of the 57-kev level in $Tb^{159}$ were too short to measure with the present equipment. An attempt is being made to reduce the coincidence resolving time by using smaller NaI crystals on photomultiplier tubes which have smaller transit time spreads.

## CHARACTERIZATION OF SHORT-LIVED FISSION PRODUCTS

### Nuclear Spectra of $Tc^{100}$[1]

G. D. O'Kelley E. Eichler
N. R. Johnson

The gamma-ray spectrum of 16-sec $Tc^{100}$ observed with a scintillation spectrometer exhibits an intense double peak with components of energies of 0.542 ± 0.006 and 0.600 ± 0.009 Mev. Less intense gamma rays of 0.71, 0.81, 0.89, 1.01, 1.14, 1.31, 1.49, and 1.8 Mev, as well as unresolved low-energy components, are also present. The 0.542-Mev gamma ray, which represents the decay from the first excited level of $Ru^{100}$, is coincident with the 0.600-Mev gamma ray, and thus an excited state at 1.14 Mev is established.

Scintillation beta-ray spectra were resolved into components of 3.38 ± 0.06 and 2.88 ± 0.07 Mev, which decay to the ground and the first excited states of $Ru^{100}$, respectively. A beta-ray group of about 2.2 Mev is in coincidence with the double gamma-ray peak at the 0.542-0.600-Mev level, as expected for the beta rays feeding the 1.14-Mev level of $Ru^{100}$.

### Production of $Ga^{74}$[2]

E. Eichler N. R. Johnson
G. D. O'Kelley

Irradiations of germanium metal containing 97.7% $Ge^{74}$ with 14-Mev neutrons from the fast-neutron facility at the Biology Division produced a nuclide with a half life of 7.8 ± 0.2 min. This nuclide has been assigned to $Ga^{74}$ because it follows the chemistry of gallium and because its beta decay excites the well-known first excited state of $Ge^{74}$ at 0.60 Mev. As a final confirmation, samples of natural germanium (36.5% $Ge^{74}$) and germanium enriched to 97.7% in $Ge^{74}$ were irradiated in the same neutron flux, and the yield of the 8-min activity was proportional to the isotopic enrichment. Preliminary gamma-ray spectra measured with a 3 × 3 in. NaI crystal spectrometer showed intense gamma rays with energies of 0.60 and 2.3 Mev, as well as weak transitions of 0.30, 0.50, 0.88, 1.1, 1.5, 1.9, and 2.8 Mev. The beta-ray spectrum observed with an anthracene scintillation spectrometer was resolved into three groups with end points at 2.65 ± 0.05, 2.0 ± 0.1, and 1.1 ± 0.1 Mev.

### Radiations from $I^{136}$[3]

N. R. Johnson G. D. O'Kelley

The radiations emitted by 86-sec $I^{136}$ have been studied with single-crystal and coincidence scintillation spectrometers. The spectrum obtained with a 3 × 3 in. NaI crystal showed gamma rays with energies of 3.18, 2.84, 2.63, 2.40, 2.25, 1.89, 1.72, 1.55, 1.321, 1.00, 0.75, 0.53, 0.46, 0.39, 0.27, and 0.20 Mev. Of these, the 1.32-Mev gamma ray was the most intense.

Scintillation spectrometer measurements with an anthracene crystal revealed two high-energy beta rays with energies of 5.62 ± 0.15 and 7.00 ± 0.10 Mev. In coincidence with the 1.32-Mev gamma ray were beta rays of 5.60 ± 0.15 and 4.23 ± 0.20 Mev and possibly a third component at about 2.7 Mev. Also coincident with the prominent 1.32-Mev gamma ray were gamma rays of 0.20, 0.27, 0.39, 0.46, 0.53, 0.75, 1.00, 1.32, 1.55, and 1.72 Mev, and a diffuse distribution at about 2.0 Mev. The above data, disagreeing somewhat with those of earlier experiments,[4] indicate that the first two excited states in $Xe^{136}$ are at 1.32 and 2.64 Mev, with a pair of 1.32-Mev gamma rays involved in the cascade process. A partial decay scheme consistent with the above observations has been formulated.

### Nuclear Spectra of $Rb^{90}$[5]

N. R. Johnson G. D. O'Kelley
E. Eichler

Extensions of both the single-crystal scintillation counter and coincidence rate measurements previously reported[6] on 2.9-min $Rb^{90}$ have been

[1] G. D. O'Kelley, E. Eichler, and N. R. Johnson, *Bull. Am. Phys. Soc.* 3, 62 (1958).

[2] E. Eichler, N. R. Johnson, and G. D. O'Kelley, *Bull. Am. Phys. Soc.* 3, 62 (1958).

[3] N. R. Johnson and G. D. O'Kelley, *Bull. Am. Phys. Soc.* 3, 63 (1958).

[4] M. McKeown and S. Katcoff, *Phys. Rev.* 94, 965 (1954).

[5] N. R. Johnson, G. D. O'Kelley, and E. Eichler, *Bull. Am. Phys. Soc.* 3, 207 (1958).

[6] G. D. O'Kelley and N. R. Johnson, Jr., *Chem. Semiann. Prog. Rep. June 20, 1956*, ORNL-2159, p 8.

made by using a Radiation Counter Lab. 256-channel pulse-height analyzer. The spectrum obtained with a single 3 × 3 in. NaI crystal spectrometer of improved resolution (7.6% at 0.662 Mev) was analyzed into gamma-ray components of 0.52, 0.72, 0.833, 1.00, 1.10, 1.23, 1.39, 1.68, 1.81, 2.15, 2.51, 2.73, 2.85, 3.05, 3.34, 4.12, 4.34, 4.60, 5.08, and 5.23 Mev. In coincidence with the intense 0.84-Mev gamma-ray transition were gamma rays at 0.52, 0.72, 0.87, 1.05, 1.11, 1.24, 1.41, 1.71, 1.82, 2.20, 2.51, 2.70, 2.83, 3.35, 3.56, and 4.4 Mev. Gamma rays at 0.5, 0.836, and 1.06 Mev appeared in coincidence with the 3.34-Mev gamma ray.

The most energetic beta ray had an end point at 6.59 ± 0.15 Mev. Beta rays at 5.81 ± 0.10 and 4.4 Mev were in coincidence with the 0.84-Mev gamma-ray transition. With the window of the pulse-height selector set on the 5.23-Mev gamma-ray peak, a coincident beta group at 1.2 Mev was observed; when the window was set to trigger on all gamma rays greater than 3.8 Mev, the beta ray in coincidence had an end-point energy of 2.21 ± 0.08 Mev.

Measurements with an end-window proportional counter and with a $4\pi$ beta counter gave a half life for $Rb^{90}$ of 2.90 ± 0.09 min. The number of 0.84-Mev gamma rays per beta disintegration was found to be 0.61.

It has been possible to formulate a partial decay scheme from the above data.

### Nuclear Structure of $Zr^{90}$[7]

G. D. O'Kelley J. H. Hamilton[9]
N. H. Lazar[8] L. M. Langer[9]
W. G. Smith[9]

The early measurements[10] of the energy levels of $Zr^{90}$ excited by the decay of 14.6-hr $Nb^{90}$ have been extended. Beta- and gamma-ray spectroscopy, utilizing both single and coincident NaI(Tl) crystals and a magnetic spectrometer, were used. The positron spectrum was resolved into components of 1.505 and 0.655 Mev; the internal-conversion electron spectrum was obtained, from which gamma-ray transitions of 0.132, 0.141, 0.372, 1.13, and 2.34 Mev were determined. The internal-conversion electron spectrum characteristic of the 1.76-Mev monopole transition in $Zr^{90}$ was also seen. The scintillation gamma-ray spectrum was resolved into components of 2.32, 2.19, 2.0, 1.85, 1.60, 1.48, 1.27, 1.13, 1.1, 0.89, 0.372, (0.43), 0.142, and 0.133 Mev.

Based on these data, a level scheme for $Zr^{90}$ was formulated with excited states at 1.76 (0+), 2.19 (2+), 2.32 (5–), 3.08 (4+), 3.45 (6+), 3.59 (8+), 4.44, 5.05, and 5.45 Mev, which may be understood qualitatively in terms of an independent-particle model.

### A REVIEW OF SOME NEUTRON ABSORPTION CROSS SECTIONS OF INTEREST TO REACTOR OPERATION[11]

R. W. Stoughton J. Halperin

Cross-section values often have been reported by different investigators which differ by a factor of 2 or more when the estimated errors indicated much greater accuracy. An analysis of some of the problems which give rise to such inconsistencies was carried out. The choice of flux conventions and of methods of monitoring and the use of imprecise definitions were shown to make substantial differences in reported cross sections.

With the use of a consistent convention and with an adequately precise definition of terms, a review was made of some cross sections of particular interest to thermal reactors.

The results preferred by the authors are shown in Table 1. Here $\sigma_0$ is the 2200-m/s cross section, $I_0$ is the resonance integral above the cadmium cutoff, and $g$ is a factor correcting for any non-$1/v$ dependence in the thermal range. The symbols $g\sigma_0$ and $\sigma_{eff}$ are defined by the equation for the reaction rate per atom, $R$, in a thermal reactor in terms of the thermal flux $\phi_{th}$ and the resonance flux per unit ln $E$, $\phi_r$:

$$R = \phi_{th}\sigma_{eff} = \phi_{th} g\sigma_0 + \phi_r I_0 \ .$$

---

[7] N. H. Lazar *et al.*, *Phys. Rev.* 110, 513–19 (1958).

[8] Physics Division, now of the Thermonuclear Experimental Division.

[9] Indiana University, Bloomington.

[10] G. D. O'Kelley and N. H. Lazar, *Chem. Semiann. Prog. Rep. June 20, 1956*, ORNL-2159, p 9.

[11] To be published as a paper for the Geneva Meeting in September 1958.

Table 1. Preferred Values of Heavy-Nuclide Cross Sections

| Nuclide | Process[a] | $\sigma_0$ (barns) | $g\sigma_0$ (barns) | $I_0$ (barns) | $\sigma_{eff}$[b] (barns) |
|---|---|---|---|---|---|
| $Th^{233}$ | c | (1350 ± 150) | 1350 ± 150 | 450 ± 150 | 1400 ± 150 |
| $Pa^{233}$ | c | (80 ± 20) | 80 ± 20 | 700 ± 200 | 140 ± 20 |
| $U^{233}$ | c | 55 ± 10 | 50 ± 10 | 100 ± 40 | 55 ± 15 |
| | abs | 590 ± 20 | 590 ± 30 | 1000 ± 200 | 670 ± 50 |
| $U^{234}$ | c | 95 ± 10 | 95 ± 10 | 700 ± 70 | 150 ± 15 |
| $U^{236}$ | c | 6 ± 2 | 6 ± 2 | 400 ± 50 | 38 ± 10 |
| $U^{238}$ | c | 2.75 ± 0.05 | 2.75 ± 0.05 | 280 ± 10 | 26 ± 3 |
| $Pu^{239}$ | c | 300 ± 20 | 340 ± 20 | 1500 ± 300[c] | 500 ± 80 |
| | abs | 1030 ± 30 | 1100 ± 30 | 3600 ± 1000[c] | 1400 ± 200 |
| $Pu^{240}$ | c | 290 ± 30 | 320 ± 30 | 9000 ± 1000 | 1100 ± 150 |

[a] c and abs represent capture and absorption, respectively.
[b] Values of $\sigma_{eff}$ are for $\phi_r/\phi_{th} = 1/12$.
[c] These values are for the resonance integral $I_0'$, with a lower limit of 0.15 ev.

## THERMAL-NEUTRON ABSORPTION CROSS SECTION OF $Pu^{240}$[12]

J. Halperin H. S. Pomerance[13]
J. O. Oliver[14]

A remeasurement of the thermal cross section of $Pu^{240}$ was made by use of the pile oscillator method with more highly enriched samples of $Pu^{240}$ than hitherto had been available (92.19% $Pu^{240}$). The $Pu^{240}$ and isotopically pure $Pu^{239}$ samples were compared with thin gold foils of almost equal response, so that only minor interpolations were necessary. The $Pu^{240}$ gave a response 2.94 times that of gold. On the basis that $\sigma_{2200}(Au) = 99$ barns, that the 1.055-ev resonance in $Pu^{240}$ has a neutron width $\Gamma_n = 2.24 \times 10^{-3}$ ev and a radiation width $\Gamma_\gamma = 37 \times 10^{-3}$ ev, that the neutron spectrum has a Maxwellian temperature of 450°C, and that the ratio of resonance to thermal flux is about 0.001, it is computed that $\sigma_{2200}(Pu^{240}) = 280 \pm 20$ barns.

[12] To be published in *J. Inorg. & Nuclear Chem.*

[13] Education Division.

[14] Analytical Chemistry Division.

## APPARENT "SOLUBILITY" OF FISSION PRODUCTS IN THE HOMOGENEOUS REACTOR

J. Halperin R. W. Stoughton
J. O. Oliver[14]

During the operation of HRE-2, in runs 13 and 14, a number of radiochemical analyses were carried out on 12 fission products: $Sr^{89}$, $Y^{91}$, $Zr^{95}$, $Mo^{99}$, $Ru^{103}$, $I^{131}$, $Te^{132}$, $Cs^{136,137}$, $Ba^{140}$, $Ce^{144}$, and $Nd^{147}$, as well as on $Np^{239}$, $U^{237}$, $S^{35}$, $Cu^{63}$, and $P^{32}$. The amount of each nuclide found analytically was compared with that expected on the basis of the number of fissions that had taken place as measured by $Cs^{137}$ activity and the history of reactor power. In general the results were in agreement with the observations made in the in-pile loops and reported previously.[15]

[15] J. Halperin, J. O. Oliver, and R. W. Stoughton, *Chem. Ann. Prog. Rep. June 20, 1957*, ORNL-2386, p 12.

# ISOLATION AND CHEMICAL PROPERTIES OF SYNTHETIC ELEMENTS

## CHEMISTRY OF TECHNETIUM

### Solvent Extraction of Technetium[1]

G. E. Boyd Q. V. Larson

The extraction of pertechnetate ion, $TcO_4^-$, contained in acid, neutral salt, and alkaline aqueous solutions was measured by using a wide variety (70) of immiscible organic liquids. These liquids included alcohols, ketones, ethers, esters, nitro compounds, nitriles, amines, hydrocarbons, and chlorocarbons, and also organophosphorus and organonitrogen compounds dissolved in nonpolar liquids.

The presence of a donor group in the organic molecule (containing either a basic oxygen or nitrogen) was necessary to obtain extraction. Steric effects and the dielectric constant of the organic liquid were of less importance. Interesting correlations of the extraction coefficient, $E_a^o$, with the oxygen-to-carbon ratio of the molecule were found for the alcohols, ketones, and ethers. Further variations of this ratio also could be effected by using solutions of alcohol or ketone in an *n*-hydrocarbon; extraction was apparently governed by the molarity of the donor group. A linear dependence of log $E_a^o$ on donor group molarity was found; at equal concentrations ketones are superior to alcohols as extractants. Comparisons of 0.1 *M* solutions of tri-*n*-octylphosphine oxide, tri-*n*-octylamine, cyclohexanone, cyclohexanol, and $\beta,\beta'$-dichlorodiethyl ether in cyclohexane show that the organophosphorus compound and the tertiary amine are vastly more efficient extractants than either the alcohol or the ketone. Measurements of the extraction of Tc(VII) and of acid by cyclohexanol from 1 *N* aqueous $H_3PO_4$, $H_2SO_4$, HCl, HBr, $HNO_3$, HI, and $HClO_4$ solutions showed that the extraction of technetium diminished as the extraction of acid increased.

Extraction from acid solutions appeared to depend on "onium" salt formation in the organic phase, where a competition occurred between the $TcO_4^-$ ion and the anion of the acid. The concentration of "onium" salt in the organic phase appeared to depend on the basicity of the donor molecule and on the activity of the hydrogen ion in the aqueous phase. The assumption of an acid-base in addition to an anion exchange equilibrium sufficed as an explanation of the occurrence of a maximum in the variation of $E_a^o$ with increasing acid concentration.

An examination of the extraction mechanism, which is of interest because $TcO_4^-$ is a member of the important class $MX_4^-$ of complex ions, was carried out by systematic studies of the dependence of the extraction coefficient, $E_a^o$, on acid concentration, salt concentration, pertechnetate ion concentration, the composition of the organic phase, and the temperature. The heat of extraction of $TcO_4^-$ from 1 *N* $H_2SO_4$, derived from the temperature variation of $E_a^o$ between 0 and 35°C, was −5.8 kcal/mole, while a larger, variable heat was found by using trioctylphosphine oxide solutions in an aliphatic hydrocarbon.

### Spectrophotometric Examination of Certain Oxidation States of Technetium and Rhenium[2]

R. H. Busey Q. V. Larson

A spectrophotometric examination of several compounds or oxidation states of technetium and rhenium in solution was made as a preliminary in the study of the oxidation states of technetium. The method of study consisted in preparing certain compounds, observing their spectra in various solvents, and observing the action of redox reagents upon the compounds in solution.

**$KTcO_4$.** – Potassium pertechnetate was found to undergo a reversible color change on heating, the color changing from white to a canary yellow. The color is evident around 200°C and becomes brilliant yellow at 500°C. The $KTcO_4$ may be fused (at about 540°C) and sublimed (at about 1000°C) without any apparent decomposition. For $KTcO_4$ in aqueous solution the ratio of the 2460-Å maximum to the 2880 maximum is 2.63, a value believed to be accurate to a few tenths of a per cent and

[1] G. E. Boyd and Q. V. Larson, *Abstracts of Papers, 133rd National Meeting of the American Chemical Society, San Francisco, April 13–18, 1958*, paper 150, p 61Q.

[2] R. H. Busey and Q. V. Larson, *Abstracts of Papers, 133rd National Meeting of the American Chemical Society, San Francisco, April 13–18, 1958*, paper 72, p 30L.

to be a valuable aid in determining the purity of a $TcO_4^-$ solution.

**$K_2TcCl_6$, $K_2TcBr_6$, $K_2TcI_6$, and $K_2ReCl_6$, $K_2ReBr_6$, $K_2ReI_6$.** – The following is a comparison of the spectra and the stability of these compounds (IV oxidation state) in hydrochloric, hydrobromic, and hydriodic acid solutions. In 1 *M* HCl, $K_2ReCl_6$ is stable but $K_2TcCl_6$ is not, the latter apparently undergoing hydrolysis; the spectrum of the $TcCl_6^{--}$ ion is similar to that of $ReCl_6^{--}$, with the absorption maximum shifted toward longer wavelengths. The spectra of the bromide compounds are not similar, and both compounds are stable in 6 *M* HBr solution. Both the $ReI_6^{--}$ and $TcI_6^{--}$ ions are unstable in concentrated HI, the latter being the more unstable. The $ReI_6^{--}$ spectrum exhibits an unusual number (12) of absorption maxima from 3000 to 8000 Å. All the above compounds show very intense absorption bands in the ultraviolet region; for example, the molar absorbancy index of $K_2ReBr_6$ at 2180 Å is 21,900.

Similar to $K_2ReI_6$ (ref 3) in 2 *M* $H_2SO_4$, technetium is extracted by ether from a solution of $K_2TcI_6$ in 2 *M* $H_2SO_4$. Although the ether phase for both compounds is very unstable, the stability may be increased by maintaining the solutions at 0°C.

**$ReCl_3$ in 12 *M* HCl and in Acetone.** – Chloride ion is necessary to stabilize the Re(III) oxidation state, undoubtedly by formation of $ReCl_4^-$ ions with a $dsp^2$ square-planar or $sp^3$ or $d^3s$ tetrahedral structure. The spectra of the compound in 12 *M* HCl and in acetone are very similar, leading to the hypothesis that the $ReCl_3$ in acetone, as in glacial acetic acid,[4] is dimerized to $Re_2Cl_6$, which would also have the square-planar or tetrahedral structure.

**$TcO_3Cl$, $ReO_3Cl$, and $ReO_3Br$.** – These compounds were prepared in 18 *M* $H_2SO_4$ and were found to be extractable with $CCl_4$, $CHCl_3$, or $C_6H_{14}$. By the method of continuous variations, a second species with two chlorides per metal atom has been shown to exist in 18 *M* $H_2SO_4$ in addition to the single-chloride species. Extraction data clearly show, however, that it is the monochloride species that is extracted by the organic phase. The spectra of these compounds show unusual detail of vibrational fine structure superimposed on the electronic absorption bands, especially in the organic phase. In the ultraviolet spectrum of $ReO_3Cl$, for example, eight vibrational bands are discernible, six of which show distinct maxima. Equal energy separations of the vibrational bands for both $ReO_3Cl$ and $ReO_3Br$ indicate that the vibration arises from the symmetric spinning top, $ReO_3$. The 900-$cm^{-1}$ separation of the fine structure bands indicates that an absorption band in the infrared spectrum at 11 $\mu$ should be observed. The infrared spectrum[5] of gaseous $ReO_3Cl$ does show a single absorption band at 10.5 $\mu$.

**Re(VI) in 18 *M* $H_2SO_4$.** – A spectrophotometric titration of $KReO_4$ in 18 *M* $H_2SO_4$ with $SnSO_4$ clearly demonstrates the existence of Re(VI) in this medium. The absorption does not follow Beer's law, and, in addition, the deviation is not the same over the visible wavelength range, indicating that the absorption is due to more than one species. Curves of the optical density at selected wavelengths vs the number of equivalents of $Sn^{++}$ per mole of Re do not show a sharp change in slope at a ratio of unity [maximum Re(VI)], which indicates a disproportionation of the Re(VI), probably into Re(V) and Re(VII). Dilution curves of Re(VI) may be interpreted on the basis that the principal Re(VI) species giving rise to the absorption is a dimer which is in equilibrium with a monomer.

With the addition of two equivalents of $SnSO_4$ per mole of Re, Re(V) results, which cannot be further reduced by the $SnSO_4$. The $KTcO_4$ in 18 *M* $H_2SO_4$ reduced with $SnSO_4$ gives no indication of a Tc(VI) or a Tc(V).

**Rhenium(VI) Chloride Complexes in 18 *M* $H_2SO_4$.** – Observation of the spectra of solutions obtained by the controlled addition of $Cl^-$ to Re(VI) in 18 *M* $H_2SO_4$ showed the existence of at least two rhenium(VI) chloride species. The first species formed has a Cl/Re ratio of approximately 5 to 6 and gives an absorption spectrum with an intense band at 5300 Å. Even before this first species is fully developed, a second chloride species begins to form as the Cl/Re ratio is increased. The second species is fully developed at high Cl/Re ratios and exhibits an

[3] W. Biltz, *Z. anorg. u. allgem. Chem.* **234**, 142 (1937).

[4] F. W. Wrigge and W. Biltz, *Z. anorg. u. allgem. Chem.* **228**, 372 (1936).

[5] C. J. Wolf, A. F. Clifford, and W. H. Johnston, *J. Am. Chem. Soc.* **79**, 4257 (1957).

intense absorption band at 4350 Å. This higher chloride complex is extractable from the 18 *M* $H_2SO_4$ with $CCl_4$, in which solution the compound shows an intense, relatively sharp absorption band at 4400 Å with a molar absorbancy index of approximately 4500.

## ISOLATION OF NEPTUNIUM. EXTRACTION STUDIES AND FLOW PLANS

P. M. Lantz W. J. Martin
G. W. Parker

Previous work on the isolation of neptunium has been reported.[6] In one of the reports, ORNL CF-57-8-34, the results of a neptunium material balance study of the nonvolatile residues resulting from the fluorination of depleted $UO_3$ were summarized. The discovery of an existing quantity of neptunium in these residues signified that a continuing source might be developed from it. A paper was presented[7] which summarized the experience in obtaining the first 100 g of neptunium. An additional 115 g was isolated from the Metal Recovery Plant concentrate from an extraction of Diffusion Plant ash. The yield from an improved neptunium-thorium ether-extraction-ion-exchange (NETHIX-1) process was estimated to be 98 to 99%. The flowsheet, which was developed and used for the final isolation of 115 g of $Np^{237}$, is shown in Fig. 1. The greatest difficulty in developing a purification procedure was caused by the nearly hundredfold thorium content relative to the neptunium. For this reason the ethyl ether extraction of Np(VI), following bromate oxidation, was found to be advisable. The procedure in the rest of this flowsheet is similar to earlier work except for the partitioning of neptunium and uranium. Since, in 1 *M* $HNO_3$, hydrogen peroxide reduces Np(VI) only as far as Np(V), it is possible to leave the uranium in the organic phase while the neptunium is being extracted into the aqueous phase.

In order to increase the efficiency of the neptunium production program in the Metal Recovery Plant, a thorium partitioning step was incorporated in the initial fluorination ash extraction process. Because

[6] G. W. Parker, P. M. Lantz, and W. J. Martin, *Chem. Ann. Prog. Rep. June 20, 1957*, ORNL-2386, p 22; G. W. Parker *et al.*, *Chem. Semiann. Prog. Rep. June 20, 1956*, ORNL-2171; P. M. Lantz and G. W. Parker, *Investigation of Paducah Ash and Metal Recovery Waste as a Large Scale Source of Neptunium-237*, ORNL CF-57-8-34 (July 31, 1957).

[7] P. M. Lantz, W. J. Martin, and G. W. Parker, *The Intermediate Scale Production and Isolation of Neptunium and Americium*, paper presented at the XVI International Congress of Pure and Applied Chemistry, Paris, July 18–24, 1957, and to be published in *Progress in Nuclear Energy, Process Chemistry, Series III*, vol II, McGraw-Hill, New York.

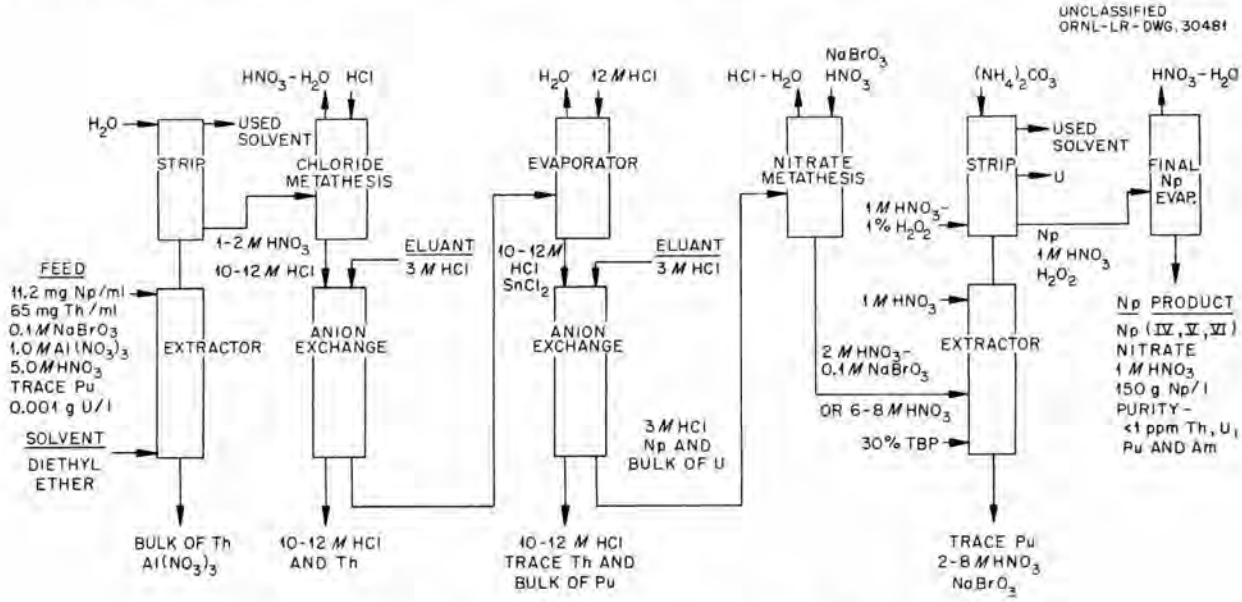


**Fig. 1. Flowsheet for NETHIX-1 Process.**

the bromate oxidation would cause excessive corrosion in stainless steel plant equipment, an alternate process had to be found. This process will be described elsewhere.

## EXPERIMENTS ON THE RELEASE OF FISSION PRODUCTS FROM MOLTEN REACTOR FUELS[8]

G. E. Creek W. J. Martin
G. W. Parker

### Particle-Forming Fission Elements Released from APPR Fuel Plate Melted in Air

Recent work has been directed toward an examination of the melt off-gas or vapor for particle-forming fission products in addition to the volatile components already characterized. Indicated below is the relative probability of finding the most important fission element activities in a radioactive cloud from a meltdown.

| Fission Product | Average Percentage Released |
|---|---|
| $Cs^{137}$ ($\gamma$) | 11.0 |
| $Zr^{95}$ ($\gamma$) | 0.05 |
| $Ce^{144}$ ($\beta$) | 0.008 |
| $Sr^{89,90}$ ($\beta$) | 0.006 |

In this experiment $\frac{3}{8}$-in. disks were punched from APPR stainless steel–$UO_2$ plate after having a 20% burnup irradiation and two years' cooling time.

The values observed for all elements except cesium are so low that they are not clearly different from zero; therefore it was not surprising when a similar result was found in the following experiment: with the use of the inductive-type heating method and an APPR fuel plate containing only long-lived fission products as the source, samples were melted in an air stream which carried the air-borne materials to a series of filters of Millipore and CWS papers. The porosity of the papers selected was such that an efficiency of greater than 99% was expected for particles down to diameters of 0.05 $\mu$.

In all cases the activity collected was found to be pure $Cs^{137}$, and this was essentially completely stopped on the 5-$\mu$ (pore diameter) paper. Table 2 summarizes the results of the collection of cesium on a two-stage filter.

These results were expected because cesium oxide is thermodynamically unstable at the temperature of molten stainless steel and therefore is vaporized as elemental cesium and re-forms the oxide at a lower temperature. Because of the deliquescent character of the cesium hydroxide, measurement of particle size was unsuccessful.

A further experiment has been completed in which the rate of release of cesium from molten APPR stainless steel has been measured for periods up to 10 min (Fig. 2). An approximate half time of 3 to 5 min for vaporization of cesium is indicated, although these samples all released the krypton in less than 30 sec. In some experiments which were also performed in air, the stainless steel pellets burned with incandescence and showed faster as well as more complete release of cesium.

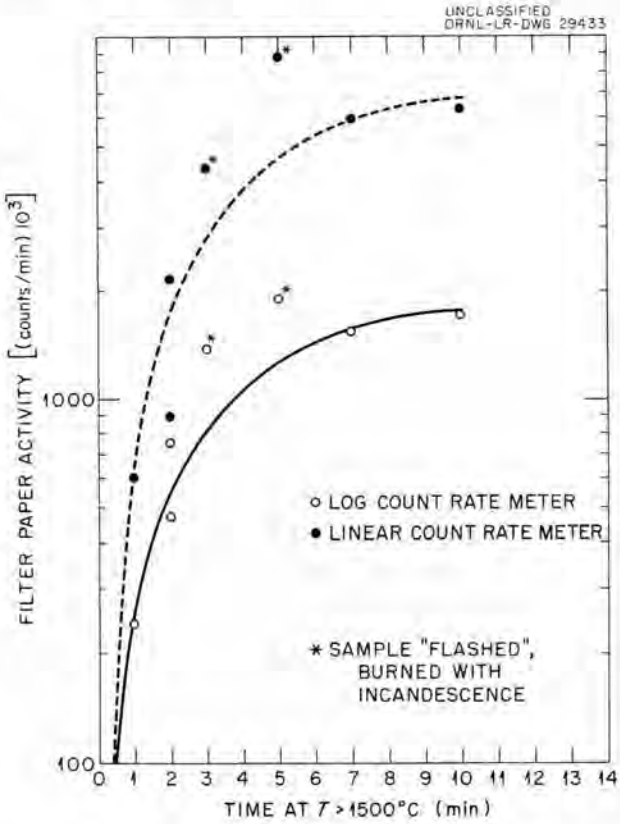


**Fig. 2. Time Dependence of the Release of Cesium from Molten APPR Fuel.**

[8] G. W. Parker and G. E. Creek, in *Reactor Safety Conference, New York City, Oct. 31, 1957*, TID-7549 (Pt. 2), p 32.

Table 2. Filtration of Particulate Cesium from Melted APPR Disks*

| Run No. | First Filter | Second Filter | Ratio of Activity Collected, $\frac{\text{Cs on first}}{\text{Cs on second}}$ |
|---|---|---|---|
| 1 | 0.8 $\mu$ (Millipore) | 0.8 $\mu$ (Millipore) | $5 \times 10^5$ |
| 2 | 5 $\mu$ (Millipore) | 0.8 $\mu$ (Millipore) | $6 \times 10^4$ |
| 3 | 0.3-mm HV-70** | 0.8 $\mu$ (Millipore) | 340 |

*15% burnup.

**Mineral fiber paper, 0.3-mm thickness.

# CHEMICAL SEPARATION OF ISOTOPES

## LITHIUM ISOTOPE SEPARATION BY ION EXCHANGE CHROMATOGRAPHY

D. A. Lee

Lithium isotope fractionation between aqueous lithium ions and lithium ions on various ion exchange resins was studied. A band elution technique with an ion exchange column was used. The elution curve was determined by lithium flame spectroscopy. From the elution curve the number of theoretical plates was calculated by using Glueckauf's plate theory.[1] Isotopic analyses were made on the lithium samples over the entire eluted lithium band. The single-stage separation factor $\alpha$ was determined from these data according to the method of Glueckauf.[2]

The influence of the degree of cross-linking on the selectivity for lithium isotopes was investigated in two series of experiments in which the sulfonated polystyrene-divinylbenzene copolymers Dowex 50-2x, -4x, -8x, -12x, -16x, and -24x were used. The first series of experiments was made with 4x, 12x, and 24x Dowex 50 and with HCl as eluant. The second series of experiments was performed with 2x, 4x, 8x, and 16x Dowex 50 and with $NH_4Cl$ as eluant. The operating data and the results of these experiments are shown in Table 3. The separation factor increases as the degree of cross-linking increases. This effect can be attributed to the decrease in the amount of hydration of the lithium ion in the resin phase as the cross-linking increases.

Separation factors for two inorganic ion exchangers were measured. Decalso, a hydrated sodium aluminum silicate, produced a single-stage separation factor of $1.003_6$. Zirconium phosphate yielded only a tentative estimate, 1.003, because of experimental and analytical difficulties.

Weakly acidic cation exchange resins were also studied. The ammonium forms of IRC-50 and Duolite CS-100, two carboxylic acid resins, were investigated, with $NH_4Cl$ as eluant. The $\alpha$ for lithium isotopes on IRC-50 was 1.0020 and that on CS-100 was 1.0026. Duolite C-60, a phosphonous cation exchanger, and Duolite C-65, a phosphonic cation exchanger, each produced a separation factor of 1.002.

The alkali metals can be separated on an anion exchange column by using ethylenediaminetetraacetate (EDTA) as a complexing agent.[3] For an evaluation of the isotopic separation potential of such systems, the $LiEDTA^{---}$–Dowex 1 system was studied. The experimental data, listed in Table 3, show that the affinity of lithium isotopes for the resin is reversed; that is, $Li^7$ instead of $Li^6$ concentrates on the resin. The single-stage separation factor was $0.999_5$. The same reversal was noted for $LiEDTA^{---}$ vs lithium ions on Dowex 50. A preliminary estimate of the separation factor is 0.994. Further studies are in progress to confirm this large effect.

## SEPARATION OF BORON ISOTOPES

A. Palko

Studies dealing with the chemical separation of boron isotopes were continued. The automatic Anco pilot plant was operated for several months to determine the extent of solvent decomposition during long periods of operation. In four runs an average decomposition rate of 0.36% of working inventory per day was observed. This amount of solvent loss is well within tolerable limits for a plant producing commercial quantities of enriched boron isotopes.

Boron trifluoride forms addition compounds with many oxygen, nitrogen, and sulfur compounds. However, most of the boron isotope separation studies undertaken thus far have dealt only with reactions involving oxygen-containing boron trifluoride addition compounds. For this reason, studies of isotopic exchange reactions involving thioether complexes of boron trifluoride were initiated. Thioether complexes have the advantage that their melting points are much lower than those of their oxygen analogs. This factor permits the exchange reaction to be carried out at much lower temperatures, where single-stage separation factors

[1] E. Glueckauf, *Trans. Faraday Soc.* **51**, 34–44 (1955).

[2] E. Glueckauf, *Theory of Chromatography. Part XI. Enrichment of Isotopes by Chromatography*, AERE C/R-2448 (Jan. 1958).

[3] F. Nelson, *J. Am. Chem. Soc.* **77**, 813 (1955).

Table 3. Summary of Lithium Isotope Separation on Ion Exchangers

| Resin | Mesh Size | Column Diameter (mm) | Column Height (mm) | Eluant | Flow Rate (cm/sec) | Lithium Loading (mg) | Number of Theoretical Plates | Separation Factor |
|---|---|---|---|---|---|---|---|---|
| Dowex 50-4x | 200–400 | 15 | 650 | 0.1 *N* HCl | $2.3 \times 10^{-3}$ | 16 | 1000 | $1.0009_5$ |
| Dowex 50-12x | 200–400 | 19 | 1100 | 0.3 *N* HCl | $2.0 \times 10^{-3}$ | 176 | 500 | $1.003_0$ |
| Dowex 50-24x | 100–200 | 15 | 650 | 0.3 *N* HCl | $3.4 \times 10^{-3}$ | 87 | 138 | $1.003_8$ |
| Dowex 50-2x | 50–100 | 34 | 492 | 0.25 *N* $NH_4Cl$ | $7.9 \times 10^{-4}$ | 95 | 533 | $1.0005_7$ |
| Dowex 50-4x | 50–100 | 26 | 1498 | 0.25 *N* $NH_4Cl$ | $1.0 \times 10^{-3}$ | 368 | 538 | $1.001_0$ |
| Dowex 50-8x | 50–100 | 34 | 494 | 0.25 *N* $NH_4Cl$ | $8.0 \times 10^{-4}$ | 59 | 637 | $1.001_8$ |
| Dowex 50-16x | 50–100 | 26 | 1485 | 0.25 *N* $NH_4Cl$ | $1.1 \times 10^{-3}$ | 360 | 816 | $1.002_5$ |
| Decalso | 100–200 | 16 | 640 | 0.1 *N* $NH_4Cl$ | $9.7 \times 10^{-4}$ | 29 | 97 | $1.003_6$ |
| Zirconium phosphate | ? (large) | 17 | 1460 | 0.2 *N* $NH_4Cl$ | $9.6 \times 10^{-3}$ | 266 | 47 | 1.003 |
| Duolite CS-100 | 270 | 19 | 1190 | 0.1 *N* $NH_4Cl$, pH 8 | $2.5 \times 10^{-3}$ | 350 | 100 | $1.002_6$ |
| IRC-50 | 100 | 15 | 630 | 0.1 *N* $NH_4Cl$ | $4.9 \times 10^{-3}$ | 120 | 82 | $1.002_0$ |
| Zeo-karb | 80–270 | 15 | 570 | 0.1 *N* $NH_4Cl$ | $1.1 \times 10^{-3}$ | 70 | 72 | $1.002_3$ |
| Duolite C-60 | 100–200 | 12 | 980 | 0.1 *N* $NH_4Cl$ | $1.7 \times 10^{-2}$ | 33 | 33 | 1.002 |
| Duolite C-65 | 100–200 | 10 | 1040 | 0.1 *N* $NH_4Cl$, pH 8 | $4.8 \times 10^{-4}$ | 70 | 130 | 1.002 |
| Dowex 1-10x | 200–400 | 25 | 1210 | 0.1 *M* $(NH_4)_4EDTA$, pH 10 | $1.4 \times 10^{-3}$ | 350 | 108 | $0.999_5$ |
| Dowex 50-8x | 50–100 | 26 | 1531 | 0.1 *M* $(NH_4)_4EDTA$, pH 10 | $1.0 \times 10^{-3}$ | 124 | 129 | $0.994_2$ |

are higher and where solvent decomposition is minimized.

The vapor pressures of various mixtures of *n*-butyl sulfide and $BF_3$ were measured at several temperatures, and the heat of association for the *n*-butyl sulfide–$BF_3$ complex was calculated. Over the composition range between 0.299 and 0.984 mole of $BF_3$ per mole of $Bu_2S$, $\Delta H$ was found to be $-12.76 \pm 0.06$ kcal/mole from $-5$ to $+26°C$.

The temperature variation of the single-stage separation factor for the reaction

$$B^{10}F_3(g) + Bu_2S{\cdot}B^{11}F_3(l) \rightleftharpoons B^{11}F_3(g) + Bu_2S{\cdot}B^{10}F_3(l)$$

was determined from $-20$ to $+28°C$. The method used has been described previously[4] for the $BF_3$-anisole system. These measurements are shown in Fig. 3.

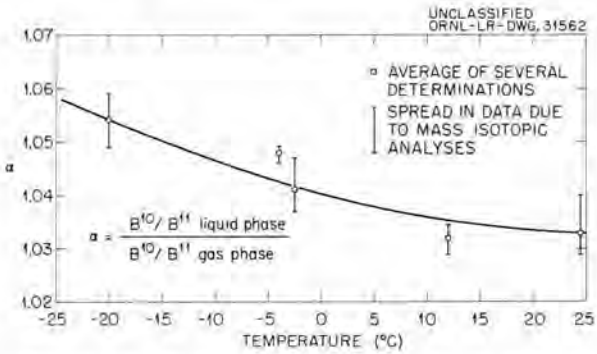


**Fig. 3. Single-Stage Separation Factor vs Temperature for *n*-Butyl Sulfide–$BF_3$ System.**

A similar study for the ethyl sulfide–$BF_3$ system is nearly complete.

## OXYGEN ISOTOPE FRACTIONATION STUDIES

L. L. Brown L. B. Yeatts

The study of chemical exchange reactions suitable for the fractionation of oxygen isotopes was continued. No system was found which is likely to be economically competitive with the water distillation method.

The isotopic separation factor for the exchange reaction

$$Et_2O^{18}(l) + LiBr{\cdot}HgI_2{\cdot}6Et_2O^{16}(l) \rightleftharpoons Et_2O^{16}(l) + LiBr{\cdot}HgI_2{\cdot}6Et_2O^{18}(l)$$

was measured in a multistage batch run and found to be $1.004 \pm 0.004$ (95% C.I.)

From the partition function ratios of Urey[5] and Weston[6] for the oxygen isotopes, a separation factor of 1.022 at 25°C was calculated for the system $NO(g)$ vs $H_2O(l)$, with $O^{18}$ concentrating in the gas phase. Studies made in this laboratory with water labeled with $O^{18}$ indicated no measurable exchange of oxygen atoms between NO and $H_2O$ in a 30-hr period. However, the addition of a small amount of $NO_2$ to the NO-$H_2O$ system should provide a mechanism for rapid exchange of the oxygen atoms in this gas-liquid system without significantly altering the fractionation factor. Experiments designed to measure the separation factor have been performed, but the presence of $O^{16}O^{16}$ interfered with the mass spectrometer measurement of the $N^{14}O^{18}$ species. New measurements are being made with $N^{15}O$ rather than with normal nitric oxide so that interference by oxygen will be eliminated.

## SEPARATION OF $N^{15}$

### Separation Factor Measurements

L. L. Brown

Previous studies of the chemistry of the Nitrox process of enriching $N^{15}$ were made at room temperature.[7] No studies had been made of the temperature dependence of the single-stage separation factor until recently, when the range was extended to 40, 55, and 70°C.

The method used was the same as that previously described for the 25°C work. The resulting nitrogen samples were analyzed in the Chemical Separation of Isotopes Section on the new ratio mass spectrometer. Analyses were obtained

[4] A. A. Palko, R. M. Healy, and L. Landau, *J. Chem. Phys.* **28**, 214–17 (1958).

[5] H. C. Urey, *J. Chem. Soc.* **1947**, 562.

[6] R. Weston, private communication, Nov. 1957.

[7] G. M. Begun *et al.*, *Chemical and Isotopic Studies of the Nitrox System for $N^{15}$ Enrichment*, ORNL-2291 (June 6, 1957).

directly from the instrument in the form

$$\frac{(N^{15}/N^{14})_{liq}}{(N^{15}/N^{14})_{gas}} .$$

This is the separation factor $\alpha$ for the isotopic exchange reaction

$$N^{15}O(g) + HN^{14}O_3(aq) \rightleftharpoons N^{14}O(g) + HN^{15}O_3(aq)$$

The results, shown in Fig. 4, reveal the usual inverse dependence on temperature.

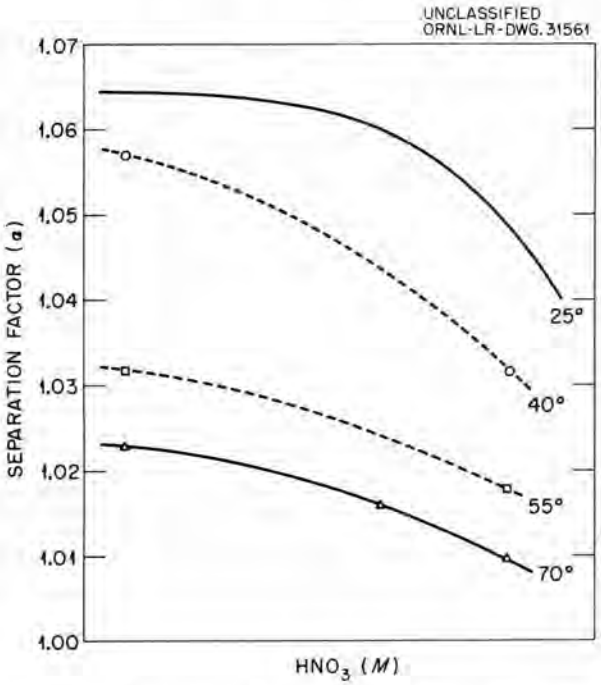


**Fig. 4. Temperature Dependence of Nitrox Separation Factor.** The 25°C curve is from G. M. Begun *et al.*, *Chemical and Isotopic Studies of the Nitrox System for $N^{15}$ Enrichment*, ORNL-2291 (June 6, 1957).

## Production of $N^{15}$

E. F. Joseph

The Nitrox two-column cascade[7] was operated during the year in order to produce enriched $N^{15}$ for AEC uses. Improvements were made in operating procedures and equipment which resulted in increased long-term reliability of the system. The longest continuous period of operation of the plant was 103 days. During this time the equipment functioned automatically, with occasional attention required on the day shift. The present rate of production is 1.7 g of $N^{15}$ per day at a concentration of approximately 95% $N^{15}$. The amount of $N^{15}$ produced to date is about 270 g, of which 235 g is contained in nitric acid assaying higher than 90% $N^{15}$.

## ENRICHMENT OF $C^{13}$

D. Zucker

Two chemical exchange reactions having attractive carbon isotope fractionation factors were found. Equilibration of carbon monoxide gas with an aqueous solution of the cuprous ammonium lactate complex of carbon monoxide produced a separation factor of 1.012 ± 0.002 (95% C.I.), with $C^{13}$ concentrating in the aqueous phase. This system is quite stable in the absence of air[8] and can be quantitatively refluxed by thermal means. Additional studies are in progress to evaluate the potentialities of this system.

The exchange of carbon between gaseous carbon monoxide and liquid iron pentacarbonyl results in the concentrating of $C^{13}$ in the liquid phase. The separation factor for the reaction is 1.020 ± 0.003 (95% C.I.). This isotopic fractionation ceases to occur if sufficient *o*-phenanthroline is added to the system to form a 1:1 mole ratio with the iron pentacarbonyl. Under these conditions the measured separation factor was 1.000 ± 0.003 (95% C.I.). Ethylenediamine, which also forms an addition compound with iron pentacarbonyl, does not behave in a similar manner. The separation factor for the reaction was observed to be essentially unchanged, 1.023 ± 0.003 (95% C.I.), in the presence of a large molar excess of this complexing agent.

## ENRICHMENT OF SULFUR ISOTOPES

A. C. Rutenberg

The study of the fractionation of sulfur isotopes between $SO_2$ gas and addition compounds of $SO_2$ to organic amines was continued. The apparatus and procedure were described in the previous report.[9] In addition to the previously reported data for the dimethylaniline·$SO_2$ addition compound,

[8] W. Gump and I. Ernst, *Ind. Eng. Chem.* **22**, 382–84 (1930).

[9] A. C. Rutenberg, *Chem. Ann. Prog. Rep. June 20, 1957*, ORNL-2386, p 32.

new data were obtained for pyridine·$SO_2$, triethylamine·$SO_2$, and aniline·$SO_2$ (Table 4). The single-stage separation factor $\alpha$ was calculated from the total separation $S$ by assuming a 50% efficiency for the bubble-plate column and correcting for the dissolved $SO_2$ in excess of the 1:1 complex.

The isotopic exchange of sulfur between $SO_2$ gas and $HSO_3^-$ has been used in the past to prepare small quantities of slightly enriched sulfur isotopes. In the operation of a column based on this system, the $SO_2$ is ordinarily absorbed at the top by an alkaline aqueous solution, while at the bottom of the column, acid is added to liberate the $SO_2$. In the present studies, an attempt was made to eliminate the chemical reflux by using a buffered, slightly acid solution which would absorb $SO_2$ to give largely $HSO_3^-$, but which would release the $SO_2$ when heated. It was found that $SO_2$ could be removed from a solution of $KH_2PO_4$ of pH ~4.1 by a short period of boiling.

The effect of temperature on the phosphate-$SO_2$-$HSO_3^-$ exchange system was studied in the 30-bubble-plate column used for the $SO_2$·amine experiments. The total separations achieved were 1.070, 1.067, and 1.059 at 30, 40, and 58°C, respectively.

## INFRARED AND RAMAN SPECTRA OF ISOTOPIC MOLECULES

In order to calculate the isotopic separation factors for exchange reactions between various chemical forms of an element, it is necessary to observe or estimate the fundamental vibrational frequencies of the molecules involved and the isotopic shift of these frequencies. The infrared and Raman spectra of isotopic molecules are being studied by members of the Chemical Separation of Isotopes Section in order to assemble data for this purpose.

### Infrared Spectra of the Isotopic Nitrous Oxides

G. M. Begun W. H. Fletcher

Nitrous oxide presents a unique spectroscopic opportunity in that four isotopic nitrogen species may be prepared and compared. Previous workers have investigated the spectra of the normal molecule and observed several of the frequencies of $N^{15}N^{14}O$ and $N^{14}N^{15}O$. No observations have been reported on $N^{15}N^{15}O$. The availability of high-purity $N^{15}$ prepared at ORNL by use of the isotopic exchange reaction between nitric acid and nitric oxide made it possible to prepare substantial samples and observe the infrared spectra of all the various species containing $N^{14}$ and $N^{15}$.

Spectra were observed on a model 112 Perkin-Elmer infrared spectrometer; NaCl, KBr, $CaF_2$, and LiF prisms were used for various regions of the spectra from 2.5 to 20 $\mu$. The frequencies of the 3 fundamental vibrational bands and the 15 overtone and combination bands were tabulated for the 3 isotopic species and compared with similar observations of the normal $N^{14}N^{14}O$ molecule.

With the use of known anharmonic constants and isotopic relations, approximate zero-order frequencies and force constants were calculated for the isotopic molecules. The zero-order frequencies are given in Table 5. The frequencies of all the observed combination bands were calculated from the fundamental frequencies and the anharmonic constants, and these frequencies were compared with the observed values. Agreement was generally within experimental error.

The fundamental vibrational frequencies may be used to calculate the partition function ratios for various isotopic species. These may in turn be used to calculate equilibrium constants for isotopic exchange reactions. An exact calculation was made by using the present data. Table 6 shows the results of the calculation.

**Table 4. Fractionation of Sulfur Isotopes by $SO_2$·Amine Addition Compounds**

| Amine | Temperature (°C) | Mole Ratio, $SO_2$/Amine | $S$ | $\alpha$ |
|---|---|---|---|---|
| Aniline | 30 | 1.47 | 1.028 | 1.0027 |
| Triethylamine | 30 | 1.82 | 1.022 | 1.0026 |
| Pyridine | 30 | 1.24 | 1.027 | 1.0022 |
| Dimethylaniline | 24 | 1.55 | 1.013 | 1.0014 |

Table 5. Zero-Order Frequencies for $N_2O$

| Species | $\omega_1$ | | | $\omega_2$ | | | $\omega_3$ | | |
|---|---|---|---|---|---|---|---|---|---|
| | Observed ($cm^{-1}$) | Calculated ($cm^{-1}$) | Error (%) | Observed ($cm^{-1}$) | Calculated ($cm^{-1}$) | Error (%) | Observed ($cm^{-1}$) | Calculated ($cm^{-1}$) | Error (%) |
| $N_2^{14}O$ | 1300.3 | 1299.7 | −0.05 | 596.5 | 596.5 | 0.00 | 2276.9 | 2277.0 | +0.004 |
| $N^{14}N^{15}O$ | 1295.6 | 1298.5 | +0.22 | 582.8 | 582.8 | 0.00 | 2228.6 | 2226.9 | −0.08 |
| $N^{15}N^{14}O$ | 1285.1 | 1281.4 | −0.29 | 593.2 | 592.9 | −0.05 | 2254.5 | 2256.7 | +0.10 |
| $N_2^{15}O$ | 1280.3 | 1280.6 | +0.02 | 578.9 | 579.2 | +0.05 | 2206.3 | 2205.9 | −0.02 |

Table 6. Partition Function Ratios for $N_2O$

| Temperature (°K) | Ratio of Partition Functions | | | |
|---|---|---|---|---|
| | $\frac{N^{15}N^{14}O^{16}}{N^{14}N^{14}O^{16}}$ | $\frac{N^{14}N^{15}O^{16}}{N^{14}N^{14}O^{16}}$ | $\frac{N^{15}N^{15}O^{16}}{N^{14}N^{15}O^{16}}$ | $\frac{N^{15}N^{15}O^{16}}{N^{15}N^{14}O^{16}}$ |
| 273.16 | 1.0874 | 1.1546 | 1.0884 | 1.1557 |
| 298.16 | 1.0772 | 1.1360 | 1.0783 | 1.1372 |
| 400 | 1.0507 | 1.0881 | 1.0510 | 1.0884 |
| 500 | 1.0360 | 1.0628 | 1.0355 | 1.0623 |
| 600 | 1.0269 | 1.0464 | 1.0267 | 1.0462 |

The equilibrium constant for the intramolecular equilibrium

$$N^{15}N^{14}O^{16} \rightleftharpoons N^{14}N^{15}O^{16}$$

can be calculated by dividing the partition function ratio for $N^{14}N^{15}O^{16}/N^{14}N^{14}O^{16}$ by that for $N^{15}N^{14}O^{16}/N^{14}N^{14}O^{16}$. This results in an equilibrium constant of 1.0545 at 25°C.

A sample of liquid $N_2^{15}O_4$ has been synthesized from high-purity $N^{15}$, and the Raman and infrared spectra of this compound are now under investigation.

### Infrared Studies of NOCl

L. Landau

The infrared spectra of $N^{14}OCl$ and $N^{15}OCl$ were obtained in the region from 2 to 40 $\mu$. Prisms of CsBr, KBr, NaCl, and $CaF_2$ were used, and all three fundamentals of each species, as well as many of the overtone and combination bands, were observed. The frequency shifts on substitution of $N^{15}$ for $N^{14}$ were tabulated, and the separation of the $P$ and $R$ branches of the bands was measured and agreed well with calculated values.

The NOCl was prepared by condensing NO on $Cl_2$ in a trap cooled with liquid nitrogen, sealing off the admitting stopcock, and then allowing the $Cl_2$ and NO to warm up and react:

$$2NO + Cl_2 \rightleftharpoons 2NOCl$$

This procedure avoided exposure of the NOCl to stopcock grease.

Table 7 gives the assignment of the frequencies, where $\nu_1$ is the N-O stretching frequency, $\nu_2$ is the N-Cl stretching frequency, and $\nu_3$ is the O-N-Cl bending frequency. Where indicated, $Q$ branches

**Table 7. Infrared Spectra of NOCl**

| Assignment | Branch | Frequency ($cm^{-1}$) | | $\Delta$, $N^{14} - N^{15}$ ($cm^{-1}$) | *P-R* Separation ($cm^{-1}$) | | $N^{14}OCl$ Frequency ($cm^{-1}$) | |
|---|---|---|---|---|---|---|---|---|
| | | $N^{14}OCl$ | $N^{15}OCl$ | | $N^{14}OCl$ | $N^{15}OCl$ | Ref *a* | Ref *b* |
| $3\nu_1$ | | 5295 | 5215 | | | | 5303 | |
| $2\nu_1 + \nu_2$ | *R* | 4164 | 4086 | | | | | |
| | | 4153.8 | 4080 | | 17 | 18 | 4160 | |
| | *P* | 4147 | 4068 | | | | | |
| $2\nu_1 + \nu_3$ | *R* | 3893.4 | 3833.4 | | | | | |
| | | 3888.4 | 3824.9 | | 16 | 18 | 3898 | 3887 |
| | *P* | 2877.3 | 3815.3 | | | | | |
| $2\nu_1$ | *R* | 3569.2 | 3511.6 | | | | | |
| | | 3563.1 | 3503.3 | | 14 | 18 | 3568 | 3560 |
| | *P* | 3555 | 3493.4 | | | | | |
| $\nu_1 + \nu_2$ | *R* | 2402.6 | 2358.0 | | | | | |
| | *Q* | 2394.7 | 2349.8 | | 19 | 19 | 2395 | 2409 |
| | *P* | 2383.3 | 2338.7 | | | | | |
| $\nu_1 + \nu_3$ | *R* | 2138.5 | 2105.4 | | | | | |
| | *Q* | 2130.5 | 2097.8 | | 20 | 20 | 2131 | 2129 |
| | *P* | 2118.6 | 2085.6 | | | | | |
| $\nu_1$ | *R* | 1808.0 | 1777.9 | | | | | |
| | *Q* | 1798.6 | 1767.8 | 30.8 | 20 | 20 | 1799 | 1800 |
| | *P* | 1789.8 | 1758.3 | | | | | |
| $3\nu_2$ | *R* | | ~1731 | | | | | |
| | *Q* | 1767[c] | 1719.0 | | | | | |
| | *P* | 1760.4 | 1712.2 | | | | | |
| $\nu_2 + \nu_3$ | *R* | 929.7 | 915.8 | | | | | |
| | *Q* | 922 | 905.2 | | 17 | 17 | 923 | 924 |
| | *P* | 913 | 899.1 | | | | | |
| $\nu_2$ | *R* | 604.3 | 590.5 | | | | | |
| | *Q* | 597.2 | 583.2 | 14.0 | 19 | 19 | 592 | 595 |
| | *P* | 585.2 | 571.2 | | | | | |
| $2\nu_3$ | | | 663 | | | | 664 | 654 |
| $\nu_3$ | | 339.8 | 337.9 | | | | | |
| | | 332.4 | 330.6 | 1.8 | | | 332[d] | 329[d] |
| | | 320.4 | 318.6 | | | | | |

[a]W. G. Burns and H. J. Bernstein, *J. Chem. Phys.* **18**, 1669 (1950).
[b]A. G. Pulford and A. Walsh, *Trans. Faraday Soc.* **47**, 347 (1951).
[c]Calculated from analogy with $N^{15}OCl$, since the *Q* and *R* branches were hidden by the $\nu_1$ band.
[d]Not measured values.

were observed; otherwise the troughs between the $P$ and $R$ branches were used as band centers.

### Raman Studies of Metal-Ammonia Complexes

A. C. Rutenberg L. Landau

As a portion of the program for calculating the isotopic fractionation between $NH_4OH$ and a series of metal-ammonia complexes, the Raman spectra of several of these complexes were observed with a Cary model 81 Raman spectrophotometer, and preparation of similar complexes containing $ND_3$ and $N^{15}H_3$ has been initiated. Compounds of $Cd(NH_3)_4^{++}$ and $Zn(NH_3)_4^{++}$ ions, both of which are tetrahedral in configuration, were given the most detailed study thus far. These particular metal-ammonia complexes were chosen because isotopic fractionation data between $N^{14}$ and $N^{15}$ have been obtained for systems containing these complexes, and also because they can be kept in solution at fairly high concentrations and do not absorb light in the region of the 4358-Å exciting frequency of the Raman spectrophotometer.

Of the four possible Raman frequencies which may be associated with the metal-nitrogen bond in a tetrahedral structure, only the totally symmetric breathing frequency $\nu_1$ was observed. The measured degree of depolarization, $\rho$, was found to be approximately 0.25.

Table 8 gives the frequencies of the metal-ammonia symmetric vibrations and, also, the frequencies of the associated N-H vibration as compared with the similar vibration in $NH_4OH$.

**Table 8. Raman Frequencies of Metal-Ammonia Complexes**

| Compound | Frequency | |
|---|---|---|
| | Metal-N $\nu_1$ ($cm^{-1}$) | N-H ($cm^{-1}$) |
| $Zn(NH_3)_4Br_2$ (3 M) | 364 | 3270 |
| $Cd(NH_3)_4(NO_3)_2$ (2.8 M) | 426 | 3290 |
| $Cu(NH_3)_5Cl_2$ | ~450 | |
| $NH_4OH$ | | 3312 |

### Infrared Spectrum of $BF_3$

J. Vanderryn[10]

In the course of investigating the spectra of complexes of $BF_3$, it was found necessary to reinvestigate the infrared spectrum of $BF_3$ itself. In the literature the assignment is uncertain between $\nu_1 + 2\nu_4$ and $\nu_3 + \nu_4$ and between $2\nu_1 + \nu_4$ and $\nu_1 + \nu_3$. Measurements made in this laboratory on $B^{10}F_3$ and $B^{11}F_3$ have resolved these uncertainties. The previously unreported $\nu_1 + \nu_3$ band also was observed. This study is now complete. The observed frequencies above 1450 $cm^{-1}$ and their assignments, together with literature and calculated values for overtone and combination frequencies, will soon be submitted for publication.

[10]Research participant, summer 1957. Department of Chemistry, Virginia Polytechnic Institute, Blacksburg.

## RADIATION CHEMISTRY

### EFFECT OF IONIZING RADIATION ON CATALYSTS

H. W. Kohn G. E. Moore
E. H. Taylor

Heterogeneous catalysis is one of the fields in which imperfections in solids are thought to play an important role. It is therefore natural to see whether the various point defects which can be introduced into solids by ionizing radiation have effects upon catalytic behavior. Earlier work[1-3] has shown the existence of such effects (both in the direction of enhancement of activity and in the direction of decrease), and a particular example, $\gamma$-alumina, has now been studied in some detail. The following paragraph is a summary from a paper on the subject.[4]

Relatively small doses of gamma rays at −78°C have been found to enhance the $H_2$-$D_2$ exchange activity of $\gamma$-$Al_2O_3$. The enhancement depends upon the presence of a catalyst poison ($H_2O$, $H_2$, or $C_2H_4$), and in the case of $H_2O$ is a function of the extent of poisoning, being greatest for the most highly poisoned samples. However, $Al_2O_3$ not activated by high-temperature treatment is not made active by prolonged irradiation. The enhancement in catalytic activity produced by radiation decays fairly rapidly at room temperature and above, and appreciable decay can be noted in some samples (highly poisoned ones, highly sensitive to radiation) even at −78°C. In a particular sample, irradiations at a series of temperatures (above the reaction temperature) indicate that the activation energy for decay of the effect is about 3 kcal/mole. Reactor radiation (fast neutrons and gamma rays) and radon produce similar enhancement, but in this case the effect does not decay markedly at room temperature. Although it is not yet possible to assign these effects surely to electron trapping (for gammas) and atom displacement (for heavy particles), these are the most attractive hypotheses at present. In any case it appears likely that further study of these phenomena will help to clarify the importance for catalysis of various crystal imperfections.

Some preliminary results, also with $H_2$-$D_2$ exchange, are available on a number of other nonmetal catalysts. Although pure ZnO shows a marked radiation enhancement, ZnO promoted (by coprecipitation) with Ti, Cd, Ga, Al, or Na is insensitive to radiation. Silica gel and anatase have shown remarkably high radiation enhancement; that of anatase is not readily annealed at room temperature. On the other hand, the enhancement of certain preparations of $ThO_2$ is very transitory, disappearing in a matter of minutes at room temperature. These and other results are summarized in Table 9.

The bulk of this work to date has been with nonmetallic catalysts, since these were expected to retain electronic displacements as well as displaced atoms, and since the possible effects of the electronic displacements were the first objects of this work. Metallic catalysts, however, are of such importance that work has been initiated with them in order to see whether atomic displacements will affect the catalytic activity of metals. Copper and germanium (a metallic semiconductor) are under study and have exhibited both increases and decreases in activity. The number of experiments is too small to permit conclusions about the nature of the effect. Neutron irradiation is being used as the principal source, although an effect has apparently been observed with gamma rays, which produce displacements as well as ionization, but at a very low rate.

[1] E. H. Taylor and J. A. Wethington, Jr., *J. Am. Chem. Soc.* **76**, 971 (1954).

[2] P. B. Weisz and E. W. Swegler, *J. Chem. Phys.* **23**, 1567 (1955).

[3] E. H. Taylor and H. W. Kohn, *J. Am. Chem. Soc.* **79**, 252 (1957).

[4] H. W. Kohn and E. H. Taylor, *Abstracts of Papers, 133rd National Meeting of the American Chemical Society, San Francisco, Calif., April 13–18, 1958*, paper 44, p 171.

### RADIOLYSIS OF CARBON MONOXIDE BY ALPHA PARTICLES

P. S. Rudolph S. C. Lind

Current interest in gas-cooled, graphite-moderated reactors has renewed interest in the irradiation of CO and its reaction products. Carbon dioxide and graphite under reactor irradiation give

Table 9. Effect of Irradiation on the $H_2$-$D_2$ Exchange Activity of Catalysts

| Catalyst | Enhancement Factor* | | Rate for Unirradiated 1-g Sample ($hr^{-1}$) | Temperature of Reaction (°C) | Annealing Time at Room Temperature After Radiation Indicated | | |
|---|---|---|---|---|---|---|---|
| | Minimum | Maximum | | | Alpha | Gamma | Reactor |
| $\gamma$-$Al_2O_3$ | 0.5 | 2,000 | 0.02–8.30 | −78 | | Days | |
| $\gamma$-$Al_2O_3$ | 3 | 10 | 2.1–4.15 | −78 | Long | | Long |
| ZnO | 3 | 10 | 0.07–0.1 | −78 | | Months | |
| ZnO promoted | 0.8 | 1.2 | 0.005–2.2 | −78 | | No observation | |
| Hydrides (*in vacuo*) | 0.1 | 1 | 0.02–4.15 | −78 | | Long? | |
| Hydrides (in $H_2$) | 1 | 10 | 0.05–5.2 | −78 | | Long | |
| $ThO_2$ | | 100 | 0.01 | −78 | | Minutes | |
| $TiO_2$ (rutile) | 1 | 1 | 0.42 | −78 | | | |
| $TiO_2$ (anatase) | 9000 | 18,000 | 0.002 | 25 | | Months | |
| $BaTiO_3$ | 13 | 20 | 0.008 | 25 | | Weeks | |
| $SiO_2$ (gel) | 9000 | 50,000 | 0.002 | 25 | | Long | |
| MgO | 3 | 6 | 2.1 | −78 | | Weeks | Long |
| $V_2O_3$ | 5 | 10 | 0.028 | −78 | | No observation | |
| $SiO_2$-$Al_2O_3$ | 10 | | 1.65 | −78 | | Weeks | |

*Reaction rate after irradiation divided by reaction rate before irradiation.

CO and $C_3O_2$ (refs 5–7). The products of CO irradiation are $CO_2$, C, and a polymer which is largely $(C_3O_2)_x$.

A mixture of 94% CO and 6% $CO_2$ was irradiated in a spherical glass reaction vessel with radon. Cryogenic separations during the experiment gave values from 2.2 to 2.5 for the ratio $-\Delta P_{CO}/+\Delta P_{CO_2}$. Final analysis of gases gave 2.07 for this ratio. The polymer was heated *in vacuo* to 450°C; the small amount of gas evolved was mainly $CO_2$. The polymer on heating turned from dark red to black. The vessel was opened in an atmosphere of $N_2$, and the solid was removed by scraping. An x-ray analysis of this solid showed only the pattern of SiC.

A sample of polymer from a CO irradiation was degassed and irradiated with radon. A cryogenic analysis, during the run, of the gases evolved showed mainly $CO_2$, with some CO and $C_3O_2$. A chemical analysis after the irradiation showed $CO_2$ and only traces of other gases. A new

[5] R. E. Woodley, *Promotion of Chemical Reaction in Gas-Graphite Systems by Gamma Radiation*, HW-31929 (May 24, 1954).

[6] P. C. Davidge and W. R. Marsh, *The Effect of Pile Radiation on the Carbon Dioxide–Graphite Reaction*, AERE C/R-1374 (Jan. 1956).

[7] V. R. Deitz and E. J. Prosen, *Nature* 181, 109 (1958).

polymer, assumed to be $(C_3O_2)_x$, was formed during the irradiation. The original polymer was dark red, and the new polymer, which could be seen on the glass at the periphery of the original polymer, was cream-colored. The polymer appears to "come down" cream-colored and to turn dark red upon continued irradiation.

An experiment was run with CO and radon. There was a continued pressure drop until the total pressure was about two-thirds the initial CO pressure. At this point there was a prolonged plateau in the pressure readings, after which the pressure again started to drop slowly.

A mixture of CO and $CO_2$ in a ratio of 3:1 was irradiated with radon. The pressure dropped regularly until the total pressure was about 82% of the initial pressure, when a prolonged period of no pressure change occurred. After this plateau the pressure dropped slowly to 78% of the initial value.

A consistent observation in the irradiation of CO with and without $CO_2$ initially present is the inhibiting action of $CO_2$. This may be due to a back reaction or to a transfer of charge or energy from the CO to the $CO_2$. C. E. Melton of the Mass Spectroscopy Group modified his spectrometer so that a second gas could be bled into the field-free region of the instrument beyond the ionization chamber. Carbon monoxide was bled in through the standard leak and ionized while $CO_2$ was bled into the modified leak where the $CO^{+2}$ could collide with the neutral $CO_2$. These preliminary experiments gave no evidence of $CO_2^+$ formed by the process

$$CO^+ + CO_2 \longrightarrow CO + CO_2^+$$

A mixture of $CO_2$ and graphite was irradiated with alpha particles from radon and its decay products. In this experiment there was an initial increase in pressure reaching a maximum of 1.2% increase in total pressure, after which there was a slight decrease in pressure.

In collaboration with W. H. Baldwin, a mixture of $H_2$ and graphite[8] was similarly irradiated. In this experiment there was a continuous decrease in pressure. When the radon was essentially decayed, the decrease in total pressure was 1.2%.

[8] A highly purified sample of graphite was furnished by the National Carbon Company.

## RADIOLYSIS OF BIPHENYL BY ALPHA PARTICLES FROM RADON

W. H. Baldwin P. S. Rudolph

Aromatic hydrocarbons are more stable to ionizing radiation than most other organic compounds, and consequently have been suggested for use in organic fluid reactors. Biphenyl was selected for studying several variables in connection with the over-all problem of organic reactor fluids. Concerning most compounds, there is insufficient information relating the yields of products to the kind of radiation. For example, quantitative information was desired for the radiolysis of biphenyl with heavy ionizing particles. Biphenyl was irradiated with radon alpha particles as the most readily available of the heavy particles.

Biphenyl (1.83 g) was melted, spread over the inside of a 67-cc glass sphere, and cooled slowly to form a uniform coat when it solidified. The sphere was degassed ($10^{-5}$ mm), and 162 mc of radon was introduced. The sphere (previously fitted with a manometer) was sealed off from the atmosphere and placed in a constant-temperature bath (25 ± 0.1°C). Within 10 min the pressure was observed to be 7 mm. Relatively little change in the pressure was noted (9.1 mm at the end of 8 and 17 days). Yellowing of the solid became evident after 4 hr. The solid slowly flaked from the walls in some areas, but it was estimated that 80% of the total energy was absorbed in the biphenyl. A blue luminescence was observed, and two days after the start of the experiment the intensity was strong enough to register on a photographic plate and provide a self-illuminated photograph.

The mixture was allowed to decay for three months, after which time the gas was removed with a Toepler pump. There was obtained $2.4 \times 10^{-5}$ mole of gas that contained 92% hydrogen (by diffusion through a palladium thimble). The residual gas consisted, for the most part, of methane.

The major portion of the unchanged biphenyl was removed by sublimation under reduced pressure. The residue in the flask was washed out with benzene and filtered, yielding 5.5 mg of a yellow insoluble polymer. The benzene was evaporated from the solution, and the polymeric residue was subjected to sublimation, yielding a further small portion of biphenyl. The residue from this sublimation (50.4 mg) was a red viscous liquid with a molecular weight of 450 (by Rast camphor

method). While attempts to separate this mixture were unsuccessful, it appeared to consist of a white crystalline material and a red viscous oil.

The yields ($G$) of products were hydrogen, 0.03; residual gas (mostly methane), 0.003; benzene-soluble polymer, 0.45; and benzene-insoluble polymer, 0.05. The polymer was assumed (for the calculation of yield) to have a molecular weight that was some multiple of the molecular weight of biphenyl, and the yields represent biphenyl converted to polymer.

Yields of gas shown above are three to five times as high as those reported by Colichman and Gercke[9] from the electron irradiation of biphenyl.

## EFFECTS OF SOLUTES ON THE "MOLECULAR" YIELDS ($H_2$ AND $H_2O_2$) IN THE DECOMPOSITION OF WATER BY GAMMA RAYS

J. W. Boyle H. A. Mahlman

In the sequence of events following the absorption of high-energy radiation in liquid water, $H_2$ and $H_2O_2$ are produced, presumably by combination of radicals as they diffuse away from the sites of formation along charged-particle tracks. Information, both on the nature of the processes leading to these products and on the initial spatial distribution of the intermediates, can be gained by studying the effects of added scavengers at various concentrations. In general, solutes that react with H atoms lower the molecular $H_2$ yield, and those that react with OH radicals lower the $H_2O_2$ yield. For irradiation by cobalt gamma rays the decrease in yield is, in a number of cases, proportional to the cube root of scavenger concentration. This dependence is consistent with the radical-diffusion model developed by Magee and co-workers and also by others.

### Effect of Sodium Nitrate Concentration on $H_2$ Yield[10]

H. A. Mahlman J. W. Boyle

Degassed sodium nitrate solutions at concentrations up to 0.3 $M$ were irradiated with cobalt gamma rays. The solutions also contained $10^{-3}$ $M$ KBr to prevent secondary reaction of the $H_2$ produced. The hydrogen yield, equivalent to the molecular hydrogen yield, $G_{H_2}$, decreased with increasing $NaNO_3$ concentration and could be expressed by the equation

$$G_{H_2} = 0.46 - 0.40[NaNO_3]^{1/3} ,$$

where concentration is expressed as molarity. The decrease in yield is attributed to scavenging of precursors of $H_2$ in the particle tracks.

### The Activity Coefficient in Radiation Chemistry

H. A. Mahlman

For $NaNO_3$ concentrations greater than 0.3 $M$, considerable deviation from the cube-root dependence mentioned above is observed. However, the cube-root dependence holds over the entire range of concentrations from $10^{-4}$ to 1.0 $M$, provided that the activity is used in place of molarity. The dependence on activity was also demonstrated by changing the ionic strength by adding NaCl at concentrations of 1.0, 3.0, and 5.0 $M$ to 0.1 $M$ $NaNO_3$ solution. The equation expressing molecular $H_2$ yield is

$$G_{H_2} = 0.46 - 0.46(\gamma[NaNO_3])^{1/3} .$$

### Effect of pH on "Molecular" Hydrogen Yield

H. A. Mahlman

Hydrogen yields from degassed nitric acid solutions at concentrations from $10^{-4}$ to 0.8 $M$ were compared with yields from $NaNO_3$ solutions (pH 5.1 to 5.8) in the same concentration range. All solutions contained $10^{-3}$ $M$ KBr to prevent secondary reaction of the $H_2$ produced. The yields from the two solutions were the same at equal nitrate concentrations, indicating no effect of acidity on the "molecular" $H_2$ yield, and also no effect of acidity on the action of $NO_3^-$ in lowering the molecular yield. It was previously found that $H_2SO_4$ in concentrations up to 0.4 $M$ had no effect on $H_2$ yield. This observed lack of acid dependence is in disagreement with results published by others,[11] who report yields of 0.46 and 0.39 for solutions at pH 2 and in 0.4 $M$ $H_2SO_4$, respectively.

[9] E. L. Colichman and R. H. J. Gercke, *Nucleonics* 14(7), 50 (1956).

[10] H. A. Mahlman and J. W. Boyle, *J. Chem. Phys.* **27**, 1434 (1957).

[11] C. J. Hochanadel and S. C. Lind, in *Annual Reviews of Physical Chemistry* (ed. by H. Eyring), vol 7, p 91, Annual Reviews, Palo Alto, Calif., 1956.

### Effect of Sodium Sulfate Concentration on Hydrogen Yield

H. A. Mahlman

The yield of hydrogen from degassed sodium sulfate solutions containing $10^{-3}$ *M* KBr was independent of sulfate concentration in the range from 0.6 to 1.8 *M*. The yield, 0.48 ± 0.02, was based on total energy absorbed. For the 1.8 *M* solution the fraction of electrons present in the solute was ~19%, and if appreciable excitation of the solute occurred, then this energy was effective in producing hydrogen. The results also indicate that sulfate is not reactive with H atoms.

### Comparison of the Effect of KBr on the Molecular Peroxide Yield in Light and Heavy Water

J. W. Boyle H. A. Mahlman

Air-saturated solutions containing KBr at concentrations from 0 to $10^{-2}$ *M* in both $H_2O$ and $D_2O$, and containing either 0.4 *M* $H_2SO_4$ or 0.4 *M* $D_2SO_4$, were irradiated with cobalt gamma rays, and the initial peroxide yields were measured. The initial peroxide yield is given by

$$G(H_2O_2)_{Br^-,O_2} = G_{H_2O_2} + \tfrac{1}{2}(G_H - G_{OH}) ,$$

from which

$$G_{H_2O_2} = \tfrac{1}{2}\left[G(H_2O_2)_{Br^-,O_2} + G_{H_2}\right] .$$

By subtracting the known molecular $H_2$ yield from the measured $H_2O_2$ yield, the "molecular" $H_2O_2$ yield, $G_{H_2O_2}$, can be calculated. The yield, $G_{H_2O_2}$, is the same, 0.81, for both $H_2O$ and $D_2O$, and the effect of KBr in lowering this yield is the same for both systems; the yield is given by

$$G_{H_2O_2} = G_{D_2O_2}$$
$$= (0.81 \pm 0.01) - (1.65 \pm 0.1)\,[KBr]^{1/3} .$$

## RADIATION-INDUCED REACTION OF REDOX COUPLES

J. W. Boyle C. J. Hochanadel

Solutions containing an oxidizing agent and a reducing agent that react thermally at a negligible rate provide useful scavenger systems for studying the intermediates in the radiation decomposition of water. Two such systems were studied: Fe(III)-Sn(II) and As(III)-Ce(IV).

### Radiation-Induced Reaction of Fe(III) and Sn(II)

J. W. Boyle C. J. Hochanadel

Cobalt irradiation induces the reaction of Fe(III) with Sn(II). In degassed 0.4 *M* $H_2SO_4$ the initial Fe(II) yield is 6.6 and is equivalent to $G_H + G_{OH}$. A mechanism is proposed in which Sn(II) is oxidized by OH radical to Sn(III), Fe(III) is reduced by Sn(III) and by H radical, and Fe(II) is oxidized by $H_2O_2$ and by H radical. Predicted initial yields are $G[Sn(IV)] = G_{H_2O_2} + G_{OH}$ and $G(H_2) = G_{H_2}$. Preliminary measurements gave a value of 2.3 for $G[Sn(IV)]$. The yields $G[Fe(II)]$ and $G[Sn(IV)]$ decrease as the concentration of Fe(II) increases. The dependence of yields on relative concentrations indicates competition of Fe(II) and Sn(II) for OH radical and of Fe(II) and Fe(III) for H radical; the latter competition is sensitive to acidity. When a solution 0.4 *M* in $H_2SO_4$ and containing Fe(III) in excess of Sn(II) is irradiated, the Sn(II) is first completely oxidized to Sn(IV). With increased dose, the Sn(IV) remains, the Fe(II) which had been produced is reoxidized, and presumably an equivalent amount of $H_2$ is produced. Further irradiation presumably produces $H_2$ and $H_2O_2$ in equivalent amounts.

### Radiation-Induced Reaction of As(III) with Ce(IV)

J. W. Boyle

Arsenic(III) enhances the yield for reduction of Ce(IV) in air-saturated 0.4 *M* $H_2SO_4$ solution from $2.4 = 2G_{H_2O_2} + G_H - G_{OH}$ to a maximum value $8.2 = 2G_{H_2O_2} + G_H + G_{OH}$; the yield increases with increasing ratio of concentrations [As(III)]/[Ce(IV)]. This indicates reaction of As(III) with OH radical [in competition with Ce(III)] to give a species, As(IV), which reduces Ce(IV). The specific rate constant for the reaction of As(III) with OH is estimated to be 10 to 15 times as large as that for the reaction of Ce(III) with OH. Competition of Ce(IV) and As(III) for $H_2O_2$ is also indicated, the ratio of specific rate constants being 3 to 4.

## KINETICS OF THE RADIATION-INDUCED REDUCTION OF Ce(IV) IN SOLUTIONS CONTAINING Ce(IV), Ce(III), $H_2$, AND $H_2SO_4$

J. W. Boyle C. J. Hochanadel

The effect of $H_2SO_4$ on the radiolysis of Ce(IV) solutions was studied in the range of acid concentrations from 0.04 to 4 *M* by irradiating solutions initially saturated with either He, air, or $H_2$, and also by irradiating solutions purged continuously with either He, $O_2$, or $H_2$ during irradiation. Particular attention was addressed to purification, not only of the water, but also of the acid, cerium salts, and gases. Results in all cases were reproducible, and for air-saturated 0.4 *M* acid solution the initial production of Ce(III) was essentially linear with dose. A plot of production of Ce(III) vs dose passed through the origin, indicating negligible effect of impurities. For acid concentrations in the range 0.04 to 0.4 *M*, $H_2$ enhances the yield for reduction, the yield increasing with increasing concentration ratios $[H_2]/[Ce(III)]$ and $[H_2]/[H_2SO_4]$. This indicates possibly a competition of these three solutes for OH radicals. If the yields of intermediates (H, OH, $H_2$, and $H_2O_2$) produced in the decomposition of water are represented by $G_H$, $G_{OH}$, $G_{H_2}$, and $G_{H_2O_2}$, the maximum initial yields for Ce(IV) reduction in the absence and presence of $H_2$ are related to these quantities by

$$G[Ce(III)] = 2G_{H_2O_2} + G_H - G_{OH} ,$$

and

$$G[Ce(III)]_{H_2} = 2G_{H_2O_2} + G_H + G_{OH} .$$

The maximum value in the presence of $H_2$ is approached only at low acidities. If it is assumed that the species produced by reaction of OH radical with $H_2SO_4$ (presumably $HSO_4$ radical) reacts readily with Ce(III) but not with $H_2$, and that Ce(IV) is reduced by the H and $HO_2$ radicals and by $H_2O_2$, the derived rate equation expresses the results if the relative reactivities of Ce(III), $H_2$, and $H_2SO_4$ with OH radicals are as 650:135:1. An effect of $O_2$ in 4 *M* acid solutions indicates possible oxidation of Ce(III) by H atoms at high acidity.

## CHEMICAL FEATURES OF THE FIXATION OF NITROGEN BY IRRADIATION OF MOIST AIR

A. R. Jones

When moist air was exposed to electron bombardment and the products were examined spectrophotometrically, it was found that nitric acid was produced at a rate linear with dose and independent of the concentration of water vapor up to the highest concentration (11 mm partial pressure) which could be examined with sodium chloride windows. The 100-ev yield (*G* value) was 2.9. At the concentration of nitric acid equal to the maximum permissible concentration as calculated stoichiometrically from the initial amount of water present, the nitric acid began to disappear, and the destruction continued linearly with dose with a *G* of 5.4.

During the disappearance of the nitric acid, nitrogen dioxide and water were produced stoichiometrically with the same *G* yield, 5.4. Subsequently to the decomposition of the nitric acid, nitrogen dioxide was produced at a rate which decreased slightly with dose, appearing to approach asymptotically the value $G = 0.28$. The other major product of the irradiation of moist air was nitrous oxide, which was produced at a rate independent of water vapor concentration over the experimental range. The 100-ev yield decreased slightly with dose, appearing to approach asymptotically the value 0.55. These facts indicate that the maintenance of humidity would certainly be a prime consideration if the fixation of nitrogen by radiation were to have industrial importance, since a partial pressure of water vapor prevents the formation of nitrogen dioxide and the consequent decrease in fixation yield.

## ORGANIC CHEMISTRY

### THE PINACOL REARRANGEMENT

#### The Phenyl-di-*p*-tolyl System

B. M. Benjamin

The pinacol rearrangement of triaryl-substituted ethylene glycols and the closely related rearrangement of substituted acetaldehydes to ketones have been under investigation. A previous report[1] gave the results of experiments on the conversion of the phenyl-di-*p*-tolyl compounds VI, VII (both threo and erythro forms), and VIII to the ketones IX and X in the presence of cold concentrated sulfuric acid (the Roman numerals refer to specific compounds, and the other symbols used are the same as those previously employed):

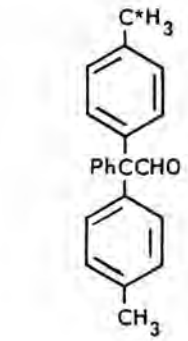

VI

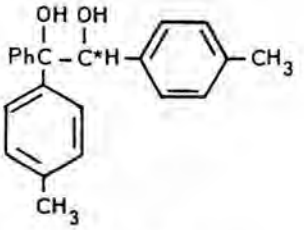

VIIa

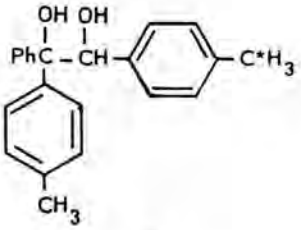

VIIc

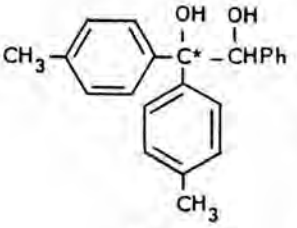

VIII

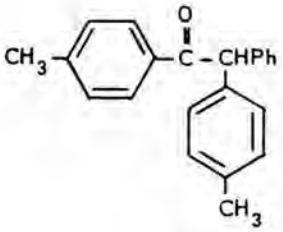

IX

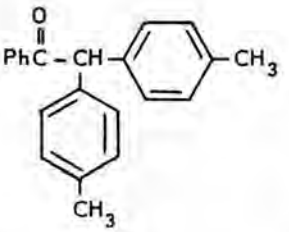

X

During an analysis of the data, certain anomalies appeared. The isotopic dilution experiments and certain of the degradative procedures were therefore repeated.

The present experimental procedure differs from the former in that the aliquots to which ketones IX and X were added for isotopic dilution analysis were not subjected directly to fractional crystallization, but instead the following procedure was used: (1) the aliquots were treated with lithium aluminum hydride; (2) the carbinol from IX was converted to the acetate, and the carbinol from X was converted to the *p*-nitrobenzoate; and (3) each derivative was then crystallized several times prior to the radioactivity assay. The conversion of each of the above aliquots to high-melting derivatives was absolutely essential in the application of the isotope dilution method of analysis, for in the earlier experiments, in which the ketones themselves were isolated, repeated crystallizations were not sufficient to provide reliable results.

The data were treated by two different methods for calculation of the mole fractions $m_i$ of the glycols VII and VIII which proceed to products by the various paths defined in Charts 1 and 2 of ref 1. In the first method the $m_i$ were calculated directly for threo-VII from the yield data and double-labeling experiments, and the value $m_e/m_d$ = 1.004 obtained therefrom was used in subsequent $m_i$ calculations for erythro-VII and VIII. In the second method the ratio of the yields of the two ketones IX and X, 49:51 = 0.961, observed upon rearrangement of aldehyde VI, was used in the same manner as that described by Raaen and Collins.[2]

The amended results calculated with the Hearon equation (Eq. 1 of ref 1) are given in Table 10.

#### The 1,2-Diphenyl-1-*o*-tolyl System

H. R. Jolley C. J. Collins

The first-order rates of rearrangement, with respect to reactant, of *dl*-erythro-1,2-diphenyl-1-*o*-tolylethylene glycol and *dl*-threo-1,2-diphenyl-1-*o*-tolylethylene glycol have now been determined

[1] L. W. Kendrick, Jr., *Chem. Ann. Prog. Rep. June 20, 1957*, ORNL-2386, p 39–44.

[2] V. F. Raaen and C. J. Collins, *J. Am. Chem. Soc.* 80, 1409 (1958).

in 3.13 *N* aqueous ethanolic sulfuric acid by a method previously employed.[3] By the use of the isotopic dilution method it was established that there is no threo-glycol formed during rearrangement of the erythro-glycol. However, it has been shown that, when the reaction of the threo-glycol is interrupted before completion, the recovered glycol consists of 32% erythro-glycol. Further, the erythro-glycol affords only 20.5% of diphenyl-*o*-tolylacetaldehyde, whereas the threo-glycol yields 50% of this same aldehyde.

The first-order rate constant for the rearrangement of erythro-glycol, calculated from seven points by the method of least squares, is $(16.202 \pm 0.017) \times 10^{-4}$ min$^{-1}$. The data for rearrangement of the threo isomer are not steady, but allow the calculation, from ten points, of an average first-order rate constant of $(35.11 \pm 0.67) \times 10^{-4}$ min$^{-1}$.

No conclusions will be drawn from the present results without further experimental data.

## ANALYSIS OF KINETIC RATE DATA BY MEANS OF THE ORACLE

M. H. Lietzke C. J. Collins

Rate constants for reactions 1, 2, and 3 as catalyzed by *p*-toluenesulfonic acid in acetic acid–acetic anhydride have been reported:[4]

(1) $$2Ph_2CH\overset{\overset{\displaystyle OCOCH_3}{|}}{C}{*}HPh \xrightarrow{k_I} Ph_2CH\overset{\overset{\displaystyle OCOCH_3}{|}}{C}{*}HPh + PhCH\overset{\overset{\displaystyle OCOCH_3}{|}}{C}{*}HPh$$

I

(2) $$3Ph_2CH\overset{\overset{\displaystyle OCOCH_3}{|}}{C}HPh{*} \xrightarrow{k_{II}} Ph_2CH\overset{\overset{\displaystyle OCOCH_3}{|}}{C}HPh{*} + 2PhCH\overset{\overset{\displaystyle OCOCH_3}{|}}{C}HPh_2^{*}$$

II

(3) $$Ph_2CH\overset{\overset{\displaystyle OCOC{*}H_3}{|}}{C}HPh \xrightarrow{k_{III}} Ph_2CH\overset{\overset{\displaystyle OCOCH_3}{|}}{C}HPh + C{*}H_3COOH$$

III

**Table 10. Summary of the Ratios Calculated for Use in or by Means of the Hearon Equation**

| Ratio | Method of Calculation | |
|---|---|---|
| | 1 | 2 |
| $m_e/m_d$ | 1.004 | 0.961 |
| $k_\phi/k_H$ | 3.95 | 4.44 |
| $(m_c + m_e)/m_d$ | | |
| Threo-VII | 1.05 | 1.05 |
| Erythro-VII | 1.11 | 1.11 |
| $k_{Tol}/k'_H$ | | |
| Threo-VII | 39.6 | 20.6 |
| Erythro-VII | 18.4 | 12.8 |
| $k_T/2k_P$ | | |
| Threo-VII | 4.4 | 1.9 |
| Erythro-VII | 2.1 | 1.2 |

The equations by which each rate constant was evaluated are as follows:

$$k_I = \frac{1}{t} \ln \frac{x_e}{x_e - x} ,$$

$$k_{II} = \frac{1}{t} \ln \frac{y_e}{y_e - y} ,$$

$$k_{III} = \frac{1}{t} \ln \frac{a}{a - z} ,$$

[3] W. T. Rainey and B. B. Smith, *Chem. Ann. Prog. Rep. June 20, 1957*, ORNL-2386, p 52–53.

[4] W. A. Bonner and C. J. Collins, *J. Am. Chem. Soc.* **77**, 99 (1955).

in which $x_e$ and $y_e$ are the equilibrium concentrations of rearranged product, $x$ and $y$ are the respective concentrations at time $t$, $a$ is the initial molar radioactivity of III, and $(a - z)$ is the molar radioactivity of III at time $t$. The estimation of first-order rate constants from these data by the previous[4] method, by graphical methods, or by ordinary least-squares calculations provides approximate values which can be compared in a semiquantitative manner.

Most of the uncertainties involved in the calculation of $k_I$, $k_{II}$, or $k_{III}$ are of the type which can be expressed as constants that can be added to $x_e$, $y_e$, or $a$ in the respective equations. Since a study was being made of the rate of racemization, $k_{IV}$, of optically active 1,2,2-triphenylethyl acetate (IV) and since $k_{IV}$ was to be compared with $k_I$, $k_{II}$, and $k_{III}$, it was important to determine the best values of these constants. By use of the Oracle the least-squares values for each $k_i$ and the sum of the squares of the residuals of the fit,[5] $\Sigma r^2$, were determined from previous[4] data over a range of values for $x_e$, $y_e$, and $a$. The $k_i$ were then plotted as functions of $\Sigma r^2$, and the value chosen for $k_i$ in each case was that for which $\Sigma r^2$ was a minimum. The two additional[6] determinations of $k_{III}$ as well as the data[6] for the rate of racemization, $k_{IV}$, of optically active (+)-1,2,2-triphenylethyl acetate were analyzed by the same method. The results, given in Table 11, are compared with values obtained by the ordinary least-squares method.

From Table 11 it appears that $k_I$ and $k_{II}$ are identical within experimental error and that $k_{III}$ and $k_{IV}$ are also identical and about 20% larger than $k_I$ and $k_{II}$. Further, values obtained for $k_I$ and $k_{III}$ in the present study are in very close agreement with the values recalculated from data[4] obtained by different individuals four years earlier. Since the racemization rate, $k_{IV}$, was measured in an experiment in which another determination of $k_I$ was made, external deviations owing to lack of duplicability of conditions in this case were eliminated. It is interesting to compare the results of calculations by the ordinary least-squares method (column 3) with the values (column 4) given for the same data by the Oracle. The differences in $k_I$, in $k_{II}$, and in $k_{IV}$ as calculated by the two different methods are relatively small, and probably represent corrections for isotope effects and for minor errors in determining $x_e$, $y_e$, or $a$. The change in $k_{III}$, however, is considerable and can hardly be attributed to the same type of error. It is significant that plots of all data for $k_I$, $k_{II}$, and $k_{IV}$ show these rate constants to be reasonably steady throughout the reaction. Plots of the data for $k_{III}$, however, show a definite curvature, and it is clear that an ordinary least-squares calculation would give an answer for $k_{III}$ which is lower than that obtained by drawing a tangent to the curve at time zero, the slope of the tangent being equivalent to the "true" value of $k_{III}$.

It is sometimes the practice, when reporting kinetic data, to consider only the points representing the first third or half of the reaction – in which a plot of log $(1/f)$ vs $t$ appears to be a straight line – and to neglect the remaining data where curvature begins ($f$ = fraction reacted). The best least-squares fit of the data for the first 40% of reaction 3 – where a fairly good straight line can be drawn – does not give a realistic value for $k_{III}$. What is required in such cases is the slope of the tangent to the whole curve at time zero. That the values for $k_{III}$ given in the fourth column of Table 11 may be considered the slopes of such tangents is demonstrated as follows: If it is assumed that some fraction $b$ of the original concentration $a$ of III reacts rapidly with solvent and becomes unavailable for reaction, then

$$\frac{dz(t)}{dt} = k_{III}\,(a - b - z)\ ;$$

hence

$$k_{III} = \frac{1}{t}\ \ln \frac{a - b}{a - b - z}\ ,$$

and $k_{III}$ is the true rate constant for the fraction of III that is capable of reacting. Similar reasoning can be applied to cases in which a competing first-order reaction or a back reaction takes place.

[5] M. Ezekiel, *Methods of Correlation Analysis*, 2d ed., p 128–131, Wiley, New York, 1949.

[6] C. J. Collins and C. A. Krauth, *Chem. Ann. Prog. Rep. June 20, 1957*, ORNL-2386, p 55–57.

Table 11. First-Order Rate Constants for Isotope Position Isomerization and Racemization of 1,2,2-Triphenylethyl Acetate

| Experiment No. | Reactant | Rate Constant ($hr^{-1}$) | | |
|---|---|---|---|---|
| | | Ordinary Least-Square Value | Oracle Least-Square Value | Average of Oracle Values |
| | | $\times 10^{-2}$ | $\times 10^{-2}$ | $\times 10^{-2}$ |
| 1 | I[a] | 2.138 ± 0.052 | 1.989 ± 0.015 | $k_I = 2.03 \pm 0.08$ |
| 2 | I[a] | 2.136 ± 0.052 | 2.155 ± 0.052 | |
| 3 | I[b] | 1.961 ± 0.034[c] | 1.961 ± 0.034 | |
| 4 | II[a] | 1.940 ± 0.044 | 2.206 ± 0.032 | $k_{II} = 2.14 \pm 0.07$ |
| 5 | II[a] | 1.903 ± 0.028 | 2.075 ± 0.023 | |
| 6 | III[b] | 1.862 ± 0.074[d] | 2.400 ± 0.010[d]<br>2.425 ± 0.010[e] | $k_{III} = 2.46 \pm 0.08$ |
| 7 | III[b] | 1.807 ± 0.057[d] | 2.490 ± 0.022[d]<br>2.360 ± 0.015[e] | |
| 8 | III[a,f] | 1.869 ± 0.061 | 2.555 ± 0.030 | |
| 9 | IV[g] | 2.349 ± 0.048 | 2.425 ± 0.048 | $k_{IV} = 2.53 \pm 0.10$ |
| 10 | IV[h] | 2.479 ± 0.055 | 2.635 ± 0.053 | |

[a]Recalculated from data of ref 4.

[b]Calculated from data of this report.

[c]Corrected for degradative isotope effect of 4%.

[d]First five points used.

[e]All six points used.

[f]This is experiment 1 of Table VI, ref 4. Experiment 2 is not included because it was performed on doubly labeled 1,2,2-triphenylethyl acetate with a consequent large subtractive error. Experiment 3 of Table VI was run with a doubled concentration of *p*-toluenesulfonic acid, and the Oracle value for $k_{III}$ calculated therefrom is $(6.50 \pm 0.05) \times 10^{-2}\ hr^{-1}$.

[g]Calculated from polarimetric data on recovered acetate.

[h]Calculated from polarimetric data on recovered carbinol.

## STEREOCHEMISTRY OF THE DEAMINATION OF 1,2,2-TRIPHENYLETHYLAMINE

C. J. Collins

By the use of the same technique previously employed[7] for the deamination of (–)-1,2,2-triphenylethyl-1-$C^{14}$-amine at 36.5°C, the (+)-isomer has now been subjected to deaminating conditions at 25°C, and the product has been separated into olefin, acetate, and carbinol fractions. The carbinol was further separated into a racemic fraction and a fraction whose $[\alpha]_D^{25}$ is 121 deg. Degradation[7] of these fractions followed by radioactivity assay disclosed the fraction of $C^{14}$ scrambling. These results are given in Table 12. The (–)-carbinol, having an $[\alpha]_D^{25}$ of –122 deg, was subjected to the conditions of deamination[7] at 80°C, followed by quantitative reisolation. The reisolated carbinol exhibited an unchanged $[\alpha]_D^{25}$ of –122 deg. The carbinol is thus stable under the conditions of the deamination.

[7]C. T. Lester and C. J. Collins, *Chem. Ann. Prog. Rep. June 20, 1957*, ORNL-2386, p 54–55.

Table 12. Summary of Radiochemical Data for Various Fractions Obtained on Deamination of (+)-1,2,2-Triphenylethyl-1-$C^{14}$-amine at 25.0°C

| Product | Yield (%) | $[\alpha]_D^{25}$ (deg) | $C^{14}$ Rearrangement (%) |
|---|---|---|---|
| $Ph_2C^* = C^*HPh$ | 2.5 | | 25.5 |
| (+)-$Ph_2C^*H\overset{OAc}{\overset{\vert}{C}}{}^*HPh$ | 5.5 | | 24.0[a] |
| (+)-$Ph_2C^*H\overset{OH}{\overset{\vert}{C}}{}^*HPh$[b] | 92 | | |
| Fraction 1 | | 0 | 28.1 |
| Fraction 2 | | +121 | 26.5 |

[a] Per cent of total acetate fraction.
[b] The carbinol had an $[\alpha]_D^{24.7}$ of +34.9 deg, corresponding to 36% net inversion.

## OPTICAL CONFIGURATION OF (+)-1,2,2-TRIPHENYLETHYLAMINE AND (+)-1,2,2-TRIPHENYLETHANOL

### Chemical Methods

J. B. Christie[8]

In order to establish whether the (+)- and (−)-1,2,2-triphenylethanol obtained through crystallization of the partially racemic acetate[7] were completely resolved, a resolution of this material by conventional methods has been undertaken. The acid succinate of *dl*-1,2,2-triphenylethanol was successfully resolved both through the cinchonidine salt and through (+)- and (−)-1,1-diphenyl-1-aminopropanol-2 (ref 9). The (+)-carbinol had a melting point of 82 to 83°C and an $[\alpha]_D^{25}$ of +123 deg. The (−)-carbinol had a melting point of 82 to 83°C and an $[\alpha]_D^{25}$ of −123 deg. The carbinol previously[7] obtained was therefore completely resolved.

Since the work of Huisgen[10] and of White[11,12] has shown that the thermal decomposition of *N*-nitroso-acyl derivatives of optically active amines proceeds with a net retention of configuration, this same reaction was applied to the *N*-nitroso-*N*-acetyl-1,2,2-triphenylethylamine obtained from (+)-1,2,2-triphenylethylamine. It is inferred from these experiments that (+)-1,2,2-triphenylethylamine and its (+)-*N*-acetyl derivative possess the same configuration as (+)-1,2,2-triphenylethanol and (+)-1,2,2-triphenylethyl acetate.

### Physical Methods

C. J. Collins

Additional evidence that (+)-1,2,2-triphenylethylamine, (+)-1,2,2-triphenylethanol, and the (+)-acetyl derivatives of each possess the same configuration was obtained through two purely physical methods: (1) The optical rotary dispersion curves[13] of (+)-*N*-acetyl-1,2,2-triphenylethylamine and (+)-1,2,2-triphenylethyl acetate are very similar. (2) The Fredga[14–17] method of solid-liquid phase relationships of enantiomers was applied to derivatives of the carbinol and the amine. Although there was no evidence of the

[8] ORINS predoctoral Fellow.

[9] Furnished by B. M. Benjamin.

[10] R. Huisgen and C. Rüchardt, *Ann. Chem., Liebigs* 601, 21–39 (1956).

[11] E. H. White, *J. Am. Chem. Soc.* 77, 6014 (1955).

[12] E. H. White and C. A. Aufdermarsh, Jr., *J. Am. Chem. Soc.* 80, 2598 (1958).

[13] Furnished by C. Djerassi.

[14] A. Fredga, in *The Svedberg* (ed. by A. Tiselius and K. O. Pedersen), p 261 ff., Almqvist and Wiksells, Uppsala, Sweden, 1945.

[15] A. Fredga, *Arkiv Kemi* 11, 23 (1957).

[16] K. Mislow and M. Heffler, *J. Am. Chem. Soc.* 74, 3668 (1952).

[17] K. Mislow and W. C. Meluch, *J. Am. Chem. Soc.* 78, 5920 (1956).

formation of quasi-racemates or eutectics, the solidi were characteristically different in the case of mixtures of (+)-1,2,2-triphenylethyl acetate with (+)- and (−)-*N*-acetyl-1,2,2-triphenylethylamine, sufficiently to allow a tentative conclusion that the two compounds of like sign possess like configuration.[18]

## DETERMINATION OF ACTIVE HYDROGEN BY MEANS OF TRITIUM EXCHANGE

V. F. Raaen

Determination of active hydrogen in organic compounds has previously been accomplished by means of reactions which lead to the formation of gases whose volumes are directly proportional to the amount of active hydrogen. This has been done commonly with Grignard reagents (to produce methane or butane), with lithium aluminum hydride (to produce hydrogen), and occasionally with diazomethane (to produce nitrogen). Each of these methods of analysis has been adequately reviewed.[19] A possible alternative method for this type of analysis is based upon exchange of active hydrogen with isotopic hydrogen, followed by assay of the organic material for change in isotopic content. Although its potential has been obvious for some time, the exchange method has not previously been subjected to a detailed evaluation for routine application. The increased availability of tritium and the development of a good general technique for the assay of tritium-labeled organic compounds[20] made such a detailed evaluation seem advisable.

The convenience and the accuracy of isotopic exchange as a routine method for determining most types of active hydrogen have now been examined. The active hydrogen in a variety of organic compounds was exchanged for tritium from excess 2-propanol-$H^3_1$ of known radioactivity. An extremely simple exchange technique was employed. The radioactivity of each organic compound was then measured and compared with that expected from the known number of active hydrogen atoms in each.

The results have been submitted for publication.[21]

## REDUCTION OF TRIPHENYLACETONITRILE BY THE α-HYDROGEN ATOM OF BENZYLMAGNESIUM CHLORIDE[22]

V. F. Raaen

Certain reactions of nitriles with Grignard reagents have been best explained[23] by the assumption of the exchange of nitrile and magnesio chloride groups:

$$(1) \qquad RCN + R'MgCl \longrightarrow R'CN + RMgCl$$

In what has appeared to be "the most clear-cut example reported,"[23] treatment of triphenylacetonitrile (I) first with benzylmagnesium chloride and then with water produced triphenylmethane (II):[24]

$$(2) \qquad \underset{\mathrm{I}}{(Ph)_3CCN} \xrightarrow[(2)\ H_2O]{(1)\ PhCH_2MgCl} \underset{\mathrm{II}}{(Ph)_3CH}$$

If exchange occurs, the reactions producing triphenylmethane could be the following:[23]

$$(3) \quad (Ph)_3CCN + PhCH_2MgCl \longrightarrow (Ph)_3CMgCl + PhCH_2CN$$

$$(4) \quad (Ph)_3CMgCl + H_2O \longrightarrow (Ph)_3CH + Mg(Cl)(OH)$$

Although Eqs. 3 and 4 seem to provide a reasonable explanation[23] of reaction 2, such an explanation is now invalidated by the following findings: (1) When the proposed intermediates, triphenylmethylmagnesium chloride (III) and phenylacetonitrile (IV), are mixed and then treated with water,

---

[18] The author is indebted to K. Mislow of the Eidgenöss. Tech. Hochschule, Zurich, for pointing out the utility of the Fredga method in the present configurational relationship.

[19] G. F. Wright, p 155, and F. G. Arndt, p 197, in *Organic Analysis* (J. Mitchell *et al.*, eds.), vol 1, Interscience, New York, 1953.

[20] K. E. Wilzbach, L. Kaplan, and W. G. Brown, *Science* 118, 522 (1953).

[21] J. F. Eastham and V. F. Raaen, *Anal. Chem.* (in press).

[22] V. F. Raaen and J. F. Eastham, *J. Am. Chem. Soc.* 79, 6088 (1957).

[23] M. S. Kharasch and O. Reinmuth, *Grignard Reactions of Nonmetallic Substances*, p 779–782, Prentice-Hall, New York, 1954.

[24] P. Ramart-Lucas and M. F. Salmon-Legagneur, *Bull. soc. chim. France* 43, D321 (1928). Ramart-Lucas isolated the hydrocarbon (II) in 70% yield from the nitrile (I) by using excess Grignard reagent in boiling toluene. Analysis by isotopic dilution showed that II was formed to the extent of 97% in the toluene solvent at 70°C.

the yield of triphenylmethane is very small. (2) When the reaction between triphenylacetonitrile and benzylmagnesium chloride is carried out as described,[24] and the reaction mixture is then treated with excess carbon dioxide before hydrolysis, no triphenylacetic acid is formed. (3) If the reaction mixture of triphenylacetonitrile and benzylmagnesium chloride is hydrolyzed with water labeled with tritium, no tritium appears in the triphenylmethane. However, when the reaction is carried out with benzylmagnesium chloride labeled on the $\alpha$-carbon atom with tritium, tritium does appear in the triphenylmethane. The transfer of tritium takes place with an isotope effect of approximately 5. *Thus the source of hydrogen found ultimately in the triphenylmethane (II, Eq. 2) is the benzyl grouping in the original Grignard reagent.*

A possibility for the course of this reaction is shown in Eq. 5:

(5)

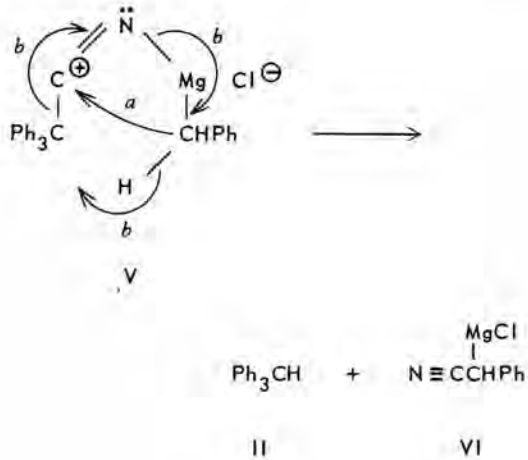


Once the complex (V) between nitrile and Grignard reagent is formed, there occurs both the commonly accepted[25] 1,3-shift of the benzyl group from magnesium to the nitrile carbon (arrow *a*) and a concerted shift of hydrogen and electrons around a six-membered quasi ring (arrows *b*). If these are the transformations which occur, phenylacetonitrile (from VI) should be isolable after hydrolysis. When the reaction was carried out with triphenylacetonitrile labeled in the nitrile group with $C^{14}$, labeled phenylacetonitrile was isolated after hydrolysis. In this run, isotopic dilution showed that the phenylacetonitrile was formed in 35% yield. All remaining $C^{14}$ was found in a nonvolatile, amorphous organic material formed presumably by polymerization[26] of VI.

## REACTION OF CYANOGEN WITH ARYLMETHYLMAGNESIUM HALIDE

V. F. Raaen

Cyanogen was found to react with various benzyl-type Grignard reagents to give *o*-cyano derivatives in 40 to 60% yield. These reactions are illustrated in Eqs. 1, 2, and 3:

(1)

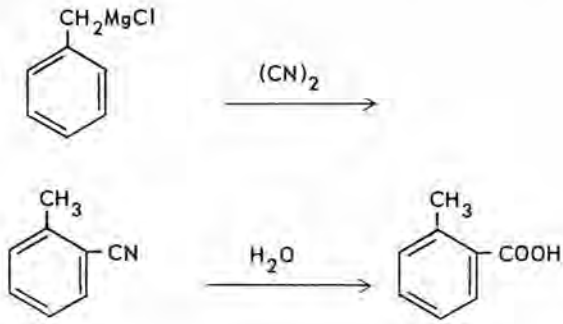


(2)

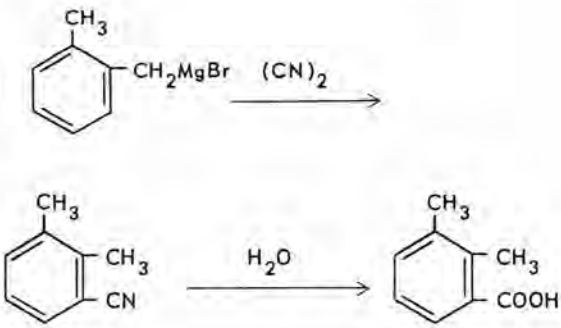


[25] C. G. Swain, *J. Am. Chem. Soc.* **69**, 2306 (1947). See also M. S. Kharasch and O. Reinmuth, *Grignard Reactions of Nonmetallic Substances*, p 767–769, Prentice-Hall, New York, 1954.

[26] A. Rondou, *Bull. soc. chim. Belg.* **31**, 231 (1922).

(3) 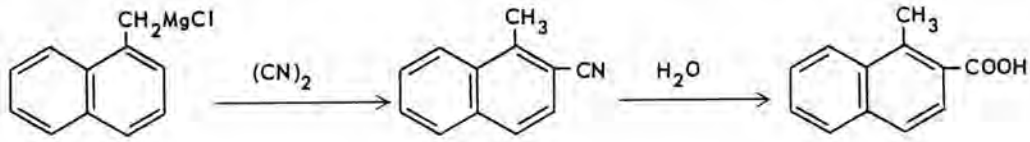


These reactions are the first examples of an ortho substitution that does not involve a carbon-oxygen linkage.

A particularly interesting example of this new ortho-substitution reaction occurs with 2,6-dimethylbenzylmagnesium chloride, in which both ortho positions are blocked (Eq. 4):

(4) 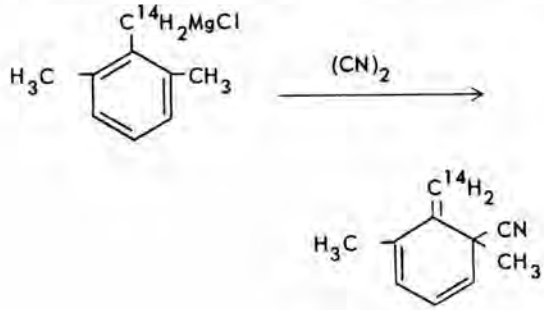


The product, 1,5-dimethyl-6-methylene-5-cyano-1,3-cyclohexadiene, was formed with interruption of benzene aromaticity. This triene proved to be unstable, and samples of it were half converted to a dimer (Eq. 5), apparently as a result of a Diels-Alder reaction:

(5) 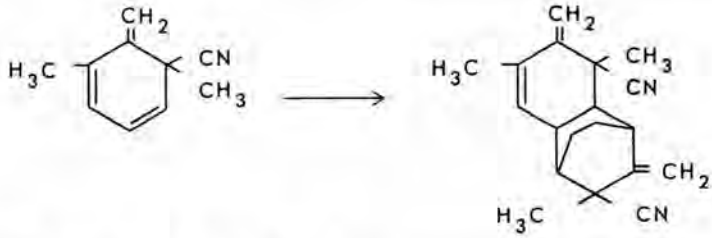


Because of these new findings, the study of the reaction of benzyl Grignard reagents with nitriles was extended to include cyanogen bromide. However, reaction between excess cyanogen bromide and benzylmagnesium chloride proceeded in the conventional manner, and benzyl bromide was formed as shown in Eq. 6:

(6) $BrCN + PhCH_2MgCl \longrightarrow PhCH_2Br + Mg(CN)Cl$

The benzyl bromide was obtained in 69% yield from benzyl chloride. A portion of the foregoing data has been published.[27]

## THE CARBON ISOTOPE EFFECT IN THE PINACOL-PINACOLONE REARRANGEMENT: A REINVESTIGATION

V. F. Raaen C. J. Collins

Intermolecular carbon-isotope effects in the acid-catalyzed rearrangements, above 80°C, of 2,3-dimethyl-2,3-butanediol-2-$C^{14}$ (I) and 2,3-dimethyl-2,3-butanediol-2-methyl-$C^{14}$ (II) have been reported recently:[28]

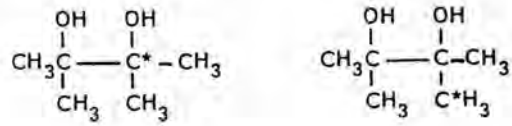


I II

The magnitude of these reported isotope effects ($k^*/k$ for I, 0.74; $k^*/k$ for II, 0.48) is astonishing, particularly in the case of II, in which the isotopic bond should never be directly involved in the initial bond-breaking process. In addition, the data of Duncan and Lynn violate, in two instances,[29] the law of conservation of mass.

[27] J. F. Eastham and V. F. Raaen, *Proc. Chem. Soc.* 1958, 149.

[28] J. F. Duncan and K. R. Lynn, *Australian J. Chem.* 10, 7–25 (1957).

[29] *Ibid.*, p 18, Table 11, line 3.

Therefore a reinvestigation was made of the intermolecular isotope effects in the acid-catalyzed rearrangements of I and II. The results showed that, in the presence of 0.295 *N* hydrochloric acid at 100°C, I exhibits an intermolecular isotope effect of 3% ($k^*/k = 0.97$) and that II exhibits no isotope effect at all ($k^*/k = 1.00$).

Acetic-1-$C^{14}$ acid was converted[30] to acetone-*carbonyl*-$C^{14}$ by passage over manganous carbonate at 420–450°C. The 2,4-dinitrophenylhydrazone of the acetone had a melting point of 125–126°C and a radioactivity assay of 2.239 ± 0.001 mc/mole. Isotope position isomer I was prepared from the foregoing acetone.[31] The hexahydrate of I had a melting point of 45.5–47°C. Periodate[28] cleavage of I produced acetone-*carbonyl*-$C^{14}$ whose 2,4-dinitrophenylhydrazone had a melting point of 125–126°C and a radioactivity assay of 2.215 ± 0.005 mc/mole.

Compound I (3.00 g, hexahydrate) was allowed to react for 30 min with 400 ml of 0.295 *N* hydrochloric acid at 100 ± 0.5°C, and the reaction was then quenched in ice water containing sodium bicarbonate. The organic material was isolated by continuous extraction with ether, and the unreacted pinacol (1.2 g) was isolated from the ether solution as the hexahydrate after addition of a minimum quantity of water. Periodate[28] cleavage of the recovered pinacol yielded acetone-*carbonyl*-$C^{14}$ whose 2,4-dinitrophenylhydrazone had a melting point of 125–126°C and a radioactivity assay of 2.240 ± 0.004 mc/mole. The pinacolone remaining in the foregoing ether solution was converted to the 2,4-dinitrophenylhydrazone, whose melting point was 126–127°C (depressed upon mixing with acetone-2,4-dinitrophenylhydrazone) and whose radioactivity assay was 4.388 ± 0.012 mc/mole.

Compound II was prepared from redistilled biacetyl (boiling point 83–84°C) and methyl-$C^{14}$-magnesium iodide. The hexahydrate of II had a melting point of 45–46.5°C. A repetition of the experiment described above (by which I was subjected to rearrangement) led to the reisolation of 2.1 g of II-hexahydrate. Cleavage of reisolated II by periodate produced acetone-*methyl*-$C^{14}$ whose 2,4-dinitrophenylhydrazone had a melting point of 125–126°C and a radioactivity assay of 2.062 ± 0.001 mc/mole (2 × 2.062 = 4.124 ± 0.002). The 2,4-dinitrophenylhydrazone of the pinacolone isolated from the same reaction mixture had a melting point of 126–127°C and a radioactivity assay of 4.122 ± 0.017 mc/mole. From the kinetic data of Duncan and Lynn[32] the conditions for both of the foregoing experiments correspond to values of $a/(a - x)$ in the first-order rate equation of 1.36, or a value of $f$ (fraction reacted) of 0.264. From these data, therefore, it can be calculated[33,34] that the isotope effects are, within experimental error, for the rearrangement of I, $\leqq 0.03$, and for the rearrangement of II, zero.

## ISOTOPIC STUDIES OF THE DECARBONYLATION OF CARBOXYLIC ACIDS IN CONCENTRATED SULFURIC ACID

G. A. Ropp

Several types of acids are known to lose carbon monoxide quantitatively when dissolved in concentrated sulfuric acid at room temperature:

$$\mathrm{RCOOH} \xrightarrow{H_2SO_4} \mathrm{ROH} + \mathrm{CO}\uparrow$$

The mechanism usually assumed involves a protonation of the carboxyl-group oxygens followed by breakup of the protonated species:

$$R-\overset{\overset{\displaystyle O}{\|}}{C}-\overset{\oplus}{O}H \xrightarrow{\text{activation}} R\overset{\alpha}{\cdots}\overset{\overset{\displaystyle O}{\|}}{C}\overset{\beta}{\cdots}\overset{\oplus}{O}H \longrightarrow$$

$$R^{\oplus} + CO + H_2O \xrightarrow{H_2SO_4} \text{product}$$

However, nothing has been previously known about whether the stretching of the bond $\alpha$ or the bond $\beta$ is critical in determining the rate.

For the case of formic acid (R = H) the low deuterium isotope effect found[35] in the decarbonylation of formic-*d* acid, DCOOH, indicated

[30] W. M. Cumming, I. V. Hopper, and T. S. Wheeler, *Systematic Organic Chemistry*, 4th ed., p 101, Constable, London, 1950.

[31] R. Adams and E. W. Adams, in *Organic Syntheses* (H. Gilman, Editor-in-Chief), coll vol I, 2d ed., p 459, Wiley, New York, 1941.

[32] J. F. Duncan and K. R. Lynn, *J. Chem. Soc.* **1956**, 3514, Table 2.

[33] W. H. Stevens and R. W. Attree, *Can. J. Research* **27B**, 807 (1949).

[34] J. Y. P. Ton and P. E. Yankwich, *J. Phys. Chem.* **61**, 540 (1957).

[35] G. A. Ropp, *Chem. Ann. Prog. Rep. June 20, 1957*, ORNL-2386, p 57.

that the bond $\beta$ was the critical bond. In the case where R is the triphenylmethyl group, the acid was labeled with $C^{14}$ to give triphenylacetic-$\alpha$-$C^{14}$ acid, $(C_6H_5)_3\ C^{14}-COOH$. The decarbonylation at 25°C was carried to 40% completion, and the relative values of the various molar specific activities reported in Table 13 indicated $k_{12}/k_{14} \leq 1.01$. The low $C^{14}$ isotope effect indicates that the bond $\beta$ is critical in the rate of this reaction also.

It may be that cleavage of the bond $\beta$ in both these cases is critical because stability of the ion $R^{\oplus}$ in the medium results in weakness of the bond $\alpha$. In the case of formic acid, $R^{\oplus}$ would represent a proton. For the case of triphenylacetic acid, $R^{\oplus}$ would represent the highly resonance-stabilized triphenylmethyl carbonium ion. It was logical to study also a case where $R^{\oplus}$ would represent a carbonium ion not so highly resonance-stabilized as the triphenylmethyl carbonium ion. The decarbonylation of benzoylformic-$\alpha$-$C^{14}$ acid was chosen. Here $R^{\oplus}$ would be the positive benzoyl ion, $C_6H_5CO^{\oplus}$, for which few resonance forms can be drawn.

The decarbonylation of benzoylformic-$\alpha$-$C^{14}$ acid was first studied to learn the origin of the carbon monoxide. Since the carbon monoxide was nonradioactive, it came from the carbonyl group just as it necessarily did in the decarbonylation of formic and triphenylacetic acids. The $C^{14}$ isotope effect data of Table 14 for two independent experiments indicate clearly a value of $k_{12}/k_{14}$ of about 1.03. The relatively large $C^{14}$ isotope effect in this reaction indicates that the breaking of bond $\alpha$ plays a significant role in the rate step. It may be that cleavages of both $\alpha$ and $\beta$ play important parts. It does appear, however, that at least two types of rate processes can control decarbonylation reaction rates in concentrated sulfuric acid and that the structure of the group R determines which process is critical in determining the reaction rate for a particular acid.

**Table 13. Isotope Fractionation Study of the Decarbonylation of Triphenylacetic-$\alpha$-$C^{14}$ Acid at 25°C**

| Compound Assayed | Per Cent Reaction | Activity (mc/mole) |
|---|---|---|
| Triphenylacetic-$\alpha$-$C^{14}$ acid | 0 | 1.940 ±0.25% |
| Triphenylcarbinol-$\alpha$-$C^{14}$ | 100 | 1.950 ±0.5% |
| | 40 | 1.930 ±0.2% |
| Triphenylacetic-$\alpha$-$C^{14}$ acid (60% recovered unreacted) | 40 | 1.942 ±0.35% |

## EXCHANGE OF CARBON MONOXIDE-$O^{18}$ WITH 96% SULFURIC ACID

G. A. Ropp

In an attempt to study the kinetic $O^{18}$ isotope effect during the decarbonylation of formic-$O^{18}$ acid in excess 96% $H_2SO_4$, an oxygen isotope

**Table 14. Isotope Fractionation Study of the Decarbonylation of Benzoylformic-$\alpha$-$C^{14}$ Acid at 25°C**

| Experiment No. | Compound Assayed | Per Cent Reaction | Sample Represents | Activity (mc/mole) |
|---|---|---|---|---|
| 1 | Benzoylformic-$\alpha$-$C^{14}$ acid | 0 | Starting acid | 1.840 ±0.7% |
| | Benzoic-$\alpha$-$C^{14}$ acid | 100 | Starting acid | 1.840 ±0.2% |
| | | 40 | Product | 1.802 ±0.8% |
| | Benzoylformic-$\alpha$-$C^{14}$ acid | 40 | Recovered unreacted starting acid | 1.897 ±0.9% |
| 2 | Benzoic-$\alpha$-$C^{14}$ acid | 100 | Starting acid | 1.845 ±0.3% |
| | | 50 | Product | 1.805 ±0.3% |
| | | 50 | Unreacted starting acid (recovered and quantitatively converted to benzoic-$\alpha$-$C^{14}$ acid) | 1.914 ±0.1% |

exchange between the reaction product carbon monoxide-$O^{18}$ and the sulfuric acid medium was observed. Table 15 was obtained from mass spectrometric data[36] and indicates the approximate rate of loss of $O^{18}$ from the carbon monoxide phase. The sample of $COO^{18}$ was obtained by complete oxidation of a formic-$O^{18}$ acid sample with chlorine gas and hence represents (after division by 2) the carbon monoxide at time zero. The formic-$O^{18}$ acid was completely converted to carbon monoxide-$O^{18}$ in the first 20 min. The three analyses of $CO^{18}$ represent successive samplings of the carbon monoxide gas.

The $C^{13}$ analyses provided a test for leakage of air into the system. If the decrease in per cent of $O^{18}$ had been caused by leakage of nitrogen (mass 28) into the carbon monoxide, the per cent $C^{13}$ would have decreased at the same rate. This was not the case, as Table 15 shows. It is possible that the $O^{18}$ exchange actually takes place between the carbon monoxide and the water in the sulfuric acid. A conceivable symmetrical intermediate which, if formed even in low concentrations, could account for the exchange is dihydroxymethylene, HO-C-OH.

## MASS SPECTROMETRIC STUDIES OF LABELED FORMIC ACIDS[37]

G. A. Ropp C. E. Melton

From mass spectrometric studies in which formic-*d* acid (DCOOH) and formic acid-*d* (HCOOD) were used, it has been shown that, upon electron impact, formic acid yields positive ions ($CHO_2^+$ and $CHO^+$) by loss of hydrogen from either position. By contrast, a negative ion of mass 45 ($HCOO^-$) is formed almost exclusively by loss of hydrogen from the oxygen attachment. A negative ion of mass 91 ($HCOOH \cdot HCOO^-$) apparently is formed by loss of hydrogen attached to oxygen in the known dimer of formic acid. Relative sensitivities of formic, acetic, and propionic acids to formation of this type of negative ion were found to be parallel to the acid strengths of these acids in solution.

## DETECTION OF CYANIDE ($CN^-$) IN A MIXTURE OF FORMIC ACID AND NITROGEN IN A RESEARCH MASS SPECTROMETER

C. E. Melton G. A. Ropp

A research mass spectrometer of 6-in. radius was modified to provide an essentially field-free region between the ionization chamber and the first accelerating plate. A gas can be introduced through the variable leak into this field-free region. Thus ions produced in the ionization chamber from a second gas can be passed at low energy through neutral molecules of the first gas. Since the pressure inside the ionization chamber is kept one order of magnitude higher than that in the field-free region,[38] little back diffusion occurs. It is therefore possible to determine which of two species furnishes the ion in an ion-molecule reaction by inverting the mode of addition of the two gases and noting the effect on the relative abundance of a product ion.

[36] Mass spectrometric analyses were performed by J. R. Sites, Analytical Chemistry Division.

[37] G. A. Ropp and C. E. Melton, *J. Am. Chem. Soc.* **80**, 3509 (1958).

[38] G. F. Wells and C. E. Melton, *Rev. Sci. Instr.* **28**, 1065 (1957).

**Table 15. Exchange of Carbon Monoxide-$O^{18}$ with 96% Sulfuric Acid**

| Sample Analyzed | Contact Time | | Per Cent $C^{13}$ | Per Cent $O^{18}$ |
|---|---|---|---|---|
| | Hot | Cold | | |
| $COO^{18}$ | | | 1.24 | 1.07* |
| $CO^{18}$ | 15 min at 80°C | 4 days | 1.13 | 0.54 |
| | 15 min at 80°C | 4 days | 1.12 | 0.49 |
| | 2 hr at 60°C | Shaken 60 hr | 1.11 | 0.35 |
| Normal composition | | | 1.1 | 0.2 |

*After division by 2.

Formic acid introduced into the ionization chamber was ionized by electrons with an indicated energy of 2.3 ev. Under these conditions essentially no positive ions[39] are produced, but instead a homogeneous beam of $HCOO^-$ ions. With the field-free region filled with nitrogen gas, a new negative ion of mass 26 was detected. Its mass was not affected by substitution of DCOOH for the formic acid. Substitution of either $HC^{13}OOH$ for formic acid or nitrogen-$N^{15}$ for nitrogen shifted the mass of the new ion to 27. Use of both $HC^{13}OOH$ and nitrogen-$N^{15}$ in the same experiment caused an ion of mass 28 to appear. When carbon monoxide or carbon dioxide was substituted for formic acid, the new ion failed to appear. It was concluded that the new negative ion was $CN^-$. Since the positive peaks known to arise from hydrogen cyanide and cyanogen[40–42] were absent even with the electron energy raised to 75 ev, neither of these substances was the precursor.

When an equimolar mixture of nitrogen and formic acid at 2 mm pressure was subjected to spark discharge, 1% hydrogen cyanide was found in the product mixture.

In the mass spectrometric study, some active species produced from formic acid in the ionization chamber apparently reacts with nitrogen molecules to give rise to $CN^-$ ions.

[39] T. Mariner and W. Bleakney, *Phys. Rev.* 72, 792 (1947).

[40] C. A. McDowell and J. W. Warren, *Trans. Faraday Soc.* 48, 1084 (1952).

[41] K. E. Dorsch and H. Kallmann, *Z. Physik* 60, 376 (1930).

[42] J. T. Tate, P. T. Smith, and A. L. Vaughan, *Phys. Rev.* 48, 525 (1935).

## EXTRACTION OF TRIBUTYL PHOSPHATE FROM NONPOLAR SOLVENTS

W. H. Baldwin C. E. Higgins

Tributyl phosphate (TBP) has become a useful reagent for the separation of uranium, thorium, and plutonium. Generally, TBP is dissolved in a nonpolar solvent (such as kerosene) for contacting aqueous solutions. Most of the TBP remains in the organic phase. We have found that the TBP can be extracted from hydrocarbon diluents into polar organic solvents (e.g., certain glycols). This observation could be useful for the purification of TBP from process solutions.

To 5-ml volumes of each of the two phases (polar and nonpolar) were added measured volumes of TBP labeled with $P^{32}$. The mixture was tumbled end over end for 45 min in a bath at 25.0 ± 0.2°C, centrifuged for 20 sec, then held undisturbed in the bath for 2 hr. Aliquots from each phase were counted for $P^{32}$ activity to estimate the distribution. A few representative results have been summarized in Table 16.

**Table 16. Distribution of Tributyl Phosphate Between Organic Solvents**

| Polar Solvent | Nonpolar Solvent | Volume Ratio of TBP, $x$* | $E_N^{P}$** |
|---|---|---|---|
| 1,2-Propanediol | Amsco 125-82 | 0.01 | 2.4 |
| | Amsco 125-82 | 0.25 | 2.7 |
| | Amsco 125-82 | 1.0 | 2.2 |
| | *n*-Hexane | 0.01 | 1.2 |
| | Dibutyl ether | 0.01 | 0.6 |
| | Carbon tetrachloride | 0.25 | 0.5 |
| | Benzene | 0.01 | 0.3 |
| Dipropylene glycol | *n*-Hexane | 0.01 | 1.9 |
| Triethylene glycol | *n*-Hexane | 0.01 | 0.5 |
| Diethylene glycol | *n*-Hexane | 0.01 | 0.5 |
| Ethylene glycol | *n*-Hexane | 0.01 | 0.1 |
| Ethanolamine | *n*-Hexane | 0.01 | 0.06 |
| 1,3-Propanediol | *n*-Hexane | 0.01 | 0.5 |

*$x$ volumes TBP, 1 volume polar solvent, 1 volume nonpolar solvent.

**Ratio of the $P^{32}$ activity (counts/min/ml) in the polar solvent to the activity in the nonpolar solvent.

The polar solvents examined were glycols or amino alcohols, while the nonpolar solvents examined were hydrocarbons, dibutyl ether, and carbon tetrachloride.

An apparent relationship was observed between the structure of the glycol and the distribution of TBP between the glycol and the nonpolar solvents. 1,2-Propanediol extracted more TBP from *n*-hexane than did either 1,3-propanediol or ethylene glycol. Ethanolamine extracted less TBP than any of the glycols mentioned.

It is to be noted that 1,2-propanediol extracted TBP readily from Amsco 125-82. The extraction as indicated by the distribution coefficient ($E_N^P$, Table 16) was not appreciably affected by the concentration of the TBP.

## EFFECTS OF ELECTROLYTES AND TEMPERATURE ON THE SOLUBILITY OF TRIBUTYL PHOSPHATE IN WATER

C. E. Higgins W. H. Baldwin
B. A. Soldano

The solubility of tributyl phosphate (TBP), labeled with $P^{32}$, in aqueous solutions of univalent electrolytes was measured at temperatures ranging from 5 to 50°C. The electrolytes used included the chlorides, bromides, and iodides of hydrogen and lithium; sodium and potassium iodides; silver nitrate; and nitric acid.

The Setchenow equation[43]

$$\log \frac{S_0}{S} = k_s C_s \ ,$$

where

$S_0$ = solubility of TBP in water,
$S$ = solubility of TBP in aqueous electrolyte solution,
$C_s$ = concentration of electrolyte,
$k_s$ = salting coefficient,

was shown to represent the data adequately.

The salting coefficient $k_s$ was essentially independent of temperature.

## DISTRIBUTION OF MONOVALENT ELECTROLYTES BETWEEN WATER AND TRIBUTYL PHOSPHATE

W. H. Baldwin C. E. Higgins
B. A. Soldano

Aqueous solutions of monovalent electrolytes were shaken with pure tributyl phosphate. The two phases were separated and analyzed. The electrolyte concentration was determined in each phase, and water was determined in the organic phase.

Two mechanisms (based upon water behavior) were observed. In one mechanism, water accompanied the electrolytes; in the other mechanism the electrolyte was not accompanied by water. A linear correlation was found to exist between the standard free energy change and the Gurney unitary partial molal entropy.[44]

## DISPERSION OF THORIUM DIOXIDE IN NONPOLAR SOLVENTS

W. H. Baldwin

Slurries of thorium or uranium oxides are potentially useful systems for fuels and blankets in reactors. It has also been proposed that organic fluids be employed in reactors. The present study was initiated with the dispersion of $ThO_2$ in biphenyl, since aromatic hydrocarbons exhibit greater stability to radiolysis than most other organic compounds.

It has been shown by Harkins *et al.*[45–47] that pigments such as $TiO_2$ can be dispersed in benzene with the aid of certain additives. They report that (1) effective dispersing agents included high-molecular-weight acids and salts of these acids, (2) the dispersing agent was adsorbed from benzene by $TiO_2$, (3) the settling rate of the pigment was reduced by the dispersing agent and was a function of the amount adsorbed on the $TiO_2$, (4) the final settled volume of $TiO_2$ was reduced by and was a function of the amount of the dispersing agent adsorbed, and (5) water competed with the dispersing agent for adsorption on the $TiO_2$.

The final settled volume of $ThO_2$ was used here as a measure of the effectiveness of dispersing agents on $ThO_2$ in molten biphenyl. Usually, 5 g of $ThO_2$ (supplied by J. P. McBride) was

---

[43] P. M. Gross, *Chem. Rev.* 13, 91 (1933).

[44] R. W. Gurney, *Ionic Processes in Solution*, McGraw-Hill, New York, 1953.

[45] W. D. Harkins and R. Dahlstrom, *Ind. Eng. Chem.* 22, 897 (1930).

[46] W. D. Harkins and D. M. Gans, *J. Phys. Chem.* 36, 86 (1932).

[47] L. W. Ryan, W. D. Harkins, and D. M. Gans, *Ind. Eng. Chem.* 24, 1288 (1932).

placed in a pyrex tube (0.9 cm ID × 30 cm, sealed and flattened on one end) and heated at 145°C for at least 20 hr. Molten biphenyl (10 g, distilled through a 20-in. column) and the desired amount of dispersing agent were then added. The tube and its contents were evacuated to 0.1 mm and degassed by a combination of freezing and thawing. The tube was sealed at this reduced pressure.

The sealed tubes were held at 145°C with occasional shaking by hand. They were then placed in a vertical position and allowed to settle for 16 hr. They were shaken again and allowed to settle again. The height of the settled column was measured, and the volume for 1 g of $ThO_2$ was calculated.

Water was shown to have no influence on the settled volume when benzoic acid (0.08 meq per gram of $ThO_2$) was the dispersing agent. Added water was displaced at the temperature used (145°C), and visible droplets condensed in the vapor space above the biphenyl when the tubes were quenched.

A few selected results (Table 17) reveal that an additive of high molecular weight, such as stearic acid, is not essential. Benzoic acid, which has a much lower molecular weight, was equally effective. Compounds other than carboxylic acids are likewise useful, for example, *p*-hydroxybiphenyl and benzenesulfonic acid.

Another useful technique was supplied by J. P. McBride. The oxide was pretreated with a commercial mixture of methylsilicon chlorides (Dri-Film), which polymerizes on surfaces and renders them water-repellent. The material so treated was dispersed in biphenyl but somewhat less effectively than material treated with some of the adsorbed materials (see Table 17).

**Table 17. Effect of Additives on the Settled Volume of $ThO_2$**

| Additive* | Settled Volume (cc per gram of $ThO_2$) |
|---|---|
| None | 0.85 |
| Stearic acid | 0.43 |
| Benzoic acid | 0.40–0.46 |
| Benzenesulfonic acid | 0.44 |
| *p*-Hydroxybiphenyl | 0.43 |
| Uranyl dibenzoate | 0.50 |
| Treated with Dri-Film | 0.57 |

*0.08 to 0.1 meq per gram of $ThO_2$.

## DETERMINATION OF EQUIVALENT WEIGHT OF ESTERS AND HALIDES WITH CATION EXCHANGE RESINS

W. H. Baldwin C. E. Higgins

A report has been published under the above title[48] summarizing some observations on the quantitative reaction of relatively inert compounds. Although the esters of sulfur and phosphorus acids and certain halides are relatively inert to the usual hydrolytic reagents (NaOH, NaOR), they do react with amines (e.g., ethanolamine), forming salts of the substituted ammonium type. These salts can then be decomposed with cation exchange resins in the hydrogen form, liberating acids that are titrated with standard alkali.

[48] W. H. Baldwin and C. E. Higgins, *Anal. Chem.* **30**, 446 (1958).

# CHEMISTRY OF AQUEOUS SYSTEMS

## PHYSICAL CHEMISTRY OF ION EXCHANGERS

### Properties of a New Strong-Base Anion Exchanger Containing Structurally Bound Tertiary Sulfonium Cations[1]

S. Lindenbaum G. E. Boyd
G. E. Myers

Selectivity coefficients, rates of anion exchange, water absorption isotherms, and the absorptions of Zn(II) and Fe(III) from concentrated electrolyte solutions were measured by using a new methylene-cross-linked strong-base anion exchanger (Stamex S-44) containing structurally bound tertiary sulfonium cations. The selectivity coefficient scale, determined by using 13 anion salt forms, was nearly identical with that for quaternary-ammonium-type anion exchangers. The greater the water uptake at saturation vapor pressure by a given salt form, the greater the bromide ion affinity. The tertiary sulfonium anion exchanger was appreciably more hydrated at low water vapor activities than was the quaternary ammonium type, whereas the converse held for high water activities. The self-exchange of bromide ion in the sulfonium exchanger at 25°C occurred with a self-diffusion coefficient of $1.18 \times 10^{-7}$ $sec^{-1}$, which is notably smaller than the coefficient observed[2] with a comparable quaternary-ammonium-type exchanger at the same temperature. Micro quantities of Zn(II) and Fe(III) were strongly absorbed from hydrochloric acid and lithium chloride solutions, and this absorption increased with electrolyte concentration in a manner similar to that found with quaternary-ammonium-type anion exchangers.

### Equilibrium Measurements with Cation and Anion Exchangers of Variable Capacity[3]

S. Lindenbaum C. F. Jumper
G. E. Boyd

Measurements at 25°C of the equilibrium selectivity coefficients for the exchange of $Na^+$ with $H^+$, $NH_4^+$, and $Cs^+$ ions and for $Cs^+$ with $NH_4^+$ ion were conducted with two series of specially synthesized[4] polystyrene sulfonic acid cation exchangers of varying exchange capacity. Selectivity coefficients for the exchange of $Br^-$ with $Cl^-$ ion were also measured by using variable-capacity, strong-base quaternary ammonium anion exchangers.[5] In all exchanges, except those with $H^+$ ion, the selectivity coefficient decreased as the capacity increased when the cross-linking was held constant. This behavior is contrary to the statistical thermodynamic theory of cross-linked ion exchangers by Rice and Harris,[6] which predicts that increased exchange capacity increases the ion binding and therewith the selectivity.

### Model Studies of Ion Exchange Mechanisms with Liquid Ion Exchangers[7]

G. E. Boyd S. Lindenbaum

Solutions of dimethyldidodecenylammonium chloride, tri-*n*-octylamine, dinonylnaphthalenesulfonic acid, and di-2-ethylhexylphosphoric acid in nonpolar organic liquids serve as analogs of cross-linked strong- and weak-base resinous anion exchangers and of the strong- and weak-acid cation exchangers, respectively. These liquid ion exchangers offer several advantages in the study of ion exchange mechanisms: (1) they can be used for studies of equilibria in concentrated electrolyte solutions without Donnan penetration of the exchanger phase; (2) the rates of exchange appear to be extremely rapid; (3) measurements of physical properties of the exchangers, such as conductivity and dielectric strength, are more conveniently performed than with resinous exchangers.

Measurements of equilibrium selectivity and of distribution coefficients with these liquid ion exchangers aid in generalizing and in elucidating the more complex behavior of cross-linked polymeric

---

[1] S. Lindenbaum, G. E. Boyd, and G. E. Myers, *J. Phys. Chem.* 62, 995 (1958).

[2] B. A. Soldano and G. E. Boyd, *J. Am. Chem. Soc.* 75, 6099 (1953).

[3] S. Lindenbaum, C. F. Jumper, and G. E. Boyd, *Abstracts of Papers, 134th National Meeting of the American Chemical Society, Chicago, Ill., Sept. 7–12, 1958*, p 181, paper 43.

[4] R. H. Wiley and J. M. Schmitt, *J. Am. Chem. Soc.* 78, 2169 (1956).

[5] R. H. Wiley and J. M. Schmitt, *J. Am. Chem. Soc.* 80, 1389 (1958).

[6] S. A. Rice and F. Harris, *Z. physik. Chem.* (Frankfurt) 8, 207 (1956).

[7] G. E. Boyd and S. Lindenbaum, *Abstracts of Papers, 134th National Meeting of the American Chemical Society, Chicago, Ill., Sept. 7–12, 1958*, p 171, paper 42.

exchangers. For example, the effect of varying exchange capacity on the selectivity coefficients for the $Br^-/Cl^-$ anion exchange was examined. As the concentration of dimethyldidodecenylammonium chloride in toluene increased, the selectivity for $Br^-$ ion decreased for all "loadings" of the liquid exchanger. This result is in agreement with experiments on variable-capacity resinous exchangers.

Measurements of the distribution of Zn(II) ion between liquid anion exchangers and aqueous hydrochloric acid or lithium chloride solutions as a function of aqueous chloride ion concentration showed pronounced similarities to the behavior found with cross-linked exchangers. The distribution of Fe(III) ion between aqueous hydrochloric acid and dinonylnaphthalenesulfonic acid dissolved in benzene, as a function of acid concentration, was also similar to that observed with a cross-linked polystyrene sulfonic acid exchanger.

### Calorimetric Measurements of the Heats of Cation Exchange[8]

F. Vaslow G. E. Boyd

The heats of exchange of $Na^+$ ion with $H^+$, $Li^+$, $K^+$, and $Cs^+$ ions in a series of six differently cross-linked polystyrene sulfonate-type cation exchangers (viz., Dowex 50) were determined at 25°C as a function of the resin "loading." Differential heats were measured by using a vacuum-walled calorimeter equipped with a 36-junction copper-constantan thermocouple, a glass pipet for holding the ion exchanger, a resistance heater for electric calibration, and a stirrer and a stirrer tube to facilitate good mixing. The heat effects were evolved within 2 to 3 min.

Integral heats of exchange, $\Delta H^0$, were estimated for the hypothetical process

$$\underset{\substack{a=1\\ \text{equilibrated with}\\ 0.1\ N\ \text{NaX}}}{R_4NX} + \underset{\substack{a=1\\ \text{aqueous}}}{NaBr} \rightleftharpoons \underset{\substack{a=1\\ \text{equilibrated with}\\ 0.1\ N\ \text{NaBr}}}{R_4NBr} + \underset{\substack{a=1\\ \text{aqueous}}}{NaX} + \underset{a_w=1}{xH_2O}$$

Equilibrium measurements previously published[9] on these same systems were used to compute $\Delta F^0$ values so that standard entropy changes, $\Delta S^0$, were obtainable.

The magnitudes of $\Delta H^0$ varied from −300 to −1800 cal per mole exchanged. The least heat was evolved in the exchanges between cations of nearly the same degree of hydration, and the most was evolved when these hydrations differed greatly. The heat evolved increased with ion exchanger cross-linking: rapidly at first, and then more slowly. In these systems the entropy changes were negative (as were $\Delta H^0$ and $\Delta F^0$) for the uptake of the preferred ion. The magnitude of $\Delta F^0$ is, of course, determined by the balance between the lowering of the enthalpy and the decrease in the entropy.

### Calorimetric Measurements of the Heats of Anion Exchange[10]

F. Vaslow G. E. Boyd

Differential heats of exchange, $\Delta\bar{H}$, of $Br^-$ ion with $F^-$, $Cl^-$, and $I^-$ ions were measured at 25°C as a function of resin "loading" by using a series of five differently cross-linked polystyrene quaternary-ammonium-type anion exchangers (viz., Dowex 2). Integral heats of exchange, $\Delta H^0$, for the hypothetical process

$$\underset{\substack{a=1\\ \text{equilibrated with}\\ 0.1\ N\ \text{MCl}}}{MR} + \underset{\substack{a=1\\ \text{aqueous}}}{NaCl} \rightleftharpoons \underset{\substack{a=1\\ \text{equilibrated with}\\ 0.1\ N\ \text{NaCl}}}{NaR} + \underset{\substack{a=1\\ \text{aqueous}}}{MCl} + \underset{a_w=1}{xH_2O}$$

[8] F. Vaslow and G. E. Boyd, *Abstracts of Papers, 133rd National Meeting of the American Chemical Society, San Francisco, Calif., April 13–18, 1958*, p 18I, paper 46.

[9] G. E. Myers and G. E. Boyd, *J. Phys. Chem.* **60**, 521 (1956).

[10] F. Vaslow and G. E. Boyd, *Abstracts of Papers, 134th National Meeting of the American Chemical Society, Chicago, Ill., Sept. 7–12, 1958*, p 18I, paper 44.

were estimated. Equilibrium measurements previously conducted[11] on these same systems were employed to compute $\Delta F^0$ values which, together with the $\Delta H^0$ values, permitted estimations of the standard entropies of exchange, $\Delta S^0$.

The observed $\Delta \bar{H}$ varied from −1200 to −2500 cal per mole exchanged, and were less dependent on the resin composition than were the smaller differential heats for similarly cross-linked polystyrene sulfonic acid cation exchangers. Further, $\Delta H^0$ varied little with exchanger cross-linking, in contrast with the behavior of $\Delta F^0$ and with the dependence of $\Delta H^0$ on cross-linking in cation exchangers. The entropies of anion exchange were negative, but, interestingly, they became *less* negative with increasing cross-linking. The heat and entropy changes in anion exchange indicate that anion binding is a predominant effect and that polymer network entropies may be relatively important. This situation is in contrast with cation exchange, wherein ion binding is unimportant and the heat and entropy changes appear to originate in strong ion-solvent interactions.

## TEMPERATURE DEPENDENCE OF THE SOLUBILITY OF SILVER SULFATE IN VARIOUS ELECTROLYTE MEDIA

M. H. Lietzke R. W. Stoughton

In previous work[12] a plot of the logarithm of the stoichiometric solubility product $S$ of silver sulfate on a molality basis vs the square root of the ionic strength $I$ at 25°C in a variety of electrolytes was shown to be essentially independent of the electrolyte medium. This was true on the basis of assumed complete dissociation, whether or not the supporting electrolyte contained a common ion, and regardless of valence type, that is, 1-1, 1-2, 2-1, 2-2, or 3-2. This fact, together with the observation that none of the curves fell above the limiting (Debye-Hückel) slope, suggested that (1) no sulfate complexing need be postulated in any system, and that (2) a single-parameter Debye-Hückel expression of the type

$$(1)\quad \log S = \log S_0 + \mathscr{S}_0 \left(\frac{D_0 T_0}{DT}\right)^{3/2} \left(\frac{\sqrt{I}}{1 + A_s \sqrt{I}} - \frac{\sqrt{3}\, s_0}{1 + A_s \sqrt{3}\, s_0}\right)$$

could be used to describe the data. In this equation $\mathscr{S}_0$ is the Debye-Hückel limiting slope for a 1-2 electrolyte at 25°C, $D$ is the dielectric constant at temperature $T$ (°K), $D_0$ and $T_0$ are the values at 25°C, $s_0$ and $S_0$ are the solubility and the solubility product of silver sulfate in pure water at temperature $T$, and $A_s$ is either a constant or a constant $A_0$ times $(D_0 T_0/DT)^{1/2}$. This last expression represents the prediction of the original Debye-Hückel theory.

In order that the validity of the two assumptions could be tested, a study of the solubility of $Ag_2SO_4$ in four electrolyte media was initiated as a function of temperature and ionic strength. The first media investigated were solutions of $KNO_3$, which involved a pure medium effect; then $K_2SO_4$, which involved both a medium and a common-ion effect; next, $H_2SO_4$, which involved effects of medium, common ion, and a weak acid; and, finally, $HNO_3$, which involved a medium effect and two weak acid constants. The measurements were carried out over a wide range of temperature and ionic strength. Then calculations were performed on the high-speed digital computer (the Oracle) to test the applicability of the Debye-Hückel type of expression in describing the solubility data.

The solubility measurements were carried out by using the fused-silica-tube technique described previously.[12] The determinations could be made only on a heating cycle, since the solutions supersaturated upon cooling.

Figures 5 through 8 show the comparison between the observed and calculated values of the solubility of $Ag_2SO_4$ in each of the four media. At higher temperatures and at higher ionic strengths the solubility of $Ag_2SO_4$ is very markedly enhanced. In the case of the $K_2SO_4$, the $H_2SO_4$, and the $HNO_3$ systems, the direction of curvature of the solubility curves changes at higher concentrations of the supporting electrolyte. At low ionic strengths in these systems and at all the ionic

[11] G. E. Boyd, S. Lindenbaum, and G. E. Myers, *Abstracts of Papers, 132nd National Meeting, American Chemical Society, New York, Sept. 8–13, 1957*, p 21, paper 4.

[12] M. H. Lietzke and R. W. Stoughton, *J. Am. Chem. Soc.* 79, 2067 (1957).

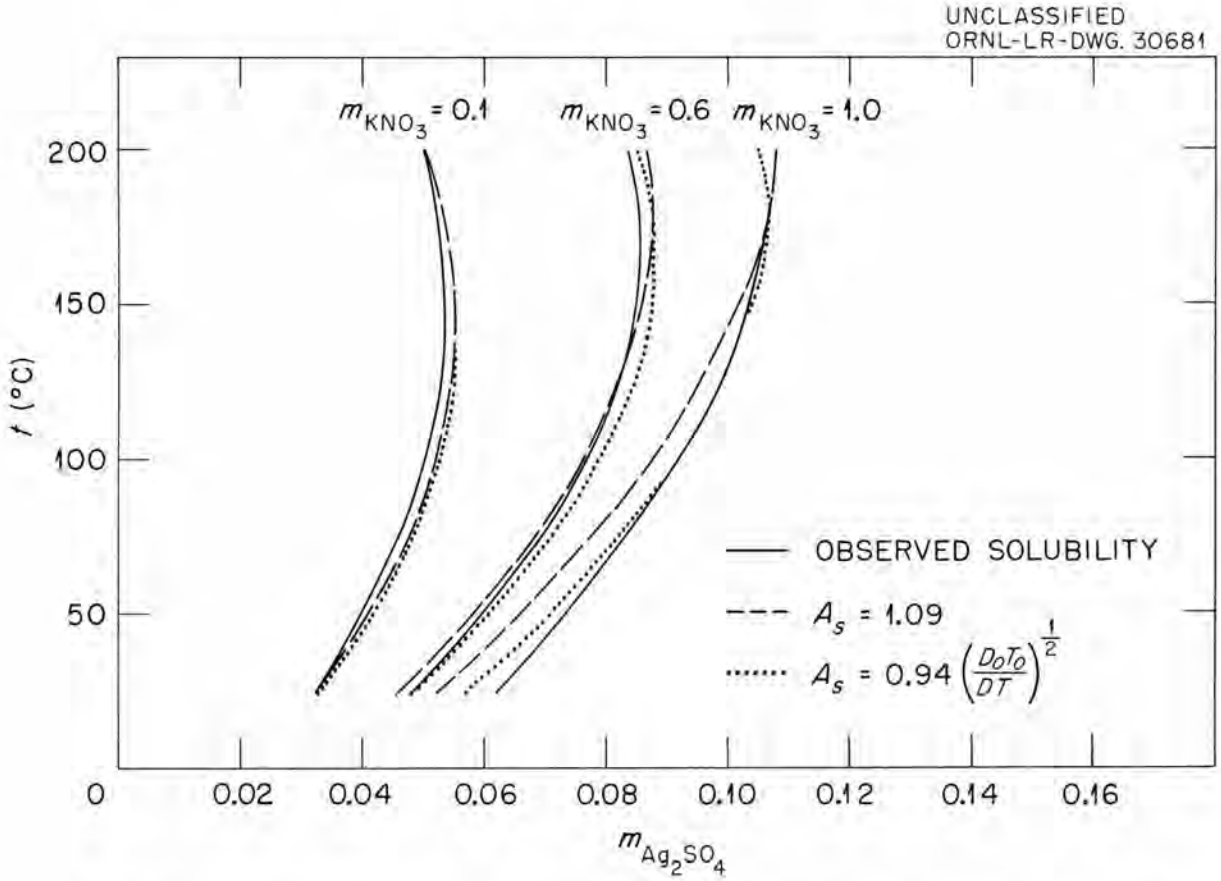


**Fig. 5. Observed and Calculated Solubilities of $Ag_2SO_4$ in $KNO_3$ Media as a Function of Temperature.**

strengths investigated in the case of the $KNO_3$ system, the curvature is the same as that for the solubility of $Ag_2SO_4$ in pure water.

The calculations of the solubility were in the nature of activity corrections applied to the solubility in pure water to allow for the higher ionic strength in the presence of each supporting electrolyte. In the $KNO_3$ system it was assumed that the only species in solution were $Ag^+$, $SO_4^{--}$, $K^+$, and $NO_3^-$; in the $K_2SO_4$ system, $Ag^+$, $SO_4^{--}$, and $K^+$; in the $H_2SO_4$ system, $Ag^+$, $SO_4^{--}$, $HSO_4^-$, and $H^+$; and in the $HNO_3$ system, $Ag^+$, $SO_4^{--}$, $H^+$, $NO_3^-$, $HNO_3$, and $HSO_4^-$. The solubility of $Ag_2SO_4$ in pure water ($s_0$) was expressed in terms of a power series in $t$ (the centigrade temperature) obtained by the method of least squares. In each case an expression for the ionic strength of the solution $I = I(m,s)$ was derived, where $s$ is the solubility of $Ag_2SO_4$ in the given solution, and $m$ is the concentration of the supporting electrolyte. In the systems involving $H_2SO_4$ or $HNO_3$ the acid quotients for the bisulfate ($K_2$) and the $HNO_3$ ($K_N$) were expressed by equations of the following form:

$$(2)\quad \ln K_2 = \ln K_2^0(T) + \frac{\mathcal{S}_0' \left(\frac{D_0T_0}{DT}\right)^{3/2} \sqrt{I}}{1 + A_2\sqrt{I}},$$

$$(3)\quad \ln K_N = \ln K_N^0(T) + \frac{\mathcal{S}_0'' \left(\frac{D_0T_0}{DT}\right)^{3/2} \sqrt{I}}{1 + A_N\sqrt{I}},$$

where the equations for $\ln K_2^0(T)$ and $\ln K_N^0(T)$

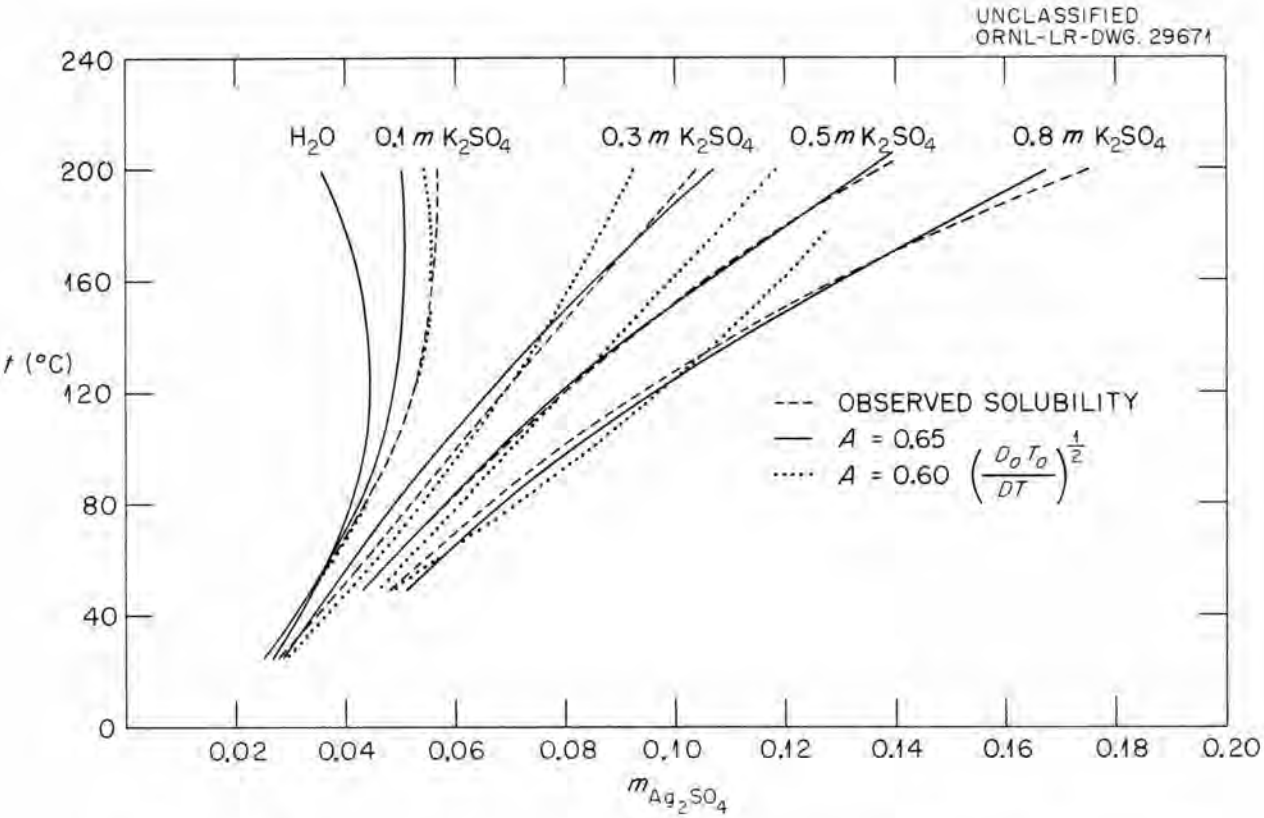


**Fig. 6. Observed and Calculated Solubilities of $Ag_2SO_4$ in $K_2SO_4$ Media as a Function of Temperature.**

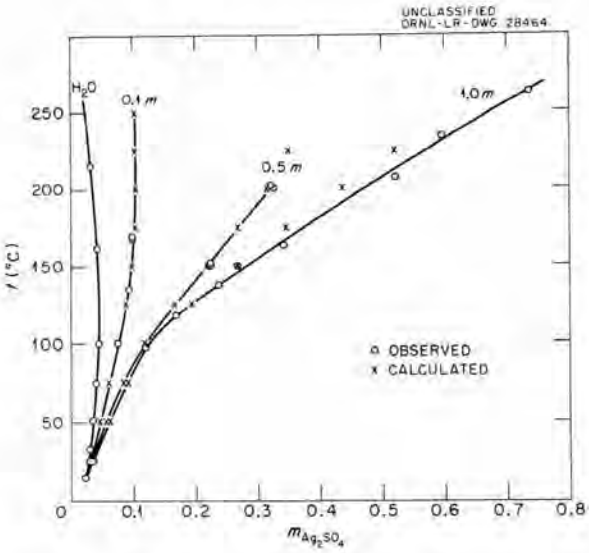


**Fig. 7. Observed and Calculated Solubilities of $Ag_2SO_4$ in $H_2SO_4$ Media as a Function of Temperature.**

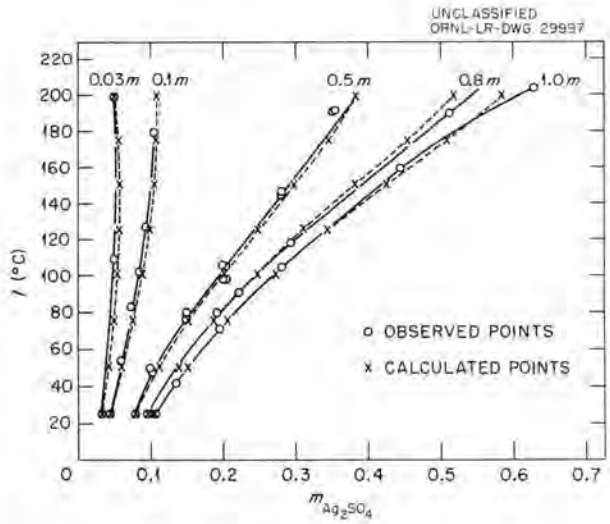


**Fig. 8. Observed and Calculated Solubilities of $Ag_2SO_4$ in $HNO_3$ Media as a Function of Temperature.**

were obtained from Young.[13] The dielectric constant of $H_2O$ was assumed to vary with temperature in accordance with the equation given by Akerlof and Oshry.[14] By combining the expressions given above, an equation was derived relating the solubility of $Ag_2SO_4$ to the parameters involved in each specific system. These equations were solved by successive approximations to give values of $s_{calcd}$. In starting the calculations at any given temperature and concentration of supporting electrolyte, an initial trial value of the ionic strength was assumed. Then a value of $s_{calcd}$ was determined. This value of $s_{calcd}$ was used to calculate a new value of the ionic strength and a new value of $s_{calcd}$. The process was continued until successive values of $s_{calcd}$ agreed to within 0.1%. The calculations were made at 25-deg intervals from 25 to 225°C.

For the calculations the $A$ parameters in Eqs. 1, 2, and 3 were varied, and "best-fit" values were obtained in each case. These values are listed below.

| $Ag_2SO_4$ in $KNO_3$ | $Ag_2SO_4$ in $K_2SO_4$ |
|---|---|
| $A_s = 1.09$ | $A_s = 0.65$ |

| $Ag_2SO_4$ in $H_2SO_4$ | $Ag_2SO_4$ in $HNO_3$ | |
|---|---|---|
| $A_s = 0.7$ | $A_s = 0.65$ | $A_s = 0.55$ |
| $A_2 = 0.4$ | $A_2 = 0.4$ or | $A_2 = 0.3$ |
| | $A_N = 0.5$ | $A_N = 0.5$ |

If best-fit values of $A_s$, $A_2$, and $A_N$ are multiplied by the factor $(DT)^{-1/2}$, the net effect is either poorer agreement or no significant improvement in agreement.

## LIQUID-PHASE SPECTROPHOTOMETRY AT ELEVATED TEMPERATURES AND PRESSURES

W. C. Waggener R. W. Stoughton

Equipment developed for studies of radioactive aqueous solutions at elevated temperatures and pressures has been briefly described previously.[15] It consists of an adaptation of a Cary model 14M recording spectrophotometer. The sample cell and reservoir assembly has a working range of 0 to 250°C and 0 to 1000 psi. The sample cell at any operating temperature and pressure is compared optically with a geometrically similar solvent cell at 25°C.

The equipment was operated at elevated temperatures and pressures for the first time in March 1957. Between March and December, ten principal high-temperature runs were made: first with $D_2O$, then with 0.1 $M$ and 1.0 $M$ $HNO_3$, and finally with 0.1 $M$ $DNO_3$, alone and with dissolved $RbNpO_2(NO_3)_3$. A total of 363 hr was logged for the equipment; 1% of the time was above 250°C, 10% was above 200°C, and between 13 and 14% was below 25°C. The special cell-reservoir assembly and spectrophotometer operated without leak or failure throughout the period covered, demonstrating the reliability of this equipment.

The fate of the neptunyl ion in a nitric acid solution was followed spectrophotometrically, from 0.6 to 1.3 $\mu$ for a period of 45 hr and over a temperature range from 4.5 to 252°C. Deuterated solutions were used to decrease both the absorbance and the effect of temperature upon the absorbance of the solvent.[16] The sample was saturated with ozone and then degassed prior to introduction into the titanium cell-reservoir assembly, which had been pretreated with 1.0 $M$ $HNO_3$ at 250°C. As the temperature was raised, Np(VI) was found to be reduced to Np(V) quantitatively and irreversibly.

The experiment was completed and the sample removed, without alpha contamination being found exterior to the sample space. Good decontamination of the sample space was achieved by very slow flushing with 1 $M$ $HNO_3$ until the effluent contained less than $10^{-3}$ $\mu$g of $Np^{237}$ per 100 ml.

The stability and reproducibility of measurements were quite comparable to those obtainable at room temperature. For example, the absorbance curve of Np(V) obtained at 252°C remained unchanged during numerous spectral scans made over a period of 3 hr at this temperature.

The stability of the Np(V) species made it possible to study in some detail the effect of

[13] T. F. Young, private communication.

[14] G. C. Akerlof and H. T. Oshry, *J. Am. Chem. Soc.* 72, 2844 (1950).

[15] W. C. Waggener and R. W. Stoughton, *Chem. Ann. Prog. Rep. June 20, 1957*, ORNL-2386, p 64–67.

[16] W. C. Waggener and R. W. Stoughton, *Chem. Ann. Prog. Rep. June 20, 1957*, ORNL-2386, p 67–69.

temperature upon the sharp, strong absorption band with a peak at about 0.98 $\mu$. This band, which is well resolved by the Cary model 14 spectrophotometer (see Fig. 9), is slightly asymmetric, the integrated absorbance of the long-wavelength side being 1 to 2% greater than that of the short-wavelength side both at 25 and 251°C. The band asymmetry measured in Fig. 9 would be reduced appreciably by replotting the data with the use of a linear energy axis (e.g., wave number rather than wavelength).

Three parameters of the 0.98-$\mu$ band are plotted as a function of temperature in Fig. 10. The position of maximum absorbance (curve A) shifts smoothly from 10,208 $cm^{-1}$ (9797 Å) at 25°C to 10,266 $cm^{-1}$ (9741 Å) at 251°C. The half-intensity bandwidth (curve B) shows a striking behavior with increasing temperature, first decreasing (12%) from 60 $cm^{-1}$ at 25°C to a minimum of 53 $cm^{-1}$ at about 170°C, then slowly increasing to 57 $cm^{-1}$ at 251°C. Finally, the product of the absorbance at the band maximum and the half-intensity bandwidth (related to integrated intensity), normalized for solvent background and density change (curve C), decreases linearly (34%) from 25 to 251°C.

The temperature effect upon the half-intensity bandwidth is further analyzed by plotting the position of the two half-intensity absorbance edges vs temperature (see Fig. 11). The difference in ordinate between the two curves at a given temperature equals the half-intensity bandwidth. The high-energy absorbance edge increases linearly with temperature at the rate of 0.246 $cm^{-1}/°C$. The temperature sensitivity of the low-energy edge,

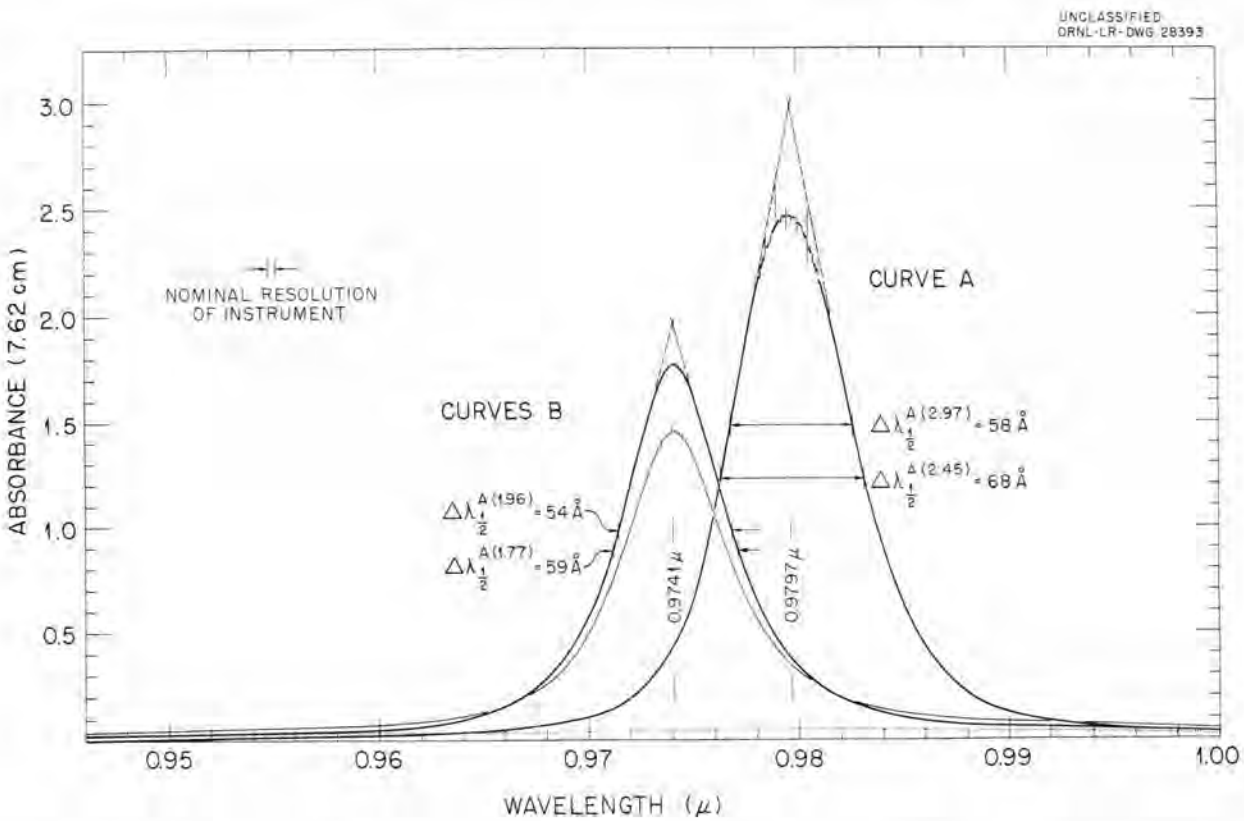


**Fig. 9. Profile of the 0.98-$\mu$ Absorption Peak of Np(V) at Room Temperature and 251°C.** Sample contained $7.43 \times 10^{-4}$ *M* Np in 0.1 *M* $DNO_3$–$D_2O$ at 25°C and was measured against a geometrically similar solvent cell held at 25°C. Curve A at 25°C: —— absorbance of sample; curves B at 251°C: ····· $\Delta T$ absorbance of solvent, —— measured absorbance of sample, —— normalized absorbance of sample (solvent background and density). Vertical lines indicate statistical variation in pen trace around absorbance maxima: ⋮ slit width ~0.1 mm, | slit width ~0.2 mm.

however, changes from 0.35 $cm^{-1}/°C$ at 25°C to 0.17 $cm^{-1}/°C$ at 252°C. Below 160 to 170°C the change with temperature of the low-energy absorbance edge is greater than that of the high-energy edge, while at higher temperatures the reverse is true. The effect of temperature upon the bandwidth is therefore directly related to the nonlinear shift of the low-energy absorbance edge.

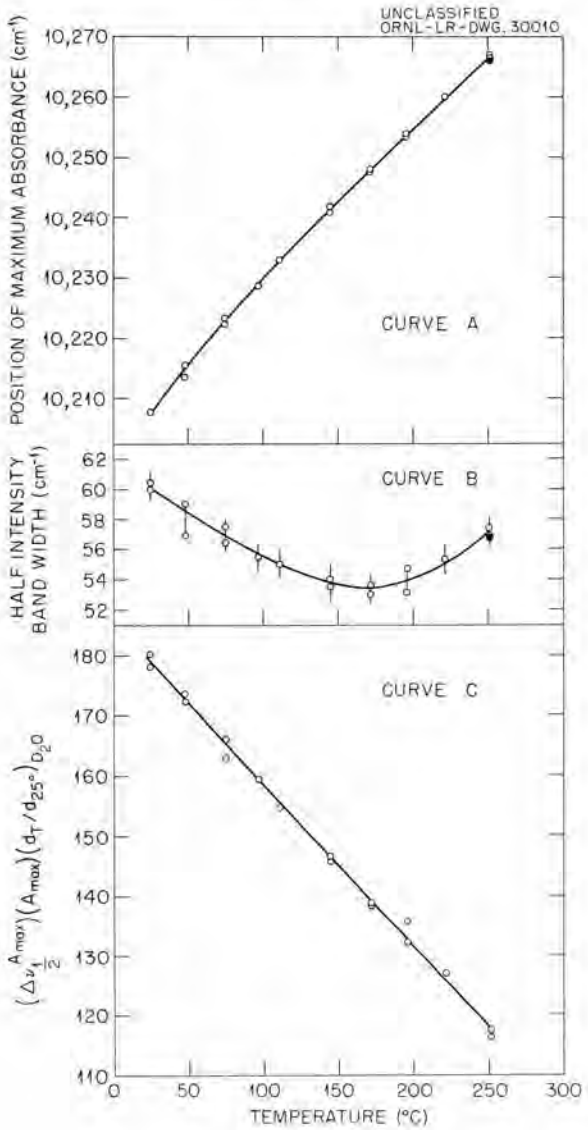


**Fig. 10. Parameters of the 0.98-$\mu$ Absorption Band of Np(V) in 0.1 *M* $DNO_3-D_2O$ as a Function of Temperature Between 25 and 251°C.** Curve A: band maximum; curve B: half-intensity band width; curve C: a function taken as proportional to the integrated band intensity. o Data taken from separate scans of unadjusted band profile; • data taken from normalized profile (adjusted for solvent background and density).

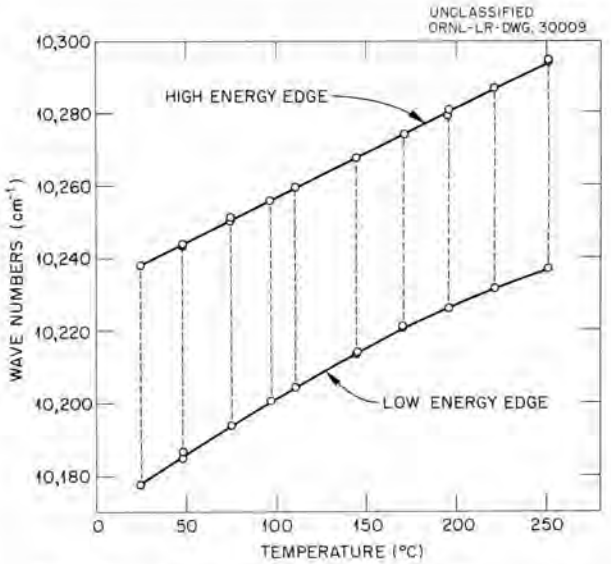


**Fig. 11. Profile of the Half-Intensity Absorbance Edges of the 0.98-$\mu$ Absorption Peak of Np(V) in 0.1 *M* $DNO_3-D_2O$ as a Function of Temperature Between 25 and 251°C.**

Ten weaker absorption bands belonging to Np(V) and Np(VI) ions have been studied in less detail in these initial experiments. The results indicate clearly, however, a great variability in the effect of temperature upon band profile among the bands measured. Further experiments, of course, will be necessary in order to establish correlations between the effect of temperature and solution environment upon these spectra.

It is planned that this first cell will be redesigned with the help of the performance data already obtained. Additional features will include methods for rapid equilibration of the liquid and vapor phases and means for independently maintaining both sample and reference cells at elevated temperatures and pressures.

## THE pH OF $UO_2SO_4$ SOLUTIONS AS A FUNCTION OF TEMPERATURE AND CONCENTRATION

M. H. Lietzke R. W. Stoughton

The pH values of four different concentrations of $UO_2SO_4$ solution were measured over the range 25 to 180°C by means of the high-temperature pH meter manufactured by Canadian Aviation Electronics, Ltd. At lower concentrations of $UO_2SO_4$

the pH values decrease slightly with increase in temperature, while at high $UO_2SO_4$ concentrations the pH values increase slightly (see Fig. 12). Within experimental error (±0.1 pH unit) all the plots are linear. For comparison, the pH plot for an $H_2SO_4$ solution (~0.005 *m*) is also shown.

## OBSERVATIONS ON THE PHASE BEHAVIOR OF THE SYSTEM $UO_2SO_4$-$CuSO_4$-$H_2SO_4$-$H_2O$ AT ELEVATED TEMPERATURES

F. E. Clark R. Slusher
J. S. Gill C. H. Secoy

The fuel solution proposed for use in the second homogeneous reactor experiment at Oak Ridge was a heavy-water solution 0.04 *m* in $UO_2SO_4$ and 0.005 *m* in $CuSO_4$. At elevated temperature, in concentration regions where a hydrolytic precipitate was not encountered, the temperature limit of homogeneity was fixed by the appearance of a second liquid phase analogous to the behavior of $UO_2SO_4$-$H_2O$ (ref 17).

Experimental methods of study, the compositions of solutions used, and the experimentally observed temperatures at which a second liquid phase appeared were given previously.[18] Plotting the temperature data against one of the composition variables yielded smooth curves from which interpolation values for isothermal phase equilibria were obtained. Figure 13 (parts I–V) shows temperature contour plots obtained in this manner for each of five acidity values. It is of interest to note that, when sufficient acid was present to prevent precipitation of a solid, pure copper sulfate–sulfuric acid–water solutions yielded a second liquid phase in a manner completely analogous to the behavior of uranyl sulfate solutions. In nearly all cases the temperature at which the solids appeared, at least the blue-green

[17] C. H. Secoy, vol 2, p 559 in *The Reactor Handbook*, ed. by J. F. Hogerton and R. C. Gross, AECD-3646 (May 1955).

[18] W. L. Marshall *et al.*, *HRP Quar. Prog. Rep. Oct. 31, 1957*, ORNL-2432, p 171.

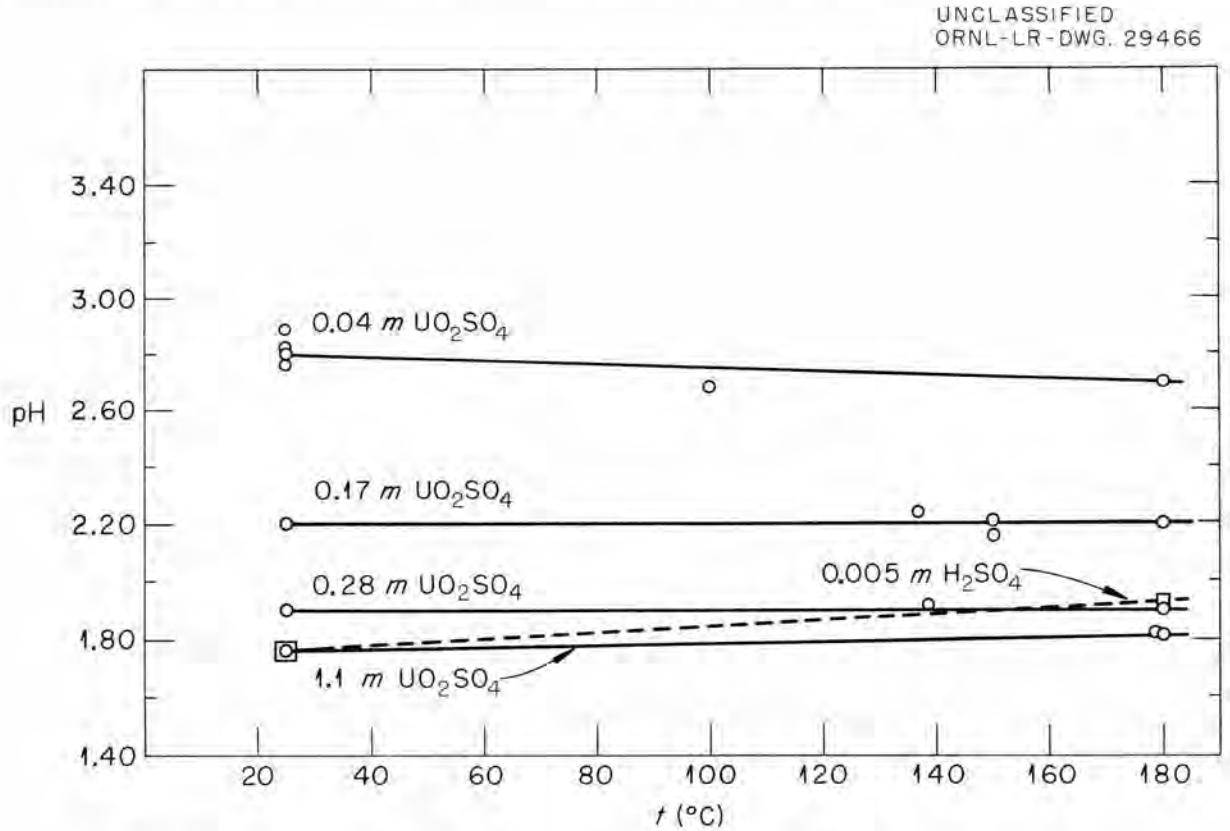


Fig. 12. Values of the Apparent pH of $UO_2SO_4$ and $H_2SO_4$ Solutions as a Function of Temperature.

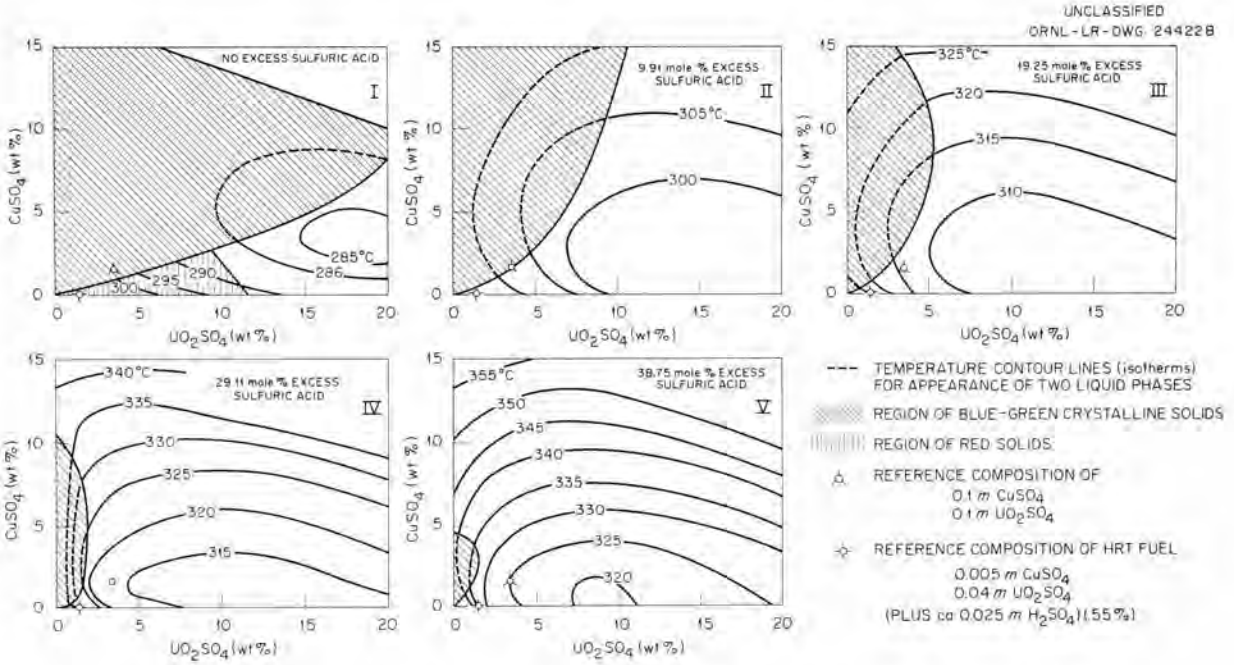


**Fig. 13. Phase Transition Temperatures in Solutions Containing $CuSO_4$, $UO_2SO_4$, and $H_2SO_4$.**

solid, was far below (100 deg or more) the two-liquid temperature region. The solid crystals could readily be classified by color into two groups: blue-green solids and red-yellow solids. We believe that the blue-green solid is probably the well-known basic copper sulfate, $3CuO{\cdot}SO_3{\cdot}2H_2O$.

Solution compositions falling within the precipitation regions are probably of no interest for reactor use because of the temperature limitation. The data for the two-liquid temperature region provide an upper temperature limit for reactor use for compositions within the scope of this study.

## CALCULATIONS OF SOLUBILITY IN MULTICOMPONENT SYSTEMS FROM SOLUBILITIES IN SIMPLER SYSTEMS

W. L. Marshall

Preliminary calculations were carried out for the solubility of antlerite ($3CuO{\cdot}SO_3{\cdot}2H_2O$) in the system $UO_3$-$CuO$-$SO_3$-$H_2O$ at 290°C by using solubility data from simpler related systems. The particular system was chosen for evaluation because (1) phase equilibrium data were available at 285 to 355°C for the system (cf. "Observations on the Phase Behavior of the System $UO_2SO_4$-$CuSO_4$-$H_2SO_4$-$H_2O$ at Elevated Temperatures," this report), (2) solubility data were available for the system $UO_3$-$SO_3$-$H_2O$ at 290°C,[19] and (3) experimental solubility data for $CuO{\cdot}SO_3$-$H_2O$ at lower temperatures could be extrapolated to 290°C. The method of calculation is given in detail in an HRP quarterly report.[20] A comparison between the calculated and experimental data at 290°C is given in Table 18, which indicates rather consistent agreement between the two sets of data.

Thus with the use of some rather simplified assumptions, solubilities in multicomponent systems were determined from solubilities in simpler three-component systems. There are many problems to be solved, however, before a clear picture can be obtained on the solubility behavior in multicomponent systems, in this case, at high temperature. Several rather formidable questions to be considered are the following: (1) which solid (or solids at an invariant point) will be the saturating *solid* phase, (2) what are the conditions for formation of *double* salts as a saturating solid, and (3) how does the existence of ionic species in

[19] W. L. Marshall, *Anal. Chem.* **27**, 1923 (1955).

[20] W. L. Marshall *et al.*, *HRP Prog. Rep. for Quarters Ending April 30 and July 31, 1958*, ORNL-2561 (in press).

**Table 18. Comparison of Calculated and Experimental Solubilities of Antlerite ($3CuO \cdot SO_3 \cdot 2H_2O$) in the System $UO_3$-$CuO$-$SO_3$-$H_2O$ (290°C)**

| Concentration of $SO_3$ ($m$) | Concentration of $UO_3$ ($m$) | Molal Solubility of Antlerite | | Absolute Difference | Deviation (%) |
|---|---|---|---|---|---|
| | | Experimental | Calculated | | |
| 1.626 | 0.820 | 0.806 | 0.785 | −0.02 | −3 |
| 1.557 | 0.359 | 1.058 | 1.029 | −0.03 | −3 |
| 1.487 | 0.102 | 1.145 | 1.124 | −0.02 | −2 |
| 1.388 | 0.135 | 1.029 | 1.023 | −0.01 | −1 |
| 1.217 | 0.167 | 0.854 | 0.855 | 0 | 0 |
| 1.181 | 0.651 | 0.530 | 0.515 | −0.02 | −3 |
| 1.002 | 0.172 | 0.668 | 0.663 | −0.01 | −1 |
| 0.886 | 0.511 | 0.375 | 0.352 | −0.02 | −6 |
| 0.882 | 0.259 | 0.544 | 0.508 | −0.04 | −6 |
| 0.763 | 0.157 | 0.481 | 0.469 | −0.01 | −2 |
| 0.655 | 0.389 | 0.266 | 0.242 | −0.02 | −9 |
| 0.509 | 0.183 | 0.280 | 0.250 | −0.03 | −11 |
| 0.461 | 0.278 | 0.183 | 0.157 | −0.03 | −14 |
| 0.444 | 0.119 | 0.253 | 0.237 | −0.02 | −6 |
| 0.285 | 0.177 | 0.108 | 0.0865 | −0.02 | −2 |
| 0.278 | 0.0869 | 0.146 | 0.130 | −0.02 | −11 |
| 0.267 | 0.116 | 0.127 | 0.107 | −0.02 | −16 |
| 0.164 | 0.0566 | 0.0811 | 0.0672 | −0.01 | −17 |
| 0.137 | 0.0852 | 0.0521 | 0.0349 | −0.01 | −33 |
| 0.104 | 0.0561 | 0.0386 | 0.0294 | −0.01 | −24 |
| 0.0750 | 0.0278 | 0.0351 | 0.0250 | −0.01 | −29 |

solution together with nonionic species complicate the solubility characteristics of any one species.

The complexity of system definition is indicated by the following example. If only five variations for each added component are considered sufficient to define a system and if the study is limited to only *one* temperature, then the following table shows the experimental work necessary to define the system both by an all-experimental approach and by a part-calculation method in some manner as mentioned above:

| Number of Components | Number of Experimental Phase Diagrams Necessary to Define System at One Temperature | |
|---|---|---|
| | All Experimental | Part Calculation |
| 2 | 1 solubility point | 1 solubility point |
| 3 | 1 phase diagram | 1 phase diagram |
| 4 | 5 phase diagrams | 2 phase diagrams |
| 5 | 25 phase diagrams | 3 phase diagrams |
| 6 | 125 phase diagrams | 4 phase diagrams |
| 7 | 625 phase diagrams | 5 phase diagrams |

For example, the present homogeneous reactor fuel containing $UO_2SO_4$, $CuSO_4$, $NiSO_4$, $H_2SO_4$, and $H_2O$ after reactor operation is a five-component system, even when the fission products are not considered.

## SOLUBILITY EQUILIBRIUM IN THE SYSTEM $NiO$-$SO_3$-$H_2O$ AT HIGH TEMPERATURE

J. S. Gill R. Slusher
W. L. Marshall

The investigation of the $NiO$-$SO_3$-$H_2O$ system at high temperature in the absence of other components was initiated (1) because of the apparent complexity of multicomponent reactor fuel systems with regard to phase stability and interpretation and (2) because of the preliminary success in calculating solubilities in a four-component system from data on two three-component systems (cf. "Calculations of Solubility in Multicomponent Systems from Solubilities in Simpler Systems," this report). This investigation is discussed in more detail in an HRP report[21] and is merely summarized here. In order that a complete picture of the general behavior of this system could be obtained, studies were carried out from 150 to 300°C and from $10^{-4}$ to 1 $m$ total $SO_3$. These data and their interpretation are to be considered along with the evaluated system $UO_3$-$SO_3$-$H_2O$ (ref 18) and with data to be obtained for the system $CuO$-$SO_3$-$H_2O$ over the same concentration and temperature ranges.

The experimental results for phase equilibria in the system $NiO$-$SO_3$-$H_2O$ are given in Figs. 14 and 15. In studying a system over a wide concentration range, it is difficult to choose any one type of graphical presentation for the best description. A plot of log $m_{NiO}$ vs log $m_{SO_3}$ (Fig. 14) covers the widest range and shows the general behavior of the system from 150 to 300°C. For working curves, however, in order to emphasize precision of data, plots were made of log $m_{SO_3}'$, where $m_{SO_3}'$ = total $m_{SO_3}$ in the solution, vs the "saturation mole ratio," that is, the number of moles of NiO which will dissolve per mole of total $SO_3$ (Fig. 15).

Solid phases were characterized by means of x-ray diffraction by R. L. Sherman of the Analytical Chemistry Division. Considerable disagreement

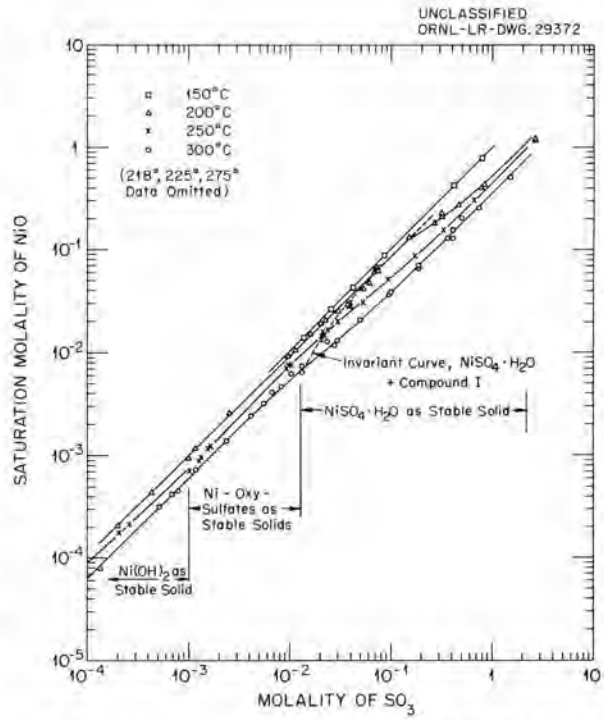


**Fig. 14. Log-Log Plot of the System $NiO$-$SO_3$-$H_2O$ at 150 to 300°C.**

and overlap of solid phases as defined by x-ray analysis was found. The relative solution composition groupings with respect to the initial solid-phase compositions would favor $\frac{1}{2}Ni(OH)_2 \cdot NiSO_4$ hydrate for compound I and $Ni(OH)_2 \cdot NiSO_4$ hydrate for compound II. At lower $SO_3$ concentrations, $Ni(OH)_2$ has been identified by x-ray diffraction. A compound III as well as a compound IV seems to exist also in the lower concentration ranges in the 200°C range.

If these data, in the region in which $NiSO_4 \cdot H_2O$ is a stable solid, are converted to $m_{NiSO_4}$ and $m_{H_2SO_4}$, and the solubility of $NiSO_4$ is plotted as a function of $m_{H_2SO_4}$ (Fig. 16), an approximate linear relationship is observed which can be extrapolated to zero molality $H_2SO_4$. From the slope at a particular temperature, a value for a hypothetical solubility was derived. These hypothetical solubilities are never achieved because of the conversion of the solid phase to the hydroxy-sulfates and hydroxides at low concentrations of $H_2SO_4$.

The slopes, $\Delta m_{NiSO_4}/\Delta m_{H_2SO_4}$, for 200, 218, and 225°C (Fig. 16) have nearly the same value,

[21] W. L. Marshall *et al.*, *HRP Prog. Rep. for Quarters Ending April 30 and July 31, 1958*, ORNL-2561 (in press).

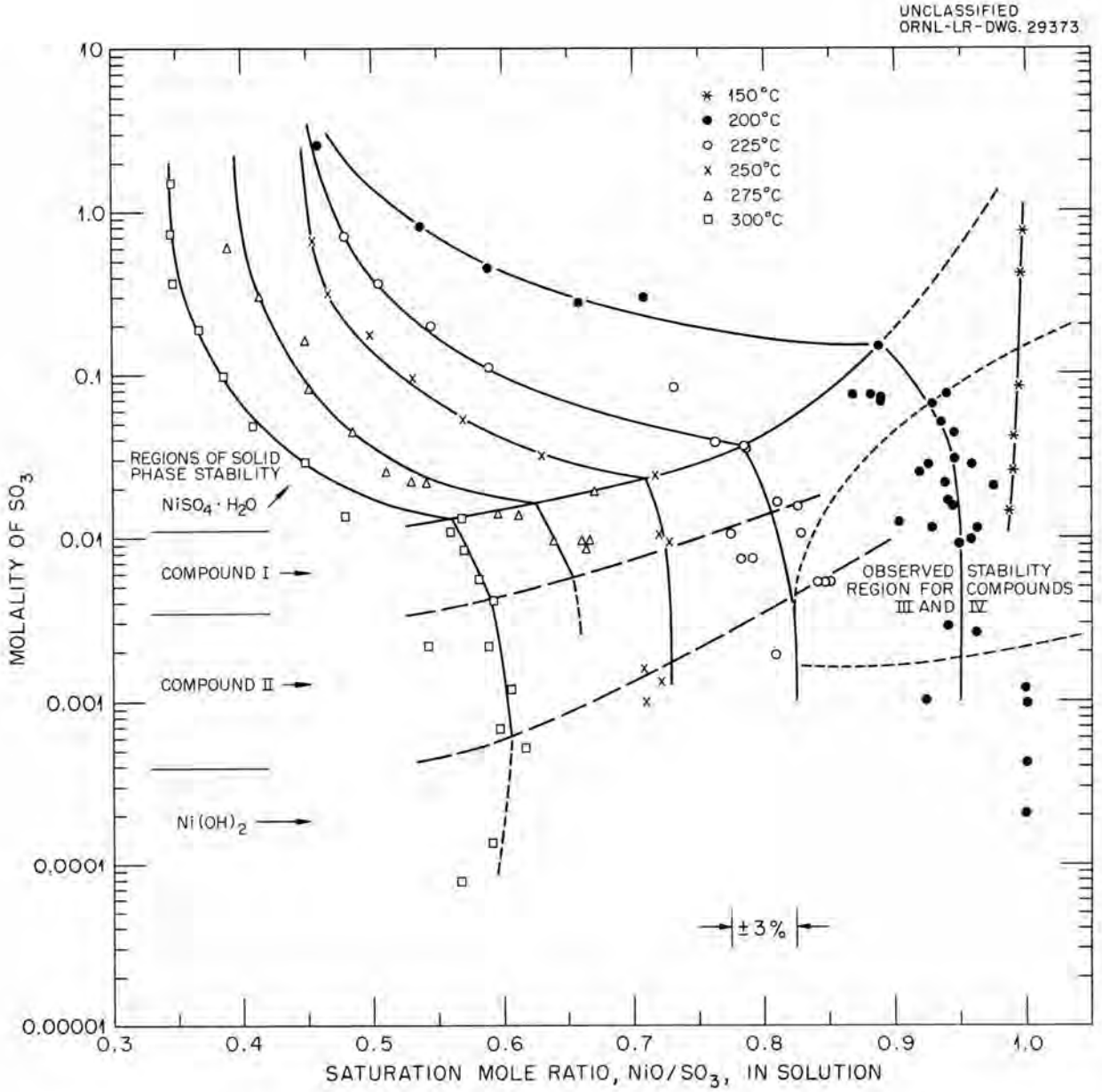


**Fig. 15. Log–Mole-Ratio Plot of the System $NiO-SO_3-H_2O$ at 150 to 300°C.**

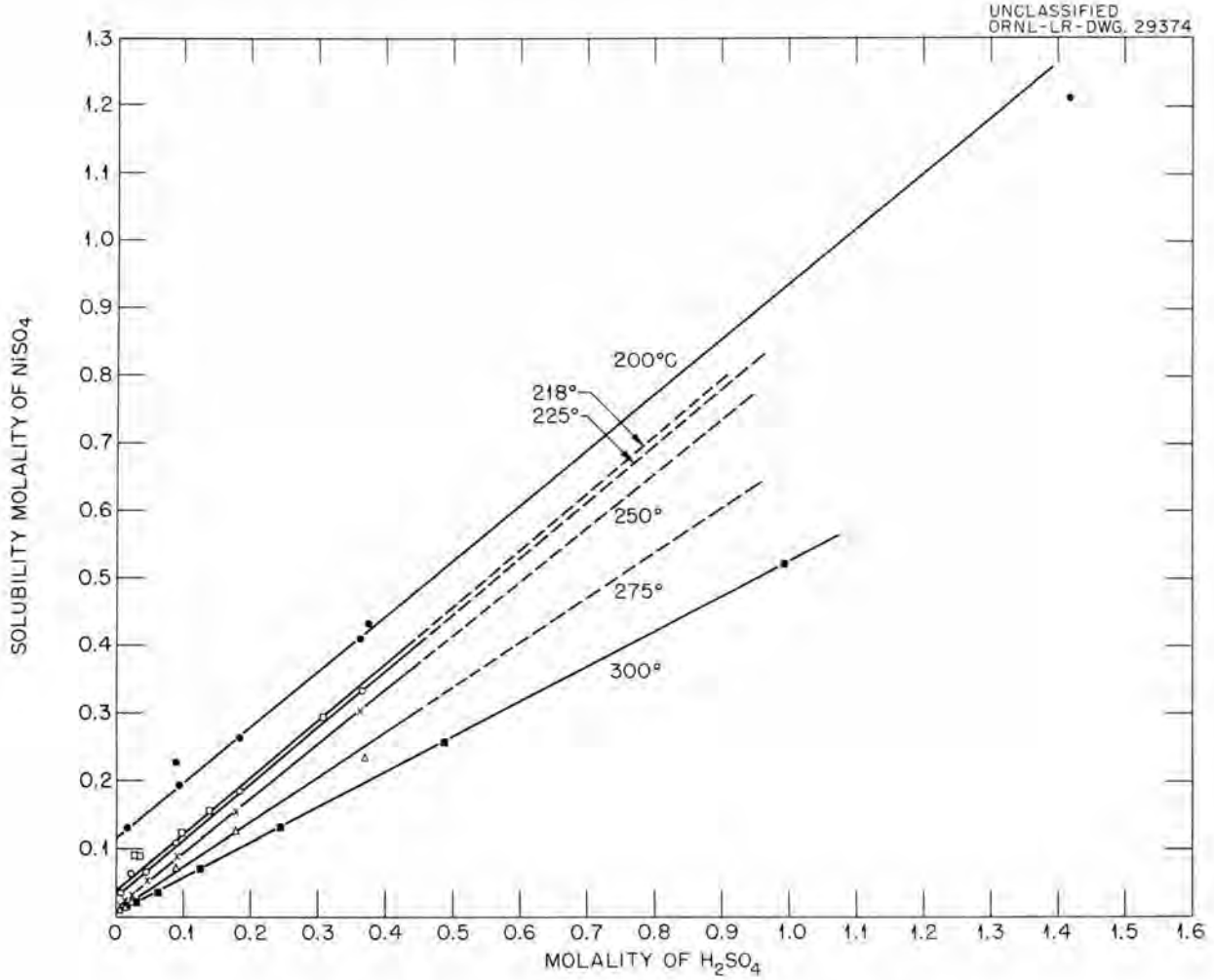


Fig. 16. Solubility of $NiSO_4$ in $H_2SO_4$-$H_2O$ at 200 to 300°C.

which is approximately 0.8. This value might indicate a complex of the type $Ni(HSO_4)_2$, or indicate $Ni^{++}$ and $HSO_4^-$ ions in solution. At 300°C the slope is 0.5, which might indicate a complex in solution of a type $Ni(HSO_4)_2 \cdot H_2SO_4$.

## MEASUREMENT OF AQUEOUS VAPOR PRESSURE AT ELEVATED TEMPERATURE AND PRESSURE

G. M. Hebert W. L. Marshall

The program of vapor-pressure measurement of aqueous systems at elevated temperature[22,23] has been resumed. The current goal of this investigation is to attain a method for measuring absolute vapor pressures of aqueous solutions to a high degree of precision and accuracy to temperatures approaching the critical temperature of water. The satisfactory development of a method will supplement the isopiestic apparatus developed in the Chemistry Division for studies of aqueous solutions at elevated temperature.[24]

The use of a differential manometer for measurement is actively being investigated. This approach seems logical, since the ultimate pressures to be encountered are of the order of 200 atm near the critical point of water.

[22] H. O. Day, Jr., and C. H. Secoy, *Chem. Semiann. Rep. Dec. 20, 1953*, ORNL-1674, p 98.

[23] H. O. Day, Jr., *HRP Quar. Prog. Rep. March 31, 1953*, ORNL-1554, p 109.

[24] B. A. Soldano, R. J. Fox, and R. W. Stoughton, *Chem. Ann. Prog. Rep. June 20, 1957*, ORNL-2386, p 74.

## EQUILIBRIUM COMPOSITIONS OF THE LIGHT AND HEAVY LIQUID PHASES IN THE SYSTEM $UO_3$-$SO_3$-$H_2O$

E. V. Jones W. L. Marshall

An investigation is under way to measure the equilibrium compositions of the light and heavy liquid phases in the systems $UO_3$-$SO_3$-$H_2O$ and $UO_3$-$SO_3$-$D_2O$. The technique involves equilibrating the two phases at temperature in a sealed glass tube, freezing the contents of the tube before intermixing of the two phases can occur, and the subsequent analyzing of both phases for $UO_3$ and $SO_3$. With stoichiometric $UO_2SO_4$ from 0.8 to 2 *m* in the $H_2O$ system, preliminary experiments at 300°C indicate the light-phase composition to be in the region of 0.38 *m* uranium, with approximately 8 mole % excess free acid. The heavy-phase composition is approximately 4.9 *m* uranium, with a 2 mole % deficiency in free acid.

## HOMOGENEOUS CATALYSIS OF THE OXIDATION OF DISSOLVED HYDROGEN

H. H. Stone H. F. McDuffie

**Reaction Rates in the Deuterium–Heavy-Water System.** – Since heavy water is used as the fuel solvent in the HRT, it was of considerable importance to determine the hydrogen-oxygen recombination rates in the HRT fuel solution for temperatures of reactor operation. Earlier reports[25,26] had indicated that the use of deuterium instead of hydrogen and the use of deuterium with heavy-water solutions would give rise to slower recombination rates than when the protium isotope was involved. Four test solutions were prepared for direct measurement of the rates in heavy-water solutions. Three of these solutions (B,C,D) were prepared with natural uranium and differed only in their copper content; the fourth (S) was prepared from enriched uranium by dilution of and copper addition to the HRT reactor stock solution. Recombination tests performed at 250, 275, and 300°C showed the rates to be essentially proportional to the copper concentration.[27] The effect of temperature, after a correction for the copper concentration, is shown in Fig. 17. These data make it possible to estimate the rate of consumption of deuterium at a given temperature and for a given partial pressure of deuterium in the reactor.

**Dichromate as the Oxidizing Agent.** – While ORNL homogeneous catalysis studies have all made use of oxygen gas as the oxidizing agent, other studies of the reactions of dissolved hydrogen have made use of dissolved oxidizing agents, such as dichromate, which do not distribute themselves between the gas and liquid phases.[28] To show the applicability of dichromate under our conditions of temperature, acidity, and

[25] H. F. McDuffie *et al.*, *The Radiation Chemistry of Homogeneous Reactor Systems. III. Homogeneous Catalysis of the Hydrogen-Oxygen Reaction*, ORNL CF-54-1-122 (Jan. 26, 1954).

[26] C. H. Secoy, in *HRP Civilian Power Reactor Conference Held at Oak Ridge National Laboratory, May 1–2, 1957*, TID-7540, p 217–220.

[27] H. F. McDuffie and H. H. Stone, *HRP Quar. Prog. Rep. Jan. 31, 1958*, ORNL-2493, p 181.

[28] E. Peters and J. Halpern, *J. Phys. Chem.* **59**, 793 (1955).

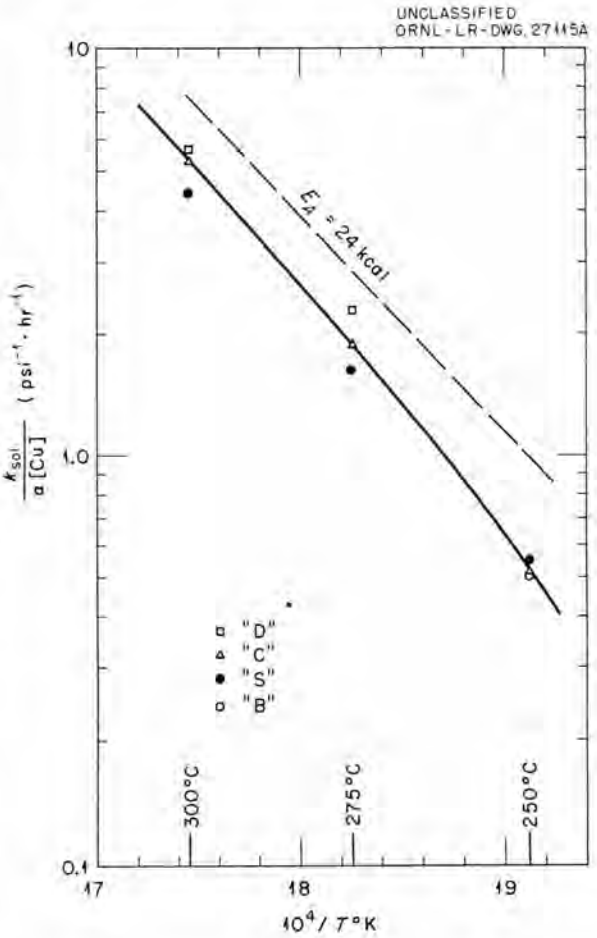


**Fig. 17. Effect of Temperature on Recombination in Heavy-Water Solutions.**

copper concentration, tests were performed at 200°C with a solution containing 0.02 $M$ $CuSO_4$, 0.20 $M$ $H_2SO_4$, and, initially, 0.1 $F$ $CrO_3$. In these tests there was no oxygen gas present with the hydrogen, and the amount of hydrogen was only slightly in excess of that needed to react with all the oxidant. The loss of hydrogen pressure with time was recorded, and the usual interpretation was given to the observed data; that is, a plot was made of the effect of the gas-to-liquid ratio upon the observed rate of pressure decrease. Within the limitations imposed by the shortness of the reaction, due to the small amount of oxidant present, and by the difficulties of measuring the low partial pressures of hydrogen, the observed data were indistinguishable from results of better precision, previously obtained in tests which made use of oxygen as the oxidant. It may be concluded from these experiments that the technique and interpretation based on oxygen as the oxidant give results which are satisfactorily in agreement with those not requiring oxygen in the vapor phase.

**Simultaneous Determination of Reaction Rates and Hydrogen Distribution Coefficients.** – The simultaneous determination of $k_{sol}$ and $\alpha$ for cupric sulfate solutions at 175 and 200°C in the presence of varying concentrations of acid and copper was discussed in the last annual report.[29] For a given solution and temperature, a plot of $1/k_\pi$ vs $V_g/V_l$ gave a linear relationship of the form $Y = mX + b$, where $b = 1/k_{sol}$, and $m = \alpha/bRT$. Two difficulties with the interpretation of the data were apparent; values of $b$ were frequently so small in absolute magnitude that the precision of the data did not permit the extrapolated value for $b$ to be determined with satisfactory precision, and the experimental values for $Y$ covered such a large range that the distribution of errors in $Y$ about the least-squares line was not normal. Progress has been made in overcoming both these difficulties. The temperature control during tests has been improved; it is now considered to be within ±0.2°C, which improves the precision of the data. The other difficulty, the increasing absolute magnitude of the error in $Y$ at larger values of $Y$, was overcome by the stratagem[30] of plotting the data in the form $Y/X = m + b/X$, which is also linear, but with the slope and intercept exchanged and with the errors more nearly normally distributed. Redetermination of the previously reported parameters is in progress; reinterpretation of the data will be made when sufficient results are available.

## DECOMPOSITION OF PEROXIDE IN AQUEOUS SOLUTIONS

L. O. Gilpatrick H. F. McDuffie

**Isotope Effects.** – Resumption of the study of the decomposition of peroxide in aqueous solutions during the past year permitted studies of the effects of changing from a hydrogen- to a deuterium-base system.[31] The temperature coefficient, below 100°C, for the decomposition of peroxide in light-water systems was essentially the same as that in the heavy-water systems, as shown by Fig. 18. Actual decomposition rates in solutions differing only in the isotopic nature of the solvent (and in any impurities adventitiously introduced with the purified solvents) were some 13% faster in heavy-water systems than in light-water systems.

An estimate of the significance of this isotope effect must await the elucidation of the mechanism of the reaction. Tentative conclusions are as follows:

1. Both the smallness of the observed effect and the fact that $k_D$ is larger than $k_H$ suggest that the rate-determining step does *not* involve the breaking of an O-H or O-D bond.[32]

2. Most acid-catalyzed reactions proceed more rapidly in heavy water than in light water.[33,34] Reported ratios of $k_D/k_H$ for a number of organic reactions fall in the range 1.2 to 10. Since this ratio is 1.13 for the present solutions, we infer that peroxide decomposition may be an acid-catalyzed reaction.

---

[29] H. F. McDuffie and H. H. Stone, *Chem. Ann. Prog. Rep. June 20, 1957*, ORNL-2386, p 83.

[30] J. B. Levy *et al.*, *J. Am. Chem. Soc.* **73**, 3792 (1951); E. Klein, J. B. McKelvey, and B. G. Webre, *J. Phys. Chem.* **62**, 286 (1958).

[31] L. O. Gilpatrick and H. F. McDuffie, *HRP Prog. Rep. for Quarters Ending April 30 and July 31, 1958*, ORNL-2561 (in press).

[32] K. B. Wiberg, *Chem. Rev.* **55**, 713 (1955).

[33] K. F. Bonhoeffer and O. Reitz, *Z. physik. Chem. (Leipzig)* **A179**, 135 (1937).

[34] K. F. Bonhoeffer, *Z. Elektrochem.* **40**, 469 (1934).

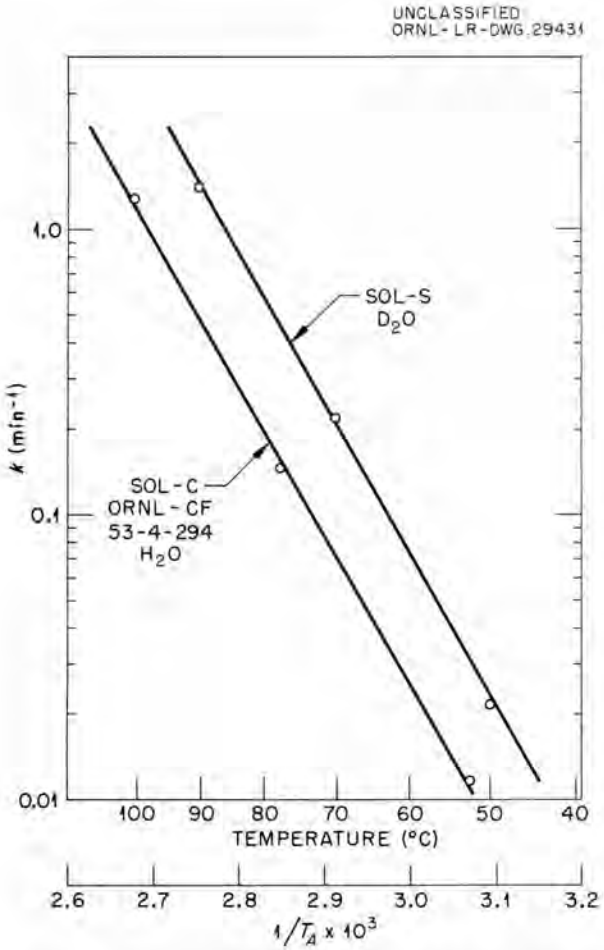


**Fig. 18. Peroxide Decomposition in Light- and Heavy-Water Solutions of Uranyl Sulfate.**

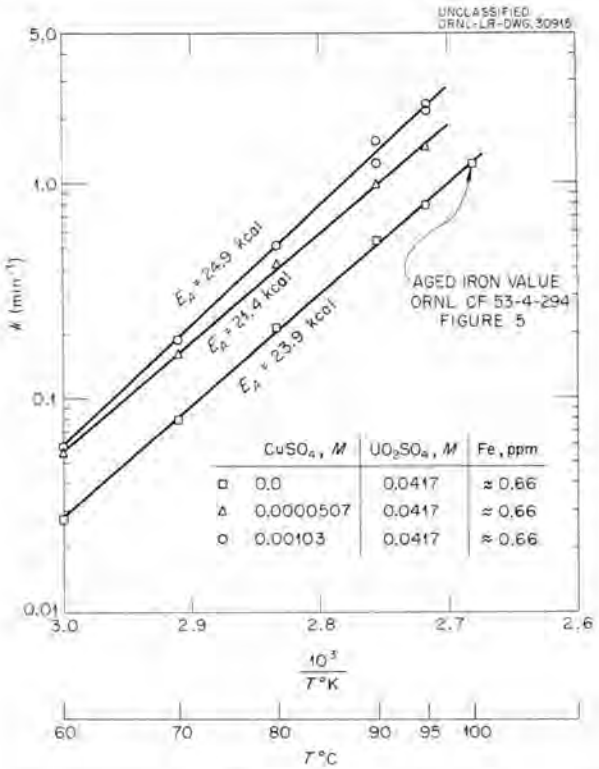


**Fig. 19. Effect of Copper Concentration on Temperature Dependence of Peroxide Decomposition.**

**Catalytic Effects.** – It is important to know the rates of peroxide decomposition at temperatures above 100°C for aqueous reactor operation. One way to estimate such rates is by extrapolation from rates measured at lower temperatures. The previously reported work of Silverman *et al.*[35] provided a basis for such extrapolation for solutions containing aged iron or no iron, as illustrated by the line for solution C, Fig. 18.

It was also previously reported[35] that the presence of cupric copper in uranyl sulfate solutions accelerated the decomposition of peroxide at 100°C. The temperature dependence has now been determined, as illustrated in Fig. 19, for peroxide decomposition in uranyl sulfate solutions containing different concentrations of cupric sulfate. Although the addition of the copper increased the decomposition rate, it did not significantly lower the activation energy. A saturation effect was noted; above a concentration of 0.0001 *M* the effect of additional copper was negligible; in the previously reported work the effect of additional copper had not disappeared at 0.0127 *M*.

## pH MEASUREMENTS IN $ThO_2$ SLURRIES

F. H. Sweeton

This work was undertaken in order to find a practical method of measuring the pH of a $ThO_2$ slurry without having the calomel electrode in direct contact with the suspension. Such contact can result in errors, which in the case of certain clay suspensions are as large as 2.0 pH units.[36]

[35] M. D. Silverman, G. M. Watson, and H. F. McDuffie, *Ind. Eng. Chem.* 48, 1238 (1956).

[36] H. R. Kruyt (ed.), *Colloid Science*, vol I, p 184–87, tr by L. C. Jackson, Elsevier, New York, 1952.

Two approaches involving measurement of a slurry supernatant were unsuccessful because complete separation of solids was not obtained when settling proceeded by gravity or by centrifugation. Another method that was tried made use of a two-compartment cell, one compartment holding the calomel electrode and the supernatant of a specially prepared $ThO_2$ slurry, and the other holding the glass electrode and the slurry under test. This approach proved to be too tedious, and the results were too erratic.

The final method[37] tested made use of a Millipore filter with 100-Å pores, so as to obtain a filtrate directly from the slurry being tested. The apparatus shown in Fig. 20 served both to collect the filtrate and to measure the pH, with this filtrate separating the calomel electrode and the slurry. Provision was made for adding $HNO_3$ solution to the slurry in order to determine the reproducibility over a range of pH readings.

The $ThO_2$ used was prepared by the Chemical Technology Division by calcining thorium oxalate at 650°C and is known as "D-16" material. Nitrogen absorption data indicated that this oxide had a specific surface area of $37._6$ $m^2/g$. Before use the material was outgassed for several hours at 600°C under an absolute pressure of 0.1 mm Hg, and it was protected from atmospheric $CO_2$ until the end of the pH measurements. The concentrations of slurries used in the runs varied between 60 and 300 g of $ThO_2$ per liter.

Data obtained by this method are shown in Fig. 21 as "regular runs." Except for the first run, which gave results about 0.5 pH unit higher than the others, the data seem reasonably reproducible and indicate that the method is practical.

For qualitative comparison another sample of D-16, not degassed, was measured while exposed to air, with the calomel electrode immersed directly in the slurry. The resulting data, labeled "special runs" in Fig. 21, show either that the calomel electrode can give considerable error with $ThO_2$ slurries, or that adsorbed $CO_2$ can

[37] A more detailed discussion is given by F. H. Sweeton, *HRP Prog. Rep. for Quarters Ending April 30 and July 31, 1958*, ORNL-2561 (in press).

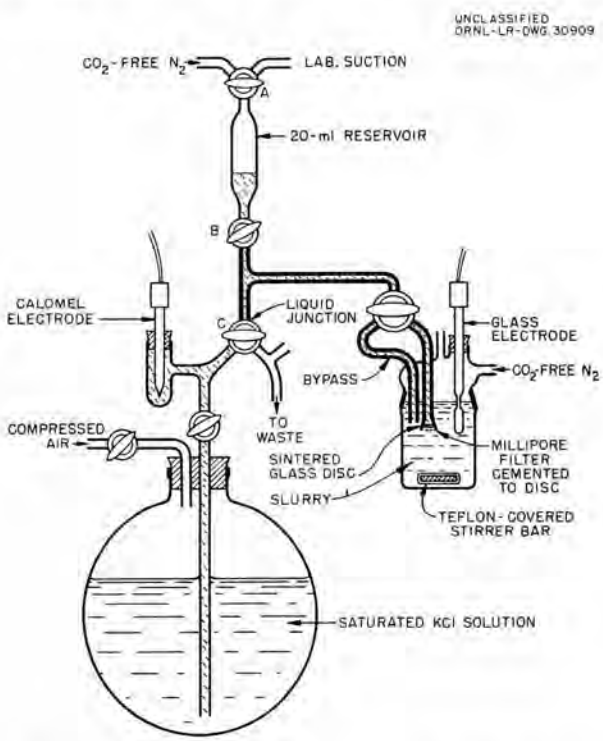


Fig. 20. Apparatus for Determining pH of Slurries.

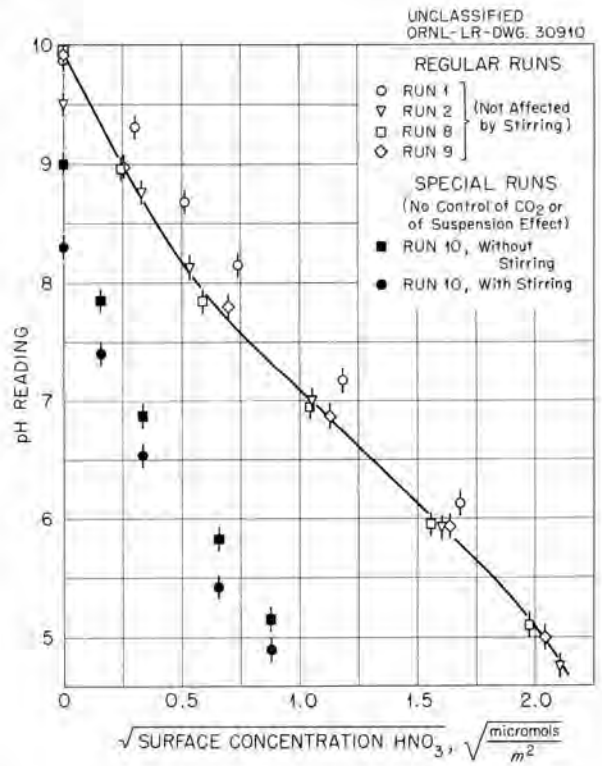


Fig. 21. Adsorption of Nitric Acid by Thorium Oxide Slurry.

affect the pH of $ThO_2$ slurries appreciably, or that both can occur.

### DISPERSIONS OF THORIUM OXIDE

T. A. Carlson J. S. Johnson
K. A. Kraus

Studies on the properties of dispersions of a high-molecular-weight, hydrolytic Th(IV) polymer were continued, and measurements on the adsorption of HCl by the polymer were extended. A potentiometric technique was used, and studies up to 90°C were carried out. Polymer concentrations ranged from 36 to 315 g of $ThO_2$ per liter. The apparent enthalpy change for the adsorption reaction $H^+ + Cl^- \rightarrow H^+_{(p)} + Cl^-_{(p)}$, where the subscript $(p)$ represents polymer, was about −5 kcal and essentially independent of polymer concentration, in spite of the fact that the most concentrated polymer dispersions showed considerable tendency to aggregate; they showed relatively high viscosity and strong Tyndall effects.

By potentiometric methods the activity of HCl in a concentrated polymer dispersion was determined as a function of NaCl concentration. The activity of HCl was relatively independent of added NaCl, although at the highest chloride concentrations there was a considerable increase in the Tyndall effect, indicating substantial increase in the degree of aggregation.

### ULTRACENTRIFUGATION AND LIGHT-SCATTERING STUDIES OF INORGANIC POLYMERIZATION

J. S. Johnson E. W. Anacker[38]
K. A. Kraus

**Multiple-Cell Rotor.** – Recently, a rotor for the Spinco ultracentrifuge became available which, in combination with an interference optical system, permits simultaneous centrifugation of five solutions. Among the tests carried out on this equipment was a centrifugation with identical solutions of 0.055 $M$ $Na_2MoO_4$ in 1 $M$ $NaClO_4$ supporting electrolyte in all cells. The average degree of polymerization $N$ of $Na_2MoO_4$, computed for the charge of the molybdate ion, is 1.05 ± 0.02 for the five cells. The spread of only 4% for such a low-molecular-weight solute in a supporting electrolyte whose molecular weight is not greatly less indicates that the precision of the equipment is good and that the techniques used to diminish the effect of cell distortion are adequate. About 2% of the difference of the mean from the known value, $N = 1$, can be attributed to neglect of the effect on the refractive index of the difference in pressure between the solvent and the solution compartment; the rest could easily arise from variations in activity coefficients of the solutes.

**Light Scattering of Electrolytes in Two-Component Systems.** – The intensity of light scattered by a two-component solution in excess of that scattered by the solvent, at an angle of 90 deg to the incident beam, may be expressed in terms of the Rayleigh ratio, $R_{90}$, as

$$R_{90} = \frac{Km_2}{\partial \ln a_2/\partial \ln m_2} = \frac{K\dfrac{w_2}{1000M_2}}{\partial \ln a_2/\partial \ln m_2},$$

where $K$ summarizes optical constants and refractive index increments, $m_2$ is the molality of the solute, $w_2$ is the concentration in grams of solute per gram of $H_2O$, $M$ is its molecular weight, and $a_2$ is its activity. It is common practice to extrapolate results to infinite dilution in order to eliminate the activity coefficient factor $(\partial \ln \gamma_2/\partial \ln m_2)$ in the activity term. However, if the solute is an electrolyte, activity must be written as an ion product for the activity coefficient term to disappear; that is,

$$\frac{\partial \ln a_2}{\partial \ln m_2} = \nu\left(1 + \frac{\partial \ln \gamma_\pm}{\partial \ln m_2}\right),$$

where $\nu$ is the number of moles of ions per mole of solute. As a consequence, with decreasing concentration the observed molecular weight will approach the number average weight of the ions, or the molecular weight of the solute divided by $\nu$.

The statement[39] is sometimes encountered that the extrapolated value of molecular weight in such a situation is a weight average of the ions. Since we believed it to be erroneous, we carried out light-scattering measurements of solutions of silicotungstic acid in water. Ultracentrifugation and light-scattering measurements carried out in

[38] Summer participant 1957, Montana State College.

[39] See, for example, P. Doty and J. T. Edsall in *Advances in Protein Chemistry* (ed. by M. L. Anson *et al.*), vol 6, p 98; D. J. Bettinger and S. Y. Tyree, Jr., *J. Am. Chem. Soc.* **79**, 3355 (1957).

a supporting electrolyte, both by the authors and by others, indicated that the formula for this material is $H_4SiW_{12}O_{40}$, and acidity measurements indicate that four protons per molecule are ionized. A weight average of the ions would be 2871.1, or almost the same as the formula weight, 2879.1; a number average would be 575.8.

Since silicotungstic acid is a 4-1 electrolyte, the ionic strength is appreciable at concentrations for which enough light is scattered to allow measurements of reasonable accuracy, and the activity coefficient team will not be negligible. If this term is neglected, the molecular weight computed from our results is about one-third the formula weight. Further, because of the changes in ionic strength with concentration, the curve for the usual function, $Kw_2/R_{90}$, does not lend itself readily to extrapolation to zero concentration. We have, therefore, computed the $\partial \ln \gamma_{\pm}/\partial \ln m$ term for each concentration from a Debye-Hückel expression, with an assumed $\mathring{a}$ "distance of closest approach" of 5 Å. The molecular weight implied by the scattering for each concentration was then computed:

| Molarity | Molecular Weight | |
|---|---|---|
| | 436 mμ | 546 mμ |
| 0.0211 | 540 | 540 |
| 0.0105 | 565 | 560 |
| 0.0063 | 580 | |
| 0.0032 | 600 | 570 |

The theoretical molecular weight for the number average of ions is 575.8.

The results of measurements, at both wavelengths utilized, scatter about the value for the number average molecular weight of the ions. It is possible that other rules hold for the scattering of solutions so dilute that substantial deviations from electroneutrality occur within scattering elements, but this does not seem to be the case for the concentration range covered here.

**Isopolymolybdates.** – The species formed upon the addition of acid to aqueous molybdate solutions have been a classical subject of interest in inorganic polymer chemistry. We are engaged in a study of this system by equilibrium ultracentrifugation.

The centrifugations were carried out in 1 *M* $NaClO_4$ supporting electrolyte as a function of degree of "neutralization" of $Na_2MoO_4$ with $HClO_4$ and of molybdate concentration. The results for about 0.05 *M* Mo(VI) are summarized in Fig. 22, a plot of apparent degree of polymerization *N* vs the average formula of the molybdate monomer unit, $Na_{2-p}H_pMoO_4$. The value of *p* is the number of moles of $HClO_4$ added to the solution, less the number of moles of free acid (determined separately by pH measurements), divided by the number of moles of Mo(VI). Since the solutions were found to be polydisperse, estimation of $z'$ was precluded, and the data are presented in the figure computed for $z' = 0$ and for the maximum plausible value of charge, $z' = 2 - p$.

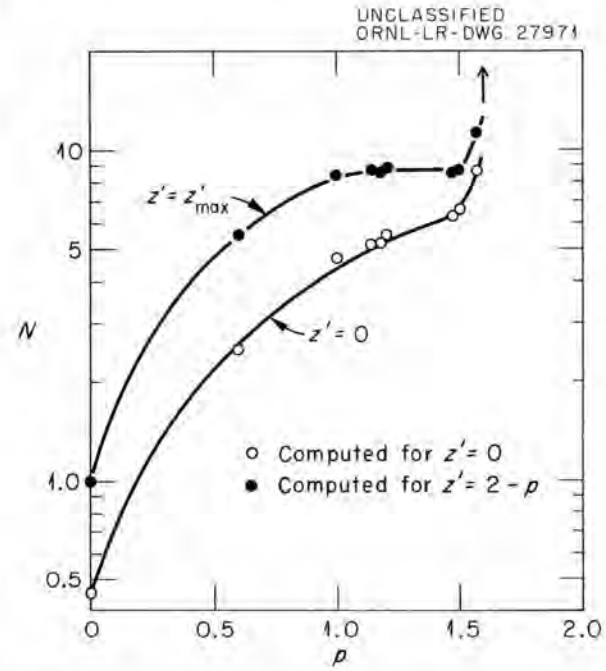


**Fig. 22. Polymerization of 0.05 *M* $Na_{2-p}H_pMoO_4$ in 1 *M* $NaClO_4$.**

The results in general agree with some of the earlier schemes proposed, for example, those based on diffusion measurements,[40] spectrophotometry,[41] and, more recently, titration studies in Sillen's laboratory. In all cases a predominance

[40] G. Jander and K. F. Jahr, *Kolloid-Beih.* 41, 1 (1935).
[41] I. Lindqvist, *Acta Chem. Scand.* 5, 568 (1951).

of polymers with $N$ between 6 and 8, for the range $p$ = 1.0 to 1.5, is postulated. However, several of our observations, particularly an apparent dependence of degree of aggregation on Mo(VI) concentration at constant $p$, raise questions concerning details of these schemes. As yet, we are not able to resolve these discrepancies or differences among the proposals of other authors.

### ADSORPTION ON INORGANIC MATERIALS

H. O. Phillips K. A. Kraus

Work on the adsorptive and ion exchange properties of inorganic materials was continued; principal emphasis remained on hydrous oxides, as in the previous period. A summary of some of the work on the ion exchange properties of hydrous oxides and acid salts has been prepared for the 1958 Geneva Conference on the Peaceful Uses of Atomic Energy.

### ADSORPTION OF $SO_2$ BY HYDROUS OXIDES

H. O. Phillips K. A. Kraus

During the investigation of the adsorptive properties of hydrous metal oxides, a qualitative study of their behavior toward acidic gases, such as $SO_2$, was made. Most of the oxides adsorbed $SO_2$, the extent of adsorption depending on pretreatment and firing temperature. Thus the oxides of Ti(IV), Zr(IV), Sn(IV), U(VI), Ta(V), and Nb(V), if dried at room temperature, adsorbed $SO_2$ readily at 25°C. If the oxides were initially in the $Cl^-$ form, 70 to 80% of $SO_2$ could be removed on treatment with a stream of $CO_2$ at 250°C.

Attempts were made to find oxides which could adsorb $SO_2$ at high temperatures. A large number of oxides were tested, including Ni(II), Cu(II), Zn(II), Pb(II), Al(III), Fe(III), Ce(III), Bi(III), Ti(IV), Zr(IV), Th(IV), Sn(IV), V(V), Nb(V), Ta(V), W(VI), and U(VI). Only a few of these adsorbed $SO_2$ appreciably after the oxide had been fired in the range of 600 to 900°C. With others, the oxide, sulfite, or sulfate melts or shrinks before the temperature is high enough to remove all the sulfur when a column is swept with air.

Of the oxides which adsorb $SO_2$ at high temperatures, Al(III) and Th(IV) seemed to have the highest uptake; cyclic loadings at 250°C followed by removal by air-sweeping at 900°C seemed successful through several cycles. Thus $Al_2O_3$ initially fired at 900°C adsorbed 0.4 mole of $SO_2$ per kilogram through five cycles. Similar uptakes could be reproduced through nine cycles with $ThO_2$.

### ANION EXCHANGE STUDIES

F. Nelson H. O. Phillips
K. A. Kraus Y. Marcus[42]

The program of investigating the properties of anion exchangers and the adsorption behavior of elements in complexing media was continued. Work on the following topics was essentially completed.

**Adsorption from HCl-HF Media.** – This system was discussed in some detail in the previous annual report, where results for 20 elements were summarized.[43] Although most of the remaining metallic elements were not expected to show significant adsorption from the media under investigation (1 $M$ HF–0.1 to 12 $M$ HCl), this assumption appeared questionable for certain elements. A study of some of these, Be(II), Al(III), Sc(III), Y(III), Eu(III) (as a typical rare earth), and Th(IV), has now been made. None of these elements show appreciable adsorbability in HCl solutions. In the presence of HF, only Be(II) and Sc(III) are adsorbable, provided the solutions are dilute enough so that difficulties from possible precipitation reactions are avoided. Beryllium(II) has a distribution coefficient of 17 near 0.05 $M$ HCl–1 $M$ HF; for Sc(III), $D$ = 6 in 0.1 $M$ HCl–1 $M$ HF. In the presence of 1 $M$ HF, adsorbability of both elements is negligible for $M_{HCl} > 1$.

**Rare Earths in Nitrate Solutions.** – Most ion exchange separations of rare-earth elements have been based on the use of cation exchangers with eluants containing organic complexing agents. Some separations involving anion exchange and organic eluants have been reported,[44] and, more recently, attention has turned toward possible utilization of anion exchangers with inorganic eluants. While the rare earths are not appreciably adsorbed from the common mineral acids HCl, $HNO_3$, and $H_2SO_4$, adsorption from slightly acidified

[42] Visiting scientist, fall and winter, 1957-58, on leave from the Israel Atomic Energy Commission.

[43] F. Nelson *et al.*, *Chem. Ann. Prog. Rep. June 20, 1957*, ORNL-2386, p 92.

[44] E. H. Huffman and R. L. Oswalt, *J. Am. Chem. Soc.* 72, 3323 (1950).

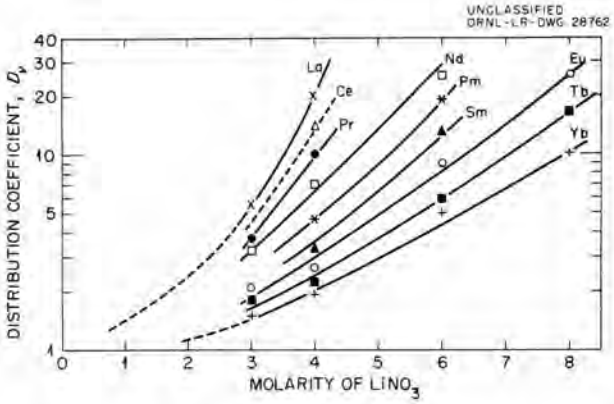


**Fig. 23. Adsorption of Rare Earths from Lithium Nitrate Solutions ($2 \times 10^{-3}$ *M* $HNO_3$, 78°C).**

ammonium nitrate solutions has been reported,[45] and adsorption has been found to be even greater from slightly acidified $LiNO_3$ solutions. Figure 23, a plot of $D_v$ vs the molarity of $LiNO_3$, summarizes adsorption results for several rare earths. On the basis of these data, separations of individual rare earths (particularly lighter rare earths) may be carried out in $LiNO_3$ media with relatively short columns. A typical separation employing a gradient elution technique is shown in Fig. 24. Further details may be found in an article recently submitted to the *Journal of the American Chemical Society*.

**Actinides in HCl Solution.** – The anion exchange behavior of U(IV) and U(VI) in HCl solutions was reported earlier,[46] and parallel studies have now been made for Np(IV), (V), (VI); Pu(III), (IV), (VI); and Am(III). While adsorption data for these elements in HCl are available from the work of Wish and Rowell,[47,48] doubt existed as to the oxidation states of the elements adsorbed by the resin under the conditions of their experiments. A systematic investigation was therefore begun, with column and equilibration techniques. Spectrophotometry was used to identify oxidation states, and counting methods were used for total metal analyses.

The results for neptunium and plutonium are summarized in Fig. 25, as plots of log $D_v$ vs molarity of HCl. Previously published data for U(IV) and (VI) are shown for comparison. As might be expected, the adsorption functions of the transuranium elements are very similar to those of uranium for corresponding oxidation states. Thus adsorption of Np(IV) and Pu(IV) begins at about 5 *M* HCl and increases with increasing molarity of HCl; adsorption of Np(VI) and Pu(VI) begins at about 1 *M* HCl and also

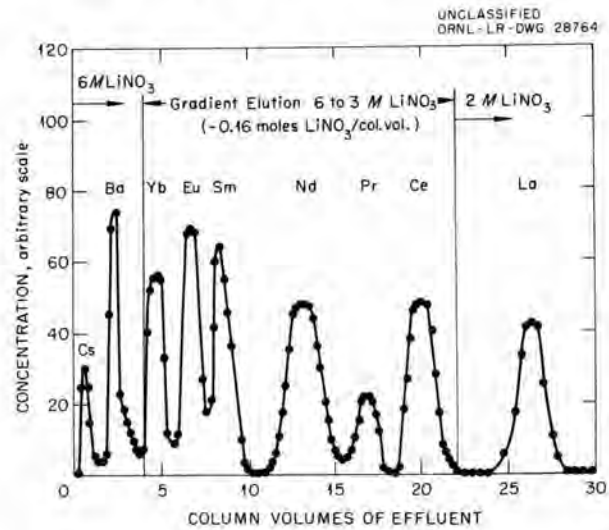


**Fig. 24. Separation of Cs, Ba, and Several Rare Earths in $LiNO_3$ Solutions (78°C, 0.25-$cm^2$ by 10.5-cm Column).**

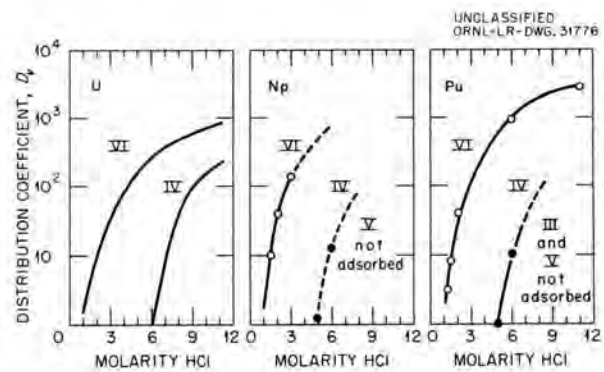


**Fig. 25. Adsorption of Uranium, Neptunium, and Plutonium from HCl Solutions.**

---

[45] K. A. Kraus and F. Nelson, *Am. Soc. Testing Materials, Spec. Tech. Publ. No. 195*, **27** (1958).

[46] K. A. Kraus, F. Nelson, and G. E. Moore, *J. Am. Chem. Soc.* **77**, 3972 (1955).

[47] L. Wish and M. Rowell, *Sequential Analysis of Tracer Amounts of Np, U, and Pu in Fission-Product Mixtures by Anion Exchange*, USNRDL-TR-117 (Oct. 11, 1956).

[48] L. Wish, *Quantitative Ion-Exchange Separations for Sequential Radiochemical Analysis*, USNRDL-TR-185 (Oct. 10, 1957).

increases with increasing molarity of HCl. Neptunium(V), which is stated in the literature to be adsorbable,[47–49] is not significantly adsorbed from 0.1 to 12 *M* HCl solutions. Plutonium(III) and Am(III) are not significantly adsorbed.

**Adsorption of $SO_2$ by Anion Exchangers.** – It was pointed out in the previous annual report[50] that organic anion exchangers may be used for the removal of various compounds from gas streams. The method was illustrated with $GeCl_4$ ($Cl^-$ form of exchanger), HCl ($Cl^-$ form), and HF ($F^-$ form). Studies on the removal of $SO_2$ from gas streams with sulfate- and sulfite-form exchangers were carried out, as well as parallel studies on removal of $SO_2$ from aqueous solutions. The apparent capacity of the exchanger for $SO_2$ is reasonably high and somewhat larger for the sulfate form than for the sulfite form. Interestingly, relatively dry resin beds have a higher uptake of $SO_2$ than moist beds. Regeneration of the beds may readily be achieved by the usual techniques and also by washing with water.

**Activity Coefficients of Some Electrolytes in the Resin Phase.** – Ratios, $\Gamma$, of activity coefficients of a number of electrolytes in the resin $[\gamma_{\pm(r)}]$ to those in the aqueous phase ($\gamma_\pm$) were evaluated from water and electrolyte uptake data. The electrolytes studied and the concentration ranges were LiCl (2–20 *m*), HCl (2–16 *m*), NaCl (0.002–6 *m*), $(NH_4)_2SO_4$ (0.8–5.8 *m*), $CoCl_2$ (0.002–4 *m*), $BaCl_2$ (0.02–1.8 *m*), and $H_2SO_4$ (0.001–7.5 *m*). At high concentrations, $\Gamma$ is remarkably constant, although, it varies substantially at low concentrations.

Activity coefficients of HCl in the resin, determined as a function of HCl activity and of cross-linking, can be correlated by a concentrated-electrolyte model of the exchanger, with the assumption that Harned's rule of the linear variation of log $\gamma_\pm$ with composition holds at constant total molality. Similar considerations, with Harned's rule generalized to higher multicomponent systems, permit at least semiquantitative evaluation of log $\gamma_{\pm HCl(r)}$ for HCl-LiCl mixtures where $\Gamma_{HCl}$ is comparatively small. Because of the relatively low activity coefficients of HCl in the resin phase at high ionic strength, separation of HCl from concentrated halide solutions is possible.

The strong adsorption of sulfuric acid by the sulfate form of the exchanger indicates that the bisulfate ion is a much weaker acid in the resin phase than in the aqueous phase. From the activity coefficients $\gamma_{\pm(r)}$ for $H_2SO_4$, the concentration quotient for the equilibrium

$$HSO^-_{4(r)} \rightleftharpoons H^+_{(r)} + SO^{--}_{4(r)}$$

has been evaluated as a function of $H_2SO_4$ invasion of the resin.[51]

**Evaluation of Complexing Reactions from Anion Exchange Data.** – The problem of obtaining information on complexing in the aqueous phase from anion exchange data has been summarized elsewhere.[52]

## TEMPERATURE DEPENDENCE OF ION EXCHANGE EQUILIBRIA

K. A. Kraus R. J. Raridon

Studies on the temperature dependence of ion exchange equilibria in pressure systems, which were first discussed in the previous annual report,[53] were continued. The studies, which in some cases were carried to 200°C, now include the cation exchange equilibria $Na^+$, $K^+$, $Rb^+$, $Cs^+$, $Be^{++}$, $Ba^{++}$, $Co^{++}$, $Zn^{++}$, $La^{+++}$, and $Eu^{+++}$ against hydrogen and $K^+$, $Rb^+$, $Cs^+$, and $Ba^{++}$ against sodium, a simple anion exchange equilibrium ($Br^-$ against chloride), and some typical equilibria involving metal complexes [Zn(II) in HCl, Ga(III) in HCl]. The anion exchange studies with Zn(II) and Ga(III) were included to illustrate that the anion exchange method could be used effectively for study of complex equilibria at high temperatures.

As pointed out previously, the measurements were carried out by a packed-column technique. A sample of the resin, uniformly loaded with an

[49] E. K. Hyde, *Proc. Intern. Conf. Peaceful Uses Atomic Energy, Geneva, 1955* 7, 296 (1956).

[50] F. Nelson *et al.*, *Chem. Ann. Prog. Rep. June 20, 1957*, ORNL-2386, p 95.

[51] F. Nelson and K. A. Kraus, *J. Am. Chem. Soc.* **80**, 4154 (1958).

[52] K. A. Kraus, "Present State of the Electrolyte Problem," Abstract No. 142A presented at the One Hundred and Eleventh Meeting of the Electrochemical Society, Washington, D. C., May 12–16, 1957.

[53] K. A. Kraus, R. J. Raridon, and D. C. Michelson, *Chem. Ann. Prog. Rep. June 20, 1957*, ORNL-2386, p 101.

appropriate tracer, is placed in a column through which various electrolyte solutions are passed. If the distribution coefficients are high, the flowing electrolyte solution will rapidly come to equilibrium with the resin bed. Under these conditions the lower portion of the column does not change significantly in composition. Distribution coefficients $D = m_{B(r)}/m_B$ of the tracer ion $B^{b+}$ are obtained by combining analyzed concentration ($m_B$) of the effluent with the previously established resin concentrations [$m_{B(r)}$]. Equipment was constructed by which the effluent may be continuously sampled in pressurized columns and at temperatures up to 200°C. The first model of the high-temperature column contained some stainless steel valves and hence was not suitable for measurements in chloride or other corrosive solutions. A modified column has been constructed in which only glass or plastic surfaces are exposed to the solution; this column was used in all experiments with chloride solutions.

**Cation Exchange Equilibria.** – From the measured distribution coefficients, concentration quotients $K^m$ for the ion exchange equilibrium

$$(1) \qquad B^{b+} + bA^+_{(r)} \rightleftharpoons bA^+ + B^{b+}_{(r)}$$

may be computed by the relationship

$$(2) \qquad K^m = \frac{K}{G} = \frac{m_{B(r)}\, m_A^b}{m_B\, m_{A(r)}^b} = D\,\frac{m_A^b}{m_{A(r)}^b} = \frac{K}{G} ,$$

where $B^{b+}$ is the tracer ion, $A^+$ is the "macro" cation, $m$ indicates concentration, subscript $(r)$ indicates the resin phase, $K$ is the equilibrium constant for the ion exchange equilibrium, and $G$ the appropriate activity coefficient quotient.

In all cases studied, log $K^m$ did not vary linearly with $1/T$ ($T$ is the absolute temperature), as might be expected if the (apparent) enthalpy change $\Delta H'$ for the ion exchange equilibrium were constant. Rather, plots of log $K^m$ show distinct curvature. The data could be fitted satisfactorily to the relationship

$$(3) \quad \log K^m = \log K_o^m + A \log \frac{T}{T_o} + B\left(1 - \frac{T_o}{T}\right) ,$$

which is derived under the assumption that the heat capacity differences $\Delta C_p$ are constant. In Eq. 3, $A$ and $B$ are constants, and subscript $o$ refers to a reference temperature, here taken as 0°C.

Through differentiation of Eq. 3,

$$(4) \quad \Delta H' = ART + 2.303BRT_o = \Delta C_p\, T + 1249.7B$$

is obtained, where $\Delta H'$ is the apparent heat of the exchange equilibrium, Eq. 1, and $R$ is the gas constant. By a second differentiation,

$$(5) \qquad \Delta C_p = AR$$

is obtained. Through combination of the values of $K^m$ and $\Delta H'$ the apparent entropy change $\Delta S'$ may be obtained.

The results of the cation exchange studies with Dowex 50-X12 are summarized in Table 19 (constants for Eq. 3, $\Delta C_p$ per equivalent, and computed temperature $T_{min}$ at the adsorption minimum) and in Table 20 ($\Delta H'$ per equivalent and $\Delta S'$ per equivalent).

**Table 19. Temperature Dependence of Cation Exchange Equilibria (Dowex 50-X12)**

| Ion | log $K_o^m$ | $A$ | $-B$ | $T_{min}$ | $\Delta C_p$/equiv |
|---|---|---|---|---|---|
| | | **Hydrogen-Form Resin** | | | |
| $Na^+$ | 0.198 | 5.2 | 3.4 | 410 | 10.4 |
| $K^+$ | 0.805 | 5.9 | 4.5 | 480 | 11.6 |
| $Rb^+$ | 0.936 | 6.1 | 5.2 | 530 | 12.1 |
| $Cs^+$ | 1.114 | 5.7 | 5.3 | 580 | 11.3 |
| $Be^{++}$ | 0.392 | 4.7 | 1.4 | 190 | 4.6 |
| $Ba^{++}$ | 1.384 | 12.7 | 7.7 | 380 | 12.6 |
| $Co^{++}$ | 0.307 | 7.1 | 3.3 | 290 | 7.1 |
| $Zn^{++}$ | 0.175 | 8.7 | 4.1 | 295 | 8.7 |
| $La^{+++}$ | 1.455 | 22.9 | 9.9 | 270 | 15.2 |
| $Eu^{+++}$ | 1.355 | 19.7 | 7.7 | 250 | 13.1 |
| | | **Sodium-Form Resin** | | | |
| $K^+$ | 0.396 | 0.4 | 0.9 | 1550 | 0.7 |
| $Rb^+$ | 0.509 | 0.7 | 1.3 | 1160 | 1.4 |
| $Cs^+$ | 0.660 | 0.7 | 1.4 | 1340 | 1.3 |
| $Ba^{++}$ | 0.932 | 6.9 | 3.0 | 275 | 6.9 |

Table 20. Apparent Enthalpy and Entropy Changes for Cation Exchange Equilibria (Dowex 50-X12; $\Delta H'$ in kcal, $\Delta S'$ in Entropy Units)

| Ion | 0°C | | 25°C | | 50°C | | 100°C | | 150°C | | 200°C* | |
|---|---|---|---|---|---|---|---|---|---|---|---|---|
| | $\Delta H'$ | $\Delta S'$ | $\Delta H'$ | $\Delta S'$ | $\Delta H'$ | $\Delta S'$ | $\Delta H'$ | $\Delta S'$ | $\Delta H'$ | $\Delta S'$ | $\Delta H'$ | $\Delta S'$ |
| **Hydrogen-Form Resin** | | | | | | | | | | | | |
| $Na^+$ | −1.4 | −4.2 | −1.2 | −3.3 | −0.9 | −2.5 | −0.4 | −1.0 | 0.2 | 0.3 | 0.7 | 1.5 |
| $K^+$ | −2.4 | −5.2 | −2.1 | −4.2 | −1.9 | −3.3 | −1.3 | −1.6 | −0.7 | −0.2 | −0.1 | 1.2 |
| $Rb^+$ | −3.2 | −7.2 | −2.8 | −6.2 | −2.5 | −5.2 | −1.9 | −3.5 | −1.3 | −2.0 | −0.7 | −0.6 |
| $Cs^+$ | −3.6 | −7.7 | −3.3 | −6.7 | −2.9 | −5.8 | −2.4 | −4.2 | −1.8 | −2.8 | −1.2 | −1.5 |
| $Be^{++}$ | 0.4 | 2.3 | 0.5 | 2.5 | 0.6 | 3.0 | 0.8 | 3.7 | 1.1 | 4.3 | 1.3 | 4.8 |
| $Ba^{++}$ | −1.4 | −1.9 | −1.1 | −0.8 | −0.8 | 0.2 | −0.1 | 2.0 | 0.5 | 3.6 | 1.1 | 5.0 |
| $Co^{++}$ | −0.1 | 0.3 | 0.1 | 0.9 | 0.2 | 1.4 | 0.6 | 2.4 | 0.9 | 3.4 | 1.3 | 4.1 |
| $Zn^{++}$ | −0.2 | −0.3 | 0.0 | 0.4 | 0.2 | 1.1 | 0.7 | 2.4 | 1.1 | 3.5 | 1.5 | 4.4 |
| $La^{+++}$ | 0.0 | 2.3 | 0.4 | 3.7 | 0.8 | 4.9 | 1.6 | 7.1 | 2.3 | 9.0 | 3.1 | 10.7 |
| $Eu^{+++}$ | 0.4 | 2.2 | 0.7 | 3.4 | 1.0 | 4.4 | 1.7 | 6.3 | 2.3 | 7.9 | 3.0 | 9.4 |
| **Sodium-Form Resin** | | | | | | | | | | | | |
| $K^+$ | −0.9 | −1.5 | −0.9 | −1.4 | −0.9 | −1.3 | −0.8 | −1.2 | −0.8 | −1.1 | −0.8 | −1.1 |
| $Rb^+$ | −1.2 | −2.1 | −1.2 | −2.0 | −1.1 | −1.9 | −1.1 | −1.7 | −1.0 | −1.5 | −0.9 | −1.4 |
| $Cs^+$ | −1.4 | −2.1 | −1.4 | −2.0 | −1.3 | −1.9 | −1.3 | −1.7 | −1.2 | −1.6 | −1.2 | −1.4 |
| $Ba^{++}$ | 0.0 | 2.1 | 0.2 | 2.7 | 0.3 | 3.2 | 0.7 | 4.2 | 1.0 | 5.1 | 1.4 | 5.8 |

*Extrapolated values, except for sodium-form resin.

The heat capacity changes are positive in all cases and hence $\Delta H'$ increases with $T$. For the exchange reactions with the hydrogen-form resin, $\Delta C_p$ is considerably larger than for exchange reactions involving the sodium-form resin; however, the differences between the two types are not constant, as might have been expected. The values of $\Delta C_p$ for the alkali metals are surprisingly similar, even though the values of $\Delta H'$ for these elements differ by several kilocalories.

Values of $\Delta H'$ and $\Delta S'$ are positive or negative, depending on the element and the temperature. While the absolute magnitudes of $\Delta H'$ and $\Delta S'$ are small, they must be considered large compared with the resulting values of $K^m$.

**Anion Exchange Studies: Bromide-Chloride Exchange.** – The adsorption of bromide tracer from 0.01 $M$ HCl on the chloride form of the anion exchanger Dowex 1-X10 was studied as a function of temperature up to 150°C. Above this temperature the results became erratic, probably because of thermal decomposition of the resin. The adsorption data as a function of temperature can be described satisfactorily by Eq. 3. The values of the parameters are log $K_o^m = 0.613$, $A = 3.2$, and $B = -2.8$. From these data, $\Delta C_p = 6.3$ cal/°C. The apparent enthalpy and entropy changes are summarized in Table 21.

**Anion Exchange Studies: Adsorption of Zn(II) and Ga(III) from HCl Solutions.** – Adsorption of these elements by the anion exchanger Dowex 1-X10 was studied as a function of temperature from 25 to 150°C and as a function of HCl concentration ($m_{HCl}$). Plots of log $D$ vs $m_{HCl}$ for these elements are characterized by a rising branch at low $m_{HCl}$, where the average charge of the ions in solution is positive, by a maximum, where the average charge is near zero, and by a falling

Table 21. Apparent Enthalpy and Entropy for Bromide Tracer–Chloride Exchange (Dowex 1-X10)

| Temperature (°C) | $\Delta H'$ (kcal) | $\Delta S'$ (e.u.) |
|---|---|---|
| 0 | −1.7 | −3.6 |
| 25 | −1.6 | −3.0 |
| 50 | −1.4 | −2.5 |
| 100 | −1.1 | −1.6 |
| 150 | −0.8 | −0.8 |
| (200)* | −0.5 | −0.1 |

*Extrapolated value.

branch with $m_{HCl}$ at high concentrations, where presumably the average charge of the ions in solution is negative. In this last region, adsorbability of both elements decreases sharply with temperature. For Zn(II) this decrease is by a factor of about 10 and for Ga(III) by a factor of about 100 for the temperature interval 25 to 150°C. It may be concluded that the enthalpy of adsorption of the negatively charged complexes of these ions is large and negative.

The adsorption maxima for both elements shift to lower HCl concentrations as the temperature is increased. This shift is only moderately large for Ga(III), where the maximum changes from $m_{HCl} = 8$ at 25°C to $m_{HCl} = 4$ at 150°C. For Zn(II) the shift is substantially greater: the maximum at 25°C is located near $m_{HCl} = 2$ and at 150°C near $m_{HCl} = 0.3$. These shifts in the maxima imply substantially greater complex formation at the higher temperatures.

This increased tendency for complex formation at high temperature is more dramatically illustrated by the slopes of the adsorption functions at low HCl concentration, where $D$ rises with $m_{HCl}$. Thus at room temperature for Zn(II) the slope at $m_{HCl} = 0.5$ is approximately +2; that is, the element is not significantly complexed by chloride ions under these conditions. At 150°C the slope is approximately +1 for $m_{HCl} = 0.02$. At this higher temperature Zn(II) is extensively complexed (average formula $ZnCl^+$) even in dilute HCl solutions. A similar increase in extent of complexing occurs with Ga(III). At room temperature $Ga^{+++}$ is presumably not complexed significantly at $m_{HCl} = 1$; however, at 150°C the data suggest that the average formula of the complexes at much lower chloride concentrations ($m_{HCl} = 0.25$) is $GaCl_2^+$.

## SOLUBILITY OF SILVER CHLORIDE IN THE TEMPERATURE RANGE 25 TO 200°C

K. A. Kraus R. J. Raridon

As pointed out in previous reports,[54,55] packed-column techniques can readily be adapted to the measurement of solubilities of insoluble salts. These measurements can be carried to relatively high temperatures by using jacketed and pressurized columns similar in design to those used in ion exchange studies at high temperatures. However, in solubility studies an additional complication arises, since sampling of the effluent from a high-temperature column is difficult when the solubility of the salt increases with temperature, as is frequently the case.

In the ion exchange columns the letdown valve used for sampling is at room temperature. Thus in the exit capillary of the column and in the valve, crystallization of the salt from the saturated solution will occur, causing an error in the analyses. This difficulty may be circumvented by analyzing the effluent from the column while it is still at high temperature. To achieve this objective the high-temperature column was modified by including with it a scintillation counter which views a small, jacketed flow cell. The cell-counter assembly is shielded from the column and, to further decrease the background, is connected to the column with a long, jacketed glass capillary.

Measurements of the solubilities $s$ of AgCl in various HCl solutions ($m_{HCl} = 0.01$, 0.1, 0.5, 1.45, and 3.06) have been carried out from 25 to 200°C with this equipment. At constant $m_{HCl}$, plots of log $s$ vs $1/T$ are straight lines. The apparent heats of solution $\Delta H'$ thus are independent of temperature at constant $m_{HCl}$; $\Delta H'$ decreases from 11.9 kcal to 6.5 kcal as $m_{HCl}$ rises from 0.01 to 3.06.

More detailed studies of the solubility of this salt are now under way with the objective of determining complexing properties of silver as a function of temperature.

[54] K. A. Kraus and D. J. Coombe, *Chem. Semiann. Prog. Rep. June 20, 1956*, ORNL-2159, p 42.

[55] K. A. Kraus and D. C. Michelson, *Chem. Ann. Prog. Rep. June 20, 1957*, ORNL-2386, p 104.

# CHEMISTRY OF CORROSION

During the past year the work in this group included the following topics: (1) the mechanism of inhibition by ions of the $XO_4^{n-}$ type; (2) kinetics of the reduction of uranyl ions at a stainless steel electrode in aerated sulfuric acid; (3) the theory and measurement of differential capacity in the system studied in (2); and (4) the electrochemistry of zirconium.

## STUDIES ON INHIBITION

R. F. Sympson[1] G. H. Cartledge

In considering the mechanism by which an inhibiting $XO_4^{n-}$ particle enables an iron electrode to become passivated in aerated solution, the suggestion was made[2] that the effect may derive from an electrostatically induced space charge at the interface. Other suggestions attribute the effect of such inhibitors either to rapid precipitation of ferrous ions as an insoluble product in pores of the protective film, or to reduction of the inhibitor on cathodic areas at such a rate that the anodic current density at active sites is sufficient to passivate them.

According to thermodynamic calculations, the pertechnetate ion cannot oxidize $Fe^{++}$ ions completely to $Fe(OH)_3$ under inhibiting conditions, as the chromate ion may do, since it is a weaker oxidizing agent and is derived from a strong acid, $HTcO_4$; it therefore has no buffering capacity such as is possessed by chromate ions. To demonstrate the inapplicability of the precipitation hypothesis in this case, the following experiment was performed. A reaction vessel was constructed which consisted of a central tube having side arms to which two bulbs were connected by ground-glass joints. The contents of these bulbs could be transferred to the central tube by rotation around the joints. The three compartments contained, respectively, solid ferrous ammonium sulfate, water, and a solution of potassium pertechnetate in excess of the amount required for complete oxidation of the ferrous salt. By alternate freezing under vacuum and thawing, the air was substantially removed,[3] the ferrous salt was then dissolved in the central tube, and the pertechnetate solution was added.

In an experiment in which the original solution of $KTcO_4$ had a pH of 6.61, no precipitated $Fe(OH)_3$ was visible after 5 hr. Air was then admitted, and the mixture was allowed to stand overnight at room temperature. A colloidal turbidity was visible. After some days this solid coagulated; it was then assayed spectrophotometrically for iron and by beta counting for technetium. The results showed that only about 0.2 mg of iron had been precipitated, of the 11 mg present, and that the reduced technetium corresponded to only 0.003% of the amount equivalent to the iron in the precipitate. It is therefore concluded that any incipient reaction between the ferrous and pertechnetate ions was quickly stopped by the consequent rise of acidity, and that such slow oxidation as was observed was caused predominantly by the oxygen finally admitted.

Other experiments were conducted to test the suggestion of Uhlig[4] that reduction of the inhibitor at cathodic areas produces high anodic current densities at active sites. Reduction of an oxidizing inhibitor may, of course, occur in the absence of oxygen, but previous experiments[5] showed that very minute amounts of $TcO_2$ deposit on the specimen during passivation in aerated solution, and also that the molybdate and tungstate ions fail to produce noble (passive) potentials on iron in the absence of oxygen, although passivation results when they are present with oxygen. Furthermore, it was shown that oxygen is able to passivate iron in the presence of either phosphate or phthalate ions, to neither of which can oxidizing properties be ascribed.

In the new experiments, carbon-steel specimens were prepared which had a tiny depression drilled at the mid-point for ease in producing an identifiable area of bare metal after passivation. The entire

[1] Summer employee, Ohio University, Athens.

[2] G. H. Cartledge, preprints, *Internationales Kolloquium über die Passivität der Metalle, Heiligenberg*, 1957; *Z. Elektrochem.* (in press).

[3] The use of R. E. Meyer's vacuum rack is gratefully acknowledged.

[4] H. H. Uhlig, discussion, Heiligenberg (1957).

[5] G. H. Cartledge, *J. Phys. Chem.* 59, 979 (1955); R. F. Sympson and G. H. Cartledge, *J. Phys. Chem.* 60, 1037 (1956).

specimen was passivated in an aerated chromate solution (0.001 *f*, 88°C). When the specimen was rinsed and subsequently exposed to a pertechnetate solution, the entire specimen (4.5 $cm^2$) had a count indicating about 0.0014 $\mu g$ of technetium. This corresponds to about $2 \times 10^{12}$ atoms/$cm^2$, or a small fraction of the amount required for a monolayer. A second specimen was passivated likewise in a chromate solution, and the central "pit" was redrilled to destroy the film locally before the specimen was placed in the pertechnetate solution for 2 hr at 88°C. The distribution of reduced technetium between the bare-metal and film-covered areas was determined by counting the beta activity before and after covering the pit with a small piece of metal. In different experiments the counts showed that the filmed area received only 0.1 to 0.5% of the reduction product, although it represented 99.4% of the exposed area. These experiments seem to confirm unequivocally the previous conclusion that the technetium found on well-washed inhibited specimens is not the result of reduction by cathodic processes *on the film,* but comes from processes associated with anodic dissolution of metal.

The two sets of experiments do not prove the adequacy of the electrostatic hypothesis, but they indicate clearly that neither the precipitation nor the reduction hypothesis is applicable in the case of inhibition by the pertechnetate ion.

In connection with the technetium work, the absorption spectrum of pertechnetate ions has been measured with a model DU Beckman spectrophotometer on a number of solutions carefully prepared from specimens of solid salt purified by W. J. Martin. The ratio of the molar extinction coefficients at the absorption peaks (2440 and 2875 Å) has also been determined on several solutions of exceptional purity but only approximately known molarity prepared by electrolytic reduction to $Tc(OH)_4$ and electrolytic reoxidation to $NH_4TcO_4$. Also, the measurements have been checked on a sample of $KTcO_4$ specially purified and intensively dried by R. H. Busey. From all these measurements over a period of five years, it is believed that the best values of the molar extinction coefficients and their ratio are as follows: 2440 Å, 6100; 2875 Å, 2320; ratio 2440/2875 = 2.63. The ratio value is particularly useful in assuring the freedom of solutions from interfering impurities when the spectrum is used for quantitative analytical purposes.

## KINETIC STUDIES ON CORROSION SYSTEMS

F. A. Posey

A previous report[6] outlined an electrochemical kinetic theory of corrosion systems which was used to analyze data on the kinetics of the reduction of cupric ion on the surface of passive stainless steel in dilute sulfuric acid. For the continuation of these studies, a precise electronic potentiostat was developed.[7] The theory and potentiostatic techniques were applied to the reduction of uranyl ion at a stainless steel electrode in aerated sulfuric acid. A procedure was also developed for determining the differential capacity of such electrode systems based upon an analysis of their potential-time behavior.

### Kinetics of the Reduction of Uranyl Ion

The results of potentiostatic measurements on the reduction of uranyl ion at a passive, electropolished stainless steel electrode are shown in Figs. 26 and 27. As was shown previously,[6] in a complex system in which the concentration of some species $x$ is varied at constant electrode potential, the increase in the steady-state current density, $|j_p - j_{p,0}|$, upon addition of $x$ at a concentration $C_x$ is related to the kinetic order $p_x$ with respect to $x$ by the equation

$$(1) \qquad \left( \frac{\partial \ln |j_p - j_{p,0}|}{\partial \ln C_x} \right)_{\Delta\phi} = p_x \ .$$

Here $j_{p,0}$ measures the rate of reduction of dissolved oxygen, since, at the potentials used, the rate of oxidation of stainless steel is negligible in comparison with the reduction of oxygen. Figure 26 shows that the reduction of $UO_2^{++}$ is first order with respect to its concentration over the whole range of potentials and concentrations studied.

Data from Fig. 26 are presented in a different form in Fig. 27. Here, the logarithm of the rate of reduction of $UO_2^{++}$, $\log |j_{UO_2^{++}}| \equiv \log |\Delta j_p|$, is plotted vs the electrode-solution potential difference

[6] F. A. Posey, *Chem. Ann. Prog. Rep. June 20, 1957,* ORNL-2386, p 110.

[7] The author is indebted to E. Fairstein and his group, of the Instrumentation and Controls Division, for the development of this instrument.

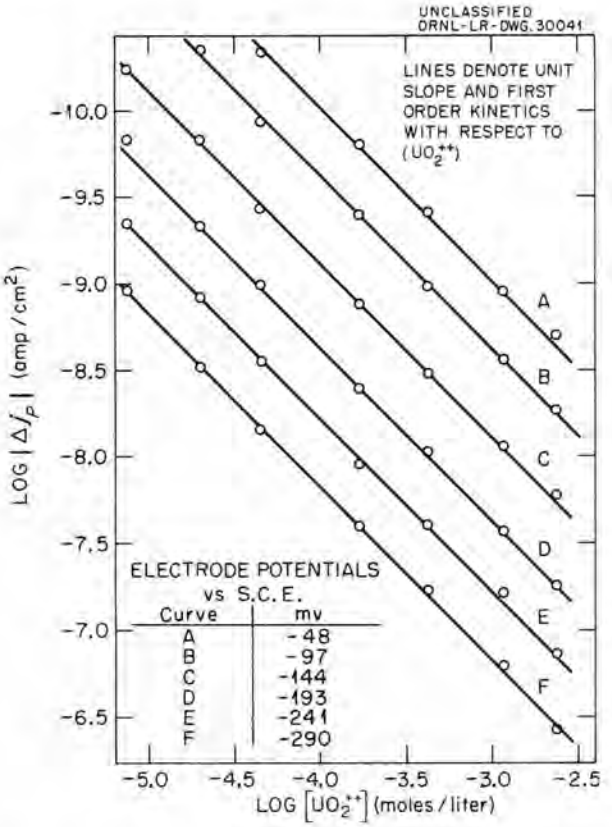


**Fig. 26. Reduction of $UO_2^{++}$ on the Surface of Passive Stainless Steel in 0.010 / $H_2SO_4$–0.090 / $Na_2SO_4$ at 44°C in Oxygen.**

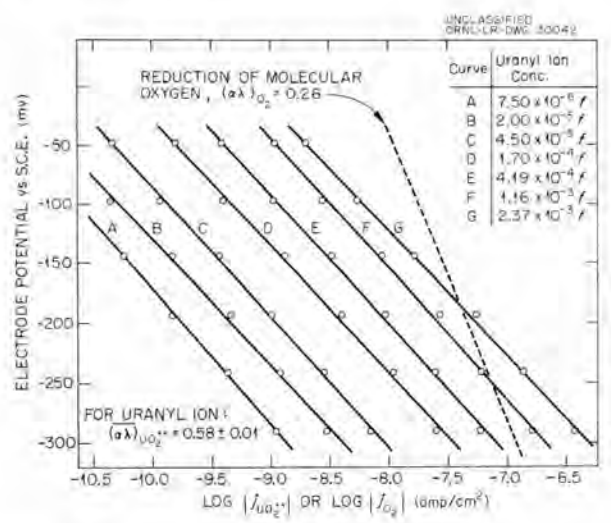


**Fig. 27. Reduction of $UO_2^{++}$ on the Surface of Passive Stainless Steel in 0.010 / $H_2SO_4$–0.090 / $Na_2SO_4$ at 44°C in Oxygen.**

vs the saturated calomel electrode, $\Delta\phi$, for several values of the concentration of uranyl ion in solution. Lines drawn through experimental points in this graph are least-squares fits to the data. The slope of this plot is related to the number of charges crossing the interphase during each elementary reaction sequence for the reduction of $UO_2^{++}$ by

$$(2)\quad \left(\frac{\partial\Delta\phi}{\partial \ln |j_{UO_2^{++}}|}\right)_{[UO_2^{++}]} = -\frac{RT}{\mathfrak{F}}\cdot\frac{1}{(\alpha\lambda)_{UO_2^{++}}},$$

where $RT/\mathfrak{F}$ has its usual significance, and the measurable quantity of kinetic interest, $(\alpha\lambda)_{UO_2^{++}}$, is the product of the electrochemical transfer coefficient $\alpha$ and the number of charges involved in the reaction of each $UO_2^{++}$ group at the interphase, $\lambda$. In Fig. 27 the notation $\overline{(\alpha\lambda)}_{UO_2^{++}}$ represents the average of the values of $(\alpha\lambda)_{UO_2^{++}}$ obtained by analyzing the six least-squares lines with Eq. 2. The reduction of $UO_2^{++}$ proceeds at the interphase between the passive oxide and the solution, and for this case it can be shown[8,9] that the best kinetic description of the passive stainless steel interphase is a dual barrier model such that $\alpha$ has expected values of the order of $\frac{1}{4}$, instead of the $\frac{1}{2}$ usually associated with simple two-phase (metal + solution) systems. Hence $\lambda_{UO_2^{++}}$ has the value 2 with $\alpha_{UO_2^{++}} = 0.29$. The rate of reduction of molecular oxygen, also at the oxide-solution interphase, is shown in Fig. 27 as a function of $\Delta\phi$. An expression similar to Eq. 2 applies here also, with $\alpha_{O_2} = 0.26$ and $\lambda_{O_2} = 1$ for the rate-determining step of the reduction of $O_2$, in agreement with a dual-barrier model and with independent studies on the mechanism of $O_2$ reduction. Extrapolation of the rate of $O_2$ reduction up to the steady-state potential for the corrosion of passive stainless steel in the present environment yields a corrosion current of $2.15 \times 10^{-9}$

[8] F. A. Posey, G. H. Cartledge, and R. P. Yaffe, *J. Electrochem. Soc.* (in press).

[9] R. E. Meyer, "Electrochemistry of Zirconium" (this report).

amp/cm$^2$. This same rate of corrosion was obtained from polarizability measurements in the vicinity of the steady-state corrosion potential.

Measurements made at 67 and 85°C gave kinetic parameters similar to those obtained at 44°C. The reduction rate increased with increasing temperature, and at quite low potentials the slope,

$$\left( \frac{\partial \Delta\phi}{\partial \log |j_{UO_2^{++}}|} \right)_{[UO_2^{++}]} ,$$

tended to become infinite. This may indicate either a diffusion-limited reduction process or the formation of an intermediate as a precursor to the electrode process.[10]

An additional feature of the measurements at 67 and 85°C and at low potentials was a linear change of the current density with time at a constant potential, that is,

$$\left( \frac{\partial j_p}{\partial t} \right)_{\Delta\phi, [UO_2^{++}]} = \text{a constant} .$$

This constant increased with the concentration of uranyl ion. A kinetic analysis showed that the quantity

$$Z = \left( \frac{\partial \ln (\partial j_p/\partial t)}{\partial \ln [UO_2^{++}]} \right)_{\Delta\phi}$$

is diagnostic for distinguishing between (1) catalysis of the reduction of $UO_2^{++}$, and (2) catalysis of the reduction of $O_2$ by the reduced uranium species. For the reduction of $UO_2^{++}$, $Z$ should be 2, and for reduction of $O_2$, $Z = 1$; the experimental result gave $Z = 1$. This conclusion was confirmed by measurements in an atmosphere of nitrogen, in which case there was no variation of current density with time, and the rate of reduction of $UO_2^{++}$ was identical with that in the presence of oxygen. The experiments do not indicate whether the "reduction product" consists of $UO_2^{++}$ ions transferred into the oxide lattice (a cathodic process) or of a $U^{4+}$ species in solution formed by a two-electron electrode process. Whichever it is, the results show that accumulation of such a product provides an improved path for the reduction of dissolved oxygen.

[10] H. Gerischer and K. J. Vetter, *Z. physik. Chem.* (*Leipzig*) 197, 92 (1951).

### Measurement of Differential Capacity

Any discussion of electrochemical systems which are not in a steady state and in which electrode potentials change with time eventually involves (or should consider) the notion of the differential capacity of an electrode-solution interphase. This property of electrode systems has been ably reviewed elsewhere[11,12] from the standpoints of the thermodynamic theory of interphases in a state of equilibrium and of kinetic theories of the structure of an electrified interphase. The differential capacity of the electrode-solution system consisting of electropolished stainless steel in oxygenated 0.010 *f* $H_2SO_4$ + 0.090 *f* $Na_2SO_4$ has been measured as a function of temperature and electrode-solution potential difference. The technique used in this study may be considered as a modification of the current-interrupter method[13] for the measurement of differential capacities. The theory of the technique used here will be outlined for the case of a system with any number of partial processes under activation control.

Consider a system to which a d-c current is applied which periodically changes in sign, that is, a square wave of current symmetrical (with time) about zero current. Then the variation of the electrode-solution potential difference with time will present the aspect of a (modified) saw-tooth wave with the frequency and phase of the square-wave applied current. The total applied current density $j_p$ is by definition the sum of the (net) Faradaic current density (c.d.) $j_F$ and the non-Faradaic c.d. $j_N$, or "condenser" c.d., at any time $t$. In order to measure the differential capacity as a function of potential, it is necessary to polarize the electrode system to some potential of interest, and this operation requires some constant applied c.d. $j_{p,1}$ superimposed on the square-wave applied c.d. $j_{p,2}$; hence it follows that $j_p = j_{p,1} + j_{p,2}$. The (net) Faradaic c.d. $j_F$ is a function only of the electrode-solution potential difference $\Delta\phi$, and

[11] D. C. Grahame, *Chem. Rev.* 41, 441 (1947).

[12] R. Parsons, *Modern Aspects of Electrochemistry* (ed. by J. O'M. Bockris), p 103, Academic Press, New York, 1954.

[13] D. C. Grahame, *J. Phys. Chem.* 57, 257 (1953).

is the difference between the total anodic and total cathodic c.d.'s of the processes proceeding at the interphase;[14] thus

$$(3)\quad j_F = \sum_i (j_{i,a} - j_{i,c})$$

$$= \sum_i \left[ K_{i,a} e^{+(\alpha\lambda)_{i,a} \mathfrak{F}\, \Delta\phi/RT} - K_{i,c} e^{-(\alpha\lambda)_{i,c} \mathfrak{F}\, \Delta\phi/RT} \right],$$

where subscripts $a$ and $c$ refer to anodic and cathodic processes, respectively, $K$ contains the potential-independent portion of the specific rate constant of a process and the concentrations of reactants, the summation extends over all processes at the interphase, and other quantities are as defined previously. The differential capacity is given by

$$(4)\qquad C \equiv \frac{d\rho}{d\Delta\phi} = \frac{d\rho/dt}{d\Delta\phi/dt} = \frac{j_N}{d\Delta\phi/dt},$$

where $C$ is the differential capacity (in units of amp·sec·v$^{-1}$·cm$^{-2}$), and $\rho$ is charge density. From the previous equations it follows that

$$(5)\quad j_{p,1} + j_{p,2}$$

$$= \sum_i \left[ K_{i,a} e^{+(\alpha\lambda)_{i,a} \mathfrak{F}\, \Delta\phi/RT} - K_{i,c} e^{-(\alpha\lambda)_{i,c} \mathfrak{F}\, \Delta\phi/RT} \right] + C \frac{d\Delta\phi}{dt}.$$

When the mathematical analysis is carried through, it turns out that the differential capacity at a chosen potential, $\Delta\phi_0$, may be found from a knowledge of the square-wave polarizing current $j_{p,2}$ and a measurement of the slope of the potential-time curve at the chosen potential; that is,

$$(6)\qquad \left(\frac{d\eta}{dt}\right)_{\eta=0} = \frac{j_{p,2}}{C},$$

where $\eta = \Delta\phi_t - \Delta\phi_0$.

The results of differential capacity measurements on the present system for several temperatures are presented in Fig. 28. The differential capacity is a measure of the change in charge density at an electrode-solution interphase necessary to effect a change in the over-all potential difference. As in the case of ordinary electrical circuits, the reciprocal of the measured differential capacity is the sum of the reciprocals of all the differential capacities in series at the electrode-solution interphase; hence the smallest differential capacity in the system contributes most to the measured value. In these measurements, all capacities approach small values at high potentials but rise very rapidly at lower potentials. This observation accounts for the unusually long times necessary for the attainment of steady-state potentials in the lower potential region in experiments on stainless steel. These measurements were performed also to ascertain how the differential capacity is affected when $UO_2^{++}$ is added to the solution. No detectable change in capacity was observed, so that the property of the passive metal interphase which contributes most to the observed capacity is not affected significantly by the presence of the additional Faradaic process, the reduction of $UO_2^{++}$. Some authorities consider that the most important contribution to the differential capacity of a passive metal system arises from the capacity associated with the oxide film itself.[15] If this

[14] F. A. Posey, *J. Electrochem. Soc.* (in press).

[15] See, however, B. N. Kabanov, preprints, *Internationales Kolloquium über die Passivität der Metalle*, Heiligenberg, 1957.

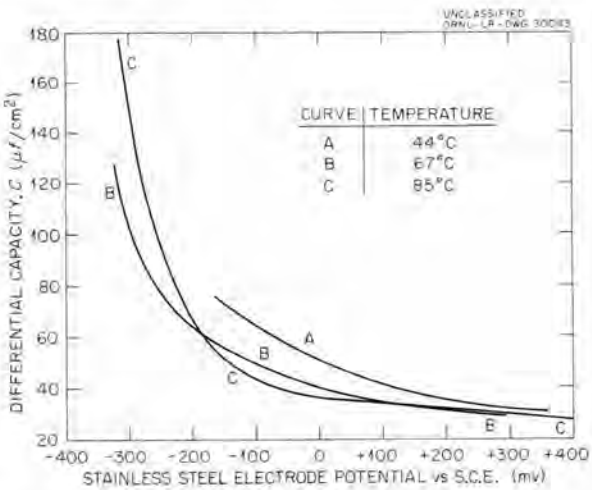


**Fig. 28. Differential Capacity of Electropolished Type 347 Stainless Steel in 0.010 *f* $H_2SO_4$–0.090 *f* $Na_2SO_4$ in Oxygen.**

hypothesis is valid for the present system, the observations would seem to suggest that the reduction of $UO_2^{++}$ does not alter the nature of the passive oxide; that is, there is no effect of the additional Faradaic process on the processes occurring in the passive oxide layer.

## ELECTROCHEMISTRY OF ZIRCONIUM

R. E. Meyer

In a previous report by Posey,[16] it was shown how the application of electrode kinetics leads to an equation from which the corrosion rate of a system may be calculated from simple electrochemical measurements. After preliminary experiments showed that the technique was feasible, this method was applied to zirconium corroding in oxygenated sodium sulfate solutions. The equation is

$$(1) \qquad r = \frac{RT}{\mathfrak{F}} \times \frac{1}{\alpha_c \lambda_c + \alpha_a \lambda_a} \times \left(\frac{di}{d\eta}\right)_{\eta \to 0} ,$$

where $r$ = the corrosion rate in amperes, $RT/\mathfrak{F}$ has the usual significance, $\alpha_c$ and $\alpha_a$ are the electrochemical transfer coefficients for the cathodic and anodic reactions, $\lambda_c$ and $\lambda_a$ are the charge numbers, and $(di/d\eta)_{\eta \to 0}$ is the slope of the current-voltage curve as the measured potential approaches the open-circuit potential. A measurement of the rate, therefore, involves the determination of $\alpha_a\lambda_a$, $\alpha_c\lambda_c$, and $(di/d\eta)$. Since the $\alpha\lambda$ factors change relatively slowly or in some cases not at all in the course of an experiment, they need be measured only occasionally.

Measurements were made as a function of time and electrode potential at temperatures of 25, 46, 66, and 88°C in 0.1 / $Na_2SO_4$ with enough added $H_2SO_4$ to give a pH of 3.5. The area of the electrodes was 2.2 $cm^2$. Extreme precautions were used to purify the solution and the cells, and the crystal-bar zirconium electrodes were annealed for several hours in a high vacuum at 750°C. As is shown in Fig. 29, the rates decreased by about a factor of 10 during the first day. (A rate of 1 $\mu$a per 2.2 $cm^2$, as shown on the graph, is approximately equivalent to 0.5 mpy.)

[16] F. A. Posey, *Chem. Ann. Prog. Rep. June 20, 1957*, ORNL-2386, p 110.

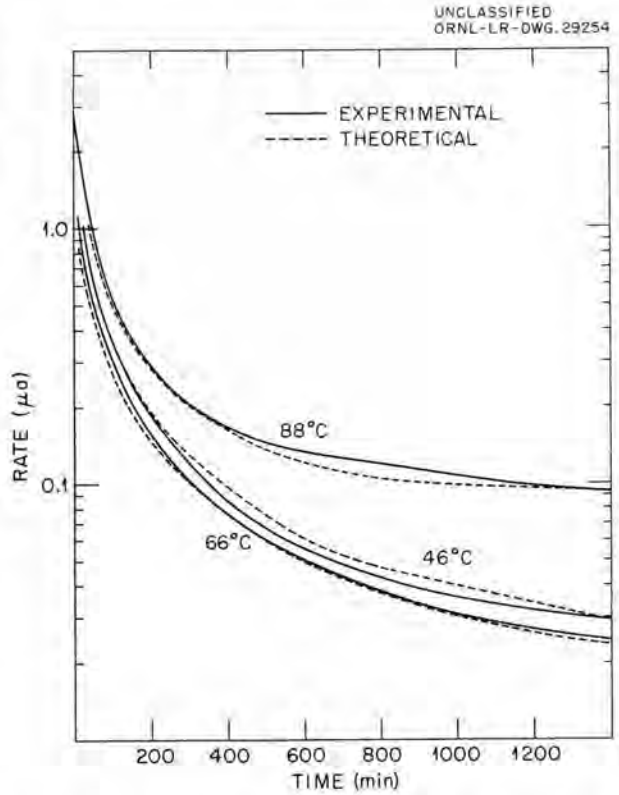


**Fig. 29. Corrosion Rates of Crystal-Bar Zirconium in Oxygenated $Na_2SO_4$ Solution.**

Figure 30 shows a galvanostatic determination of $\alpha_c\lambda_c$ and $\alpha_a\lambda_a$. It should be noted that an independent check on the rate can be made by extrapolating the linear portion of the cathodic current line to the open-circuit potential. Since it is often difficult to obtain $\alpha_a\lambda_a$ measurements by direct polarization, the $\alpha_a\lambda_a$ factor can be determined by using the fact that the total applied current is equal to the difference between the anodic and cathodic currents. In Fig. 30 the anodic current points were determined by subtracting the net current from the extrapolated cathodic current. The direct polarization method can be used for obtaining $\alpha_a\lambda_a$ if the total charge passed does not alter the course of the run, for example, by forming significant additional quantities of film.

In Fig. 31 the open-circuit potentials of the 88°C electrodes are given for the first 1000 min. These potentials were recorded continuously during a run on a Brown recorder. Smooth curves such as those shown were obtained only when

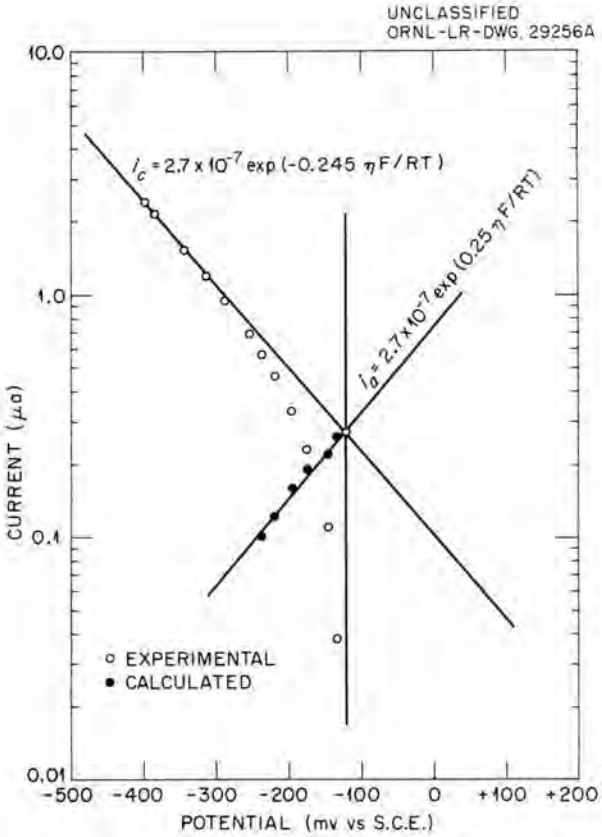


**Fig. 30. Experimental Current-Potential Plot in Oxygenated $Na_2SO_4$ Solution at 88°C.**

the solution and the electrodes were carefully prepared and purified.

Most of the $\alpha\lambda$ factors for the cathodic process cluster about the value 0.25, although values ranging from 0.17 to 0.35 have been recorded. This behavior would be consistent with a dual-barrier model similar to that proposed for stainless steel.[17] It is easy to show from elementary electrode kinetics that for such a system of two barriers, with no appreciable reverse current over either one, the cathodic current will follow the equation

$$(2)\quad i_c = \left( k_1 \prod_i a_1^{p_i} \right)_1^{\alpha_2\lambda_2/(\alpha_1\lambda_1 + \alpha_2\lambda_2)} \left( k_2 \prod_j a_j^{p_j} \right)_2^{\alpha_1\lambda_1/(\alpha_1\lambda_1 + \alpha_2\lambda_2)} \exp\left[ -\frac{\alpha_1\lambda_1\alpha_2\lambda_2\phi_T\mathfrak{F}}{(\alpha_1\lambda_1 + \alpha_2\lambda_2)\,RT} \right],$$

where the $k$'s are constants for the two barriers, the $\prod_i a_1^{p_i}$ factors are the products of the activities raised to the kinetic orders, $\phi_T$ is the over-all

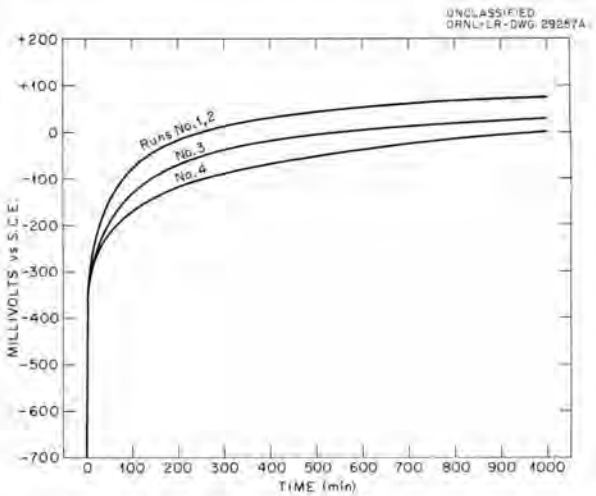


**Fig. 31. Potential-Time Curves for Crystal-Bar Zirconium at 88°C in $Na_2SO_4$ Solution.**

potential drop, and each $\alpha$ factor expresses the fraction of the total potential drop which operates across that particular barrier. If the two barriers have $\alpha\lambda$ factors which are approximately equal to 0.5, the measured $\alpha\lambda$ factor will be equal to $(0.5 \times 0.5)/(0.5 + 0.5)$, or 0.25, as observed. Furthermore, the measured order of the reaction with respect to an added reactant should be equal to the order $p$ raised to the fractional power $\alpha_n\lambda_n/(\alpha_1\lambda_1 + \alpha_2\lambda_2)$, depending on which barrier is affected. For a reactant which has an order $p$ equal to unity, the measured order should therefore be 0.5 if both the $\alpha\lambda$ factors are equal to 0.5. In preliminary experiments on the reduction of various ions, fractional orders in the neighborhood of 0.50 to 0.68 were obtained for the reduction of $Cu^{++}$, $H^+$, and $H_2O_2$ on the surface of zirconium electrodes, although the experiments show some complicated secondary effects. This phase of the investigation is being pursued further.

Preliminary results show that the order of reduction with respect to $O_2$ is zero for the very low current densities used in this work (less than

[17] F. A. Posey, G. H. Cartledge, and R. P. Yaffe, *J. Electrochem. Soc.* (in press).

$10^{-6}$ amp/cm$^2$). This zero order shows that the transfer of $O_2$ to the surface is not one of the slow steps of the reaction. Some other possible slow steps are the transfer of electrons through an insulating film to the film-solution interface, the transfer of an electron through the double layer at the film-solution interface to an $O_2$ molecule or intermediate, or the transfer of a reduction product of $O_2$ back to the solution.

The reduction current at a given potential does not change significantly during a run. There is generally a small decrease during the first hours, and beyond this the current stays relatively constant.

On the other hand, the anodic current at a given potential decreases sharply with time. The decrease in anodic current at constant potential explains the rise of potential with time shown in Fig. 31, since the anodic and cathodic currents must always be equal at open circuit. The $\alpha_a\lambda_a$ factor also decreases with time. This latter effect is barely noticeable at 25°C, but, at 88°C, $\alpha_a\lambda_a$ decreases so rapidly that in a few days it is not significantly different from zero. This behavior can be explained on the assumption that an energy barrier is lowered by the field acting upon a charged particle and that the field, which is equal to the potential across the film divided by the thickness, is steadily reduced by the growth of the film. In other words, the thickness of the film at any time is given by $l_0 + Q \int i\, dt$, where $l_0$ is the initial thickness, $\int i\, dt$ is the charge, and $Q$ is the factor relating charge to thickness. The field is then

$$\frac{\alpha_a\phi_T}{l_0 + Q\int i\, dt},$$

where $\alpha_a\phi_T$ is that portion of the total measured potential existing across the film. The anodic current should follow the equation

$$(3) \qquad i_a = K_a \exp\left[\frac{d\alpha_a\lambda_a\phi_T\mathfrak{F}}{(l_0 + Q\int i\, dt)\, RT}\right],$$

where $d$ is the distance over which the force of the field acts in surmounting a single barrier, and $\lambda_a$ is the charge number. Any reverse current in the film is neglected in this equation. If the potential barrier opposing the charged particle is sufficiently unsymmetrical, or if the term in the exponential is sufficiently large, this is a good approximation. Since the reduction current approximately follows the equation

$$(4) \qquad i_c = K_c \exp\left(-\frac{\alpha_c\lambda_c\phi_T\mathfrak{F}}{RT}\right),$$

Eqs. 3 and 4 may be combined to give, after suitable manipulation,

$$(5) \qquad \frac{di}{dt} = -Ai^2\left(\ln\frac{i}{K_a}\right)^2,$$

where

$$A = \frac{\alpha_c\lambda_c\, Q}{\alpha_a\lambda_a\, d \ln (K_c/K_a)}.$$

In general, the variation in the term $[\ln (i/K_a)]^2$ will be small as compared with the variation in the term $i^2$. If $[\ln (i/K_a)]^2$ is assumed to remain constant, the integration may then be carried out to give

$$(6) \qquad \frac{1}{i} = A\left(\ln\frac{i}{K_a}\right)^2 t + C,$$

where $C$ is an integration constant.

Equation 5 was integrated graphically from $i/K_a = 10^5$ to $i/K_a = 10$. The dotted lines in Fig. 29 show attempts to fit the rate data with Eqs. 5 or 6. The runs at 46 and 66°C were fitted by Eq. 6, and the 88°C run was fitted by Eq. 5 for $i/K_a$ ranging from about $10^5$ to $10^3$. The agreement is satisfactory, but it must be admitted that the $i/K_a$ term is an arbitrary constant. The constants were evaluated from two points on the experimental rate-time curve. At times greater than those shown on the graph, the fit is not good, since the approximations used in the derivation are not valid. As the field in the film is reduced to a negligible value, the reverse current in the film will no longer be small as compared with the forward current, and the variation of $K_a$ with time may become quite important.

It appears, therefore, that the method of measuring corrosion rates described here is satisfactory for a film-covered electrode and that the results so obtained can be interpreted with the help of a simple model based on electrode kinetics.

# NONAQUEOUS SYSTEMS AT HIGH TEMPERATURES

## HETEROGENEOUS ISOTOPIC EXCHANGE REACTIONS OF FLUORINE-CONTAINING COMPOUNDS

W. H. Christie

Fluorine exchange reactions between solid metallic fluorides and gaseous fluorocarbons, utilizing $F^{18}$ as a tracer, were first reported by Gens and Brosi.[1] The fluorocarbons studied were found to exchange more readily with alkali fluorides than with $CdF_2$, $CrF_2$, $PdF_2$, $MgF_2$, $NiF_2$, or $CuF_2$. Perfluoropropene with any single alkali fluoride exchanged more readily than $CF_4$, $C_4F_{10}$, or $(C_2F_5)_2O$. Fast exchange corresponding to the equivalent of several hundred lattice layers was observed in the system $C_3F_6$–alkali fluoride.

In all the experiments reported by Gens the exchange process was followed by observing the transfer of $F^{18}$ activity from the solid to the gas phase. This technique, coupled with the 1.87-hr half life of $F^{18}$, made detailed attention to the preparation of the labeled crystal phase impossible.

In the present study, exchange was followed by observing the removal of activity from the gas phase by the solid phase. This method allowed detailed attention to be paid to the preparation of the solid crystalline phase. By using the reaction of Gens

$$CsF^*(s) + C_3F_6(g) \xrightarrow{300^\circ} CsF(s) + C_3F_6^*(g)$$

it was possible to prepare $C_3F_6^*$ of high specific activity. Labeled $C_3F_6$ made in this fashion was then used in exchange studies with LiF and CsF. Preliminary calculations indicate that the rate of exchange is dependent on the mode of preparation and pretreatment of the solid phase. Findings in this work are in general agreement with those reported by Gens.

## SELF-DIFFUSION IN MOLTEN SALTS

A. S. Dworkin R. B. Escue[2]

The self-diffusion coefficients of the ions were measured in $LiNO_3$ from 265 to 320°C, and in $AgNO_3$ from 220 to 290°C, by using radioactive $Ag^{110}$ and the stable isotopes $Li^6$ and $N^{15}$. The data for $NaNO_3$, $KNO_3$, and $CsNO_3$ were reported previously,[3] as was the capillary method used for the measurement.[4]

The rate equations of the form

$$D = Ae^{-\Delta H^{\ddagger}/RT}$$

for $Li^+$ and $NO_3^-$ in $LiNO_3$ obtained by means of least-squares calculations are

$$(1) \qquad D_{Li^+} = 2.47 \times 10^{-3} e^{-5490/RT} ,$$

$$(2) \qquad D_{NO_3^-} = 1.95 \times 10^{-3} e^{-6340/RT} .$$

The straight lines obtained by plotting log $D$ vs $1/T$ are shown in Fig. 32. The probable errors are as follows: in $D_{Li^+}$, $\pm 0.02 \times 10^{-5}$ cm$^2$·sec$^{-1}$ (1 to 1.5%); for $\Delta H^{\ddagger}_{Li^+}$, ±110 cal (2%); in $D_{NO_3^-}$, $\pm 0.018 \times 10^{-5}$ cm$^2$·sec$^{-1}$ (2 to 3.5%); and for $\Delta H^{\ddagger}_{NO_3^-}$, ±270 cal (4%).

The equations for $Ag^+$ and $NO_3^-$ in $AgNO_3$ (Fig. 33) are

$$(3) \qquad D_{Ag^+} = 0.49 \times 10^{-3} e^{-3730/RT} ,$$

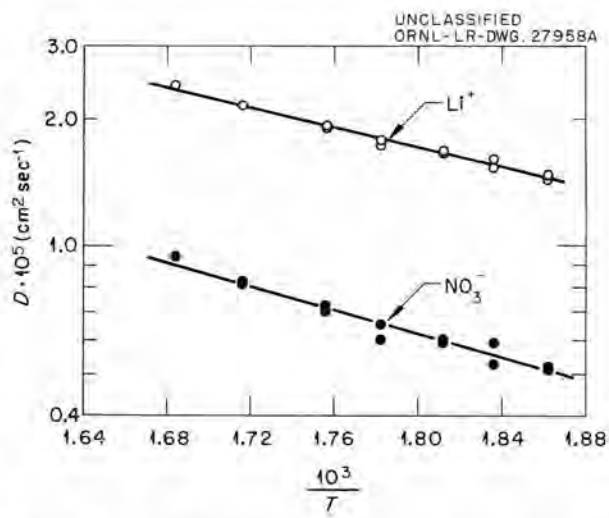


Fig. 32. Self-Diffusion Coefficients in Molten $LiNO_3$.

[1] T. A. Gens and A. R. Brosi, *Chem. Ann. Prog. Rep. June 20, 1957*, ORNL-2386, p 117.

[2] Summer research participant, 1957, North Texas State College, Denton.

[3] A. S. Dworkin, *Chem. Ann. Prog. Rep. June 20, 1957*, ORNL-2386, p 117.

[4] A. S. Dworkin and D. Brown, *Chem. Semiann. Prog. Rep. Dec. 20, 1955*, ORNL-2046, p 23.

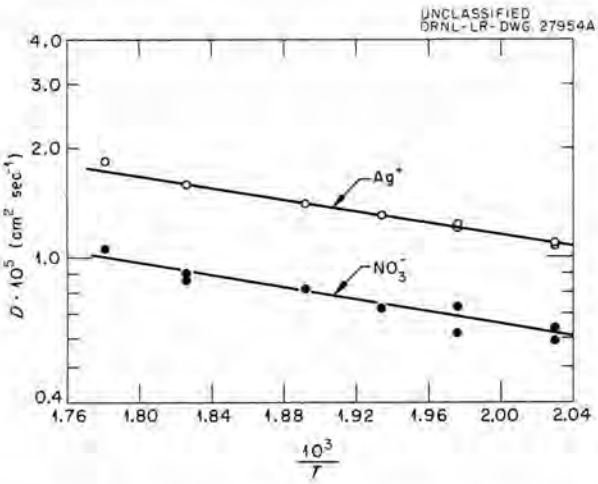


**Fig. 33. Self-Diffusion Coefficients in Molten $AgNO_3$.**

$$(4) \qquad D_{NO_3^-} = 0.31 \times 10^{-3} e^{-3840/RT} .$$

The probable errors are as follows: in $D_{Ag^+}$, $\pm 0.01 \times 10^{-5}$ cm$^2$·sec$^{-1}$ (1%); for $\Delta H^{\ddagger}_{Ag^+}$, $\pm 80$ cal (2%); in $D_{NO_3^-}$, $\pm 0.034 \times 10^{-5}$ cm$^2$·sec$^{-1}$ (3.5 to 5%); and for $\Delta H^{\ddagger}_{NO_3^-}$, $\pm 370$ cal (9.5%).

The heats of activation for the five measured nitrates are tabulated below:

| | $\Delta H^{\ddagger}_{+}$ (Cation) (kcal) | $\Delta H^{\ddagger}_{-}$ (Anion) (kcal) |
|---|---|---|
| $LiNO_3$ | 5.5 | 6.3 |
| $NaNO_3$ | 5.0 | 5.1 |
| $KNO_3$ | 5.5 | 5.7 |
| $CsNO_3$ | 5.6 | 6.3 |
| $AgNO_3$ | 3.7 | 3.8 |

With the exception of $LiNO_3$, the values for cation and anion are approximately the same within experimental error. (The errors involved in the $CsNO_3$ measurements were somewhat larger than those with the other nitrates.) The values for both cation and anion in $AgNO_3$ are significantly lower than those for the alkali-metal nitrates.

The self-diffusion coefficients for cation and anion at 350°C are listed below in order of increasing cation radius:

| | $D_+$ (cm$^2$·sec$^{-1}$) $\times 10^{-5}$ | $D_-$ (cm$^2$·sec$^{-1}$) $\times 10^{-5}$ |
|---|---|---|
| $LiNO_3$ | 2.93 | 1.15 |
| $NaNO_3$ | 2.33 | 1.48 |
| $AgNO_3$ | 2.40 | 1.40 |
| $KNO_3$ | 1.52 | 1.35 |
| $CsNO_3$ | (1.22) | (1.11) |

For the alkali-metal nitrates, the self-diffusion coefficient of the cation decreases as the cation radius increases; $AgNO_3$ does not fit in this order. However, since the $\Delta H^{\ddagger}$ of the ions in $AgNO_3$ is significantly different from the others, it is difficult to compare the self-diffusion coefficients at any given temperature. It can also be shown that the product of the self-diffusion coefficient of the cation and the cation radius is essentially constant for the alkali-metal nitrates and again is much higher for $AgNO_3$.

## MOLTEN SALT–METAL SOLUTIONS[5]

### Phase Equilibria

M. A. Bredig J. E. Sutherland
A. S. Dworkin

**Rubidium–Rubidium Halide Systems.** – With work on the chloride and fluoride systems, the study of the liquid-liquid phase equilibria in the rubidium–rubidium halide systems was almost completed. The rubidium systems are of interest not only because of possible applications in reactor technology, but also because of their intermediate position between the cesium systems, which exhibit complete miscibility in the liquid state, and the potassium systems, all of which show partial immiscibility. The occurrence of a miscibility gap over a very small temperature range, 873 to 890°C in the fluoride system (Fig. 34), and 694 to 706°C in the chloride system, makes the bromide system[6]

[5]Frequent discussions with Professor W. T. Smith, Jr., Chemistry Department, University of Tennessee, consultant, are gratefully acknowledged.

[6]M. A. Bredig and J. W. Johnson, *Chem. Ann. Prog. Rep. June 20, 1957*, ORNL-2386, p 122.

the only rubidium system in which no such gap occurs. The apparent greater ideality of the bromide system, compared with that of either the chloride or the iodide system, has thus been firmly established in the RbX-Rb as well as in the KX-K and NaX-Na systems[7] as a general feature of the alkali-metal–halide systems. It is also planned to demonstrate this in the solubility curve for solid cesium bromide in liquid cesium metal.

**Lithium–Lithium Fluoride Systems.** – A study of the lithium systems was started with work on the fluoride systems. It was hampered by the great difficulty of containing lithium metal at high temperatures, the highest thus far encountered in the alkali-metal systems. However, molten salt–metal mixtures of moderate lithium metal content could be held at temperatures up to 1400°C in a stainless steel capsule for short times just sufficient for thermal analysis. At lower temperatures and at low salt or metal concentrations, where the thermal halts for liquid-liquid separation become hardly observable because of the small temperature dependence of the solubility, the equilibration-and-sampling method furnished data which are believed reliable at least for the composition of the metal-rich phase. They are included in Fig. 34, which gives a comparison of all five alkali-metal–fluoride systems. The regular trend in the miscibility of the alkali metals with their molten fluorides, which is representative of the trend in the alkali halides, is very apparent. This trend is a rapid increase in miscibility with increase in the atomic number of the alkali metal, that is, with the decrease in internal pressure of both salt and metal.

**Symmetry of the Liquid-Phase Coexistence Equilibria.** – An astonishingly simple relationship, almost entirely empirical in nature, of the form

$$\left(\frac{N_{\text{metal}}}{N_{\text{salt}}}\right)_{\text{crit}} = 1.18\,\frac{r_- - b(r_0 - r_+)}{r_+}$$

was noted (Fig. 35), which in the alkali-metal–halide systems connects the degree of asymmetry of the immiscibility area represented by the consolute mole ratio metal:salt with the size of the ions

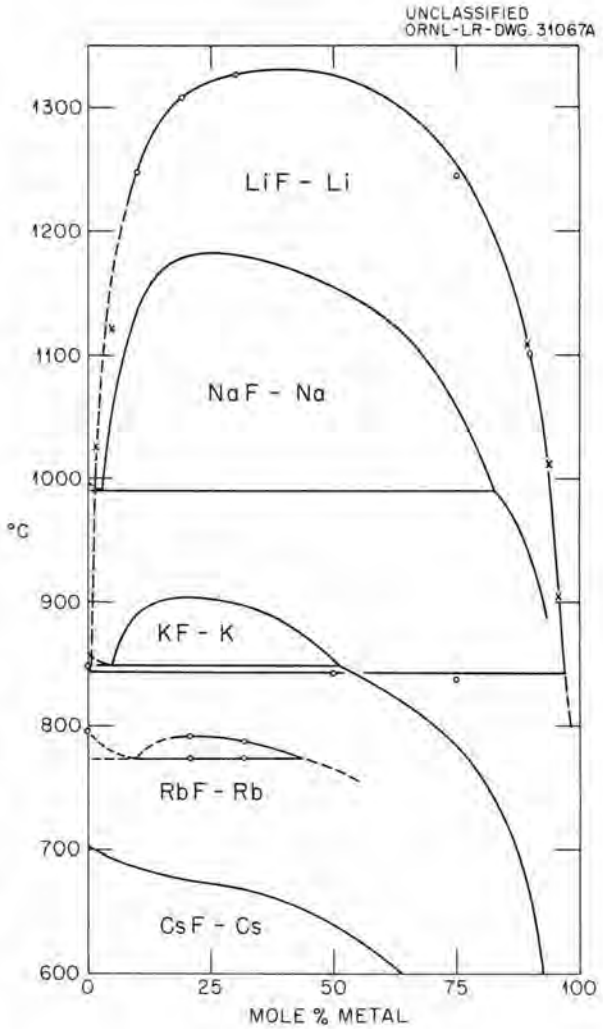


**Fig. 34. Liquid Metal–Salt Phase Equilibria in the Alkali Metal–Fluoride Systems.**

and atoms of the components. In the equation, $r_-$, $r_+$, and $r_0$ denote crystal radii of the anion, cation, and metal atom, respectively. The parameter $b$ varies slightly: 1.09, 1.13, 1.07, and 1.07 for the Li, Na, K, and Rb systems, respectively. This relationship reflects the influence of the size of the ions and, very roughly, of the space occupied by an electron in the metal $(r_0 - r_+)$. Its particular form is not understood at present. This relationship is about to receive a further test with the LiI-Li system, which, among the alkali halide systems, is expected to show the greatest solubility of the metal in the molten salt (70 mole % Li) near the critical solution temperature.

[7] M. A. Bredig and J. E. Sutherland, *Chem. Ann. Prog. Rep. June 20, 1957*, ORNL-2386, p 120–121, Figs. 53 and 54.

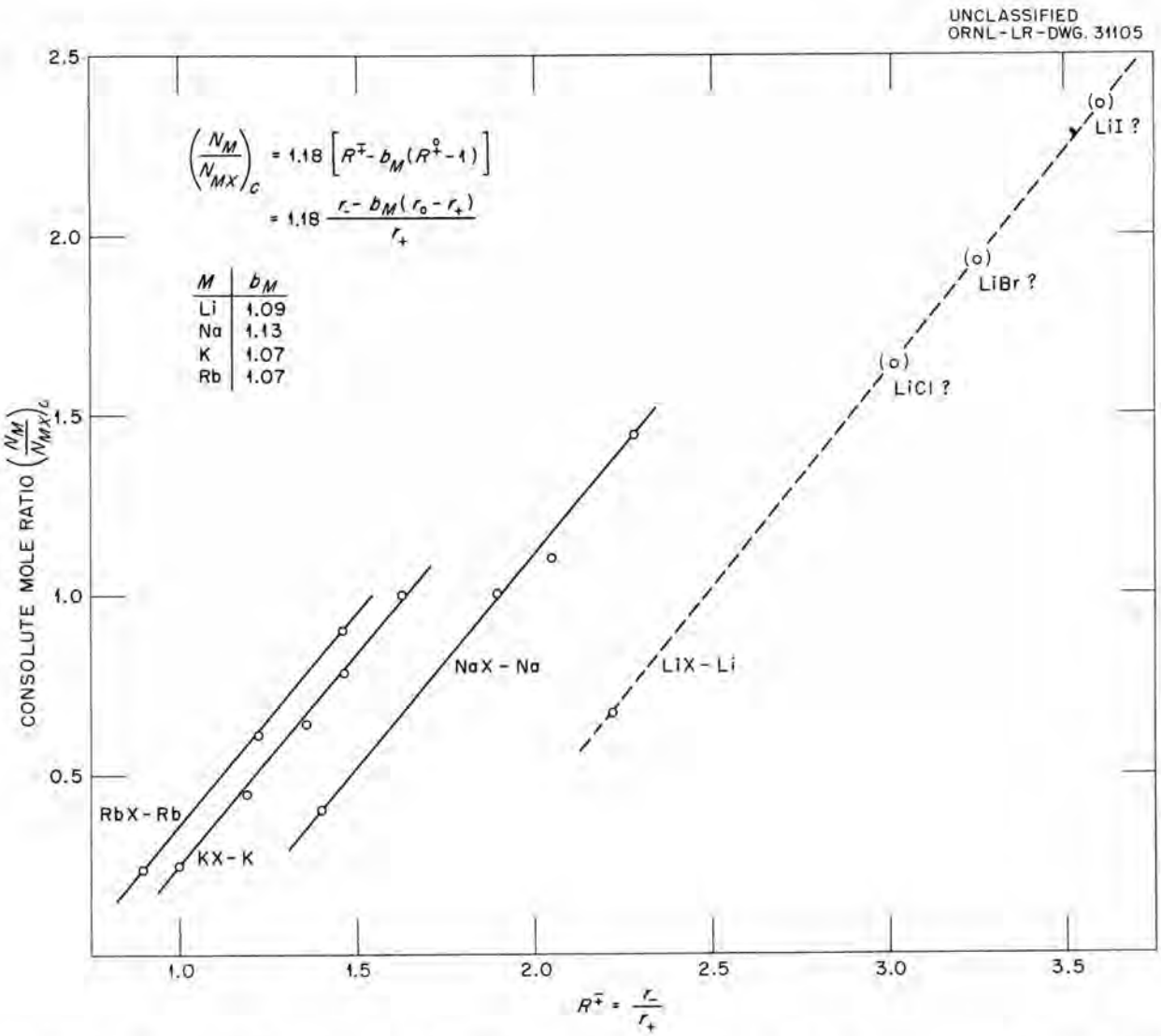


**Fig. 35. Symmetry of Liquid-Liquid Phase Equilibria in the Alkali Metal–Halide Systems as a Function of the Crystal Radii of the Ions.**

## Electrical Conductivity of Solutions of Sodium and Potassium Metals in Their Molten Iodides

H. R. Bronstein M. A. Bredig

The study, by means of electrical conductivity measurements, of the nature of the solutions of alkali metals in their molten halide salts was continued. The results obtained with chloride and bromide systems, which had shown a remarkable difference between the sodium and the potassium metals at the test temperatures,[8] were duplicated by the new data for the iodide systems NaI-Na and KI-K (Fig. 36). Specific conductivity rises monotonically with metal concentration in both these systems. However, the equivalent conductance of the metal, which *rises* monotonically in the KI-K system, was again found to *drop* sharply in the NaI-Na system, namely, from more than 11,000 $ohm^{-1}\cdot cm^2\cdot mole^{-1}$ at "infinite dilution" to a minimum of 5000 $ohm^{-1}\cdot cm^2\cdot mole^{-1}$ at 7 mole % Na (900°C). At 800 and 700°C, the minima occurring at slightly lower metal concentrations are 4000 and 2000 $ohm^{-1}\cdot cm^2\cdot mole^{-1}$, as estimated by

[8] H. R. Bronstein and M. A. Bredig, *Chem. Ann. Prog. Rep. June 20, 1957*, ORNL-2386, p 124, Figs. 57 and 58 (the captions on the figures were unfortunately interchanged); H. R. Bronstein and M. A. Bredig, *J. Am. Chem. Soc.* 80, 2077–81 (1958).

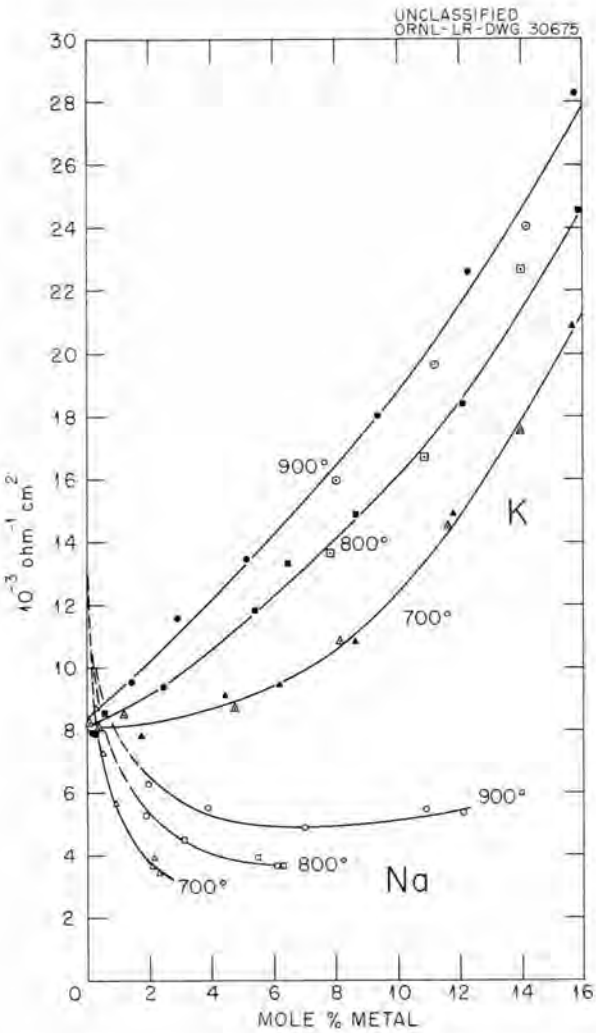


**Fig. 36. Equivalent Conductance of Sodium and Potassium Metals Dissolved in Their Molten Iodides.**

extrapolation (of the curves for conductivity vs metal concentration) beyond the solubility limits of 6 and 3 mole % Na, respectively. The large drop from 11,000 to 2000 ohm$^{-1}$·cm$^{2}$·mole$^{-1}$ at 700°C, in combination with the only moderate deviation from Raoult's law,[8] seems to suggest that not only the number of metal particles per metal equivalent, but also lower energy states of the electrons in intermediate stages of metal association, possibly $Na_2$ molecules, influence the equivalent conductance.

It appears that, as predicted, the connection of the equivalent conductance with the state of association of the metal, especially in solutions of intermediate metal concentration, is also reflected, although to a much lesser degree, in the potassium system K-KI: The temperature coefficient of the equivalent conductance of the metal in the temperature interval between 700 and 800°C, below and near the critical solution temperature of 717°C, is much larger than that between 800 and 900°C, where the metal solution is much more nearly ideal, or monodisperse. Measurements at the highest metal concentrations reached thus far, approximately 40 mole % K, indicate that the temperature coefficient all but vanishes in that region; it must become negative at still higher concentrations, as it is in pure metal.

It should further be noted that again[8] the equivalent conductance of sodium metal at "infinite dilution," greater than 11,000, is considerably higher than that of potassium, approximately 8000 ohm$^{-1}$·cm$^{2}$·mole$^{-1}$.

## THERMODYNAMICS OF DILUTE SOLUTIONS OF $AgNO_3$ AND KCl IN MOLTEN $KNO_3$ FROM EMF MEASUREMENTS

M. Blander F. F. Blankenship
R. F. Newton

Measurements of the activities of $AgNO_3$ were made in a fused-salt concentration cell, *A*, at various temperatures ranging from 344 to 436°C for dilute solutions of $Ag^+$ and $Cl^-$ ions:

$$(A) \qquad Ag \left| \begin{matrix} KNO_3 \\ AgNO_3 \end{matrix} \right\| \begin{matrix} KNO_3 \\ AgNO_3 \\ KCl \end{matrix} \left| Ag \right.$$

The activities of $AgNO_3$ obeyed the Nernst law at the low concentrations of $AgNO_3$ measured when no $Cl^-$ ions were present. The dissolution of KCl in an $AgNO_3$-$KNO_3$ mixture lowered the activity of $AgNO_3$. The lowering was proportional to the amount of KCl added and for a given concentration of KCl was larger the smaller the initial concentration of $AgNO_3$. This shows that the Nernst law is not obeyed for $AgNO_3$ in the presence of $Cl^-$ ion. Measurements of the solubility of AgCl in $KNO_3$ by a visual method were compared with measurements of the activity of $AgNO_3$ in the saturated cell:

$$(B) \qquad Ag \left| \begin{matrix} KNO_3 \\ AgNO_3 \end{matrix} \right\| \begin{matrix} KNO_3 \\ AgCl(s) \end{matrix} \left| Ag \right.$$

The measured solubilities were higher than those calculated from emf measurements of $AgNO_3$

activities in cell $B$. This was consistent with the lowered activity coefficients as measured in the unsaturated cell, $A$.

From the measurements on the saturated cell, $B$, the heat of solution of AgCl (solid) in $KNO_3$ was found to be 20.1 kcal/mole, as compared with a predicted value of 19.9 kcal/mole. A theory based on the assumption of random mixing of the cations and of the anions amongst themselves leads to

$$\log \gamma_{AgNO_3} = N_{Cl^-} \frac{\Delta H'}{2.303RT}, \tag{1}$$

where $N_{Cl^-}$ is the anion fraction of $Cl^-$, and $\Delta H'$ is approximated by the heat change for the reaction

$$AgNO_3(l) + KCl(l) \rightleftharpoons KNO_3(l) + AgCl(l)$$

which is −16.8 kcal/mole. Measured values of $-\log \gamma_{AgNO_3}$ are about 20 times larger than those calculated from Eq. 1 and are dependent on $N_{Ag^+}$.

A preferential distribution of $Cl^-$ ions about the $Ag^+$ ions was postulated, and a distribution function based on a quasi-lattice model was used to calculate the heat of dilution of $AgNO_3$. The energy of interaction of the Ag-Cl pair was taken as $\Delta H'/z$, where $z$, the coordination number of the quasi lattice, is 4. The form of $(\overline{H} - H^*)/2.303RT$ as a function of both $N_{Cl^-}$ and $N_{Ag^+}$ is strikingly similar to that of the experimental values of log $\gamma_{AgNO_3}$ (although the actual values are 25% smaller, which may be due to the crude method of estimating $\Delta H'/z$ or to the partial molar excess entropy). This physical theory was proposed as an alternate to the vague concept of complex ions.

## SOLUBILITIES OF NOBLE GASES IN MOLTEN FLUORIDE MIXTURES

N. V. Smith G. M. Watson

A systematic examination of the solubilities of the noble gases in molten fluoride mixtures of interest as reactor fuels is in progress. The method consists simply in saturating the melt under study by sparging with the test gas, transferring a measured portion of the liquid phase to an isolated section of the apparatus, stripping the dissolved gas by continuous sparging of the melt with a known volume of a second inert gas in a closed system, and determining by mass spectrometry the relative concentrations of the two gases in the final mixture. Isolation of the two sections of the apparatus is readily accomplished by freezing a plug of the molten fluoride in the connecting line.

Solubilities of He, Ne, A, and Xe were examined at pressures from 0.5 to 2 atm in $NaF\text{-}ZrF_4$ (53-47 mole %) at 600, 700, and 800°C. The solubility of each gas examined increases linearly with applied pressure of the gas and increases with temperature; the data obtained with helium, whose behavior is typical of all the gases studied, is shown in Fig. 37. Plots of the logarithm of the Henry's law constant in moles of solute gas·cm$^{-3}$ of soln·atm$^{-1}$ vs $1/T$ (°K) for all these gases in the $NaF\text{-}ZrF_4$ mixture are shown in Fig. 38. The plots are linear; the solubility decreases and the heat of solution increases with increasing atomic number of the solute gas. Solubilities and heats of solution for He and Xe in $NaF\text{-}ZrF_4\text{-}UF_4$ (50-46-4 mole %) are very similar to the values ob-

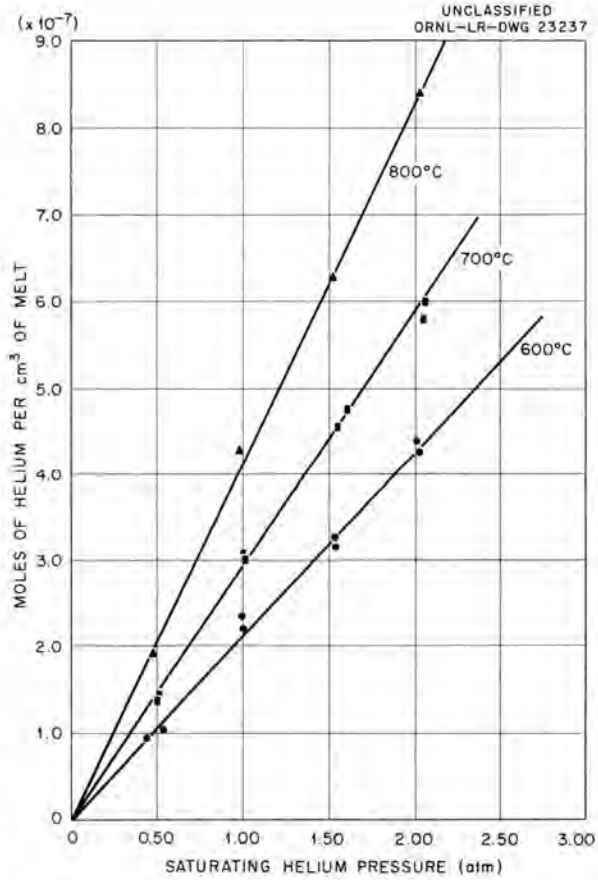


**Fig. 37. Solubility of Helium in $NaF\text{-}ZrF_4$ (53-47 Mole %).**

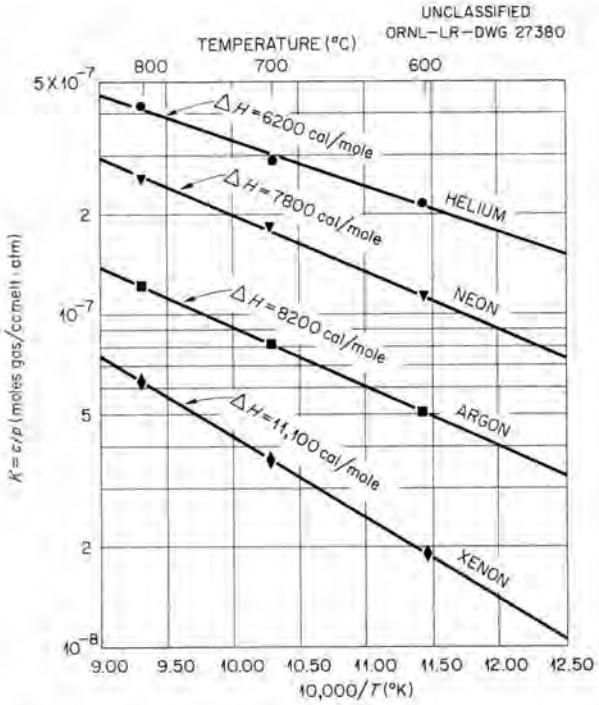


**Fig. 38. Temperature Dependences of Solubilities of Noble Gases in NaF-ZrF$_4$ (53-47 Mole %).**

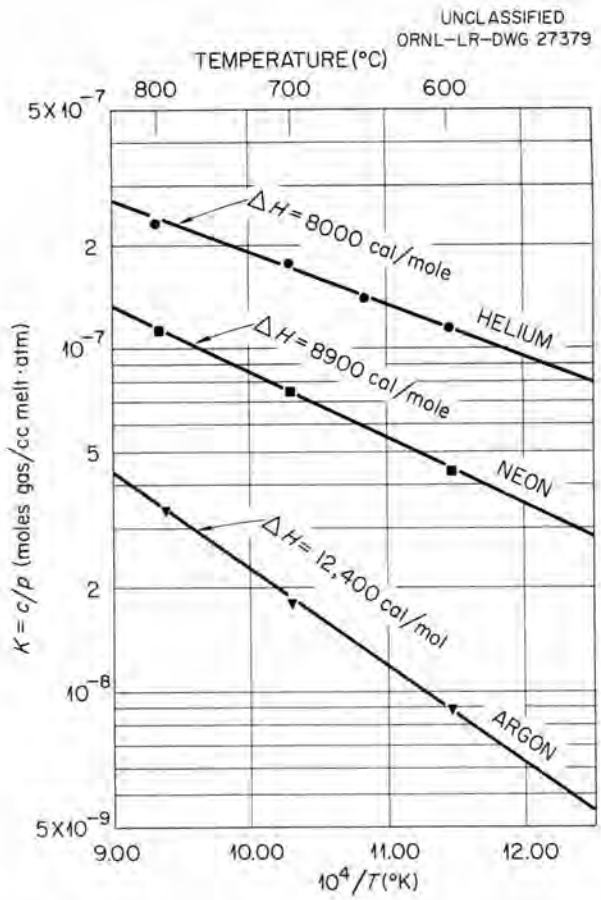


**Fig. 39. Temperature Dependences of Solubilities of Helium, Neon, and Argon in KF-NaF-LiF (11.5-42.0-46.5 Mole %).**

tained with these gases in the NaF-ZrF$_4$ mixture;[9] no studies of Ne and A have been performed with this ternary solvent.

More recently, the same procedure has been applied to the determination of the solubility of He, Ne, and A in the ternary eutectic LiF-NaF-KF (46.5-11.5-42.0 mole %) over the pressure range from 1 to 2 atm. Solubility behavior is very similar to that observed in the NaF-ZrF$_4$ mixtures, although, as Fig. 39 indicates, absolute solubilities are substantially lower and heats of solution are somewhat more positive in the ternary alkali eutectic.

The equilibrium process of dissolving a noble gas X at 1 atm in a molten salt is represented by

$$X(g,C_g) \rightleftharpoons X(d,C_d) \ ,$$

where $g$ and $d$ indicate gaseous and dissolved states, and $C_g$ and $C_d$ are the concentrations in moles per liter of the noble gas in each state at equilibrium. The enthalpy change for this process is that read from Figs. 38 and 39, while the entropy change is, obviously, given by $\Delta H/T$. Since a noble gas at high temperatures is very nearly ideal, the entropy change for isothermal expansion over the same concentration interval is

$$\Delta S = R \ln \frac{C_g}{C_d} \ .$$

The difference between these entropy values represents the entropy change on solution of a mole of the gas, with equal concentrations in gaseous and dissolved states:

$$X(g,C_d) \rightleftharpoons X(d,C_d) \ .$$

These enthalpy and entropy changes are summarized in Table 22. The entropy change on solution is obviously quite small.

[9] These data have been incorporated in "Solubilities of Noble Gases in Molten Fluorides: I. In Mixtures of NaF-ZrF$_4$ (53-47 mole %) and NaF-ZrF$_4$-UF$_4$ (50-46-4 mole %)," by W. R. Grimes, N. V. Smith, and G. M. Watson, *J. Phys. Chem.* (in press).

Table 22. Enthalpy and Entropy Changes on Solution of Noble Gases in Molten Fluoride Mixtures at 1000°K

| Solvent | Gas | Enthalpy Change (cal/mole) | Entropy Change (e.u.) | |
|---|---|---|---|---|
| | | | $X(g, C_g) \rightleftharpoons X(g, C_d)$ | $X(g, C_d) \rightleftharpoons X(d, C_d)$ |
| LiF-NaF-KF | He | 8,000 | 8.3 | −0.3 |
| (46.5-11.5-42.0 mole %) | Ne | 8,900 | 9.9 | −1.0 |
| | A | 12,400 | 12.5 | −0.1 |
| $NaF-ZrF_4$ | He | 6,200 | 7.2 | −1.0 |
| (53-47 mole %) | Ne | 7,800 | 8.2 | −0.4 |
| | A | 8,200 | 9.7 | −1.5 |
| | Xe | 11,100 | 11.2 | −0.1 |

Some calculations of the solubilities of noble gases in molten fluoride mixtures based on the surface tension of the solvent and on the atomic radii of the gases are presented in the next section.

## A SIMPLE METHOD FOR THE ESTIMATION OF GAS SOLUBILITIES

M. Blander G. M. Watson

Solutions of inert gases in liquids are amenable to simple treatment. If a gas does not interact with the liquid in which it is dissolved, then the free energy change of solution is related to the "surface" energy of the hole created by the gas molecule or atom.[10-12] The following treatment is similar to that of Uhlig.[12] The solubility of a gas in a continuous fluid medium can be estimated from the free energy changes in the following steps:

1. Expand the gas in the gas phase from $C_g$ (the concentration in the gas phase at which it is in equilibrium with the dissolved gas) to a concentration equal to $C_d$ (the concentration of gas dissolved in the liquid). The free energy change for this is

$$\Delta F_1 = RT \ln \frac{C_d}{C_g} . \tag{1}$$

2. Shrink each particle to a point and add the liquid. The free energy change for this process is zero.

3. Expand the point particles. (The surface tension of the liquid could have been decreased, the liquid mixed with the finite-sized atoms, and the surface tension then increased, to obtain this result, as suggested by Scatchard.) The free energy change for this is

$$\Delta F_3 = KA\gamma_{mic} , \tag{2}$$

where $A$ is the surface area of the hole created by the particle, $\gamma_{mic}$ is a microscopic surface tension, and $K$ is a constant necessary to obtain the correct units of energy. For spherical atoms $A = 4\pi r^2$, where $r$ is the radius of the hole. To obtain $\Delta F$ in calories, $K = 18.08/4\pi$ when $r$ is in angstroms.

The sum of the free energy changes of steps 1 to 3 is zero if the gas phase is at equilibrium with the gas in the liquid, and

$$-RT \ln \frac{C_d}{C_g} = KA\gamma_{mic} . \tag{3}$$

The exact estimation of the quantities $A$ and $\gamma_{mic}$ is difficult, since real systems cannot be considered continuous. It is interesting to speculate, however, that $\gamma_{mic}$ is related to the macroscopic value. The area $A$ is at least as large as the surface area of the spherical gas molecules. Because of thermal motions it might be expected that the area of the hole taken up by the gas molecule increases with temperature, so that at finite temperatures the use of the atomic radius for spherical molecules will lead to a low value of $A$. In Table 23 are listed values of $C_d/C_g$ calculated for the rare gases, assuming that the radius of the

[10] P. H. Emmett, private communication.

[11] D. D. Eley, *Trans. Faraday Soc.* 35, 1281, 1421 (1939).

[12] H. H. Uhlig, *J. Phys. Chem.* 41, 1215 (1937).

**Table 23. Comparison of Calculated and Observed Values of Henry's Law Constants**

| Solvent | Gas | Temperature (°C) | $K_x$ ($= C_d/C_g$) Experimental | Calculated | Exp/Calc |
|---|---|---|---|---|---|
| | | | $\times 10^{-3}$ | $\times 10^{-3}$ | $\times 10^{-3}$ |
| $NaF\text{-}ZrF_4$ | He | 600 | 15.5 | 137 | 0.11 |
| | | 700 | 23.3 | 188 | 0.12 |
| | | 800 | 37.0 | 243 | 0.15 |
| | Ne | 600 | 8.09 | 45.9 | 0.18 |
| | | 700 | 14.7 | 74.9 | 0.20 |
| | | 800 | 21.7 | 112 | 0.20 |
| | A | 600 | 3.62 | 7.33 | 0.49 |
| | | 700 | 6.44 | 16.0 | 0.40 |
| | | 800 | 10.6 | 30.2 | 0.35 |
| | Xe | 600 | 1.39 | 1.77 | 0.79 |
| | | 700 | 2.84 | 4.84 | 0.59 |
| | | 800 | 5.56 | 10.7 | 0.52 |
| NaF-KF-LiF | He | 600 | 8.09 | 28.3 | 0.29 |
| | | 700 | 14.0 | 46.8 | 0.30 |
| | | 800 | 20.3 | 70.7 | 0.29 |
| | Ne | 600 | 3.12 | 3.94 | 0.79 |
| | | 700 | 6.00 | 8.63 | 0.70 |
| | | 800 | 9.84 | 16.4 | 0.60 |
| | A | 600 | 0.645 | 0.146 | 4.4 |
| | | 700 | 1.43 | 0.509 | 2.8 |
| | | 800 | 2.99 | 1.41 | 2.1 |
| | Xe | 600 | | 0.011 | |
| | | 700 | | 0.057 | |
| | | 800 | | 0.212 | |

hole is the Goldschmidt radius and that $\gamma_{mic} = \gamma_{mac}$. The values of the macroscopic surface tension are listed in Table 24. A comparison of the calculated and measured values of $C_d/C_g$ in Table 23 shows unexpectedly good agreement, in view of the naivete of the model.

The prediction from this model of the correct order of the solubilities with size of the gas atom is significant. Although the values of the solubility may be estimated in this manner, relatively large errors in the temperature coefficients of solubility can enter from even small effects which have been neglected, since the derivative of a small number may be relatively large. In the

**Table 24. Surface Tension of Molten Fluoride Mixtures**

| Temperature (°C) | Surface Tension (ergs/cm$^2$) $NaF\text{-}ZrF_4$* (53-47 mole %) | NaF-KF-LiF** (11.5-42.0-46.5 mole %) |
|---|---|---|
| 600 | 128 | 230 |
| 700 | 120 | 220 |
| 800 | 112 | 210 |

*F. W. Miles and G. M. Watson, Oak Ridge National Laboratory, unpublished work.

**Estimated from extrapolated values for the pure components [see F. M. Jaeger, *Z. anorg. u. allgem. Chem.* **101**, 17 (1917)], assuming additive surface tension.

relation

$$(4) \qquad \frac{d\Delta F_3}{dT} = -\Delta S^0 = KA\frac{d\gamma}{dT} + K\gamma\frac{dA}{dT} ,$$

$d\gamma/dT$ is always negative. In Table 25 it is seen, however, that the standard entropy of solution of these gases is small. Since $\Delta S^0$ is small for all the gases listed, there must be a compensating factor which is probably related to the cause of the decrease of $\gamma$ with increase in temperature. Since it is thermal motions of the atoms of the liquid and expansion of the liquid with an increase of temperature which lead to the decrease of $\gamma$ with increase in $T$, the speculation might be made that the surface area of the hole created by the gas increases with the expansion of the liquid so that the product $\gamma A$ remains constant.

In the last column of Table 23 are listed the ratios of the experimental to the calculated values of $C_d/C_g$. These ratios increase in order for He, Ne, A, Xe. If $\gamma_{mic}$ does not vary with the size of the hole, then this trend might be ascribed to polarization of the gas molecule, an effect which has been neglected. The electronic polarizabilities[13] of the rare-gas atoms in $cm^3 \times 10^{-24}$ are He, 0.201; Ne, 0.390; A, 1.62; Xe, 3.99. As yet no calculations have been attempted for this effect.

Equation 4 leads to an interesting conclusion. If a nonspherical molecule is dissolved in the liquid, the increase of $A$ with an increase of temperature will be due not only to the thermal motion of the liquid molecules but also to the rotation of the gas molecule itself. At higher temperatures the rotation of the dissolved gas in the liquid becomes more free. This would lead to a more negative entropy of solution for nonspherical gases ($N_2$, $O_2$, etc.) and is consistent with the observation that the standard entropy of solution of nonspherical molecules in a given solvent is generally larger than those of the rare gases.[14]

These same conclusions could have been derived in terms of free volume ($V_f$) and potential functions. With such an interpretation, the more negative entropies of solution of nonspherical molecules would be explained by the loss of part of the rotational degrees of freedom of the molecule upon dissolution. These quantities cannot be easily related to a physical picture of the causes of the observed properties and do not easily lend themselves to a simple method of estimating solubilities.

[13] L. Pauling, *Proc. Roy. Soc. (London)* A-114, 181 (1927).

**Table 25. Standard Entropy Changes of Solution of Noble Gases in Molten Fluoride Mixtures**

| Solvent | Gas | $\Delta S^0$ |
|---|---|---|
| NaF-LiF-KF (11.5-42-46.5 mole %) | He | −0.3 |
| | Ne | −1.0 |
| | A | −0.10 |
| $NaF-ZrF_4$ (53-47 mole %) | He | −1.0 |
| | Ne | −0.4 |
| | A | −1.5 |
| | Xe | −0.1 |

## SOLUBILITY OF HF IN MOLTEN $NaF-ZrF_4$ MIXTURES

J. H. Shaffer G. M. Watson

Processes for purification of molten fluoride mixtures for use as reactor fuels and processes for dissolution of reactor fuel elements in molten fluoride mixtures for uranium recovery include sparging of the melts with anhydrous HF. Therefore a study was made of the solubility of HF in mixtures of NaF and $ZrF_4$. The method consists simply in saturating the melt by sparging with HF, transferring a measured portion of the liquid phase to an isolated section of the apparatus, stripping the HF by sparging with helium, absorbing the stripped HF in a standard solution of aqueous alkali, and determining the amount of HF recovered by acidimetric titrations.

The solubility of HF in each composition studied varies directly with the pressure of HF and decreases as the temperature is increased. Figure 40 shows the Henry's law constants in moles of $HF \cdot cm^{-3}$ of $soln \cdot atm^{-1}$ at 600, 700, and 800°C for the compositions examined. Since mixtures containing less than 35 mole % $ZrF_4$ freeze at temperatures too high for direct investigation, the values shown for 20 and 35 mole % $ZrF_4$ were obtained by extrapolation of data obtained at

[14] H. S. Frank, *J. Chem. Phys.* 13, 478 (1945).

higher temperatures. Pure NaF melts at a temperature too high to make such a procedure feasible. Accordingly, values for the $ZrF_4$-free mixture were obtained by using the ternary eutectic of LiF, NaF, and KF as the solvent.

Heats of solution obtained from plots of log $K$ vs $1/T$ for HF in the various mixtures studied are shown in Fig. 41. These heats of solution remain negative and increase approximately threefold as the $ZrF_4$ concentration is diminished from 55 to 0 mole %. Figure 41 also shows the entropy changes for the process

$$HF(g,C_d) = HF(d,C_d)$$

where $g$ and $d$ represent gaseous and dissolved states, and $C_d$ is the concentration (in moles/liter) of HF in solution in equilibrium with HF at 1 atm. These values for entropy of solution are negative, considerably larger in magnitude than those observed for the rare gases in similar solvents, and appear to pass through a maximum when the solvent contains 20 to 30 mole % $ZrF_4$.

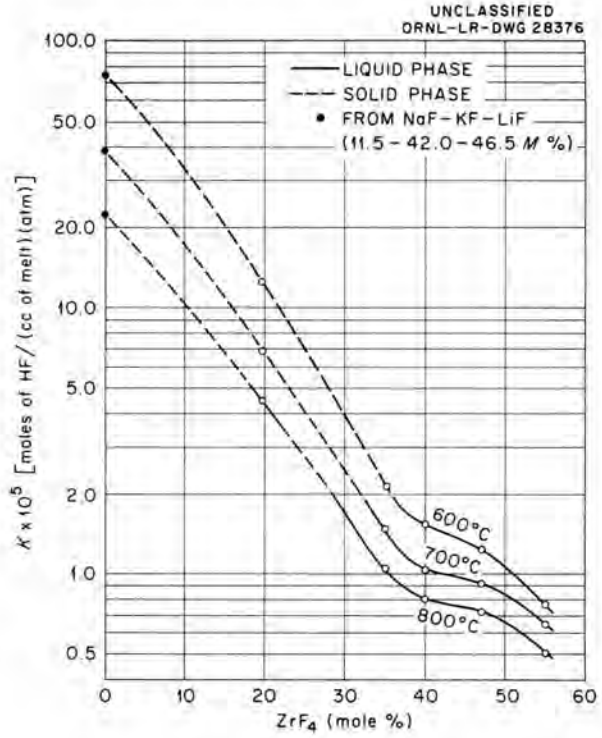


**Fig. 40. Henry's Law Constants for HF in NaF-$ZrF_4$ Mixtures.**

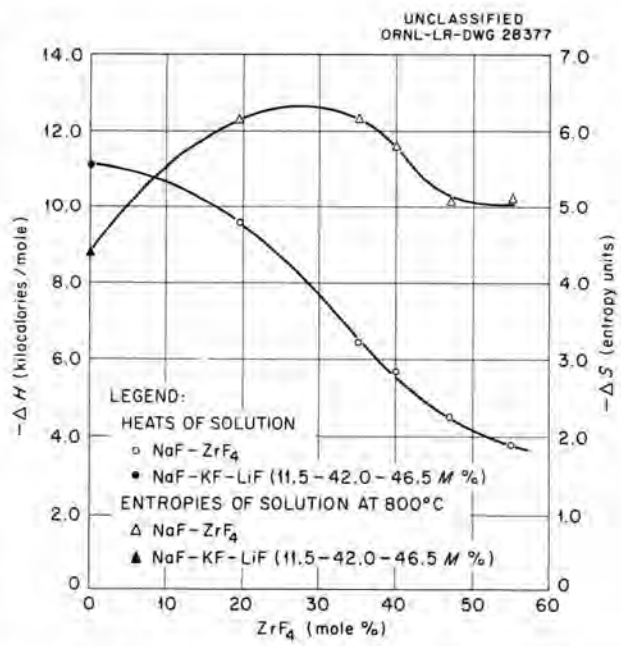


**Fig. 41. Temperature Dependence of Henry's Law Constant for the Solubility of HF in NaF-$ZrF_4$ (53-47 Mole %).**

## SOLUBILITY RELATIONS AMONG SOME FISSION PRODUCT FLUORIDES IN MOLTEN FLUORIDE MIXTURES

W. T. Ward R. A. Strehlow
G. M. Watson

Molten fluoride mixtures are of potential value as circulating fuels for high-temperature nuclear reactors. Since precipitation of fission product fluorides might terminate the reactor operation and since simple side-stream processing to remove nuclear poisons seems an attractive possibility, studies of solubility behavior of important fission product fluorides are being conducted. Yttrium and the lanthanides constitute the most abundant fission product family; and samarium, europium, and gadolinium account for more than half the nuclear poisoning by nongaseous fission product species. Much of the work has accordingly been concerned with behavior of the rare-earth fluorides.

The experimental procedure was relatively simple. Weighed quantities of the rare-earth fluoride labeled with a suitable radiotracer and of the purified solvent mixture were melted in a closed reactor vessel of nickel. The mixture was maintained under an atmosphere of pure dry helium and was stirred by sparging with this gas. After sufficient time to achieve equilibrium at

each temperature, samples of the melt were withdrawn through a sintered-metal filter; $La^{140}$ (40-hr), $Ce^{141}$ (32-day), $Sm^{151}$ (47-hr), $Y^{91}$ (58-day), and $Ba^{133}$ (9.5-year) were used to label the corresponding inert fluorides. Comparison of the counting rate for samples of the liquid with that of standards prepared from the solvent and the labeled fluoride served as the method of analysis. Where more than one rare earth was added, the filtrates were counted after selected intervals; the tracers chosen had decay rates sufficiently different to permit determination of both species in the same sample. Precision of the results, as indicated by repeated studies using fresh materials and variously modified equipment design, was ±5% of the reported value. Examination of the solidified melts with a petrographic microscope served to identify the phases present in these systems.

Values obtained for the solubility of $LaF_3$, $CeF_3$, $SmF_3$, and $YF_3$ in a 50-46-4 mole % mixture of NaF, $ZrF_4$, and $UF_4$ are shown in Fig. 42. Solubilities of the rare-earth trifluorides decrease with increasing size of the cation. The effect of composition of the NaF-$ZrF_4$ solvent on solubility of $CeF_3$ is shown in Fig. 43. From melts containing less than 42 mole % $ZrF_4$ the primary phase is NaF-$CeF_3$. At higher $ZrF_4$ concentrations $CeF_3$ precipitates as the simple trifluoride.

Barium fluoride is very soluble in such a melt. Addition of as much as 33 mole % of this compound failed to saturate the solution at 550°C. The solubility of $BaF_2$ was not greatly affected by addition of a large excess of $CeF_3$. However, the solubilities of the rare-earth fluorides are appreciably lowered by addition of $BaF_2$.

The rare-earth trifluorides are much less soluble in $BeF_2$-bearing fuel solvents. Values for the solubility of $CeF_3$ in NaF-$BeF_2$ and LiF-$BeF_2$ mixtures of varying alkali fluoride content are shown in Fig. 44. The solubility appears to pass through a minimum at about 63 mole % alkali fluoride in both cases.

When solutions containing more than one rare-earth fluoride are examined, the primary phase is a solid solution of the rare-earth fluorides. Figure 45 shows a portion of the pseudoternary system $CeF_3$-$SmF_3$-solvent (NaF-$ZrF_4$-$UF_4$ mixture). This behavior suggests that a simple scheme for removal of the nuclearly harmful rare-earth fission

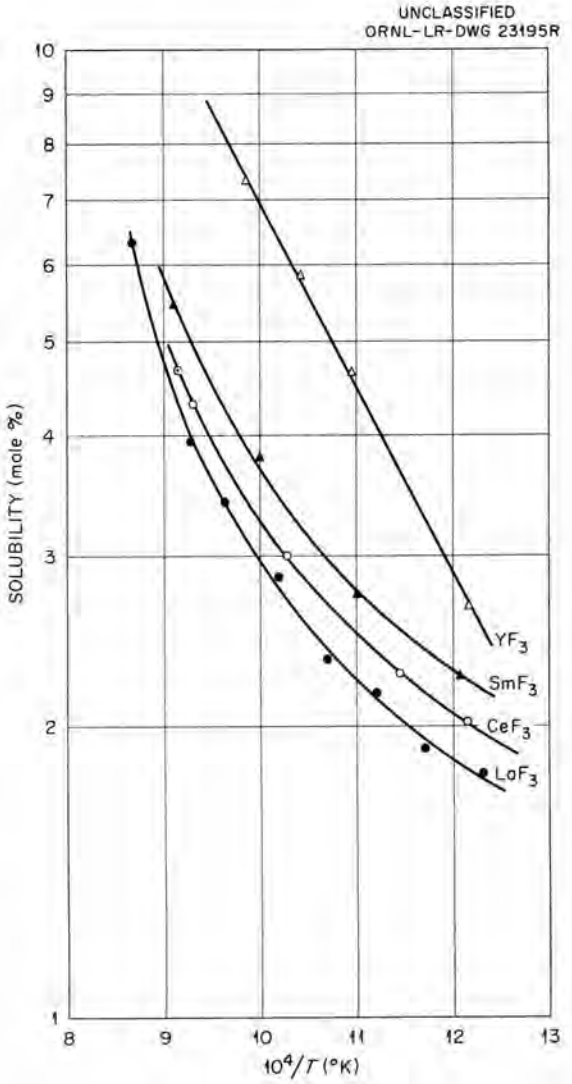


**Fig. 42. Solubility of $CeF_3$, $LaF_3$, $SmF_3$, and $YF_3$ in NaF-$ZrF_4$-$UF_4$ (50-46-4 Mole %).**

products may be based on the following reaction:

$$CeF_3(s) + LaF_3(d) \longrightarrow LaF_3(ss) + CeF_3(d)$$

where $s$, $d$, and $ss$ indicate, respectively, that the designated species is solid, dissolved in the molten fuel, or in solid solution in excess $CeF_3$. By equilibration of a bypass stream of fuel with a bed of $CeF_3$ at a temperature well below the reactor heat-exchanger outlet, high-cross-section rare-earth fission products could be reduced in concentration by replacement with $CeF_3$, which is relatively innocuous.

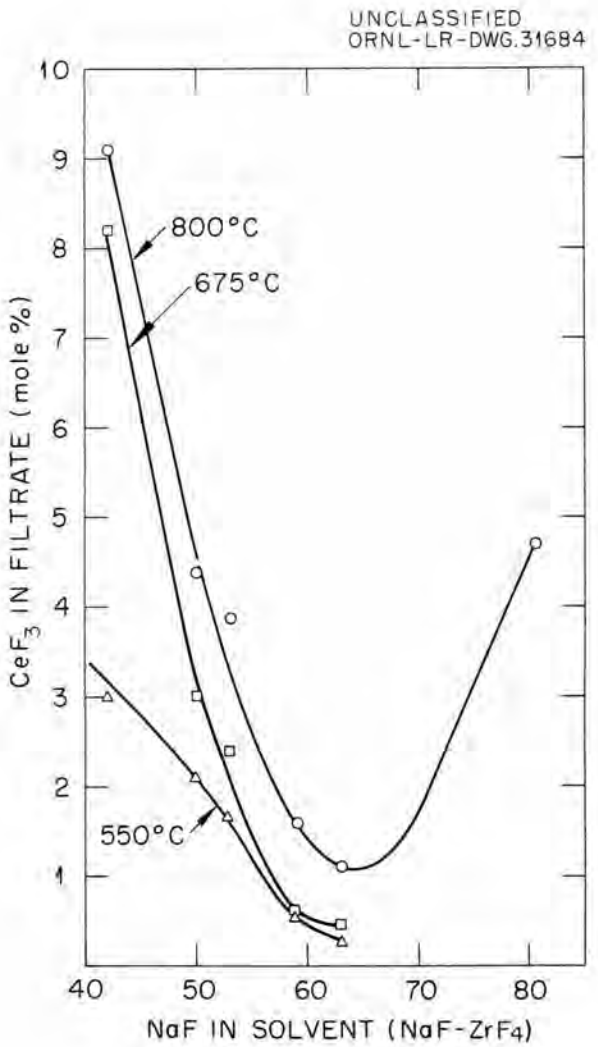


**Fig. 43. Effect of Composition of $NaF-ZrF_4$ Solvent on Solubility of $CeF_3$.**

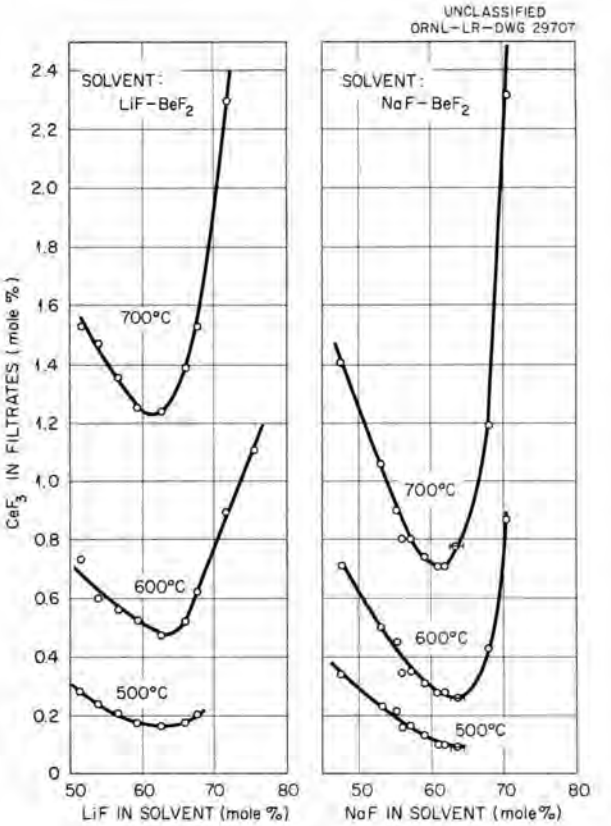


**Fig. 44. Solubility of $CeF_3$ in Alkali Fluoride–Beryllium Fluoride Solvents.**

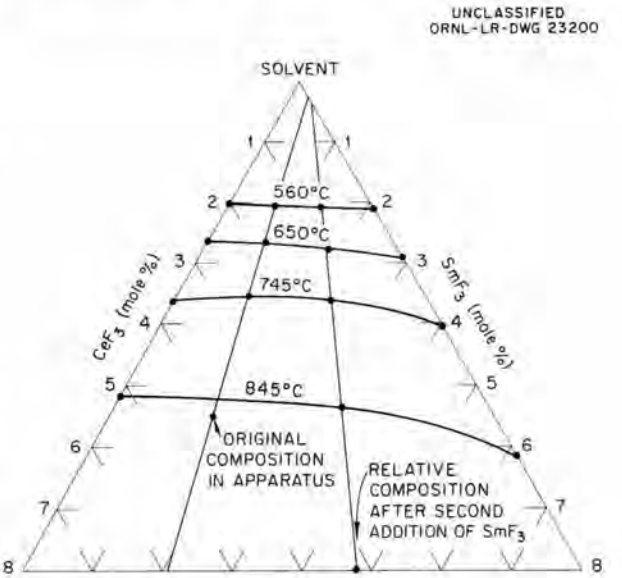


**Fig. 45. Portion of Pseudoternary System $CeF_3$-$SmF_3$-Solvent.**

## VAPOR PRESSURE MEASUREMENTS ON MOLTEN FLUORIDES

S. Cantor F. F. Blankenship

In connection with investigations of activities in molten fluoride solutions, vapor pressures as a function of temperature were measured by a method which yields total pressures. For the alkali fluorides the vapor pressures can be expressed by the equations in Table 26.

In all cases where comparisons could be made, the total pressures in Table 26 are significantly lower than literature values based on carrier-gas

Table 26. Vapor Pressures of Alkali Fluorides

| Salt | Equation | Experimental Range | |
|---|---|---|---|
| | | Temperature (°K) | $p$ (mm Hg) |
| LiF | $\log p = -13{,}890/T - 4.021 \log T + 23.165$ | 1328–1575 | 1.3–30.8 |
| NaF | $\log p = -14{,}609/T - 3.518 \log T + 21.863$ | 1381–1592 | 1.7–26.6 |
| KF | $\log p = -11{,}910/T - 3.518 \log T + 21.002$ | 1199–1505 | 1.8–81.4 |
| RbF | $\log p = -11{,}373/T - 3.518 \log T + 20.995$ | 1154–1451 | 2.2–106 |
| CsF | $\log p = -9{,}845/T - 3.518 \log T + 20.556$ | 1009–1379 | 1.7–242 |

techniques, with the usual assumption of a monomeric vapor. Association in the vapor phase accounts for the discrepancy; however, the extent of association is only roughly indicated by existing data.

Vapor pressures as functions of composition have also been measured for the $CsF\text{-}BeF_2$ system from 850 to 1050°C. A minimum in the total pressure occurs at 30 mole % $BeF_2$. The results at 950°C are representative; here CsF has a vapor pressure of 43 mm Hg and $BeF_2$ 35.5 mm, while the vapor pressure of the 30 mole % $BeF_2$ mixture is 11 mm and that of the 80 mole % $BeF_2$ is 33 mm. Between 80 and 100 mole % $BeF_2$ the total pressure is virtually independent of composition throughout the temperature range.

A transpiration apparatus to provide data on composition and weight of the saturated vapor is being constructed. This information, combined with the total-pressure data, will be useful in obtaining the partial pressures of the vapor species.

## SOLUBILITY AND STABILITY OF $PuF_3$ IN MOLTEN ALKALI FLUORIDE–BERYLLIUM FLUORIDE MIXTURES

C. J. Barton R. A. Strehlow

An extensive experimental program has established that solutions of $UF_4$ in several molten fluoride mixtures are of possible value as fuels in high-temperature circulating-fuel reactors. Mixtures of LiF or NaF with $BeF_2$ are among the most promising solvents for such fuels. Since phase behavior of $PuF_4$ and $UF_4$ should be quite similar, it seems very likely that, from the phase-behavior point of view alone, similar solutions could serve as fuels for plutonium burners. However, the available thermochemical data[15] suggest that $PuF_4$ is a much stronger oxidant than $UF_4$, while $PuF_3$ is much more stable toward disproportionation than is $UF_3$. Since it appeared that $PuF_3$ must be the source of fissionable material for a plutonium burner fueled with molten fluorides, an examination of the solubility and stability of this compound in likely fuel solvents is under way.

Studies with $PuF_3$ are conducted in interconnected glove boxes similar to those in use at Los Alamos Scientific Laboratory and in the Isotopes Division of ORNL. The dry, inert atmosphere in these boxes is maintained at a pressure below that in the laboratory. A petrographic microscope in one of the boxes permits identification of phases present in the cooled melt. Problems associated with the fact that Pu-Be mixtures are neutron sources are largely avoided by use of small samples of relatively low plutonium concentration.

The $PuF_3$ used in these studies is a high-purity preparation supplied by LASL. Solvent mixtures were used after purification by repeated sparging with HF and $H_2$ at 800°C in nickel equipment. Occasionally, desired changes in solvent composition were effected by addition of optical LiF from The Harshaw Chemical Co., or of $BeF_2$ which had been treated at 800°C with HF and $H_2$. The $PuF_3$ was maintained in the trivalent state in solution by use of a sparge or cover gas consisting of 20% $H_2$ in argon.

[15] A. Glassner, *The Thermochemical Properties of the Oxides, Fluorides, and Chlorides to 2500°K*, ANL-5750 (1957).

The solubility data were obtained simply by chemical analysis of samples drawn through filters of sintered nickel from saturated solutions contained under the reducing atmosphere in nickel equipment.

Although the specimens have been carefully examined, no evidence of disproportionation of $PuF_3$ has been observed in these studies. The solubility of $PuF_3$ in both the $LiF\text{-}BeF_2$ and $NaF\text{-}BeF_2$ solvents increases with temperature in all cases studied. As Figs. 46 and 47 indicate, plots of log solubility vs reciprocal temperature yield satisfactorily straight lines for each solvent. A minimum in the plot of solubility vs solvent composition occurs at 63 mole % LiF in $LiF\text{-}BeF_2$ and at 57 mole % NaF in $NaF\text{-}BeF_2$; solubilities of $PuF_3$ in these mixtures at 565°C are 0.25 and 0.18 mole %, respectively. Solubility in either solvent system increases slowly as $BeF_2$ is added to the composition exhibiting minimum solubility, but increases rapidly as alkali fluoride is added to this composition. The $LiF\text{-}NaF\text{-}BeF_2$ mixture containing 16 mole % LiF and 56 mole % NaF dissolves 1.2 mole % $PuF_3$ at 565°C.

The only plutonium-bearing species observed with the polarizing microscope in $LiF\text{-}BeF_2\text{-}PuF_3$ mixtures was $PuF_3$. However, an additional compound (which is almost certainly $NaPuF_4$) was found in the $NaF\text{-}BeF_2\text{-}PuF_3$ mixture containing 64 mole % NaF and in the $LiF\text{-}NaF\text{-}BeF_2\text{-}PuF_3$ mixture showing the high solubility of $PuF_3$.

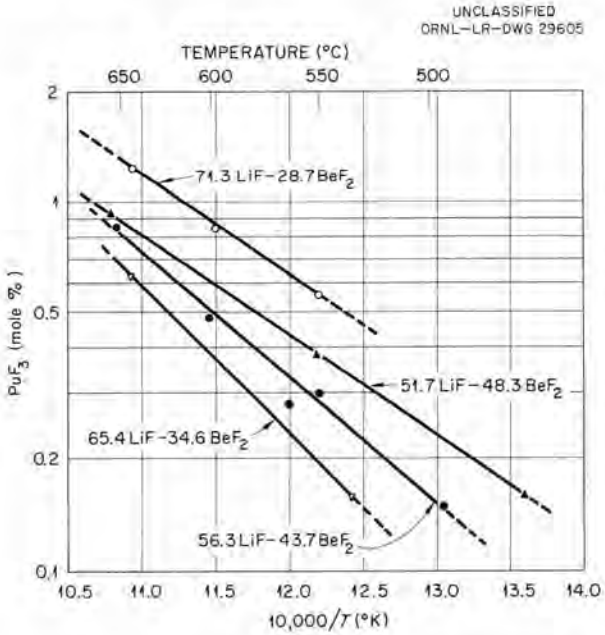


**Fig. 46. Solubility of $PuF_3$ as a Function of Temperature for $LiF\text{-}BeF_2$ Solvents.**

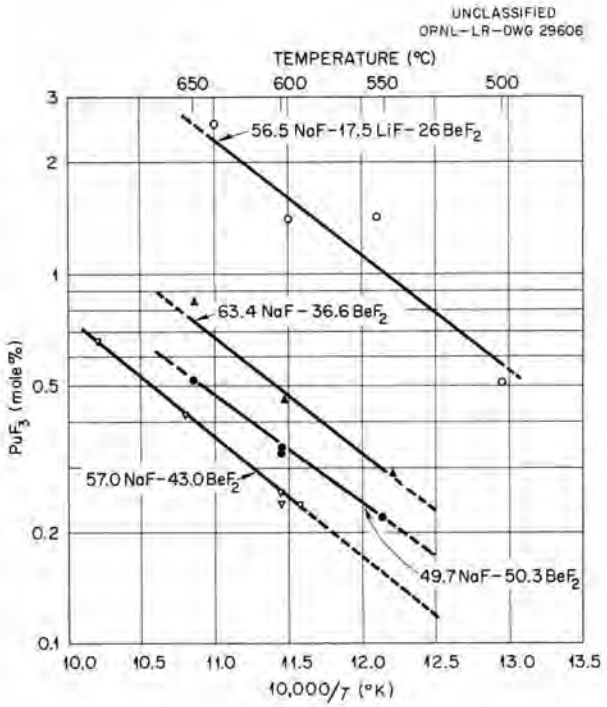


**Fig. 47. Solubility of $PuF_3$ as a Function of Temperature for $NaF\text{-}BeF_2$ and $NaF\text{-}LiF\text{-}BeF_2$ Solvents.**

Although $PuF_3$ is rather sparingly soluble in molten $LiF\text{-}BeF_2$ and $NaF\text{-}BeF_2$, it appears that sufficient $PuF_3$ can be dissolved to allow operation of a plutonium burner fueled with such mixtures.

## PHASE BEHAVIOR IN FLUORIDE SYSTEMS

R. E. Thoma
H. Insley
H. A. Friedman
C. F. Weaver
R. A. Strehlow
R. E. Moore

Phase behavior in salt systems of interest in nuclear fuel technology continues to be the subject of a comprehensive study. Of prime interest to this program are fluoride mixtures suitable as media for reprocessing reactor fuel elements and/or as circulating fuels or breeder blankets for high-temperature reactors.

The experimental data from which the diagrams were derived were obtained by thermal analysis,

equilibration followed by quenching, visual observation of phase changes, and filtration at high temperature; samples for all these techniques are examined by x-ray diffraction, and all species are identified by use of the petrographic microscope. Materials used have been, in each case, the commercially pure chemicals. These materials have been given further purification by alternate sparging in the molten state with HF and $H_2$ or by addition of $NH_4HF_2$ before fusion. All handling of the purified materials, prior to final examination, has been accomplished in dry boxes or under inert atmospheres.

It was demonstrated that $LiF\text{-}BeF_2$ mixtures can dissolve sufficient $UF_4$ and $ThF_4$ to provide a fuel for a high-temperature $U^{233}$ converter. The system $LiF\text{-}BeF_2\text{-}ThF_4\text{-}UF_4$ is, accordingly, of considerable potential importance. Efforts during the past year have included examination of several of the related binary and ternary systems; phase diagrams for most of these systems are essentially complete.

The $BeF_2\text{-}ThF_4$ system shows a simple eutectic at 1.5 mole % $ThF_4$ at 530°C without formation of compounds or solid solutions. The $ThF_4\text{-}UF_4$ system shows a continuous series of solid solutions without a temperature minimum. Four compounds, $3LiF\cdot ThF_4$, $7LiF\cdot 6ThF_4$, $LiF\cdot 2ThF_4$, and $LiF\cdot 4ThF_4$, occur in the $LiF\text{-}ThF_4$ binary diagram; eutectics at 22.5 and 29 mole % $ThF_4$ (568 and 565°C, respectively) are observed. The ternary systems of this family are characterized by numerous examples of solid solution between analogous and nonanalogous compounds. As a typical example of this characteristic, $3LiF\cdot UF_4$ has been observed to be metastable in the $LiF\text{-}UF_4$ binary system;[16] $3LiF\cdot ThF_4$ is a stable phase in the corresponding $LiF\text{-}ThF_4$ system. In mixtures containing 75 mole % LiF, the solubility of $UF_4$ as $3LiF\cdot UF_4$ in solid $3LiF\cdot ThF_4$ decreases from 15 mole % at the solidus (500°C) to 7 mole % at 475°C. This solubility thus represents the partial miscibility of metastable $3LiF\cdot UF_4$ in stable $3LiF\cdot ThF_4$. Figure 48 shows the phase diagram for the $LiF\text{-}UF_4\text{-}ThF_4$ system.

The phase diagram for $LiF\text{-}BeF_2\text{-}ThF_4$ is shown as Fig. 49. Suitable breeder blankets appear to be

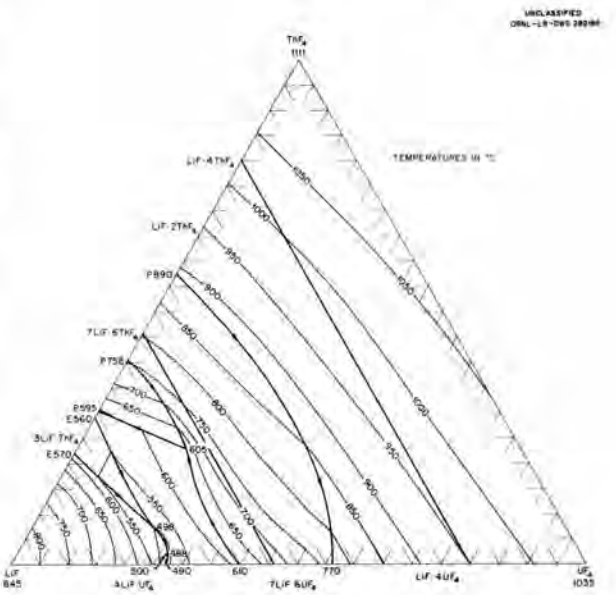


Fig. 48. The System $LiF\text{-}UF_4\text{-}ThF_4$.

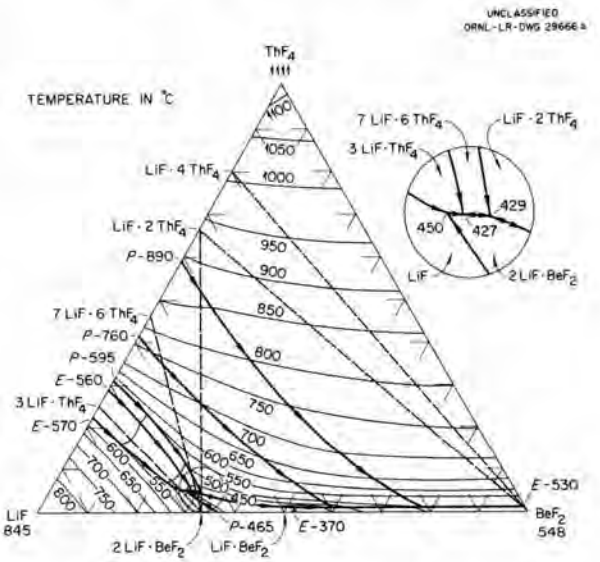


Fig. 49. The System $LiF\text{-}BeF_2\text{-}ThF_4$.

available within this system,[17] for which liquidus and solidus temperatures may be claimed with good precision. However, solubility of $BeF_2$ in solid $LiF\text{-}ThF_4$ phases still obscures complete understanding of several of the ternary solid-phase relationships.

[16] C. J. Barton *et al.*, *J. Am. Ceram. Soc.* 41, 63 (1958).

[17] R. E. Thoma *et al.*, *MSR Quar. Prog. Rep. June 30, 1958*, ORNL-2551, p 83.

Comparisons of properties of the system $NaF$-$BeF_2$-$ThF_4$-$UF_4$ with those of $LiF$-$BeF_2$-$ThF_4$-$UF_4$ are of value in appraising the use of the lithium quaternary system. Preliminary phase studies, accordingly, have been started in the systems $NaF$-$ThF_4$, $NaF$-$BeF_2$-$ThF_4$, and $NaF$-$ThF_4$-$UF_4$. Six compounds have been identified in the system $NaF$-$ThF_4$: they are $4NaF \cdot ThF_4$, $2NaF \cdot ThF_4$, $3NaF \cdot 2ThF_4$, $7NaF \cdot 6ThF_4$ (metastable), $NaF \cdot ThF_4$, and $NaF \cdot 2ThF_4$. Eutectics occur in the system at 24.5 mole % $ThF_4$ (mp 617°C), 37 mole % $ThF_4$ (mp 690°C), and 41.5 mole % $ThF_4$ (mp 702°C). No ternary compounds have been observed in the ternary systems $NaF$-$BeF_2$-$ThF_4$ and $NaF$-$ThF_4$-$UF_4$. These two systems appear to be very similar to their LiF counterparts with regard to compositions and temperatures at which invariant equilibria occur and with respect to comparable solid solution phenomena.

Phase studies are in progress or have recently been completed on the fused-salt systems $NaF$-$LiF$-$BeF_2$, $NaF$-$RbF$-$BeF_2$, $KF$-$UF_4$ (ref 18), $RbF$-$UF_4$ (ref 18), $NaF$-$LiF$-$UF_4$ (ref 18), and $NaF$-$HfF_4$. The system $NaF$-$HfF_4$ is strikingly similar to the system $NaF$-$ZrF_4$.[19] Isostructural polymorphs of the compound pairs occur:

$$3NaF \cdot ZrF_4 - 3NaF \cdot HfF_4$$
$$\alpha\text{-}5NaF \cdot 2ZrF_4 - \alpha\text{-}5NaF \cdot 2HfF_4$$
$$\beta\text{-}5NaF \cdot 2ZrF_4 - \beta\text{-}5NaF \cdot 2HfF_4$$
$$\beta\text{-}2NaF \cdot ZrF_4 - \beta\text{-}2NaF \cdot HfF_4$$
$$\gamma\text{-}2NaF \cdot ZrF_4 - \gamma\text{-}2NaF \cdot HfF_4$$
$$7NaF \cdot 6ZrF_4 - 7NaF \cdot 6HfF_4$$
$$NaF \cdot ZrF_4 - NaF \cdot HfF_4$$

Members of the compound pairs $7NaF \cdot 6ZrF_4$–$7NaF \cdot 6HfF_4$ and $NaF \cdot ZrF_4$–$NaF \cdot HfF_4$, however, display dissimilar melting relationships.

Optical measurements have been made on several alkali fluoride–thorium fluoride compounds. The optical properties of these phases are shown in Table 27.

Crystal parameter measurements were made on several compounds discovered during the course of the phase equilibrium studies. These measurements were made on the phases $3RbF \cdot UF_4$ (ref 20), $7NaF \cdot 6UF_4$, $7KF \cdot 6UF_4$, $7RbF \cdot 6UF_4$, $7LiF \cdot 6UF_4$ (ref 21), $2RbF \cdot ThF_4$, $2RbF \cdot ZrF_4$, $2CsF \cdot ZrF_4$ (ref 22), $5NaF \cdot 3UF_4$, $3NaF \cdot 2ThF_4$ (ref 23), $RbF \cdot 6UF_4$ (ref 24).

**Table 27. Optical Properties of Some Alkali Fluoride–Thorium Tetrafluoride Compounds**

| | |
|---|---|
| $\alpha$-$4NaF \cdot ThF_4$ | Isotropic<br>$N = 1.400$ |
| $\beta$-$4NaF \cdot ThF_4$ | Biaxial (–), twinning<br>$N\gamma = 1.402$<br>$N\alpha = 1.397$<br>2 V small |
| $\beta$-$NaF \cdot ThF_4$ | Biaxial (–), twinning<br>$N \cong 1.503$<br>Birefringence low<br>2 V low |
| $\gamma$-$NaF \cdot ThF_4$ | Biaxial (–)<br>$N\alpha = 1.506$<br>$N\gamma = 1.540$<br>2 V $\cong 40°$ |
| $\alpha$-$NaF \cdot ThF_4$ | Isotropic<br>$N = 1.506$ |
| $NaF \cdot 2ThF_4$ | Isotropic<br>$N = 1.550$ |
| $3NaF \cdot 2ThF_4$ | Isotropic<br>$N = 1.474$ |
| $7NaF \cdot 6ThF_4$ | Uniaxial (–)<br>$N\omega = 1.475$<br>$N\epsilon = 1.470$ |
| $7RbF \cdot 6ThF_4$ | Uniaxial (–)<br>$N\omega = 1.486$<br>$N\epsilon = 1.482$ |
| $7KF \cdot 6ThF_4$ | Uniaxial (–)<br>$N\omega = 1.474$<br>$N\epsilon = 1.470$ |

[18] R. E. Thoma, *J. Am. Ceram. Soc.* (in press).

[19] C. J. Barton *et al.*, *J. Phys. Chem.* 62, 665–76 (1958).

[20] L. A. Harris, *The Crystal Structure of $Rb_3UF_7$*, ORNL CF-58-1-26 (Jan. 6, 1958).

[21] L. A. Harris, *The Crystal Structures of 7:6 Type Compounds of Alkali Fluorides with Uranium Tetrafluoride*, ORNL CF-58-3-15 (March 6, 1958).

[22] L. A. Harris, *A Preliminary Survey of Some Fluoride Compounds. I*, ORNL CF-58-3-44 (March 10, 1958).

[23] L. A. Harris, *A Preliminary Survey of Some Fluoride Compounds. II*, ORNL CF-58-5-17 (May 14, 1958).

[24] L. A. Harris, *The Crystal Structure of $RbU_6F_{25}$*, ORNL CF-58-5-63 (May 15, 1958).

# CHEMICAL PHYSICS

## MICROWAVE AND RADIO-FREQUENCY SPECTROSCOPY

### Hydrogen Gas and Atomic Hydrogen Yields from Irradiated Acids

R. Livingston A. Weinberger

Aqueous solutions of sulfuric, phosphoric, and perchloric acids were irradiated at 77°K with gamma rays from $Co^{60}$ and then melted and assayed for molecular hydrogen and oxygen by conventional vacuum-line techniques. These frozen, irradiated acids were also examined in a paramagnetic resonance spectrometer to determine the concentration of atomic hydrogen present before melting in order to see whether there is a correlation with the molecular hydrogen yield. In a previous report,[1] gas yield data and a few preliminary atomic hydrogen assays for sulfuric acid were presented; a definite correlation between molecular and atomic hydrogen yields was noted. Molecular gas yield measurements have now been completed on all three acids. The atomic hydrogen assays are under way. Thus far the atomic hydrogen yields are being determined relative to the yield in one concentration of sulfuric acid (0.143 mole fraction). An accurate absolute assay of this reference sample will soon be attempted.

Measurements of relative atomic hydrogen yields are nearing completion for the three acids. The perchloric acid results are illustrated in Fig. 50. Figure 50*b* shows the molecular hydrogen yields (molecules per 100 ev of absorbed energy), and Fig. 50*a* shows the relative atomic hydrogen yield over the same concentration range. Neither the atomic nor molecular yields appeared to be greatly affected by attempts to prepare purely glassy or polycrystalline solids by controlling the conditions of freezing. The principal region of disagreement for the curves is at high dilution. In the limit of zero mole fraction of acid (ice) the yield of stably trapped atomic hydrogen is zero, whereas the yield of molecular hydrogen is 0.1 (molecules per 100 ev). The concentration for maximum yield and the region of rapid drop in yield for increasing concentration are essentially the same for the two cases.

[1]A. Weinberger and R. Livingston, *Chem. Ann. Prog. Rep. June 20, 1957*, ORNL-2386, p 128.

### Effect of Environmental Nuclei in Electron Spin Resonance Spectroscopy

G. T. Trammell[2] H. Zeldes
R. Livingston

Occasionally an electron paramagnetic resonance absorption line is accompanied by satellite lines which result from a weak magnetic dipole-dipole interaction, coupling the electron spin to a neighboring nuclear spin. The satellites correspond to a change of spin state of the neighbor nucleus concurrent with the change in spin state of the electron. Theoretical expressions for the energy levels and transition probabilities of a spin-only electron coupled to a neighboring nucleus have been developed. Details were recently published.[3]

### Paramagnetic Resonance Studies of Liquids During Intense Irradiation

R. Livingston R. Holmberg

In a previous report,[4] brief mention was made of the start of an experiment in which an attempt was

[2]Physics Division.

[3]G. T. Trammell, H. Zeldes, and R. Livingston, *Phys. Rev.* **110**, 630 (1958).

[4]H. Zeldes, R. Livingston, and R. Holmberg, *Chem. Ann. Prog. Rep. June 20, 1957*, ORNL-2386, p 130.

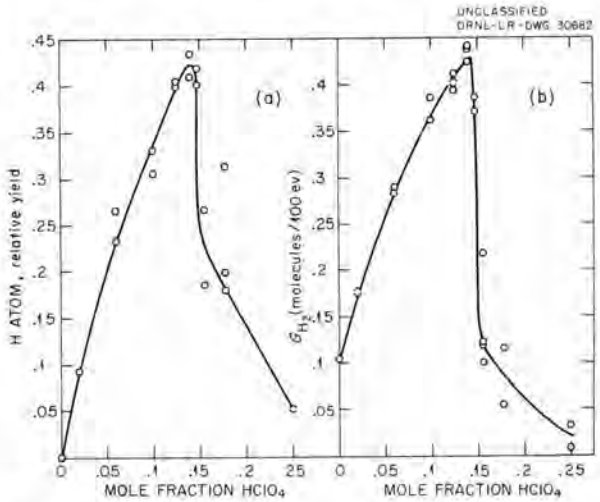


**Fig. 50. Atomic and Molecular Hydrogen Yields for Perchloric Acid Solutions Irradiated at 77°K with $Co^{60}$ Gamma Rays.** (*a*) Relative atomic hydrogen yields at 77°K; (*b*) molecular hydrogen yields (molecules/100 ev) after melting.

made to detect free radicals during the course of the irradiation of liquids with electrons from a Van de Graaff generator. A special magnet had been designed and constructed for this purpose. The magnet was set up at the generator, and it has been found possible to focus essentially the entire electron beam through a hole in one of the poles and into a microwave cavity in the gap of the magnet. A very simple paramagnetic resonance spectrometer was built and has been operated with the Van de Graaff generator also operating. No positive results have been obtained in preliminary experiments with several organic liquids which were flowed through the cavity during irradiation. However, this spectrometer has low sensitivity, and additional instrument development is being carried out which should enable an improvement in sensitivity by a factor of 100 over that initially available.

### Paramagnetic Resonance Studies of Methanol and Ethanol Irradiated at 77°K

H. Zeldes R. Livingston

Suitably prepared samples of methanol and ethanol cooled to liquid-nitrogen temperature and irradiated with gamma rays give a characteristic three- or five-line paramagnetic resonance spectrum at the low temperature. One group[5] has interpreted these spectra as arising from the $CH_2^+$ or $C_2H_4^+$ radicals, respectively, where the electron interacts equally with each of the protons. In order to understand these systems more fully, paramagnetic resonance measurements have been made on several of the deuterated alcohols at several temperatures. The results are quite complex.

If either alcohol is gamma-irradiated in darkness as a glass at 77°K, it becomes intensely colored, and this color can be bleached by incandescent illumination[6] while the samples are at the low temperature. A paramagnetic resonance spectrum associated with the color has been found. It appears partly superimposed upon the basic three- or five-line spectrum of the bleached materials. It is a precursor for at least a part of the species in the bleached materials. As the color is bleached and the precursor species vanishes, the basic spectrum becomes much more intense. Some of the properties of the precursor species have been determined. The results are not definitive but are consistent, for example, with the interpretation that the precursor is the alcohol ion.

The experiments on ethanol and deuterated ethanols show that the five-line pattern originates from a species containing four of the five hydrogen atoms on the two carbon atoms of the parent alcohol and not containing one of the hydrogens which was originally on the α-carbon. No evidence for the presence (or definite absence) of a hydroxyl hydrogen in the radical species could be found, and no decision could be made, for example, between $C_2H_4^+$ or $CH_3CHOH$. Similarly, in methanol no decision could be made between $CH_2^+$ and $CH_2OH$. Further details of this work were submitted for publication.[7]

## NEUTRON AND X-RAY DIFFRACTION STUDIES

### Single-Crystal Neutron Diffraction Study of Hydrogen Peroxide

W. R. Busing H. A. Levy

The single-crystal neutron diffraction study of $H_2O_2$ reported previously[8] has been continued, and the intensities of 38 reflections of the $hbl$ zone have been measured. A Fourier projection was made, followed by a least-squares treatment of the old and new data in which the anisotropic temperature factor $\exp\left(-\sum_{ij} B_{ij}h_ih_j\right)$ was used. A weighted discrepancy factor of 7.1% in $F^2$ was obtained. The refined parameters are given below, together with their standard errors:

| | Oxygen | Hydrogen |
|---|---|---|
| $x$ | 0.0733 ± 0.0008 | 0.220 ± 0.001 |
| $y$ | 0.1687 ± 0.0008 | 0.455 ± 0.002 |
| $z$ | 0.2220 ± 0.0004 | 0.388 ± 0.003 |
| $4a^2B_{11}$ | 1.15 ± 0.13 | 2.0 ± 0.3 |
| $4a^2B_{22}$ | 1.85 ± 0.16 | 4.0 ± 0.4 |
| $4c^2B_{33}$ | 1.36 ± 0.13 | 1.0 ± 0.5 |
| $4a^2B_{12}$ | 0.22 ± 0.07 | −0.5 ± 0.2 |
| $4acB_{13}$ | −0.09 ± 0.10 | −0.5 ± 0.3 |
| $4acB_{23}$ | −0.04 ± 0.11 | 0.4 ± 0.5 |

[5] C. F. Luck and W. Gordy, *J. Am. Chem. Soc.* 78, 3240 (1956).

[6] R. S. Alger and T. H. Anderson, *Radiation-Induced Electronic Processes in Simple Organic Materials*, USNRDL-TR-110 (1956).

[7] H. Zeldes and R. Livingston, "Paramagnetic Resonance Study of Irradiated Glasses of Methanol and Ethanol," *J. Chem. Phys.* (submitted for publication).

[8] W. R. Busing and H. A. Levy, *Chem. Ann. Prog. Rep. June 20, 1956*, ORNL-2386, p 137.

These results must still be considered to be preliminary, since the hydrogen atoms were not well resolved in the *hhl* zone. A study of the *h0l* zone should remove this difficulty.

The hydrogen bonding postulated by Abrahams, Collin, and Lipscomb[9] in their x-ray study of $H_2O_2$ was confirmed, but the hydrogen atom does not lie on the line of centers between the oxygen atoms. Instead, the O-H bond makes an angle of 7.5 ± 0.5 deg with this line. The O-H distance is 0.94 ± 0.02 Å, and the peroxide O-O distance is 1.460 ± 0.009 Å. The O-O-H angle is 101.5 ± 0.5 deg. The dihedral angle between planes each defined by the peroxide link and one hydrogen atom is 89 ± 2 deg. On the other hand the dihedral angle between planes defined not by the hydrogen atoms but by the oxygen atoms to which they are hydrogen-bonded is 93.8 ± 0.3 deg, in excellent agreement with the 93° 51′ reported by Abrahams, Collin, and Lipscomb.[9]

### Computer Program To Process the Results of Crystal Structure Refinements

W. R. Busing H. A. Levy

In the study of crystal structures by x-ray or neutron diffraction, the data are often analyzed by the method of least squares to obtain the best values of atomic coordinates and temperature factor coefficients. Usually of greater interest than these parameters themselves are various functions of them such as interatomic distances or bond angles. The least-squares procedure also makes available a variance-covariance matrix which describes the standard errors and the correlations between the errors of the parameters, and which can be used to compute the standard error of any derived quantity.

An Oracle program has been prepared which takes the least-squares parameters, the variance-covariance matrix, and the unit-cell dimensions with their standard errors and computes various functions of these parameters together with the standard errors of these functions. Some of the quantities which have been evaluated in this way are interatomic distances; bond angles; the dihedral angle between two planes, each of which is defined by three atoms; the root-mean-square thermal displacement of an atom in a direction defined by some interatomic vector; the root-mean-square displacement of an atom along a principal axis of thermal motion; the angle between a principal axis of thermal motion and an axis of a coordinate system defined by the positions of some specified atoms; the sum of several bond angles; and the difference between chemically equivalent distances or angles. A mode of operation is also available which computes all interatomic distances less than a prescribed limit.

The code used to compute each function is in the form of a subroutine which is entered several times for the numerical evaluation of the partial derivatives needed for the error computation. The programmer selects the function subroutines and specifies the atoms involved by means of an instruction input, which is readily prepared. The atoms thus chosen may be related to the basic atoms by symmetry transformations and unit-cell translations.

The output includes a description of the function, its computed value, and its standard error with and without the contributions of the errors in the unit-cell dimensions.

### Determination of the Principal Axes of the Anisotropic Temperature Factor[10]

W. R. Busing H. A. Levy

The following method for computing the principal axes of thermal motion from the anisotropic temperature factor coefficients was derived by Waser.[11] Let the expression for the temperature factor of an atom be $\exp(-\sum_{ij} B_{ij} h_i h_j)$, where the $h_i$ are the indices of the reflection, and the $B_{ij}$ are the temperature factor coefficients. Then the equations to be solved are

$$(1) \qquad \sum_i [B_{ij} - \lambda(\mathbf{b}_i \cdot \mathbf{b}_j)] q_i = 0 \ , \qquad j = 1, 2, 3,$$

where the $\mathbf{b}_i$ are the reciprocal lattice vectors, and the $q_i$ describe the vector $\mathbf{Q} = \sum_i q_i \mathbf{b}_i$. Solution of the secular determinant yields three roots, $\lambda^{(r)}$, corresponding to the three principal axis directions, and substitution of each $\lambda^{(r)}$ in Eq. 1 gives a vector $\mathbf{Q}^{(r)} = \sum_i q_i^{(r)} \mathbf{b}_i$ which defines the

[9] S. C. Abrahams, R. L. Collin, and W. N. Lipscomb, *Acta Cryst.* 4, 15 (1951).

[10] W. R. Busing and H. A. Levy, *Acta Cryst.* 11, 450 (1958).

[11] J. Waser, *Acta Cryst.* 8, 731 (1955).

direction of the $r$th principal axis. The mean-square atomic displacement along this axis is $\lambda^{(r)}/2\pi^2$.

The purpose of this section is to point out that Eq. 1 may be recast in two ways which offer computational advantage:

$$(2) \quad \sum_k [\sum_i (\mathbf{a}_k \cdot \mathbf{a}_i) B_{ij} - \lambda \delta_{jk}] q_k = 0 \ , \quad j = 1, 2, 3,$$

$$(3) \quad \sum_k [\sum_j B_{ij} (\mathbf{a}_j \cdot \mathbf{a}_k) - \lambda \delta_{ki}] p_k = 0 \ , \quad i = 1, 2, 3.$$

Here the $\mathbf{a}_i$ represent the direct-lattice vectors, and the $p_k$ are the components of $\mathbf{Q}$ in terms of these vectors:

$$(4) \qquad \mathbf{Q} = \sum_k q_k \mathbf{b}_k = \sum_k p_k \mathbf{a}_k \ .$$

In the determinants of Eqs. 2 and 3 the unknown $\lambda$ appears only in the diagonal elements, which simplifies the solution of the secular equation. (Note, however, that these determinants are no longer symmetric.) Moreover, solution of the linear equations 3 yields the direct-lattice components $p_k^{(r)}$ of the principal axis vectors. These will sometimes be preferred to the components $q_k^{(r)}$.

Derivation of Eqs. 2 and 3 is most convenient in matrix notation. Equation 1 may be written

$$(1a) \qquad (\mathbf{B} - \lambda \mathbf{g})\, \mathbf{q} = 0 \ ; \qquad \mathbf{g} = [\mathbf{b}_i \cdot \mathbf{b}_j] \ .$$

Taking the scalar product of Eq. 4 with $\mathbf{b}_j$ and noting that $\mathbf{a}_i \cdot \mathbf{b}_j = \delta_{ij}$ yields $\mathbf{p} = \mathbf{g}\mathbf{q}$. A similar product of Eq. 4 with $\mathbf{a}_j$ shows that $\mathbf{g}^{-1} = [\mathbf{a}_i \cdot \mathbf{a}_j]$, since $\mathbf{q} = \mathbf{g}^{-1}\mathbf{p}$.

Premultiplying Eq. 1$a$ by $\mathbf{g}^{-1}$ gives

$$(2a) \quad (\mathbf{g}^{-1}\mathbf{B} - \mathbf{g}^{-1}\lambda \mathbf{g})\, \mathbf{q} = (\mathbf{g}^{-1}\mathbf{B} - \lambda \mathbf{1})\, \mathbf{q} = 0 \ .$$

Substituting $\mathbf{q} = \mathbf{g}^{-1}\mathbf{p}$ into Eq. 1$a$ yields

$$(3a) \quad (\mathbf{B} - \lambda \mathbf{g})\, \mathbf{g}^{-1}\mathbf{p} = (\mathbf{B}\mathbf{g}^{-1} - \lambda \mathbf{1})\, \mathbf{p} = 0 \ .$$

These are the matrix equivalents of Eqs. 2 and 3.

### Structure of Acetylglycine

H. A. Levy S. W. Peterson
V. Schomaker

The structure of acetylglycine was discussed in some detail in the previous annual report.[12] During the present year, refinement of this structure has been completed with very satisfactory results. Some new neutron diffraction data were collected, and an extensive re-evaluation of the previously collected data was made. Weight assignments were completely revised, and least-squares refinement procedures were applied to the revised data. No major changes resulted; however, the resulting structure parameters and bond distances and angles came into better agreement with the x-ray values. The precision of the determination improved considerably; the $R$ factor

$$\frac{\Sigma \, ||F_o| - |F_c||}{\Sigma \, |F_o|}$$

is 4.6%, while the standard deviation of an observation of unit weight is 1.02 where the expectation value is unity. The improvement in the latter quantity is due largely to the new weight assignments. Bond lengths with their precisions are compared in Table 28 with the x-ray and earlier neutron values.

### Crystal Structure of Potassium Hydrogen Maleate

S. W. Peterson H. A. Levy

Evidence from infrared spectra for the existence of an especially strong intramolecular hydrogen bond in the hydrogen maleate ion was presented by Cardwell, Dunitz, and Orgel,[13] and the suggestion was made that a symmetric (centered) hydrogen bond may occur. This report contains preliminary results of a neutron diffraction study in which the previously unknown structure of potassium hydrogen maleate was solved, the existence of a short, strong hydrogen bond was confirmed, and the ion was shown to be at least statistically symmetrical.

The probable space groups[13] $Pbcm$ and $Pbc2_1$ were confirmed by the neutron absences. A complete set of intensities in the $0kl$ zone was collected with a neutron wavelength of 1.062 Å out to $(\sin \theta)/\lambda = 0.756$. Consideration of the expected size and shape of the molecules in relation to the unit-cell dimensions[13] and a least-squares adjustment of parameters describing the position and orientation of the molecule led to a suitable trial configuration. An attempted refinement in space group $Pbc2_1$ by using Fourier and least-squares methods failed to produce an

[12] H. A. Levy, R. D. Ellison, and S. W. Peterson, *Chem. Ann. Prog. Rep. June 20, 1957*, ORNL-2386, p 136.

[13] H. M. E. Cardwell, J. D. Dunitz, and L. E. Orgel, *J. Chem. Soc.* **1953**, 3740.

Table 28. Bond Lengths in Acetylglycine

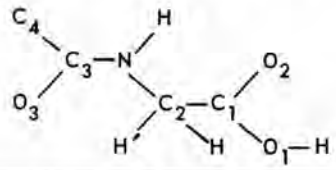


| Bond | Length (Å) | | | Standard Deviation |
|---|---|---|---|---|
| | X Ray | First Neutron | Present Neutron | |
| $C_1$-$C_2$ | 1.506 | 1.470 | 1.470 | 0.007 |
| $C_2$-N | 1.448 | 1.464 | 1.445 | 0.004 |
| N-$C_3$ | 1.323 | 1.364 | 1.343 | 0.005 |
| $C_3$-$C_4$ | 1.503 | 1.491 | 1.484 | 0.006 |
| $C_1$-$O_1$ | 1.312 | 1.331 | 1.322 | 0.006 |
| $C_3$-$O_3$ | 1.243 | 1.214 | 1.230 | 0.006 |
| $O_1$-H | | 1.028 | 1.057 | 0.016 |
| $C_2$-H | | 1.078 | 1.063 | 0.009 |
| $C_2$-H′ | | 1.067 | 1.088 | 0.012 |
| N-H | | 0.956 | 1.004 | 0.009 |

acceptable structure; refinement in *Pbcm* was, however, successful. In this space group the molecule must possess a mirror plane of symmetry.

Figure 51 shows a difference Fourier projection, along the short (4.54-Å) crystal axis *a*, from which the carbon, oxygen, and potassium contributions have been removed. It is seen that the carboxyl hydrogen atom is represented by approximately circular contours about the mid-point of the O-H-O hydrogen bond. Least-squares refinement of the position parameters and asymmetric temperature factor coefficients, with the carboxyl hydrogen constrained to the mirror plane, led to the values listed in Table 29. The conventional discrepancy factor is 8.6%, with unobserved reflections omitted.

Because only one projection of the structure is presently available, only distances between mirror-equivalent and diad-equivalent atoms can be quoted; of these, the intramolecular distances $O_2$-$O_1'$ = 2.42 Å and $C_2$=$C_2'$ = 1.37 Å and an intermolecular contact $O_1$-$O_1''$ = 2.66 Å are of interest. Whether the hydrogen atom is truly or only statistically centered cannot be directly determined

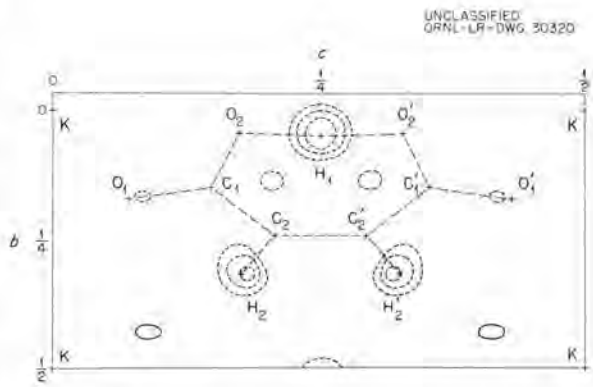


Fig. 51. Neutron Fourier Projection Along *a* of the Hydrogen Atoms in Potassium Hydrogen Maleate. Contributions of the other atoms, as given by the least-squares parameters, were subtracted. The crosses give the least-squares atomic positions. Contours are at equal intervals of 0.25 Fermi units per square angstrom; negative contours are dotted, and zero contours are omitted. The plane of the molecule is presumably tilted some 40 deg from the *b*-*c* plane.

Table 29. Position Parameters and Temperature Factor Coefficients*

| Atom | $y$ | $z$ | $B_{kk}$ | $B_{ll}$ | $B_{kl}$ |
|---|---|---|---|---|---|
| $C_1$ | 0.148 | 0.147 | 1.42 | 0.98 | −0.06 |
| $C_2$ | 0.241 | 0.207 | 1.27 | 1.74 | 0.17 |
| $O_1$ | 0.170 | 0.072 | 2.30 | 1.50 | −0.09 |
| $O_2$ | 0.045 | 0.175 | 2.93 | 1.23 | −0.19 |
| $H_1$ | 0.050 | (0.250) | 2.11 | 3.39 | (0.00) |
| $H_2$ | 0.317 | 0.176 | 4.81 | 4.75 | 0.97 |
| K | (0.000) | (0.000) | 1.15 | 1.91 | −0.17 |

*Parentheses enclose values fixed by symmetry considerations. The temperature factors are coefficients in the expression $\frac{1}{4}(B_{kk}b^{*2}k^2 + B_{ll}c^{*2}l^2 + 2B_{kl}b^*c^*kl)$.

from this study; in fact, a model in which one-half hydrogen was placed at 1.05 Å from each $O_2$ gave agreement essentially equivalent to that of the centered model. Similar difficulty in distinguishing true from statistical centering has been experienced in other cases, namely, $KH_2PO_4$ (refs 14 and 15), sodium sesquicarbonate,[16] and potassium hydrogen bis-phenylacetate.[17]

Examination of the temperature factors, however, provides direct evidence bearing on the nature of the carboxyl hydrogen atom, $H_1$. The temperature factors listed in Table 29 show that the mean-square component of displacement in the $b$ direction (i.e., normal to the hydrogen bond direction) is greater for $O_2$ than for $H_1$. Previous studies of hydrogen-containing crystals have always shown greater displacements for H than for neighboring atoms, in agreement with the picture of the light hydrogen atom "riding" on its heavier ligand with superposition of independent motion. We are led to conclude that, in the present case, H is strongly linked to both neighboring oxygen atoms and that there exists a mode of correlated motion of considerable amplitude in which the oxygen atoms are displaced but H is not. Coupled rotary oscillations about the two C-C single bonds, in a sense that would maintain a diad symmetry axis, is suggested. We submit that at least a close approach to actual centering is implied by the foregoing interpretation.

[14] S. W. Peterson and H. A. Levy, *J. Chem. Phys.* **21**, 2084 (1953).

[15] G. E. Bacon and R. S. Pease, *Proc. Roy. Soc. (London)* **A220**, 397 (1953).

[16] G. E. Bacon and N. A. Curry, *Acta Cryst.* **9**, 82 (1956).

[17] G. E. Bacon and N. A. Curry, *Acta Cryst.* **10**, 524 (1957).

## Diffraction Studies of Liquids

P. A. Agron  M. D. Danford  H. A. Levy

During the report period the emphasis of the study of liquids by both x-ray and neutron diffraction shifted from fused salts at high temperatures to a number of aqueous solutions of heavy elements at room temperatures that were suspected of containing or had been found by means of ultracentrifugation and other measurements[18–20] to contain polymeric species. The liquids studied included aqueous solutions of the uranyl ion, namely, various concentrations of uranyl fluoride, chloride, nitrate, and perchlorate at varying acidity. Among these solutions, only $UO_2F_2$ showed extensive formation of a complex species containing more than one uranium atom. A trimeric species is indicated both in stoichiometric $UO_2F_2$ solutions and in solutions containing a slight excess of HF. In an aqueous solution of 5.81 *M* $BiOClO_4$ and 0.95 *M* $HClO_4$, evidence was obtained for the complex species $Bi_6(OH)_{12}^{6+}$. The diffraction data are consistent with an octahedral arrangement of bismuth atoms, any two of which are linked by an oxygen bridge. On the other hand, as expected, bismuth trichloride solutions containing an excess of HCl gave no indication of appreciable complex formation.

The structure of the anion $SiW_{12}O_{40}^{4-}$ in aqueous silicotungstic acid solution was found to be similar to the known structure of $PW_{12}O_{40}^{3-}$ in the crystal form.

The work on both fused salts and aqueous solutions is continuing.

[18] J. S. Johnson and K. A. Kraus, *J. Am. Chem. Soc.* **74**, 4436 (1952).

[19] J. S. Johnson, K. A. Kraus, and T. F. Young, *J. Am. Chem. Soc.* **76**, 1436 (1954).

[20] R. W. Holmberg, K. A. Kraus, and J. S. Johnson, *J. Am. Chem. Soc.* **78**, 5506 (1956).

### Crystal Phase Transformations by Mechanical Deformation (Grinding)

M. A. Bredig R. D. Ellison

In continuation of earlier observations[21] on the transformation of the stable crystal modification of calcium carbonate (calcite) into aragonite, the form metastable at room temperature and atmospheric pressure, practically complete transformation was obtained after 11 days of grinding in a small laboratory ball mill. A 24-hr period of grinding, which had sufficed to produce 80% transformation with automatic mortar and pestle (force of 2 kg), did not produce a detectable amount of aragonite in the ball mill. This seems to confirm the explanation given earlier[21] that a combination of a minimum hydrostatic pressure with a shearing force is needed to produce aragonite, one of the high-pressure forms of calcium carbonate. Vaterite, better designated $\mu$-$CaCO_3$, prepared from aqueous solutions showed no transformation into either calcite or aragonite but became amorphous to x rays.

Calcite precipitated or digested in aqueous solutions of magnesium, zinc, or cadmium salts at the boiling temperature was stable against mechanical transformation into aragonite. This agrees with expectation, as the carbonates of the smaller cations of Mg, Zn, and Cd are known only in the calcite type of structure. In contrast, the carbonates of the larger cations of Sr, Ba, etc., occur in the aragonite type of structure.

### Bent-Crystal Monochromator for Single-Crystal X-Ray Diffraction Studies

R. D. Ellison

In order to obtain single-crystal x-ray diffraction data, with monochromatic molybdenum $K\alpha$ x rays of maximum available intensity, a doubly bent and ground, point-focusing crystal monochromator was designed and built. Both symmetric and asymmetric mountings were tried with NaCl and Al monochromating crystals; the most satisfactory arrangement was found to be the symmetrically mounted NaCl crystal. The crystal was bent to a barrel shape with radii of curvature of 33 and 0.52 in.

This monochromator is being used with the Weissenberg goniometer to gather full three-dimensional diffraction data on a single crystal of the $\beta_3$ phase of $Na_2UF_6$.

### Cell Size of Dimethyl-$\gamma$-Pyrone

R. D. Ellison

As an aid in the determination (by G. Brown, University of Maryland, summer research participant with the Chemical Physics Group) of the detailed structure of DM$\gamma$P, a precision refinement of the unit-cell dimensions of this compound was made. The Debye-Scherrer camera and chromium $K\alpha$ radiation were used for this determination. The monoclinic cell dimensions were found to be $a = 7.653 \pm 0.006$ Å, $b = 7.198 \pm 0.007$ Å, $c = 13.863 \pm 0.012$ Å, and $\beta = 121° 2' \pm 5'$.

## CALORIMETRY

### Low-Temperature Heat Capacity Calorimeter

R. B. Bevan, Jr. R. A. Gilbert

The construction of a specific-heat calorimeter designed to operate in the temperature range 10 to 310°K and to utilize liquid helium as a refrigerant to produce the lowest temperature was completed. The cryostat, which is similar to that of Westrum *et al.*,[22] was modified by omitting the second adiabatic shield and by replacing the outermost radiation shield with a metal Dewar.

A calorimeter utilizing liquid helium instead of liquid hydrogen as the refrigerant to cool the cryostat to the lowest temperatures requires a heat exchanger in the apparatus to utilize the cooling capacity of the helium gas vaporized from the liquid helium in addition to the relatively small cooling effect obtainable from the heat of vaporization. Otherwise, the amount of liquid helium required to cool the apparatus would be prohibitive. The cryostat constructed required only approximately 3 liters of liquid helium for measurements below 60°K.

The heat capacity of a Calorimetry Conference standard sample of benzoic acid was measured over the temperature range 10 to 310°K. These preliminary results are consistently 0.6% high. The cause of the discrepancy is being investigated.

---

[21] J. H. Burns and M. A. Bredig, *J. Chem. Phys.* **25**, 1281 (1956).

[22] E. F. Westrum, Jr., J. B. Hatcher, and D. W. Osborne, *J. Chem. Phys.* **21**, 419 (1953).

### High-Temperature Heat Content Calorimeter

R. A. Gilbert

The construction of a high-temperature (0 to 1100°C) heat content apparatus utilizing a Bunsen ice calorimeter was completed. The apparatus is similar to that now used routinely at the National Bureau of Standards and described by Ginnings *et al.*[23] The method consists, essentially, in heating a sample in a furnace to a known temperature, measured either by a platinum resistance thermometer or a Pt, Pt-Rh thermocouple depending upon the temperature range, and dropping the sample into an ice calorimeter to measure the heat evolved in cooling it to 0°C. The heat capacity of the empty sample container and the heat lost by the container during the drop are accounted for by "blank" experiments made with the empty container at temperatures the same as those with the filled sample container. In order to extend the temperature range of the present furnace to 1100°C for brief periods, nickel cylinders were substituted[24] for the silver cylinders used in the NBS apparatus. Several minor construction and operational difficulties were encountered but are being eliminated. Measurements on a Calorimetry Conference standard sample of $Al_2O_3$ are in progress.

## MOLECULAR AND IONIC BEAM STUDIES IN CHEMICAL KINETICS

S. Datz R. E. Minturn E. H. Taylor

The development of the apparatus[25] designed for the study of chemically interesting collisions between a beam of low-energy protons and a deuterium molecular beam was continued. The proton source operates dependably, yielding steady currents of about 600 μa at 3 kv. Some difficulty was encountered in achieving the desired monoenergetic beam, and the spread in energy observed was thought to be due to two effects: (1) a high proton density in the region of the first retarding grid caused reflection of some high-energy protons which should have been accepted by this grid; (2) penetration of the reaccelerating field through the second retarding grid caused acceptance of low-energy protons which should have been reflected. Both problems are being studied, the first by injection of electrons into the region of the first retarding grid, and the second by the use of double grids at the second retardation in order to assure attainment of the true grid potential. The initial results of these modifications appear promising.

The energy distribution of protons from the r-f source has been measured semiquantitatively for two different probe tip designs.[26,27] The results are plotted in Fig. 52.

[23] D. C. Ginnings, T. B. Douglas, and A. F. Ball, *J. Am. Chem. Soc.* 73, 1236 (1951).

[24] R. A. Oriani and W. K. Murphy, *J. Am. Chem. Soc.* 76, 343 (1954).

[25] S. Datz and E. H. Taylor, *Chem. Ann. Prog. Rep. June 20, 1957*, ORNL-2386, p 142.

[26] C. D. Moak, H. Reese, Jr., and W. M. Good, *Nucleonics* 9(3), 18 (1951).

[27] J. Erö, *Acta Phys. Acad. Sci. Hung.* 5, 391 (1956).

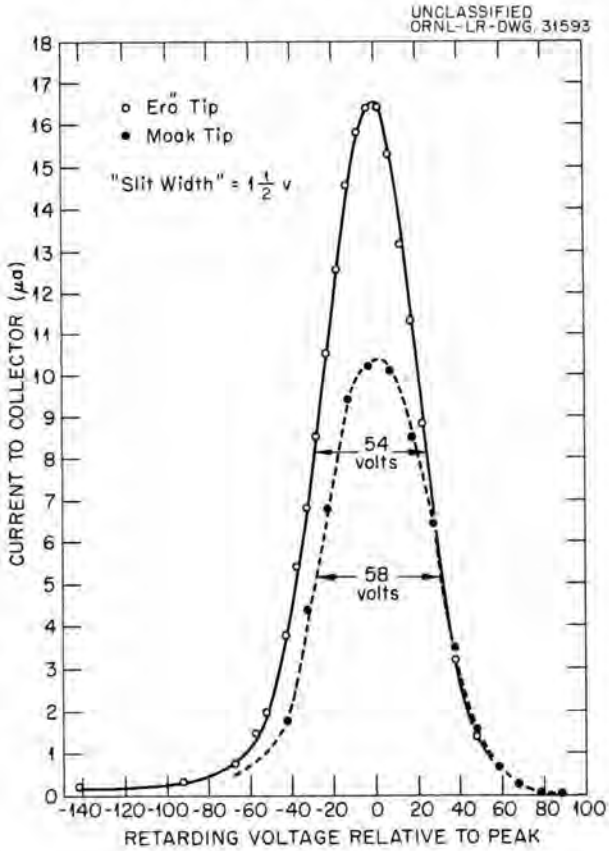


**Fig. 52. Proton Current to the Collector vs Retarding Voltage (Relative to Peak) for a "Slit Width" of 1½ v.**

## THERMAL EMISSION OF ALKALI POSITIVE ION PULSES FROM CLEAN AND OXYGENATED TUNGSTEN

R. E. Minturn S. Datz

Thermal emission of alkali positive ions from heated tungsten constitutes the major source of noise in the use of the surface ionization gage as a molecular beam detector. In addition, oxygenation markedly increases this emission. A study of the nature of this positive ion emission was made in order to ascertain whether this phenomenon could be used for investigating high-temperature diffusion and surface oxidation mechanisms, as well as to determine optimum signal-to-noise conditions for molecular beam detection. A tungsten surface ionization gage[28] with a Tektronix type 531 oscilloscope was used for studying the time dependence of the ion current. The composition of the ion current was determined with the modified G-E 6-in.-radius 60-deg-sector mass spectrometer.[29]

At temperatures between 1200 and 2400°K, thermal ion emission from aged tungsten is primarily in the form of discrete bursts of alkali ions, each burst being of short duration ($< 100\ \mu$sec on clean tungsten) and having a relatively low recurrence rate. The frequency of the bursts and the average number of ions per burst are strongly dependent on both filament temperature and oxygen pressure, which was varied from $2 \times 10^{-7}$ to $5 \times 10^{-5}$ mm Hg. A proposed mechanism consists in diffusion of the alkali impurities from the crystallites to the interstices and consequent eruption of pulses of surface ions upon crystallite reorientation. Inferences concerning the stability of surface oxide films as a function of pressure and temperature may be drawn from the shapes of positive ion pulses obtained under varying conditions. Since almost all heated metals exhibit some form of alkali ion emission, this method is suggested as a tool in studies of high-temperature behavior.

## DETERMINATION OF VAPOR DENSITIES OF ALKALI HALIDE SALTS

S. Datz R. E. Minturn

The vapor pressure data obtained previously for NaCl and KCl by the modified Knudsen effusion method[30] are valid and accurate only insofar as the degree of association in the vapor phase is known. Contradictory literature reports on the degree of association[31,32] have made necessary an additional definitive measurement of the amount of association, and the measurement of vapor densities has been chosen as the most direct and unambiguous technique. The high temperatures necessary for such measurements and the enhanced chemical activity of salts at these temperatures have increased the experimental difficulties. The quartz sickle gage technique failed because of the high-temperature permeability of thin-walled quartz to argon, which was used to balance the vapor pressure of the salt. Some qualitative results were obtained from a modified Victor Meyer apparatus, and association approximately to the extent reported by Miller and Kusch[31] was indicated. The reproducibility of the method was poor, however, probably because of irreproducible mixing of the salt vapor with the inert gas. A more promising technique is being investigated in which a small sample of the salt under consideration is contained in a fused silica flask to which is sealed a gold-filled manometer. The manometer is maintained at a temperature above the melting point of gold, and the manometer level is held constant by the application of a balancing pressure of inert gas. The gas pressure necessary to maintain constant volume in the salt vessel indicates the pressure exerted by the salt at a given temperature. Rough preliminary results indicate about 30% association in NaCl vapor, and work on the experiment is in progress.

## DISSOCIATION OF $C_6H_5T$ FOLLOWING BETA DECAY

T. A. Carlson F. Pleasonton[33]
A. H. Snell[33]

The relative abundance of the various charged fragments formed following the beta decay of monotritiated benzene was measured. A specially designed mass spectrometer was utilized for

[28] S. Datz and E. H. Taylor, *J. Chem. Phys.* **25**, 389 (1956).

[29] G. F. Wells and C. E. Melton, *Rev. Sci. Instr.* **28**, 1065 (1957).

[30] S. Datz and R. E. Minturn, *Chem. Ann. Prog. Rep. June 20, 1957*, ORNL-2386, p 125.

[31] R. C. Miller and P. Kusch, *J. Chem. Phys.* **25**, 860 (1956).

[32] W. Klemperer and S. A. Rice, *J. Chem. Phys.* **26**, 618 (1957).

[33] Physics Division.

this study. Low pressures of about $3 \times 10^{-6}$ mm Hg were used to ensure against secondary interactions before collection.

Thirty-one singly charged fragments were found. Of these, only 0.1% is represented by $(He^3)^+$, while about 70% is found as $C_6H_5^+$. The C-He bond probably breaks in most cases after a single vibration, the $C_6H_5^+$ often being left with enough energy to dissociate into further fragments. The presence of about 3% of the total number of fragments in the form of a carbon skeleton, completely stripped of hydrogen ($C_n$, where $n = 1$ to 6), suggests the existence of a fairly energetic process, since from electron impact studies such fragments have appearance potentials from 40 to 45 ev. Further, since according to calculation the maximum energy available from the recoil of beta emission in $C_6H_5T$ is only 3 ev, some extra excitation from the nonadiabatic nature of the process must be postulated. All these observations are in agreement with data on $CH_3T$ by Snell and Pleasonton[34] and on $C_2H_5T$ and $C_3H_7T$ by Wexler and Hess[35].

Comparison of the fragmentation of $C_6H_5T$ with the electron impact study of benzene with 72-ev electrons shows an over-all qualitative similarity, the initially ionized fragment $C_6H_6^+$ representing about half the products, while secondary fragments are distributed over a wide spectrum of species. A comparison of the results for fragments containing five or less carbon atoms reveals that the average number of hydrogens is 1.6 in the case of $C_6H_5T$ and 2.7 in the case of electron impact studies, reflecting the fact that the parent ion in the case of beta recoil, $C_6H_5^+$, has one fewer hydrogen than the parent species $C_6H_6^+$ of the electron impact study.

## MASS SPECTROMETRY AND RELATED TECHNIQUES

### Research Mass Spectrometers

G. F. Wells C. E. Melton C. R. Baldock

In anticipation of realizing the highest possible "abundance sensitivity" in the two-stage mass spectrometer previously described,[36] it was postulated that research in such processes as ion-molecule collisions, charge exchange, etc., would be fruitful. This postulate has been found by White *et al.*[37] to be especially true of a three-stage mass spectrometer. As a first step, a single-stage 6-in.-radius mass spectrometer described elsewhere[38] was built for this research. All data incorporated in the research reports which follow were obtained on this machine. Two recent modifications have greatly extended the application of the instrument: (1) a thoria-iridium filament,[39] which replaced the conventional tungsten filament for producing ionizing electrons, has made possible extensive investigations of such materials as formic acid, chlorine, etc., and (2) a 14-stage electron multiplier and associated counting circuitry has made possible the investigation of negative ion processes in which the probability of ion formation is several orders of magnitude less than in comparable positive ion processes.

In preparation for final assembly of the two-stage mass spectrometer, tests of the first stage are essentially complete and are quite satisfactory.

### Dissociation of Ions of Formic Acid and Deuteroformic Acids by Ion-Molecule Collision[40]

C. E. Melton G. A. Ropp

The dissociation of 5.1-kev $HCOOH^+$, $DCOOH^+$, and $HCOOD^+$ ions by ion-molecule collision with $H_2$, $D_2$, He, $N_2$, A, and Kr has been investigated by means of a mass spectrometer. By use of isotopically labeled formic acid reactants, the origin of the products was reliably determined. Approximate values for the cross sections for forming the given fragment ions from the reactions with hydrogen are shown in Table 30. These data indicate that the positive ion fragments

[34] *Oak Ridge National Laboratory Status and Progress Report Sept. 1957*, ORNL-2411, p 18 (classified).

[35] D. C. Hess and S. Wexler, *Physics Division Summary Report, April Through June, 1957*, ANL-5754, p 68; *Physics Division Summary Report, October, November, December, 1957*, ANL-5818, p 82.

[36] G. F. Wells and C. R. Baldock, *Chem. Ann. Prog. Rep. June 20, 1957*, ORNL-2386, p 139.

[37] F. A. White, F. M. Rourke, and J. C. Sheffield, *Appl. Spectroscopy* 12, 46–52 (1958).

[38] G. F. Wells and C. E. Melton, *Rev. Sci. Instr.* 28, 1065 (1957).

[39] C. E. Melton, *Rev. Sci. Instr.* 29, 250 (1958).

[40] C. E. Melton and G. A. Ropp, *J. Chem. Phys.* 29, 400 (1958).

**Table 30. Approximate Values for Absolute Cross Sections[a] for Dissociation of 5.1-kev $HCOOD^+$ and $DCOOH^+$ Ions by Ion-Molecule Collision**

| Reaction[b] | Cross Section ($cm^2$) |
|---|---|
| | $\times 10^{-17}$ |
| $HCOOD^+ + H_2 \rightarrow HCO^+ + (H_2) + (OD)$ | 4.0 |
| $\rightarrow HCOO^+ + (H_2) + (D)$ | 2.0 |
| $\rightarrow COOD^+ + (H_2) + (H)$ | c |
| $\rightarrow COD^+ + (H_2) + (OH)$ | 0.7 |
| $\rightarrow CO^+ + (H_2) + (HOD)$ | 0.5 |
| $\rightarrow OD^+ + (H_2) + (HCO)$ | 0.2 |
| $DCOOH^+ + H_2 \rightarrow DCO^+ + (H_2) + (OH)$ | 5.0 |
| $\rightarrow DCOO^+ + (H_2) + (H)$ | c |
| $\rightarrow COOH^+ + (H_2) + (D)$ | 4.0 |
| $\rightarrow COH^+ + (H_2) + (OD)$ | 0.7 |
| $\rightarrow CO^+ + (H_2) + (HOD)$ | 0.5 |
| $\rightarrow OH^+ + (H_2) + (DCO)$ | 0.2 |

[a]Calculations based on assumptions given elsewhere: C. E. Melton, *J. Chem. Phys.* 28, 359 (1958).

[b]Species in parentheses are possible, but not known products.

[c]Not evaluated because of coincidence of masses with other ions.

$CHO^+$ and $CHO_2^+$ are produced by loss of hydrogen from rupture of either the C-H bond or the O-H bond. Studies[41] of the dissociation of HCOOH induced by electron impact indicated a similar dissociation pattern.

Relative cross sections for dissociation of $HCOOH^+$, $CO^+$, and $N_2^+$ are shown in Table 31. The relative cross sections for dissociation of $HCOOH^+$ into $CHO_2^+$ are approximately in direct proportion to the mass and/or size of the noble gas atoms. However, the relative cross sections for dissociation of $N_2^+$ and $CO^+$ are approximately inversely proportional to the mass. The different mass effects in these studies might be related

[41]G. A. Ropp and C. E. Melton, *J. Am. Chem. Soc.* 80, 3509 (1958).

**Table 31. Relative Cross Section for Collision-Induced Dissociation**

| Reaction[a] | Relative Cross Section |
|---|---|
| $HCOOH^+ + He \rightarrow CHO_2^+ + (He) + (H)$ | 35 |
| $HCOOH^+ + A \rightarrow CHO_2^+ + (A) + (H)$ | 55 |
| $HCOOH^+ + Kr \rightarrow CHO_2^+ + Kr + (H)$ | 100 |
| $CO^+ + He \rightarrow C^+ + (He) + (O)$ | 100[b] |
| $CO^+ + A \rightarrow C^+ + (A) + (O)$ | 55[b] |
| $CO^+ + Kr \rightarrow C^+ + (Kr) + (O)$ | 35[b] |
| $N_2^+ + He \rightarrow N^+ + (He) + (N)$ | 100[c] |
| $N_2^+ + A \rightarrow N^+ + (A) + (N)$ | 40[c] |
| $N_2^+ + Kr \rightarrow N^+ + (Kr) + (N)$ | 30[c] |

[a]Species in parentheses are possible, but not known products.

[b]C. E. Melton and G. F. Wells, *J. Chem. Phys.* 27, 1132 (1957).

[c]G. F. Wells and C. E. Melton, *Rev. Sci. Inst.* 28, 1065 (1957).

to the fact that the energy required for dissociation of $CO^+$ and $N_2^+$ is much higher than that for $HCOOH^+$. Consequently, the ionization potential of the neutral gas might be a more important factor in determining the cross sections for dissociation of $CO^+$ and $N_2^+$ through the competition of a possible charge exchange process with the observed dissociation reaction.

## Bimolecular, Ion-Molecule Reactions of Aliphatic Acids and of Deuteroaliphatic Acids

G. A. Ropp C. E. Melton

An investigation was carried out to study ion-molecule reactions[42-44] of the type

$$CH_4^+ + CH_4 \longrightarrow CH_5^+ + CH_3$$

[42]D. P. Stevenson and D. O. Schlissler, *J. Chem. Phys.* 23, 1353 (1955).

[43]J. J. Mitchell, R. H. Perkins, and F. F. Coleman, *J. Chem. Phys.* 16, 835 (1948).

[44]V. L. Talroze and A. K. Lyubimova, *Doklady Akad. Nauk. S.S.S.R.* 86, 909 (1952).

by use of formic acid, deuteroformic acids, and acetic acid. It was thought that the reactive portion of the molecule could be determined by means of isotopic labeling. By comparing the values of the bimolecular rate constants for formic acid and acetic acid, the relative reaction rates for the two species could be determined.

Results obtained for formic acid and deuteroformic acids are shown in Table 32. The relative abundance of the products is much higher than that normally observed in a mass spectrometer at this pressure because of the special design feature[45] of the instrument. Results from deuterium labeling clearly show that the products are formed by loss of hydrogen from rupture of either the C-H bond or the O-H bond, but that rupture of the C-H bond is preferred.

In an equimolar mixture of HCOOH and $CH_3COOH$ the ratio $HCOOH{\cdot}H^+/HCOOH^+$ was equal to the ratio $CH_3COOH{\cdot}H^+/CH_3COOH^+$. This observation, combined with the observed high value of the rate constant, $K = 1 \times 10^{-9}$ cc/molecule/sec, led to the suggestion that the ion reacts at each collision with the neutral molecule.

### Charge Permutation by Ion-Molecule Collision[46]

C. E. Melton

Studies of ion-molecule reactions[47,48] indicate that in some instances negative ions are formed by positive-ion–molecule collision reactions and that positive ions result from negative-ion–molecule collision reactions. Formic acid is well suited for investigating reactions of this type because of its large cross sections for forming negative ions. Approximate values for the absolute cross section of the reactions studied are shown in Table 33.

[45] C. E. Melton and G. A. Ropp, *J. Am. Chem. Soc.* **80**, 3509 (1958).

[46] C. E. Melton, *J. Chem. Phys.* **28**, 359 (1958).

[47] S. C. Lind and D. C. Bardwell, *J. Am. Chem. Soc.* **48**, 2335 (1926).

[48] S. E. Kuprianov and V. K. Pelepov, *Doklady Akad. Nauk. S.S.S.R.* **103**, 449 (1955).

**Table 33. Absolute Cross Section for Collison Processes**

| Reaction* | Cross Section ($cm^2$) |
|---|---|
| | $\times 10^{-19}$ |
| $HCOOH^+ + Kr \rightarrow O^- + (Kr) + (HCOH)$ | 1 |
| $HCOOH^+ + Kr \rightarrow OH^- + (Kr) + (HCO)$ | 0.6 |
| $HCOOH^+ + Kr \rightarrow HCOO^- + (Kr) + H$ | 0.1 |
| | $\times 10^{-18}$ |
| $HCOO^- + He \rightarrow HCO^+ + (He) + (O)$ | 3 |
| $HCOO^- + He \rightarrow CO^+ + (He) + (OH)$ | 1 |
| $HCOO^- + He \rightarrow CO_2^+ + (He) + (H)$ | 1 |
| $HCOO^- + He \rightarrow HCOO^+ + (He)$ | 0.4 |

*It is not known whether the species indicated by parentheses are ions or neutrals; nor is their composition known.

**Table 32. Positive Ion-Molecule Reactions of Formic Acid and of Deuteroformic Acids**

| | Mass | Probable Reaction | Relative Abundance* |
|---|---|---|---|
| HCOOH | 46 | $HCOOH + e \rightarrow HCOOH^+ + 2e$ | 100 |
| | 47 | $HCOOH^+ + HCOOH \rightarrow HCOOH{\cdot}H^+ + COOH$ | 100 |
| DCOOH | 47 | $DCOOH + e \rightarrow DCOOH^+ + 2e$ | 100 |
| | 48 | $DCOOH^+ + DCOOH \rightarrow DCOOH{\cdot}H^+ + DCOO$ | 40 |
| | 49 | $DCOOH^+ + DCOOH \rightarrow DCOOH{\cdot}D^+ + COOH$ | 60 |
| HCOOD | 47 | $HCOOD + e \rightarrow HCOOD^+ + 2e$ | 100 |
| | 48 | $HCOOD^+ + HCOOD \rightarrow HCOOD{\cdot}H^+ + COOD$ | 80 |
| | 49 | $HCOOD^+ + HCOOD \rightarrow HCOOD{\cdot}D^+ + HCOO$ | 30 |

*At an indicated pressure of $5 \times 10^{-4}$ mm Hg.

The linear pressure dependence of the relative abundance for all the transitions, given in Fig. 53 (tube pressure-dependence curves for positive ion fragments formed from 5.1-kev $HCOO^-$ ions by negative-ion–molecule reactions), clearly shows that they are due to single-collision processes.

### Mass Spectrometric Observations of Triatomic Ions in Chlorine and Bromine Gases

C. E. Melton G. A. Ropp P. S. Rudolph

The mass spectra of bromine, chlorine, and their binary mixture were obtained in the especially constructed[49] mass spectrometer shown schematically in Fig. 54. Positive and negative ions of $Cl_3$ and $Br_3$ were observed (Figs. 55 and 56). Although the stability of these radicals was calculated as early as 1936 by Eyring *et al.*,[50] they had not previously been observed. In a rather extensive investigation of these trimer ions, it was not found possible to determine conclusively their origin.

[49] G. F. Wells and C. E. Melton, *Rev. Sci. Instr.* **28**, 1065 (1957).

[50] H. Eyring, J. O. Hirschfelder, and H. S. Taylor, *J. Chem. Phys.* **4**, 479 (1936).

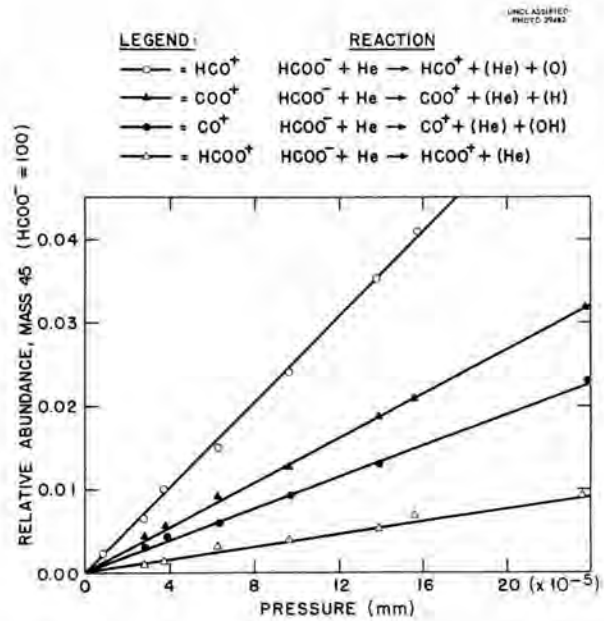


Fig. 53. Pressure-Dependence Curves for Positive Ion Fragments.

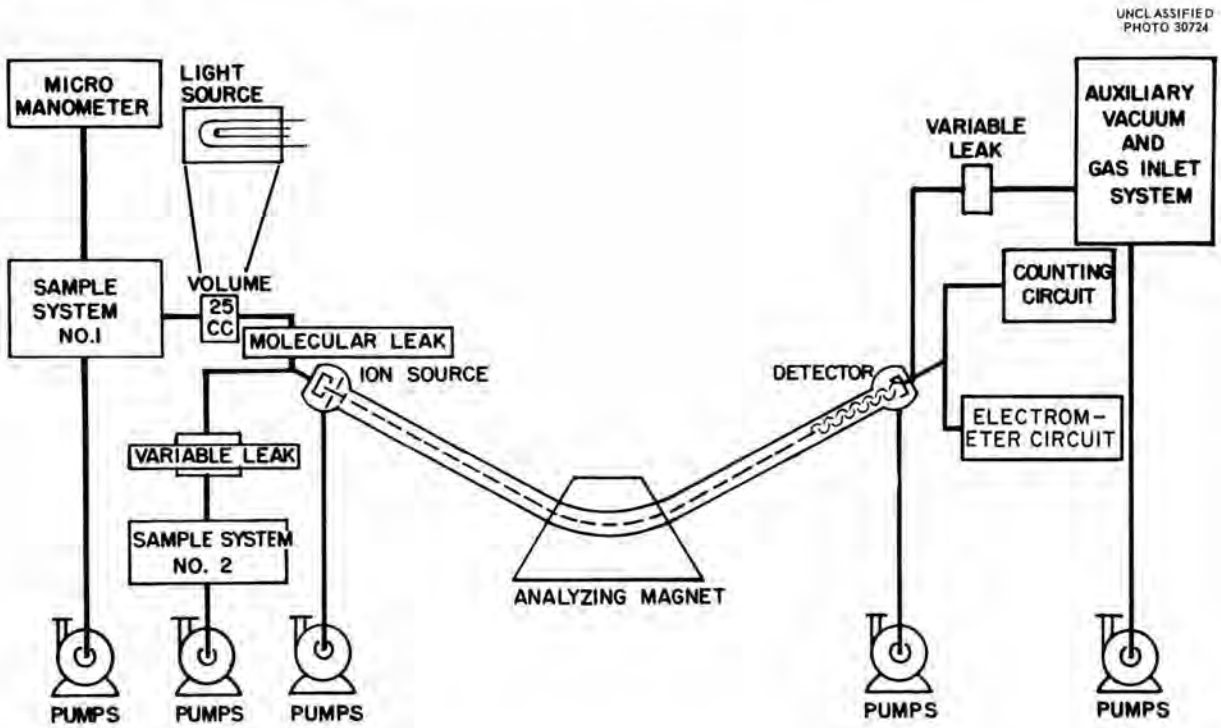


Fig. 54. Block Diagram for Mass Spectrometer RS1.

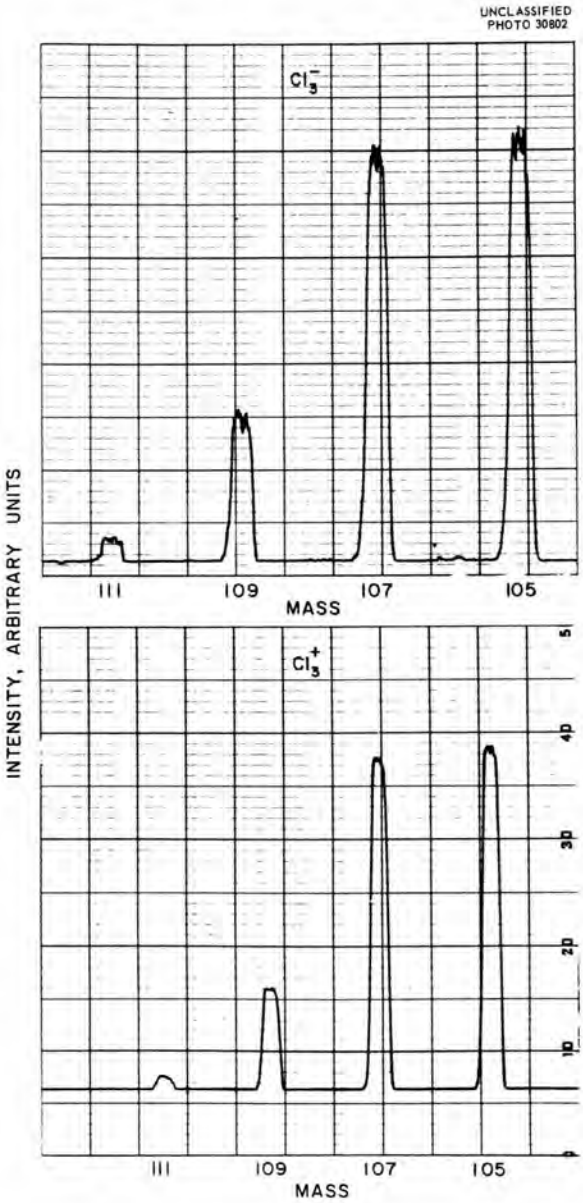


Fig. 55. Typical Mass Spectra of $Cl_3^-$ and $Cl_3^+$ Ions.

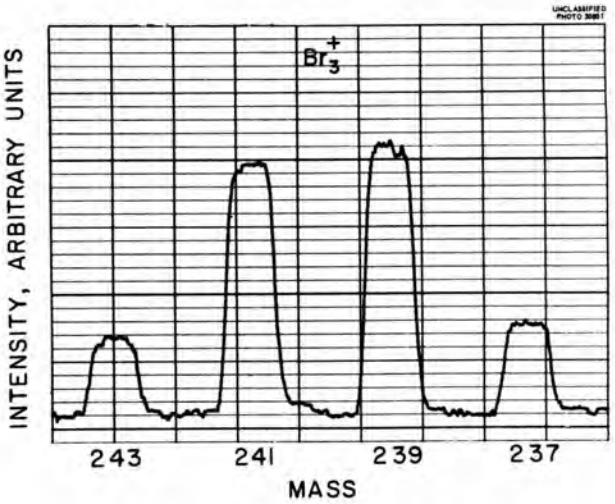


Fig. 56. Typical Mass Spectrum of $Br_3^+$ Ion.

## PUBLICATIONS

### NUCLEAR CHEMISTRY

E. C. Campbell and F. Nelson, "Metastable State of $Ge^{73}$," *Phys. Rev.* **107**, 502–3 (1957).

J. Halperin, J. O. Blomeke, and D. A. Mrkvicka, "Effective Reactor Cross Sections in MTR Fuel Assemblies," *Nuclear Sci. and Eng.* **3**, 395–402 (1958).

N. R. Johnson and G. D. O'Kelley, "Nuclear Decay of $Br^{84}$ and the Level Scheme in $Kr^{84}$," *Phys. Rev.* **108**, 82–90 (1957).

N. H. Lazar, G. D. O'Kelley, J. H. Hamilton, L. M. Langer, and W. G. Smith, "Nuclear Structure of $Zr^{90}$," *Phys. Rev.* **110**, 513–19 (1958).

G. D. O'Kelley, book review of *La Chimie Nucleaire et ses Applications* by M. Haissinsky, *Arch. Biochem. Biophys.* **75**, 296–97 (1958).

G. T. Seaborg, J. W. Gofman, and R. W. Stoughton, "A New Fissionable Isotope of Uranium: $U^{233}$," paper 1.1, p 1–15 in *Production and Separation of $U^{233}$, Collected Papers*, TID-5223, Part 1 (1952).

R. W. Stoughton and J. Halperin, "On the Effective Capture Cross Section of Pu-240 for Reactor Neutrons," *Nuclear Sci. and Eng.* **2**, 481–87 (1957).

### ISOLATION AND CHEMICAL PROPERTIES OF SYNTHETIC ELEMENTS

G. E. Boyd, "Production, Availability, and Economics of Reactor By-Products," p 161 in *Proceedings of the Conference on Peaceful Uses of Atomic Energy, May 13–17, 1957, Tokyo, Osaka, and Nagoya, Japan*, The Atomic Industrial Forum, Inc., New York.

E. G. Bohlmann, J. G. Barrick, G. A. Creek, K. K. Kennedy, J. P. McBride, F. W. Schuler, F. L. Steahly, and R. W. Stoughton, "Removal of Uranium from Thorium by Means of a Semicontinuous Solvent Extractor: Some General Solvent-Extraction Considerations," paper 3.8, p 143–158 in *Production and Separation of $U^{233}$, Collected Papers*, TID-5223, Part 1 (1952).

L. I. Katzin and R. W. Stoughton, "A Manganese Dioxide Procedure for Isolation and Concentration of Protactinium from Irradiated Thorium Compounds," paper 3.2, p 126–130 in *Production and Separation of $U^{233}$, Collected Papers*, TID-5223, Part 1 (1952).

F. W. Schuler, F. L. Steahly, and R. W. Stoughton, "Dissolution of Thorium Metal and Thorium Dioxide in $HNO_3$-HF and $HNO_3$-$(NH_4)_2SiF_6$ Mixtures," paper 7.1, p 307–317 in *Production and Separation of $U^{233}$, Collected Papers*, TID-5223, Part 1 (1952).

R. W. Stoughton, "Methods of Separation," chap. 3, p 51–83 in *Production and Separation of $U^{233}$, Survey*, TID-5222 (1951).

P. M. Lantz and G. W. Parker, ORNL CF-57-8-34 (July 31, 1957) (classified).

P. M. Lantz, p 81 in *Neptunium Information Meeting Proceedings, Oak Ridge National Laboratory, March 7 and 8, 1957*, TID-7542 (Oct. 1957) (classified).

G. W. Parker, *Neptunium Information Meeting Proceedings, Oak Ridge National Laboratory, March 7 and 8, 1957*, TID-7542 (Oct. 1957) (classified).

W. C. Waggener, "Measurement of the Absorption Spectra of Neptunium Ions in Heavy Water Solution from 0.35 to 1.85 $\mu$," *J. Phys. Chem.* **62**, 382 (1958).

## CHEMICAL SEPARATION OF ISOTOPES

R. M. Healy and A. A. Palko, "Separation of Boron Isotopes. I. Boron Trihalide Addition Compounds," *J. Chem. Phys.* **28**, 211–13 (1958).

A. A. Palko, R. M. Healy, and L. Landau, "Separation of Boron Isotopes. II. The $BF_3$ Anisole System," *J. Chem. Phys.* **28**, 214–17 (1958).

## RADIATION CHEMISTRY

J. W. Boyle and H. A. Mahlman, "Radiation Induced Decomposition of Thorium Nitrate Solutions," *Nuclear Sci. and Eng.* **2**, 492–500 (1957).

J. G. Burr, Jr., "A Comparison of the Radiolysis and Mass Spectrometry of Several Deuterated Ethanols," *J. Am. Chem. Soc.* **79**, 751–52 (1957).

J. G. Burr, "A Correlation Between Mass Spectra and Radiolysis Data," *J. Phys. Chem.* **61**, 1483–85 (1957).

J. G. Burr, "The Radiolysis of Deuterated and Tritiated Acetic Acids," *J. Phys. Chem.* **61**, 1481–83 (1957).

J. G. Burr, "The Radiolysis and Mass Spectrometry of Several Deuterated Ethanols," *J. Phys. Chem.* **61**, 1477–80 (1957).

J. A. Ghormley, "Nucleation of Bubbles in Superheated Aqueous Solutions by Fast Particles," *J. Nuclear Energy* **6**, 300–302 (1958).

C. J. Hochanadel and T. W. Davis, "Radiolysis of Solid Nitrates," *J. Chem. Phys.* **27**, 333–34 (1957).

A. R. Jones, "Radiation-Induced Reactions of Potassium Bromide with Air," *Science* **127**, 234 (1958).

S. C. Lind and P. S. Rudolph, "Retardation of a Radiochemical Reaction by Charge Transfer in a Bimolecular Mixture of Gases," *J. Chem. Phys.* **26**, 1768–69 (1957).

H. A. Mahlman and J. W. Boyle, "Hydrogen Yields in Aqueous Sodium Nitrate Solution by Cobalt-60 Gamma-Ray Radiation," *J. Chem. Phys.* **27**, 1434 (1957).

H. A. Mahlman and J. W. Boyle, "Free Radical and Molecular Yields in the Gamma-Ray Decomposition of Heavy Water," *Radiation Research* **7**, 436 (1957).

H. A. Mahlman and J. W. Boyle, "Primary Cobalt-60 Radiolysis Yields in Heavy Water," *J. Am. Chem. Soc.* **80**, 773 (1958).

H. A. Mahlman and G. K. Schweitzer, "Radiation-Induced Nitrate Formation from Concentrated Nitrate Solutions," *J. Inorg. Nuclear Chem.* **5**, 213 (1958).

T. J. Sworski, "Photoreduction of Ceric Ion in Sulfuric Acid Solutions. Effect of Thallous Ion," *J. Am. Chem. Soc.* **79**, 3655 (1957).

## ORGANIC CHEMISTRY

W. H. Baldwin and C. E. Higgins, "Determination of Equivalent Weight of Esters and Halides with Cation Exchange Resins," *Anal. Chem.* **30**, 446 (1958).

J. F. Eastham and V. F. Raaen, "A New *ortho*-Substitution Reaction of the Benzyl-Type Grignard Reagent," *Proc. Chem. Soc. (London)* **1958**, 149.

V. F. Raaen and J. F. Eastham, "The Reduction of Triphenylacetonitrile by the $\alpha$-Hydrogen Atom of Benzylmagnesium Chloride," *J. Am. Chem. Soc.* **79**, 6088 (1957).

B. M. Benjamin, H. J. Schaeffer, and C. J. Collins, "Molecular Rearrangements. XI. The Deamination of 1,1-Diphenyl-2-amino-1-propanol," *J. Am. Chem. Soc.* **79**, 6160 (1957).

V. F. Raaen and C. J. Collins, "Molecular Rearrangements. XII. The *o*-Tolyl/Phenyl Migration Ratios in the Pinacol Rearrangement and in the Deamination Reaction," *J. Am. Chem. Soc.* **80**, 1409 (1958).

L. W. Kendrick, Jr., B. M. Benjamin, and C. J. Collins, "Molecular Rearrangements. XIII. Additional Evidence for the Mechanism of the Aldehyde-Ketone Rearrangement," *J. Am. Chem. Soc.* **80**, 4057 (1958).

G. A. Ropp, C. J. Danby, and D. A. Dominey, "Studies Involving Isotopically Labelled Formic Acid and Its Derivatives. II. Relation of the Absolute Reaction Rates to the Magnitudes of the Isotope Effects in the Oxidation of Formic-$C^{13}$ Acid by Halogen Atoms," *J. Am. Chem. Soc.* **79**, 4944 (1957).

G. A. Ropp and C. E. Melton, "Studies Involving Isotopically Labelled Formic Acid and Its Derivatives. III. Positive and Negative Ions Produced by Electron Impact in Formic and Deuteroformic Acids," *J. Am. Chem. Soc.* **80**, 3509 (1958).

## CHEMISTRY OF AQUEOUS SYSTEMS

G. M. Hebert, H. F. McDuffie, and C. H. Secoy, "The Densities of Heavy Water Liquid and Saturated Vapor at Elevated Temperatures," *J. Phys. Chem.* **62**, 431 (1958).

K. A. Kraus and F. Nelson, "Radiochemical Separations by Ion Exchange," *Ann. Rev. Nuclear Sci.* **7**, 31–46 (1957).

K. A. Kraus, "Ion Exchange," p 34–101 in *Trace Analysis*, ed. by J. H. Yoe and H. J. Koch, Wiley, New York, 1957.

K. A. Kraus and F. Nelson, "Metal Separations by Anion Exchange," *Am. Soc. Testing Materials, Spec. Tech. Publ. No. 195*, 27 (1958).

M. H. Lietzke and R. W. Stoughton, "On the Solubility of $Ag_2SO_4$ in Various Electrolyte Media. Effects of the Solubility of $Ag_2SO_4$ and AgCl on the Ag, $Ag_2SO_4$ and the Ag, AgCl Electrodes," *J. Am. Chem. Soc.* **79**, 2067 (1957).

J. V. Vaughen and M. H. Lietzke, "A Study of the Effect of Dissolved $Ag_2SO_4$ on the Activity of $H_2SO_4$ Solution by Means of E.M.F. Measurements," *J. Am. Chem. Soc.* **79**, 4266 (1957).

## CHEMISTRY OF CORROSION

G. H. Cartledge, "The Activation and Passivation of Stainless Steel in Aerated Sulfuric Acid," *J. Electrochem. Soc.* **104**, 420 (1957).

G. H. Cartledge and R. F. Sympson, "The Existence of a Flade Potential on Iron Inhibited by Ions of the $XO_4^{n-}$ Type," *J. Phys. Chem.* **61**, 973 (1957).

G. H. Cartledge, *Report of European Travel, August–September 1957*, ORNL CF-57-10-27 (Oct. 15, 1957).

## NONAQUEOUS SYSTEMS AT HIGH TEMPERATURES

H. R. Bronstein and M. A. Bredig, "The Electrical Conductivity of Solutions of Alkali Metals in Their Molten Halides," *J. Am. Chem. Soc.* **80**, 2077 (1958).

J. W. Johnson and M. A. Bredig, "Miscibility of Metals with Salts in the Molten State. III. The Potassium-Potassium Halide Systems," *J. Phys. Chem.* **62**, 604 (1958).

A. A. Palko, A. D. Ryon, and D. W. Kuhn, "The Vapor Pressures of Zirconium Tetrachloride and Hafnium Tetrachloride," *J. Phys. Chem.* **62**, 319–22 (1958).

G. W. Parker and G. E. Creek, "Experiments on the Release of Fission Products from Molten Reactor Fuels," p 32 in *Reactor Safety Conference, New York City, October 31, 1957*, TID-7549, Part 2 (April 1958).

G. W. Parker and G. E. Creek, *Experiments on the Release of Fission Products from Molten Reactor Fuels*, ORNL CF-57-6-87 (March 11, 1958).

S. Cantor, R. F. Newton, W. R. Grimes, and F. F. Blankenship, "Vapor Pressures and Derived Thermodynamic Information for the System $RbF-ZrF_4$," *J. Phys. Chem.* **62**, 96 (1958).

C. J. Barton, H. A. Friedman, W. R. Grimes, H. Insley, R. E. Moore, and R. E. Thoma, "Phase Equilibria in the Alkali Fluoride-Uranium Tetrafluoride Fused Salt Systems: I. The Systems $LiF-UF_4$ and $NaF-UF_4$," *J. Am. Ceram. Soc.* **41**, 63–9 (1958).

C. J. Barton, W. R. Grimes, H. Insley, R. E. Moore, and R. E. Thoma, "Phase Equilibria in the Systems $NaF-ZrF_4$, $UF_4-ZrF_4$, and $NaF-ZrF_4-UF_4$," *J. Phys. Chem.* **62**, 665–76 (1958).

R. E. Thoma, *X-Ray Diffraction Results*, ORNL CF-57-7-39 (July 15, 1957).

W. R. Grimes and D. R. Cuneo, ORNL CF-57-9-35 (Sept. 12, 1957) (classified).

R. E. Thoma, *Results of X-Ray Diffraction Phase Analyses of Fused Salt Mixtures*, ORNL CF-58-2-59 (Feb. 18, 1958).

L. G. Overholser, ORNL CF-58-4-112 (April 29, 1958) (classified).

J. P. Blakely, *Molten Salt Compositions*, ORNL CF-58-6-58 (June 12, 1958).

R. E. Thoma and W. R. Grimes, ORNL-2295 (June 24, 1957) (classified).

W. T. Ward, R. A. Strehlow, W. R. Grimes, and G. M. Watson, *Solubility Relations Among Some Fission Product Fluorides in $NaF-ZrF_4-UF_4$ (50-46-4 mole %)*, ORNL-2421 (Jan. 15, 1958).

C. J. Barton, W. R. Grimes, and R. A. Strehlow, *Solubility and Stability of $PuF_3$ in Fused Alkali Fluoride-Beryllium Fluoride Mixtures*, ORNL-2530 (June 11, 1958).

## CHEMICAL PHYSICS

H. A. Levy and S. W. Peterson, "Neutron Diffraction Studies of Hydrogen Containing Crystals," *Revs. Modern Phys.* **30**, 101 (1958).

J. E. Worsham, Jr., H. A. Levy, and S. W. Peterson, "The Positions of Hydrogen Atoms in Urea by Neutron Diffraction," *Acta Cryst.* **10**, 319 (1957).

W. R. Busing and H. W. Morgan, "Infrared Spectrum of $Ca(OH)_2$," *J. Chem. Phys.* **28**, 998 (1958).

W. H. Fletcher and G. M. Begun, "Fundamental of $N^{15}O$," *J. Chem. Phys.* **27**, 579 (1957).

G. M. Begun and W. H. Fletcher, "Infrared Spectra of the Isotopic Nitrous Oxides," *J. Chem. Phys.* **28**, 414 (1958).

G. T. Trammell, H. Zeldes, and R. Livingston, "Effect of Environmental Nuclei in Electron Spin Resonance Spectroscopy," *Phys. Rev.* **110**, 630 (1958).

C. E. Melton and G. F. Wells, "Dissociation of $CO^+$ and $CO^{++}$ Ions by Collision with Neutral Molecules," *J. Chem. Phys.* **27**, 1132 (1957).

G. F. Wells and C. E. Melton, "Mass Spectrometer for the Study of Ion Molecule Collision Processes," *Rev. Sci. Instr.* **28**, 1065 (1957).

C. E. Melton, "Charge Permutation by Ion-Molecule Collision," *J. Chem. Phys.* **28**, 359 (1958).

C. E. Melton, "Application of Thoria-Iridium as the Source of Ionizing Electrons in Mass Spectrometry," *Rev. Sci. Instr.* **29**, 250 (1958).

### MISCELLANEOUS TOPICS

G. E. Boyd, "Energy Relations in Monolayer Formation: The Spreading of Long-Chain Fatty Acids on Aqueous Surfaces," *J. Phys. Chem.* **62**, 536 (1958).

G. E. Boyd and J. Schubert, "Energy Relations in Unimolecular Film Formation: The Spreading of Cetyl Alcohol and Palmitic Acid on Aqueous Surfaces," *J. Phys. Chem.* **61**, 1271 (1957).

G. E. Boyd and F. Vaslow, "Surface Viscosities of Mixed Unimolecular Films," *J. Colloid Sci.* **13**, 275 (1958).

## PAPERS PRESENTED AT SCIENTIFIC AND TECHNICAL MEETINGS

### NUCLEAR CHEMISTRY

A. Chetham-Strode, Jr., "The Actinide Elements," Office of Naval Research, Ninth Annual Nuclear Sciences Seminar, Oak Ridge, December 1–14, 1957

E. Eichler,* N. R. Johnson, and G. D. O'Kelley, "Production of $Ga^{74}$," American Physical Society, New York, January 1958 [*Bull. Am. Phys. Soc.* **3**, 62 (1958)]

G. D. O'Kelley,* E. Eichler, and N. R. Johnson, "Nuclear Spectra of $Tc^{100}$," American Physical Society, New York, January 1958 [*Bull. Am. Phys. Soc.* **3**, 62 (1958)]

N. R. Johnson and G. D. O'Kelley,* "Radiations from $I^{136}$," American Physical Society, New York, January 1958 [*Bull. Am. Phys. Soc.* **3**, 63 (1958)]

N. R. Johnson,* G. D. O'Kelley, and E. Eichler, "Nuclear Spectra of $Rb^{90}$," American Physical Society, Washington, D. C., May 1958 [*Bull. Am. Phys. Soc.* **3**, 207 (1958)]

G. D. O'Kelley, "Nuclear Spectra and Level Structure of Some Medium-Weight Nuclides," American Chemical Society, San Francisco, April 13–18, 1958 [ACS abstract of 133rd meeting, p 51Q]

A. Galonsky,* H. B. Willard, A. R. Brosi, B. H. Ketelle, H. O. Cohn, and N. H. Lazar, "Spherical Electrostatic Spin-Rotator for Electron Polarization Measurements," American Physical Society, Southeastern Section Meeting, Huntsville, Alabama, April 10–12, 1958 [*Bull. Am. Phys. Soc.* **3**, 305 (1958)]

J. Halperin and R. W. Stoughton,* "Review of Some Heavy Nuclide Reactor Cross Sections," American Chemical Society, San Francisco, April 13–18, 1958 [ACS abstract of 133rd meeting, p 41K]

### ISOLATION AND CHEMICAL PROPERTIES OF SYNTHETIC ELEMENTS

G. E. Boyd, "The Discovery, Production, and Properties of the Synthetic Elements Technetium and Promethium," American Chemical Society, San Francisco, April 13–18, 1958 [ACS abstract of 133rd meeting, p 19F]

G. E. Boyd* and Q. V. Larson, "Solvent Extraction of Heptavalent Technetium," American Chemical Society, San Francisco, April 13–18, 1958 [ACS abstract of 133rd meeting, p 61Q]

---

*Denotes speaker.

R. H. Busey* and Q. V. Larson, "Spectrophotometric Examination of Certain Oxidation States of Rhenium and Technetium," American Chemical Society, San Francisco, April 13–18, 1958 [ACS abstract of 133rd meeting, p 30L]

G. W. Parker* and G. E. Creek, "Summary of Fission Product Release Program," meeting of Section Committee N6 on Reactor Safety Standards, Cincinnati, April 9, 1958

G. W. Parker,* P. M. Lantz, W. J. Martin, D. O. Campbell, and R. A. Rainey, "The Intermediate Scale Production and Isolation of Neptunium and Americium," XVI International Congress of Pure and Applied Chemistry, Paris, France, July 18–24, 1957 [Proceedings of the Divisions of Inorganic and Physical Chemistry, p 395]

## RADIATION CHEMISTRY

H. W. Kohn* and E. H. Taylor, "Ionizing Radiation in the Study of Heterogeneous Catalysts," American Chemical Society, San Francisco, April 13–18, 1958 [ACS abstract of 133rd meeting, p 17I]

A. R. Jones* and R. H. Johnson, "Chemical Features of the Fixation of Nitrogen by Irradiation of Moist Air," American Chemical Society, San Francisco, April 13–18, 1958 [ACS abstract of 133rd meeting, p 43K]

G. E. Moore, "The Effect of High-Energy Radiations on Heterogeneous Catalysts," Department of Chemistry, University of Tennessee, graduate seminar, May 15, 1958

C. J. Hochanadel, chairman of the Gordon Research Conference on Radiation Chemistry, New Hampton, New Hampshire, July 1957

C. J. Hochanadel, "Review of the Radiation Chemistry of Water with Special Emphasis on Stopping Power," seminar given for the Biology Division of the Oak Ridge National Laboratory, January 9, 1958

## ORGANIC CHEMISTRY

B. M. Benjamin* and C. J. Collins, "A Study of Certain Stereospecific Reactions," American Chemical Society, San Francisco, April 13–18, 1958 [ACS abstract of 133rd meeting, p 11N]

C. J. Collins* and B. M. Benjamin, "Evidence for Open Carbonium Ions in the Deamination of Aminoalcohols," International Conference on Radioisotopes in Research, Paris, France, September 13, 1957 [abstract No. 58, session 10-A]

C. J. Collins, "Carbon-14 and Organic Chemistry," lectures for American Chemical Society before local sections at Davenport, Iowa City, and Ames, Iowa; Vermillion, South Dakota; and Lincoln and Omaha, Nebraska; March 11–18, 1958

C. J. Collins, "The Mechanism of the Deamination Reaction," Institut für organische Chemie, ETH, Zürich, September 24, 1957; Institut für organische Chemie, University of Munich, September 26, 1957; Department of Chemistry, Ohio University, Athens, April 16, 1958

G. A. Ropp,* C. J. Danby, and D. A. Dominey, "Carbon-13 Isotope Effects in the Photochemical Reaction of Formic-$C^{13}$ Acid with Halogen Atoms," American Chemical Society, New York, September 8–13, 1957 [ACS abstract of 132nd meeting, p 84P]

G. A. Ropp, "Isotope Fractionation in the Decarbonylation of Isotopically Labelled Formic Acids in Concentrated Sulfuric Acid," American Chemical Society, Southeastern Regional Meeting, Durham, North Carolina, November 1957

G. A. Ropp, "Isotope Fractionation and the Mechanism of Decarbonylation of Formic Acid by Sulfuric Acid," Chemistry Department, Georgia Institute of Technology, Atlanta, November 1957

*Denotes speaker.

## CHEMISTRY OF AQUEOUS SYSTEMS

G. E. Boyd,* S. Lindenbaum, and G. E. Myers, "A Thermodynamic Calculation of Anion-Exchange Selectivity Coefficients," American Chemical Society, New York, September 8–13, 1957 [ACS abstract of 132nd meeting, p 2I]

S. Lindenbaum,* G. E. Boyd, and G. E. Myers, "Properties of a New Sulfonium-Type Strong-Base Anion Exchanger," American Chemical Society, New York, September 8–13, 1957 [ACS abstract of 132nd meeting, p 21I]

F. Vaslow* and G. E. Boyd, "Calorimetric Measurements of the Heats of Cation Exchange," American Chemical Society, San Francisco, April 13–18, 1958 [ACS abstract of 133rd meeting, p 18I]

J. S. Johnson* and K. A. Kraus, "Ultracentrifugation Studies of Inorganic Solvents," American Chemical Society, Southeastern Regional Meeting, Durham, North Carolina, Nobember 1957

J. S. Johnson, "Hydrolytic Inorganic Polymerization," ORINS Lecture, Department of Chemistry, University of Virginia, Charlottesville, March 21, 1958

M. H. Lietzke, "High Temperature E.M.F. Measurements," Seventh Annual AEC Corrosion Symposium, Knolls Atomic Power Laboratory, Schenectady, New York, May 1958

M. H. Lietzke and R. W. Stoughton,* "Solubility of Silver Sulfate in Potassium Nitrate, Potassium Sulfate, and Sulfuric Acid Media as a Function of Temperature," American Chemical Society, San Francisco, April 13–18, 1958 [ACS abstract of 133rd meeting, p 57Q]

F. E. Clark, J. S. Gill, R. Slusher, and C. H. Secoy,* "Phase Stability at Elevated Temperatures for the System, Uranium Trioxide–Cupric Oxide–Sulfur Trioxide–Water," American Chemical Society, San Francisco, April 13–18, 1958 [ACS abstract of 133rd meeting, p 34K]

G. E. Moore* and E. L. Compere, "High Temperature Circulation of Aqueous Thorium Oxide Slurries in Small-Scale Tests," American Nuclear Society, Third Annual Meeting, Pittsburgh, June 10–12, 1957 [abstract No. 14-4, p 45]

T. A. Carlson,* K. A. Kraus, and J. S. Johnson, "Cation Exchange Properties of Zirconium(IV)–Tungsten(VI) Precipitates," American Chemical Society, New York, September 8–13, 1957 [ACS abstract of 132nd meeting, p 58S]

K. A. Kraus, "Ion Exchange," First Annual Conference, Analytical Chemistry in Nuclear Reactor Technology, Gatlinburg, Tennessee, November 1957

K. A. Kraus, "Separations by Ion Exchange," American Chemical Society, Southeastern Regional Meeting, Chapel Hill, North Carolina, November 1957

J. S. Johnson and K. A. Kraus,* "Equilibrium Ultracentrifugations of Hydrolytic Polymers," American Chemical Society, San Francisco, April 13–18, 1958 [ACS abstract of 133rd meeting, p 17L]

E. W. Anacker,* J. S. Johnson, and K. A. Kraus, "Ultracentrifugation of Polymolybdate Solutions," American Chemical Society, San Francisco, April 13–18, 1958 [ACS abstract of 133rd meeting, p 55Q]

H. F. McDuffie, "Homogeneous Catalysis," ORINS Traveling Lecture, University of Mississippi, Louisiana State University, and University of Alabama, February 10–12, 1958; University of Virginia, May 22, 1958

---

*Denotes speaker.

## CHEMISTRY OF CORROSION

G. H. Cartledge, "The Passivation Process in the Presence of the $XO_4^{n-}$ Inhibitors," Internationales Kolloquium über die Passivität der Metalle, Heiligenberg, Germany, 1957 [preprints]

G. H. Cartledge, "The Action of the $XO_4^{n-}$ Inhibitors," National Association of Corrosion Engineers, San Francisco, March 1958 [*Corrosion* (1958)]

G. H. Cartledge, "The Chemical and Electrochemical Aspects of Reactor Corrosion," lectures for the Europäische Föderation für Korrosion, symposium, Frankfurt, Germany, 1958, the Max Planck Institut für Metallforschung, Stuttgart, Germany, and the Institute of Inorganic, Analytical, and Physical Chemistry, University of Bern, Switzerland

## NONAQUEOUS SYSTEMS AT HIGH TEMPERATURES

T. A. Gens,* A. R. Brosi, and J. A. Wethington, Jr., "Rapid Exchange of Fluorine-18 Between Fluorocarbons and Alkali Fluorides," American Chemical Society, New York, September 8–13, 1957 [ACS abstract of 132nd meeting, p 8I]

M. A. Bredig, "Solutions of Alkali Metals in Their Halides in the Molten State," Gordon Research Conference on Inorganic Chemistry, New Hampton, New Hampshire, August 21, 1957

M. A. Bredig, "Miscibility of Liquid Metals with Salts. IV. The Sodium–Sodium Halide Systems at High Temperature," American Chemical Society, New York, September 8–13, 1957 [ACS abstract of 132nd meeting, p 27S]

M. Blander, "Structure and Thermodynamic Considerations in Reciprocal Molten Salt Systems," Molten Salt Symposium, Oak Ridge, July 17, 1957

C. C. Beusman, "Vapor Association in the $KCl\text{-}FeCl_2$ System," Molten Salt Symposium, Oak Ridge, July 17, 1957

M. B. Panish, "Activities in LiCl-AgCl and NaCl-AgCl Systems in the Molten and Solid States," Molten Salt Symposium, Oak Ridge, July 18, 1957

W. R. Grimes, "The System $NaF\text{-}ZrF_4\text{-}UF_4$," Molten Salt Symposium, Oak Ridge, July 19, 1957

G. M. Watson, "Activities from Hydrogen Reduction Equilibria," Molten Salt Symposium, Oak Ridge, July 19, 1957

L. E. Topol, "Activities from Daniell Cells," Molten Salt Symposium, Oak Ridge, July 19, 1957

S. Cantor, "Activities from Vapor Pressures," Molten Salt Symposium, Oak Ridge, July 19, 1957

C. J. Barton, W. R. Grimes,* H. Insley, R. E. Moore, and R. E. Thoma, "Phase Equilibria in the Systems Sodium Fluoride–Zirconium Tetrafluoride, Uranium Tetrafluoride, Uranium Tetrafluoride–Zirconium Tetrafluoride, and Sodium Fluoride–Zirconium Tetrafluoride–Uranium Tetrafluoride," American Chemical Society, New York, September 8–13, 1957 [ACS abstract of 132nd meeting, p 29S]

S. Cantor,* R. F. Newton, W. R. Grimes, and F. F. Blankenship, "Vapor Pressures of the Systems Potassium Fluoride–Zirconium Tetrafluoride and Rubidium Fluoride–Zirconium Tetrafluoride," American Chemical Society, New York, September 8–13, 1957 [ACS abstract of 132nd meeting, p 29S]

C. M. Blood, W. R. Grimes, and G. M. Watson,* "Activity Coefficients of Ferrous Fluoride and of Nickel Fluoride in Molten Sodium Fluoride–Zirconium Fluoride Solutions," American Chemical Society, New York, September 8–13, 1957 [ACS abstract of 132nd meeting, p 30S]

*Denotes speaker.

L. E. Topol, R. F. Newton, W. R. Grimes,* and F. F. Blankenship, "Electrometric Determination of the Solubilities and Activities of Some Transition Metal Fluorides in Molten Fluoride Solutions," American Chemical Society, New York, September 8–13, 1957 [ACS abstract of 132nd meeting, p 30S]

D. R. Cuneo, "Chemical Aspects of the Aircraft Reactor Experiment," American Nuclear Society, Iowa State Chapter, November 1957

G. M. Watson, "Chemical Reactions in Molten Salt Media," ORINS Traveling Lecture, University of Oklahoma, Oklahoma State University, and University of Mississippi, November 1957

W. R. Grimes, "Molten Salts as Breeder Fuels," Thorium-$U^{233}$ Reactor Symposium, Brookhaven National Laboratory, January 1958

W. R. Grimes, "Some Chemical Problems of Nuclear Reactors Fueled with Molten Fluorides," tour for American Chemical Society at Wayne State University, Detroit, March 18, 1958, and Hope College, Holland, Michigan, March 20, 1958

W. R. Grimes, "Chemical Behavior of Some Molten Fluoride Mixtures," tour for American Chemical Society at Wayne State University, Detroit, and Michigan State University, Lansing, March 19, 1958

G. M. Watson, J. H. Shaffer,* N. V. Smith, and W. R. Grimes, "Solubility of HF and Some Noble Gases in Molten $NaF-ZrF_4$ Mixtures," American Chemical Society, San Francisco, April 13–18, 1958 [ACS abstract of 133rd meeting, p 23K]

R. B. Evans, III,* F. F. Blankenship, W. R. Grimes, and G. M. Watson, "Some Aspects of Corrosion of Inconel by Molten Fluorides," AEC Corrosion Symposium, Schenectady, May 1958

W. R. Grimes, "Some Separation Processes from Molten Fluoride Solutions," American Chemical Society, Analytical Division Meeting, Schenectady, June 1958

R. E. Thoma,* H. Insley, B. S. Landau, H. A. Friedman, and W. R. Grimes, "Phase Equilibria in Alkali Fluoride–Uranium Tetrafluoride Fused Salt Systems. II. The Systems $KF-UF_4$ and $RbF-UF_4$," American Ceramic Society, Pittsburgh, April 1958 [abstract bulletin, vol 37, No. 4 (1958)]

R. E. Thoma,* H. Insley, B. S. Landau, H. A. Friedman, and W. R. Grimes, "Phase Equilibria in the Alkali Fluoride–Uranium Tetrafluoride Fused Salt Systems: III. The System $NaF-LiF-UF_4$," American Ceramic Society, Pittsburgh, April 1958 [abstract bulletin, vol 37, No. 4 (1958)]

## CHEMICAL PHYSICS

Ralph Livingston, "Applications of Paramagnetic Resonance and Nuclear Quadrupole Spectroscopy to Inorganic Chemistry," Gordon Research Conference on Inorganic Chemistry, New Hampton, New Hampshire, August 21, 1957

Ralph Livingston, "Paramagnetic Resonance Studies of Free Radicals Produced by Radiation of Solids," American Chemical Society, New York, September 8–13, 1957

Ralph Livingston, "Studies of Stably Trapped Free Radicals in Solids by Paramagnetic Resonance," symposium on the Formation and Stabilization of Free Radicals, National Bureau of Standards, Washington, D.C., September 1957

Ralph Livingston, "Pure Quadrupole Spectroscopy," conference on Radio and Microwave Spectroscopy, Office of Naval Research, Air Force Office of Scientific Research, and Office of Ordnance Research, Durham, North Carolina, November 1957

---

*Denotes speaker.

Ralph Livingston, "Nuclear Quadrupole Spectroscopy," seminar, Department of Chemistry, University of Cincinnati, October 25, 1957

Ralph Livingston, "Applications of Nuclear Quadrupole Spectroscopy to Inorganic Chemistry," Physical and Inorganic Group of the Pittsburgh Section of the American Chemical Society, Pittsburgh, October 28, 1957

Ralph Livingston, "Applications of Paramagnetic Resonance and Nuclear Quadrupole Spectroscopy to Chemistry," seminar, Department of Chemistry, Michigan State University, East Lansing, October 29, 1957; seminar, Department of Chemistry, Pennsylvania State University, University Park, October 31, 1957

Ralph Livingston, "Paramagnetic Resonance Studies of Free Radicals Produced by Radiation," testimony before the Subcommittee on Research and Development, Joint Congressional Committee on Atomic Energy, Washington, D. C., February 1958; seminar, Free Radicals Research Section, National Bureau of Standards, Washington, D.C., February 7, 1958

Ralph Livingston, "Chemical Applications of Pure Quadrupole Spectroscopy," a "Frontiers in Chemistry" lecture, Wayne State University, Detroit, February 1958

Ralph Livingston, "Electron Spin Resonance Spectroscopy," Research Laboratories of Merck, Sharp, and Dohme, Rahway, New Jersey, April 23, 1958

H. Zeldes, "Paramagnetic Resonance Studies of Irradiated Materials," Graduate School, Oklahoma State University, Department of Physics, University of Oklahoma, March 4–5, 1958; Department of Physics, Baylor University, Physics Department, A & M College of Texas, Department of Chemistry, Louisiana State University, April 14–16, 1958

W. R. Busing* and H. A. Levy, "A Computer Program to Process the Results of Crystal Structure Refinements," American Crystallographic Association, Marquette University, Milwaukee, June 24, 1958 [abstract No. G-4]

W. R. Busing* and H. A. Levy, "A Single-Crystal Neutron Diffraction Study of Hydrogen Peroxide," American Crystallographic Association, Marquette University, Milwaukee, June 25, 1958 [abstract No. H-7]

H. A. Levy, "Neutron Diffraction Studies of Hydrogen-Containing Crystals," conference on Current Problems in Crystal Physics, Massachusetts Institute of Technology, Cambridge, July 2, 1957

H. A. Levy* and S. W. Peterson, "Analysis of Thermal and Electron Asymmetry of Urea from Combined Neutron and X-Ray Data," Fourth International Congress of Crystallography, Montreal, July 1957 [abstract No. 15.3]

H. A. Levy, "Study of Molecular Structure by Neutron Diffraction," testimony before the Subcommittee on Research and Development, Joint Congressional Committee on Atomic Energy, Washington, D.C., February 1958

S. W. Peterson,* H. A. Levy, and V. Schomaker, "Neutron Diffraction Study of N-Acetyl Glycine," Fourth International Congress of Crystallography, Montreal, July 1957 [abstract No. 15.2]

P. A. Agron,* M. D. Danford, M. A. Bredig, H. A. Levy, and P. C. Sharrah, "Apparatus, Techniques, and Methods in Molten-Salt Diffraction Studies," Fourth International Congress of Crystallography, Montreal, July 1957 [abstract No. 1(i)4]

M. D. Danford, P. A. Agron,* M. A. Bredig, and H. A. Levy, "Structural Analysis of Molten Salt," Fourth International Congress of Crystallography, Montreal, July 1957 [abstract No. 12.5]

---

*Denotes speaker.

H. G. Smith* and R. E. Rundle, "Structure Refinement of the Silver Perchlorate–Benzene Complex," American Crystallographic Association, Marquette University, Milwaukee, June 26, 1958 [abstract No. M-1]

G. M. Brown* (University of Maryland), H. G. Norment, Jr., and H. A. Levy, "The Crystal Structure of 2,6-Dimethyl-γ-pyrone," Fourth International Congress of Crystallography, Montreal, July 1957 [abstract No. 7.30]

J. H. Burns* and H. A. Levy, "The Hydrogen Positions in Glycine by Neutron Diffraction," American Crystallographic Association, Marquette University, Milwaukee, June 1958 [abstract No. H-9]

Russell Baldock, C. E. Melton,* G. A. Ropp, and G. F. Wells, "Application of the Mass Spectrometer to the Study of Photochemical Reactions of Chlorine," Sixth Annual Meeting of A.S.T.M. Committee E-14 on Mass Spectrometry, New Orleans, June 2–6, 1958

G. F. Wells,* C. E. Melton, and Russell Baldock, "Mass Spectrometer Techniques in a Study of Ion-Molecule Reactions," Sixth Annual Meeting of A.S.T.M. Committee E-14 on Mass Spectrometry, New Orleans, June 2–6, 1958

C. E. Melton,* G. A. Ropp, Russell Baldock, and G. F. Wells, "Dissociation of Formic Acid and Deuteroformic Acids by Ion-Molecule Collision," Sixth Annual Meeting of A.S.T.M. Committee E-14 Spectrometry, New Orleans, June 2–6, 1958

Russell Baldock, C. E. Melton,* G. A. Ropp, and G. F. Wells, "Charge Permutation by Ion-Molecule Collision," Sixth Annual Meeting of A.S.T.M. Committee E-14 on Mass Spectrometry, New Orleans, June 2–6, 1958

## MISCELLANEOUS TOPIC

H. F. McDuffie, "The Meaning of Oak Ridge," 1958 Summer Institute for High School Juniors and Seniors, University of Cincinnati, June 19, 1958

---

*Denotes speaker.

**ORNL-2584**
**Chemistry-General**
**TID-4500 (13th ed., Rev.)**
**February 15, 1958**

*INTERNAL DISTRIBUTION*

1. C. E. Center
2. Biology Library
3. Health Physics Library
4-6. Central Research Library
7-26. Laboratory Records Department
27. Laboratory Records, ORNL R.C.
28. Reactor Experimental Engineering Library
29. A. M. Weinberg
30. L. B. Emlet (K-25)
31. J. P. Murray (Y-12)
32. J. A. Swartout
33. E. H. Taylor
34. E. D. Shipley
35. S. C. Lind
36. M. L. Nelson
37. W. H. Jordan
38. R. R. Dickison
39. F. L. Culler
40. A. H. Snell
41. A. Hollaender
42. M. T. Kelley
43. R. A. Charpie
44. K. Z. Morgan
45. T. A. Lincoln
46. A. S. Householder
47. C. S. Harrill
48. C. E. Winters
49. H. E. Seagren
50. D. Phillips
51. J. A. Lane
52. G. E. Boyd
53-65. M. A. Bredig
66. R. W. Stoughton
67. R. B. Briggs
68. G. W. Parker
69. C. J. Borkowski
70. G. H. Jenks
71. K. A. Kraus
72. H. A. Levy
73. R. S. Livingston
74. T. E. Willmarth
75. C. H. Secoy
76. C. J. Hochanadel
77. W. H. Baldwin
78. A. R. Brosi
79. R. N. Lyon
80. S. A. Reynolds
81. P. F. Thomason
82. E. G. Bohlmann
83. C. P. Keim
84. C. D. Susano
85. P. M. Reyling
86. R. Livingston
87. G. H. Cartledge
88. E. R. Van Artsdalen
89. G. C. Williams
90. R. W. Johnson
91. J. R. McNally, Jr.
92. G. D. O'Kelley
93. M. J. Skinner
94. D. S. Billington
95. H. G. MacPherson
96. J. L. Gabbard
97. R. H. Busey
98. J. J. Pinajian
99. D. W. Sherwood
100. C. R. Baldock
101. F. F. Blankenship
102. C. J. Collins
103. J. S. Drury
104. W. R. Grimes
105. J. S. Johnson
106. W. L. Marshall
107. H. F. McDuffie
108. G. J. Nessle
109. S. W. Peterson
110. G. A. Ropp
111. G. M. Watson
112. R. F. Newton
113. R. E. Thoma
114. D. R. Cuneo
115. P. H. Emmett (consultant)
116. G. T. Seaborg (consultant)
117. C. E. Larson (consultant)
118. E. P. Wigner (consultant)
119. B. Crawford (consultant)
120. T. H. Davies (consultant)

*EXTERNAL DISTRIBUTION*

121. Division of Research and Development, AEC, Washington
122. Division of Research and Development, AEC, ORO
123. Boeing Airplane Company
124. Union Carbide and Carbon Chemical Company (South Charleston)
125. North America Aviation, Inc.
126-680. Given distribution as shown in TID-4500 (13th ed., Rev.) under Chemistry-General category (75 copies – OTS)

Chemistry Division progress reports previously issued in this series are as follows:

| | |
|---|---|
| ORNL-65 | March, April, May, 1948 |
| ORNL-176 | June, July, August, 1948 |
| ORNL-229 | September, October, November, 1948 |
| ORNL-336 | December, 1948, January and February, 1949 |
| ORNL-286 | Period Ending June 30, 1949 |
| ORNL-499 | Period Ending September 30, 1949 |
| ORNL-607 | Period Ending December 31, 1949 |
| ORNL-685 | Period Ending March 31, 1950 |
| ORNL-795 | Period Ending June 30, 1950 |
| ORNL-870 | Period Ending September 30, 1950 |
| ORNL-1036 | Period Ending December 31, 1950 |
| ORNL-1053 | Period Ending March 31, 1951 |
| ORNL-1116 | Period Ending June 30, 1951 |
| ORNL-1153 | Period Ending September 30, 1951 |
| ORNL-1260 | Period Ending December 31, 1951 |
| ORNL-1285 | Period Ending March 31, 1952 |
| ORNL-1344 | Period Ending June 30, 1952 |
| ORNL-1432 | Period Ending September 30, 1952 |
| ORNL-1482 | Period Ending December 31, 1952 |
| ORNL-1587 | Period Ending June 20, 1953 |
| ORNL-1674 | Period Ending December 20, 1953 |
| ORNL-1755 | Period Ending June 20, 1954 |
| ORNL-1832 | Period Ending December 20, 1954 |
| ORNL-1940 | Period Ending June 20, 1955 |
| ORNL-2046 | Period Ending December 20, 1955 |
| ORNL-2159 | Period Ending June 20, 1956 |
| ORNL-2386 | Period Ending June 20, 1957 |